

**Analytical Graphical Approach for Predicting
Ground Conditions in TBM-based Tunneling
Construction**

by

Beatriz Goncalves Klink

B.S. Civil Engineering, Centro Universitario de Brasilia (2018)

Submitted to the Department of Civil and Environmental Engineering
in partial fulfillment of the requirements for the degree of
Master of Science in Civil and Environmental Engineering
at the

MASSACHUSETTS INSTITUTE OF TECHNOLOGY

June 2023

©2023 Beatriz G. Klink: The author hereby grants MIT a nonexclusive, worldwide, irrevocable, royalty-free license to exercise any and all rights under copyright, including to reproduce, preserve, distribute and publicly display copies of the thesis, or release the thesis under an open-access license.

Author
Department of Civil and Environmental Engineering
May 12, 2023

Certified by.....
Herbert H. Einstein
Professor of Civil and Environmental Engineering
Thesis Supervisor

Accepted by
Colette L. Heald
Professor of Civil and Environmental Engineering
Chair, Graduate Program Committee

This page intentionally left blank.

Analytical Graphical Approach for Predicting Ground Conditions in TBM-based Tunneling Construction

by

Beatriz Goncalves Klink

B.S. Civil Engineering, Centro Universitario de Brasilia (2018)

Submitted to the Department of Civil and Environmental Engineering
in partial fulfillment of the requirements for the degree of
Master of Science in Civil and Environmental Engineering
at the

MASSACHUSETTS INSTITUTE OF TECHNOLOGY

June 2023

©2023 Beatriz G. Klink: The author hereby grants MIT a nonexclusive, worldwide, irrevocable, royalty-free license to exercise any and all rights under copyright, including to reproduce, preserve, distribute and publicly display copies of the thesis, or release the thesis under an open-access license.

Authored by: Beatriz Goncalves Klink
Department of Civil and Environmental Engineering
May 12, 2023

Certified by: Herbert H. Einstein
Professor of Civil and Environmental Engineering
Thesis Supervisor

Accepted by: Colette L. Heald
Professor of Civil and Environmental Engineering
Chair, Graduate Program Committee

This page intentionally left blank.

Analytical Graphical Approach for Predicting Ground Conditions in TBM-based Tunneling Construction

by

Beatriz Goncalves Klink

Submitted to the Department of Civil and Environmental Engineering
on May 12, 2023, in partial fulfillment of the
requirements for the degree of
Master of Science in Civil and Environmental Engineering

Abstract

The present master's thesis addresses the use of Artificial Intelligence (AI) and Machine Learning (ML) algorithms to predict geology based on Tunnel Boring Machine (TBM) data. The use of mechanized tunneling has become frequent over the last decade, and their performance is critical for project management and safety. Numerical simulation methods have become prevalent in predicting TBM performance metrics, and the use of AI/ML techniques for prescient applications using TBM-generated data has become ubiquitous. The current research aims to propose an exploratory look into the correlation between specific TBM parameters and ground conditions. The methodology seeks to classify rings based on three main ground classes: rock, soil, and mixed, through the observation of clear patterns, found to be representative of these ground classes, which are demonstrated. A techno-economic assessment of the current use of AI/ML tools for geology prediction in TBM-based tunneling construction, is also presented, analyzing both the potential and shortcomings of the technology. For the purpose of the study, the Porto Metro project (Portugal) is introduced, used as a case study for the proposed methodology. As the mining and drilling market is projected to almost double from 2020-2030, and with the increasing use of TBMs, improving ground condition prediction is paramount to the advancement of tunneling automation efforts. The present thesis aims to further develop the field and open dialogue on the use and effectiveness of using purely AI/ML modelling methods for this application.

Thesis Supervisor: Herbert H. Einstein

Title: Professor of Civil and Environmental Engineering

Thesis Supervisor: Herbert H. Einstein Authored by: Beatriz Goncalves Klink

Title: Professor of Civil and Environmental Engineering

Acknowledgments

First, I would like to show my appreciation and gratitude for my advisor, Professor Herbert H. Einstein. He has been such an important mentor, advocate and teacher. After learning that I had been admitted into MIT, he was the first person I called. He had been one of the faculty members that I knew had reviewed my application, and I was just so thrilled to be heading to the best Engineering School in the world! He told me at the time that I was on his list of people to reach out to and was happily surprised when I called him first. My time at MIT was shaped and guided by Professor Einstein, I learned so much from his experience and passion for research.

I would also like to express my deepest gratitude to Professor Rita Sousa and Saadeldin Moustaffa (Saad) from the Stevens Institute of Technology. I am truly thankful for all the insights, joint research effort and support along the way. Saad, I wish you all the best in your PhD, I know you will succeed brilliantly! And to Professor Sousa, my utmost admiration and appreciation, it was so empowering and heartwarming to work with a fellow Portuguese speaker, *muchito obrigada!*

I would like to thank my loving family. Their continual encouragement and support, especially throughout the application process, was paramount for my success. I am so thankful for my grandfathers, who inspired me to study Civil Engineering and always fed into my analytical and entrepreneurial mindset. My grandmothers, for their incredible strength, courage, and, mostly, for their stories, that brought nature and science into my life at such an early age. Lastly, to all my aunts and uncles, and dear cousins, I am so grateful for the sheer amount of love I receive and experience with you all!

To my parents, Carlos and Adriana, I wish to express my deepest love and appreciation. Thank you for my upbringing, and the true honor of being your child. I know how much of a privilege it is to grow up with scientist parents that always stimulated and supported my insatiable curiosity! Thank you for teaching me about the life-changing power of knowledge, and for instilling in me the sense that anything is possible! Without you, I would have never gotten this far. And, obviously, my

brother, Tomas, for being the best big brother. Thank you for helping me through the tough times, and always bringing a smile to my face. It is truly a blessing to have so many incredible people who care and root for you, I thank and appreciate you all so much!

I also want to thank my roommates, Thais and Amanda for becoming my family here. Thank you for so many conversations, meals (sitting on the kitchen floor), books, flowers, laughs. And, especially, for helping me through the several hurdles, stressful days, dramatic breakups, and the countless illnesses brought on by winter. You have truly made me feel like I had a home here. Thank you my bbs, I love you to bits!

Thank you to all of my research group members (Eve, Paris, Rafa, Omar, Randy, Ignacio, Majed) and classmates, you have been an essential source of knowledge and support. I want to especially thank Katya and Ivo for being my CEE ride or dies, thank you for showing me the way and helping me navigate this whole experience. Ivo, I will never be able to thank you enough for all you did for me here. You brought me so many incredible people and experiences, gave me so much support and true friendship. Katya, girl, you know we are kindred spirits. Finding you was one of the best things to come out of this experience, and I am so grateful! Of course, to all the Brazilian friends I found here, that made this cold land of the north seem like home, Wellington, Matheus, Cristiano, and Carlo, thank you for all the love, good times, great conversations, and in sharing hope for the future of our beautiful country.

I am immensely grateful for finding such incredible people here. In the end, I believe that is the true highlight of my MIT experience, people. The friends I made here, the ideas I have come in contact with, the stories and journeys. It has been extremely beautiful and life-changing!

For the friends back home, my chosen family, I want to thank you so much! Without your love and support I would never have gotten here. You are all so uniquely special to me and I love you deeply. Can't wait to see you all in June!

Last but certainly not least, I want to thank Brazil. I feel so much gratitude for being brought up in such a gorgeous country. Brazil is my past, and my future. It's

my biggest love and pride. I believe that things can, and will be better! Although there is still much to be done to build the country that we dream of, it is possible. For me, Brazil is the country of the future, we have so much to teach and share with the world. You are and will always be my greatest source of inspiration. I end these acknowledgements with a lyric from one of my favorite bands, Braza, which, as I learned here, perfectly defines how I present myself to the world: "*De cabeça erguida ostento o orgulho tupiniquim*".

Contents

1	Introduction	27
1.1	Motivation and Objectives	27
1.2	Porto Metro Project	31
1.3	Thesis Outline	32
2	Background	35
2.1	Tunneling	35
2.1.1	Historical Aspects	35
2.1.2	Tunnel Construction Methods	43
2.2	Tunnel Boring Machines (TBM)	47
2.2.1	Historical Aspects	47
2.2.2	Tunnel Boring Machine (TBM) Designs	51
2.3	Porto Metro	54
2.3.1	The Project	57
2.3.2	Infrastructure	58
2.3.3	Ticketing	60
2.3.4	Communication Systems	61
2.3.5	Financial considerations	61
3	Geological and Geotechnical Aspects	63
3.1	The Geomorphology of Portugal	63
3.2	The City of Porto	66
3.2.1	Geological Conditions	69

3.3	Porto Metro Project	72
3.3.1	Projected Geological Profile	74
3.3.2	Encountered Geology	74
3.3.3	Face mappings	75
4	Methodology & Results	89
4.1	Contextual Aspects of Mechanized Tunneling Automation	90
4.1.1	TBM Data	90
4.1.2	The Future of Tunneling	92
4.2	An Introduction to Artificial Intelligence and Machine Learning	95
4.2.1	Previous work in Geology Prediction using TBM Data	96
4.2.2	Porto Metro Data	101
4.3	Relating Ground Conditions to Machine-Generated Data	103
4.3.1	Proposed Approach	103
4.3.2	Evaluated Parameters	103
4.3.3	Importance of Chosen Parameters	105
4.3.4	Correlating Graphical Data to Ground Conditions	108
4.3.5	Tunnel Sections Analyzed	108
4.4	Results	109
4.4.1	Time-series Plots	109
4.4.2	Scatter Plots	158
4.5	Interpretation & Conclusions	214
5	Novel Approach to Improving Geological Prediction in TBM Operations	219
5.1	Intent	219
5.2	Methodologies	220
5.2.1	Confidence Learning	220
5.2.2	Scattergram Approach	223
5.3	Applications	224
5.3.1	Confidence Learning Labels	224

5.3.2	Comparison Scattergrams for High Confidence Labeled Rings .	226
5.3.3	Comparison Scattergrams for Low Confidence Labeled Rings .	232
5.4	Comparison & Conclusions	238
6	Techno-Economic Assessment (TEA)	241
6.1	Contextual Aspects	241
6.2	The use of Artificial Intelligence (AI) in Tunnel Boring Machines (TBMs)	242
6.3	TEA Project Scope	243
6.3.1	Literature Review	244
6.3.2	Stakeholders	247
6.3.3	Implementation	248
6.4	Market Analysis	250
6.4.1	Current Applications	250
6.4.2	Expected Market Growth	251
6.4.3	Main Players	253
6.4.4	Market Macro-Trends	256
6.4.5	Challenges to Implementation	258
6.5	Technical Requirements	259
6.5.1	Hardware and Software Requirements	259
6.5.2	Feasibility and Scalability	262
6.6	Cost Estimates	263
6.7	Benefit Analysis	265
6.7.1	Potential Improvements	265
6.7.2	Return on Investment (ROI)	266
6.8	Associated Risks	267
6.8.1	Data	268
6.8.2	Cybersecurity Threats	269
6.8.3	Regulation	270
6.8.4	Technical Failure	271
6.8.5	Lack of Skilled Labor	271

6.8.6	Implementation Pushback	272
6.8.7	Considerations on Automation Technology	273
6.9	Conclusions and Recommendations	274
7	Summary and Conclusions	279
7.1	Future Research	281

List of Figures

1-1	The image shows the Gripper TBM, with both sets of mechanical jacks visible in black, as provided by Robins.	29
1-2	Sample geologic section (between rings 611-689) showing the division into 1 meter sections, or rings [Metro do Porto, 2010b].	30
1-3	Map of Porto Metro [Metro do Porto, 2010b].	33
2-1	Pausilippo tunnel as depicted by Louis-Jean Desprez (1781-1784). The tunnel, built by the Romans was 4,800-foot-long, 25-foot-wide and 30-foot-high [Renard, 2020].	36
2-2	Canal du Midi, France [Grand Site Canal du Midi, 2020].	37
2-3	Allegheny Portage Railroad tunnel [National Parks Service, 2022].	38
2-4	Hoosac Tunnel, Massachusetts, 1908 [Burns, 2022].	39
2-5	Mont Cenis tunnel, France [Cottet Dumoulin and Schueler, 2020].	39
2-6	Scheme of boring machine used in the construction of the Mont Cenis tunnel [Routledge, 1903].	40
2-7	Simplon tunnel construction, 1900s [Wonders, 2010].	41
2-8	Wapping-Rotherhithe Tunnel, horseshoe section of 22 ft by 37 ft. London, 1841 [Mediastorehouse, 2019].	42
2-9	Greathead tunneling technique, joining shields and air compression [Diamond and Kassel, 2018].	43
2-10	Holland Tunnel in 1928 [The Port Authority, 2016].	44
2-11	Michigan Central Railway Tunnel (also known as Detroit River Tunnel), 1910. [Gleit, 2016].	44

2-12	Paris Metro, early 20 th century [Archives Photographiques, 1906]. . .	46
2-13	Section of the SR 99 tunnel, built through the cut-and-cover method. Seattle, 2015 [Washington State Department of Transportation, 2020].	46
2-14	Gadhara Aqueduct in Jordan, 90-210 A.D. [Pafnutius, 2023].	48
2-15	Saint Lucia tunnel between Bologna and Florence, 2020 [Formiche, 2020].	49
2-16	Shipworm digging through wood, inspiring the creation of Tunnel Bor- ing Machines [Fickling, 2020].	49
2-17	Model of Wilson Patent Stone Cutting Machine model used in the Hoosac Tunnel construction [Kelley, 2017].	50
2-18	First hard-rock TBM, developed in 1952 for the Oahe Dam construc- tion in the Missouri River [Tunnel Business Magazine, 2017].	51
2-19	Slurry TBM [Ugitech, 2019].	52
2-20	Gripper TBM, where both sets of mechanic jacks can be seen in black (Courtesy of Robins).	53
2-21	Single-shield TBM [Robbins, 2021].	54
2-22	Cross-section of a double-shield TBM [Zhao et al., 2012].	54
2-23	Comparison between different TBM shields and the ground-types they are employed in [Robbins, 2021].	55
2-24	Cross-section of TBM with parts highlighted and identified. In the image we can see the machine’s main digging and thrust components [Ugitech, 2019].	55
2-25	Porto Metro full system map throughout the city of Porto’s metropoli- tan area [Mapa Metro, 2010].	57
2-26	Marques Underground Station (Line D)[Guedes, 2017].	59
2-27	Eurotram used in the Porto Metro system [Guedes, 2017].	59
2-28	Andante Ticketing stations in a Porto Metro station [Guedes, 2017]. .	60

3-1	General lithology of Portugal. In the legend, 1, 2 and 4 are sedimentary formations; 3 represents igneous rocks; 5 shows the intrusive formations; 6 the porphyrys; the continuous line (7) shows the main geologic faults present in the country while the dashed line (in 8) gives the limits of the Iberian Massif [Vieira et al., 2020]).	64
3-2	Schematic image showing the formation process of the Variscan Cordillera [Johnston and Gutierrez-Alonso, 2010]).	65
3-3	Tectonic placement of Portugal. In the image, the white arrows (1 in the legend) represent the movement of coinciding tectonic plates; the continuous (2) and dashed (3) white lines show the known and approximate locations of geologic faults, respectively. Finally the blurred segment (4) between the Iberian Peninsula and African continent shows the region where continental plates collide [Vieira et al., 2020]). . . .	66
3-4	Topographic map of Portugal. Where the darker lines (represented by 1 in the legend) show the currently active geological faults within the territory and the faded lines (2) represent the geologic lines that may conform to active faults [Vieira et al., 2020]).	67
3-5	Porto. Depicted by H. Duncalf and William Henry Toms, English royal envoys sent to the city in 1736 [Arquivo Municipal do Porto, 2022]). . .	68
3-6	Porto's historical city center today [Vieira et al., 2020]).	68
3-7	Partial geomorphological map of Portugal. The city of Porto is located in the bottom-left corner, where the main rivers flowing by the city can be seen. Also notable is that Porto is located well within the Portuguese litoral platform [Vieira et al., 2020].	69
3-8	Topographical map of the Porto region and main geologic faults. Where the main road networks are represented by the red lines and geologic faults in black. The historic city center is shown by the black and white circle, located in the margins of the Douro River [Vieira et al., 2020]).	70

3-9	Main geological subdivisions around the city of Porto. From the map it is clear that the Porto regions is composed mainly of medium grained, two mica granite, named Oporto Granite (represented in light pink). There is also presence of fluvial and lacustrine deposits from the Douro River basin (light green) [Vieira et al., 2020]).	71
3-10	The top map shows Porto’s geomorphology while the bottom represents the city’s relief cross-section. Varying from 40 to 140 meters above sea level, Porto is mostly composed of granitoid formations (represented by the crosses from Pinheiro Manso to Campanhã), followed by metasedimentary formations (slashes) in Parque da Cidade and after Campanhã. Some landfills, metamorphic and superficial formations are also present along the city [Vieira et al., 2020]).	73
3-11	Distribution of Oporto Granite amongst the Douro River valley. The metropolitan area of the city of Porto is indicated in red [Sousa, 2010].	74
3-12	Line C (partial) tunnel section showcasing the location of surveyed borings. The pink lines represent the final tunnel alignment. Red and orange circles show locations of boring holes. Courtesy of Normetro.	76
3-13	Geotechnical Profile Rings 533-610. Where the x axis shows the longitudinal distance and y the altitude (both measured in meters). The distance between two consecutive rings is 1 meter. This complete profile is based on several boring holes (represented in the figure alongside boring logs). Where g1, g2, g3 and g4 are rock-like materials and g5 represents soils. Courtesy of Normetro.	77
3-14	Geotechnical Profile Rings 611-689. Distance and altitude are represented by the x and y axis respectively (both measured in meters). The distance between two consecutive rings is 1 meter. This complete profile is based on several boring holes (represented in the figure alongside boring logs) and other geotechnical investigations. Where g1, g2, g3 and g4 are rock-like materials and g5 represents soils. Courtesy of Normetro.	78

3-15 Geotechnical Profile Rings 690-814. Distance and altitude are represented by the x and y axis respectively (both measured in meters). This complete profile is based on several boring holes (represented in the figure alongside boring logs) and other geotechnical investigations (distance between two consecutive rings is 1 meter). Where g1, g2, g3 and g4 are rock-like materials and g5 represents soils. Courtesy of Normetro.	79
3-16 Geotechnical Profile Rings 815-942. Distance and altitude are represented by the x and y axis respectively (both measured in meters). The distance between two consecutive rings is 1 meter. This complete profile is based on several boring holes (represented in the figure alongside boring logs) and other geotechnical investigations. Where g1, g2, g3 and g4 are rock-like materials and g5 represents soils. Courtesy of Normetro.	80
3-17 Predicted geomechanical conditions (top) versus encountered geomechanical (bottom) conditions for Rings 533-610. Where g1, g2, g3 and g4 are rock-like materials and g5 represents soils. As seen in the image, from Rings 535 to 561 they encountered only soil-like material (g5) different from what was predicted. This pattern is followed by the section between rings 561 and 610, where g3 and g4 sections were different from what was predicted. Courtesy of Normetro.	81
3-18 Predicted geomechanical conditions versus encountered geomechanical conditions for Rings 611-689. Where g1, g2, g3 and g4 are rock-like materials and g5 represents soils. As seen in the image, from Rings 535 to 561 they encountered only soil-like material (g5) different from what was predicted. This pattern is followed by the section between rings 630 and 661, where g3 and g4 sections were different from what was predicted and g2 material was found. Also, from rings 661 to 688 predicted and encountered geology diverged, with soil-like material (g5) more abundant than originally imagined. Courtesy of Normetro.	82

3-19	Predicted geomechanical conditions versus encountered geomechanical conditions for Rings 690-814. Where g1, g2, g3 and g4 are rock-like materials and g5 represents soils. From rings 690 to 745 they encountered unexpected rock-like material (g4). From rings 746 - 814 they found similar patterns to what was predicted but different concentrations, coming accross more rock-like material (g3, g4) than what was expected. Courtesy of Normetro.	83
3-20	Predicted geomechanical conditions versus encountered geomechanical conditions for Rings 815-942. Where g1, g2, g3 and g4 are rock-like materials and g5 represents soils. Expected geology contrasted widely with conditions confronted in the construction process. Soil-like material (g5) was greatly overestimated especially from rings 815 - 850. Location of rock-like ground (g3, g4) was also uncertain and diverged from the encountered geology throughout most of the section. Courtesy of Normetro.	84
3-21	Face mappings and corresponding geologic section: Rings 533-610. Courtesy of Normetro.	85
3-22	Face mappings and corresponding geologic section: Rings 611-689. Courtesy of Normetro.	86
3-23	Face mappings and corresponding geologic section: Rings 690-814. Courtesy of Normetro.	87
3-24	Face mappings and corresponding geologic section: Rings 815-942. Courtesy of Normetro.	88

4-1	Images showing an accident that occurred in the construction of a new metro line in Sao Paulo, Brazil. The accident was caused by unforeseen geological conditions encountered by the TBM (left-hand side) during tunnel construction. A slight course modifications led by adverse ground conditions along the original tunnel line, made the machine’s vibration felt on the surface, collapsing a nearby highway and bursting sewage pipes [Garcia, 2022]).	91
4-2	Graph showing the UN’s prediction on urbanization rates by 2050 [Ritchie and Roser, 2018]).	92
4-3	Graph showing the predicted growth of the Tunnel Boring Machine (TBM) Market [Pasalkar, 2023]).	93
4-4	A computational rendering of the variable density TBM operating in Malaysia [Mass Rapid Transit Corporation, 2013]).	94
4-5	Image of the ATBM being setup in a large public transport infrastructure construction site in Malaysia, 2018 [Byrd, 2016]).	95
4-6	Diagram of the EPBM TBM used during the excavation of the Line C tunnel of the Porto Metro project [Guglielmetti et al., 2008].	102
4-7	Sample data-set for a soil tunnel section (Ring 877). Where W0001-W107 represent different parameters.	102
4-8	Time series plots relating Thrust Force and Cutting Wheel Speed of Rotation for rock and rock-like mixed.	112
4-9	Time series plots relating Thrust Force and Cutting Wheel Speed of Rotation for soil and soil-like mixed.	113
4-10	Time series plots relating Pressure Force Cutting Wheel and Thrust Force for rock and rock-like mixed.	116
4-11	Time series plots relating Pressure Force Cutting Wheel and Thrust Force for soil and soil-like mixed.	117
4-12	Time series plots relating Torque Cutting Wheel and Pressure Force Cutting Wheel for rock and rock-like mixed.	120

4-13	Time series plots relating Torque Cutting Wheel and Pressure Force Cutting Wheel for soil and soil-like mixed.	121
4-14	Time series plots relating Penetration and Torque Screw for rock and rock-like mixed.	124
4-15	Time series plots relating Penetration and Torque Screw for soil and soil-like mixed.	125
4-16	Time series plots relating Penetration and Thrust Force for rock and rock-like mixed.	128
4-17	Time series plots relating Penetration and Thrust Force for soil and soil-like mixed.	129
4-18	Time series plots relating Penetration and Advance Speed for rock and rock-like mixed.	132
4-19	Time series plots relating Penetration and Advance Speed for soil and soil-like mixed.	133
4-20	Time series plots relating Penetration, Actually Excavated Material Flow Belt, Quantity of Excavated Material (Advance) and Quantity of Excavated Material (Total) for rock and rock-like mixed.	136
4-21	Time series plots relating Penetration, Actually Excavated Material Flow Belt, Quantity of Excavated Material (Advance) and Quantity of Excavated Material (Total) for soil and soil-like mixed.	137
4-22	Time series plots relating Actually Excavated Material and Quantity of Excavated Material 1 for rock and rock-like mixed.	140
4-23	Time series plots relating Actually Excavated Material and Quantity of Excavated Material 1 for soil and soil-like mixed.	141
4-24	Time series plots relating Cutting Wheel Speed of Rotation, Cutting Wheel High Pressure and Thrust Pressure for rock and rock-like mixed.	144
4-25	Time series plots relating Cutting Wheel Speed of Rotation, Cutting Wheel High Pressure and Thrust Pressure for soil and soil-like mixed.	145

4-26	Time series plots relating Penetration, Torque Cutting Wheel, Pressure Force Cutting Wheel, Thrust Force, Torque Screw, Actually Excavated Material and Quantity of Excavated Material for rock and rock-like mixed.	148
4-27	Time series plots relating Penetration, Torque Cutting Wheel, Pressure Force Cutting Wheel, Thrust Force, Torque Screw, Actually Excavated Material and Quantity of Excavated Material for soil and soil-like mixed.	149
4-28	Time series plots relating Thrust Pressure and Thrust Pressure Groups A, B, C, D, E, F for rock and rock-like mixed.	152
4-29	Time series plots relating Thrust Pressure and Thrust Pressure Groups A, B, C, D, E, F for soil and soil-like mixed.	153
4-30	Time series plots relating Thrust Pressure Groups A, B, C, D, E, F for rock and rock-like mixed.	156
4-31	Time series plots relating Thrust Pressure Groups A, B, C, D, E, F for soil and soil-like mixed.	157
4-32	Scatter plots and histograms relating Torque Cutting Wheel and Pressure Force Cutting Wheel for rock and rock-like mixed.	160
4-33	Scatter plots and histograms relating Torque Cutting Wheel and Pressure Force Cutting Wheel for soil and soil-like mixed.	161
4-34	Scatter plots and histograms relating Thrust Force and Pressure Force Cutting Wheel for rock and rock-like mixed.	164
4-35	Scatter plots and histograms relating Thrust Force and Pressure Force Cutting Wheel for soil and soil-like mixed.	165
4-36	Scatter plots and histograms relating Penetration and Torque Screw for rock and rock-like mixed.	168
4-37	Scatter plots and histograms relating Penetration and Torque Screw for soil and soil-like mixed.	169
4-38	Scatter plots and histograms relating Penetration and Actually Excavated Material for rock and rock-like mixed.	172

4-39	Scatter plots and histograms relating Penetration and Actually Exca- vated Material for soil and soil-like mixed.	173
4-40	Scatter plots and histograms relating Penetration and Advance Speed for rock and rock-like mixed.	176
4-41	Scatter plots and histograms relating Penetration and Advance Speed for soil and soil-like mixed.	177
4-42	Scatter plots and histograms relating Penetration and Thrust Force for rock and rock-like mixed.	180
4-43	Scatter plots and histograms relating Penetration and Thrust Force for soil and soil-like mixed.	181
4-44	Scatter plots and histograms relating Penetration and Screw Conveyor Speed Measuring for rock and rock-like mixed.	184
4-45	Scatter plots and histograms relating Penetration and Screw Conveyor Speed Measuring for soil and soil-like mixed.	185
4-46	Scatter plots and histograms relating Penetration and Screw Conveyor Pressure for rock and rock-like mixed.	188
4-47	Scatter plots and histograms relating Penetration and Screw Conveyor Pressure for soil and soil-like mixed.	189
4-48	Scatter plots and histograms relating Penetration and Earth Pressure 1 for rock and rock-like mixed.	192
4-49	Scatter plots and histograms relating Penetration and Earth Pressure 1 for soil and soil-like mixed.	193
4-50	Scatter plots and histograms relating Penetration and Quantity Exca- vated Material 1 (Total) for rock and rock-like mixed.	196
4-51	Scatter plots and histograms relating Penetration and Quantity Exca- vated Material 1 (Total) for soil and soil-like mixed.	197
4-52	Scatter plots and histograms relating Penetration and Quantity Exca- vated Material 2 (Advance) for rock and rock-like mixed.	200
4-53	Scatter plots and histograms relating Penetration and Quantity Exca- vated Material 2 (Advance) for soil and soil-like mixed.	201

4-54	Scatter plots and histograms relating Penetration and Quantity Excavated Material 2 (Total) for rock and rock-like mixed.	204
4-55	Scatter plots and histograms relating Penetration and Quantity Excavated Material 2 (Total) for soil and soil-like mixed.	205
4-56	Scatter plots and histograms relating Advance Speed and Screw Conveyor Speed Measuring for rock and rock-like mixed.	208
4-57	Scatter plots and histograms relating Advance Speed and Screw Conveyor Speed Measuring for soil and soil-like mixed.	209
4-58	Scatter plots and histograms relating Thrust Force and Cutting Wheel Speed of Rotation for rock and rock-like mixed.	212
4-59	Scatter plots and histograms relating Thrust Force and Cutting Wheel Speed of Rotation for soil and soil-like mixed.	213
5-1	Parameter comparison scatterplots for Penetration x Torque Screw for high-confidence labels.	227
5-2	Parameter comparison scatterplots for Penetration x Screw Conveyor Speed Measuring for high-confidence labels.	228
5-3	Parameter comparison scatterplots for Penetration x Earth Pressure 1 for high-confidence labels.	229
5-4	Parameter comparison scatterplots for Advance Speed x Screw Conveyor Speed Measuring for high-confidence labels.	230
5-5	Parameter comparison scatterplots for Thrust Force x Cutting Wheel Speed of Rotation for high-confidence labels.	231
5-6	Parameter comparison scatterplots for Penetration x Torque Screw for low-confidence labels.	233
5-7	Parameter comparison scatterplots for Penetration x Screw Conveyor Speed Measuring for low-confidence labels.	234
5-8	Parameter comparison scatterplots for Penetration x Earth Pressure 1 for low-confidence labels.	235

5-9	Parameter comparison scatterplots for Advance Speed x Screw Conveyor Speed Measuring for low-confidence labels.	236
5-10	Parameter comparison scatterplots for Thrust Force x Cutting Wheel Speed of Rotation for low-confidence labels.	237
6-1	Picture of MMC Gamuda’s Tunneling Centralized Command and Control Center [Berhad, 2020]).	251
6-2	Expected Tunnel Boring Machine market growth in the decade from 2020 - 2030 [Data Bridge Market Research, 2021]).	252
6-3	Predicted market growth of tunnel construction in the decade from 2018 - 2028 [Business Research Insights, 2021]).	253
6-4	MMC Gamuda’s A-TBM on the site of the Klang Valley Mass Rapid Transit (KVMRT), using Herrenknecht hardware [Construction, 2021]).	254
6-5	Example of a Robbins TBM [Robbins, 2021]).	255
6-6	Virtual depiction of the CREG’s autonomous tunnel boring machine [Chan, 2022]).	256
6-7	MMC Gamuda’s analytics dashboard for its proprietary A-TBM system [Byrd, 2016]).	261

List of Tables

3.1	Location of face mappings (in meters) along Rings 533 - 942.	75
4.1	General classification of TBM-output data.	93
4.2	Machine Learning classification and examples [Dasgupta and Nath, 2016].	96
4.3	Papers on use of Machine Learning (ML) algorithms for geology prediction using TBM-generated data.	99
4.4	Time-series plots.	104
4.5	Scatter plots.	104
4.6	Rings analyzed in the present study, from Ring 461 to 1310.	109
4.7	Terminology used to describe characteristics of data-points.	159
5.1	High Confidence Labels.	225
5.2	Low Confidence Labels.	226
5.3	Comparison between ground class labels generated by the Confidence Learning Model and Geologic Profiles.	238
5.4	Comparison between ground class labels generated by the Scattergrams and Geologic Profiles.	239
5.5	Comparison between ground class labels generated by the Scattergrams and Geologic Profiles.	239
6.2	Cost estimation for the implementation components of the use autonomous tunnel boring machine systems, interpreted from the following sources [Janbaz, 2017, Ferrein et al., 2012, Berhad, 2019].	265

This page intentionally left blank.

Chapter 1

Introduction

1.1 Motivation and Objectives

Tunnel boring machines (TBM) are frequently used in tunnel construction. Such mechanized tunneling has been demonstrated to be a safer, more environmentally friendly, and effective alternative to traditional excavation methods such as blasting [Jung et al., 2019, Sun et al., 2018]. As the use of these machines becomes widespread, foreseeing tunnel boring machine performance in many ground conditions has been a continual research focus within geotechnical engineering [Xu et al., 2019]. Prediction of TBM performance, especially penetration and advance rates, can greatly reduce risks and costs of the operation [Sun et al., 2018, Xu et al., 2019, Maidl et al., 2013].

As the mining and tunnel markets are projected to almost double in the decade from 2020-2030, and the use of TBMs becomes ubiquitous, it is especially important to increase safety and efficiency [Allied Market Research, 2022]. As geological risks are the most prominent in TBM operations, it is critical to develop tools to predict ground conditions [Jung et al., 2019].

As tunneling automation continues to advance, Artificial Intelligence (AI) and Machine Learning (ML) algorithms have become increasingly prevalent for predicting geology ahead of the tunnel face. However, while several approaches have been suggested, there is still limited evidence to support the real-time implementation of these technologies for ground condition prediction during TBM tunneling projects.

In this regard, a review of current research using AI/ML techniques for predictive applications in TBM operations will be attempted. The review will assess the feasibility of applying these modelling approaches to TBM tunneling projects and the potential for real-time ground condition prediction.

The need for more fundamental research on the parameter-data output by Tunnel Boring Machines (TBMs) and the relations between machine parameters, as well as how they may relate to surrounding geology have not been widely discussed. In this sense, the current thesis aims to propose an exploratory look into these intricate relationships and their correlation to ground conditions. Erharter (2021) comments on how, in tunneling, predicting rockmass conditions ahead of the face is crucial for taking appropriate countermeasures, and that although machine learning (ML) models have been used to forecast geology, but such projections are mostly delayed and slightly altered versions of input data, lacking true predictive value, which reinforces the need for further research in the field [Erharter and Marcher, 2021].

Tunnel boring machines (TBMs) advance in a step-by-step manner, which is closely related to the progress of the main jacks. This step-by-step advancement is often linked to the installation of pre-fabricated concrete liner rings. The fact that this happens in steps provides valuable information for predicting and accessing the geology in a systematic manner. It is therefore logical to try to assess and predict geologic conditions related to the section defined by these rings, and the term "ring" will be used throughout this thesis to refer to these sections. Figures 1-1 and 1-2 illustrate the TBM with its main jacks and a sample geologic profile, respectively. The geologic profile is divided into rings, highlighting the importance of this concept in the thesis.

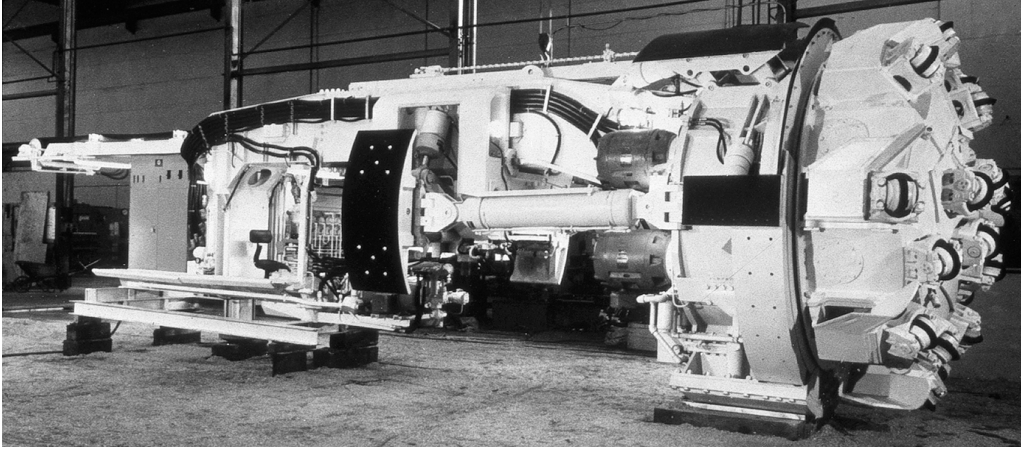


Figure 1-1: The image shows the Gripper TBM, with both sets of mechanical jacks visible in black, as provided by Robins.

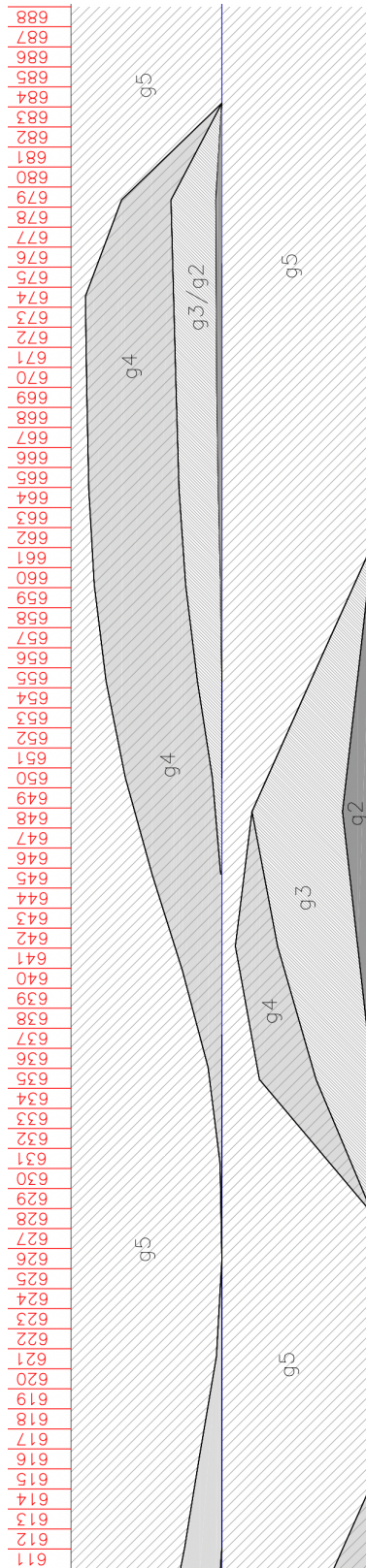


Figure 1-2: Sample geologic section (between rings 611-689) showing the division into 1 meter sections, or rings [Metro do Porto, 2010b].

The methodology presented aims to assist and increase reliability and the validity of AI/ML models for geology prediction in Tunnel Boring Machine (TBM) tunneling. By surveying several TBM parameters and their output graphical relations, as well as of four main ground classes: rock, soil, rock-like mixed and soil-like mixed. Out of the 26 parameter combinations evaluated, for all evaluated rings, pairwise distinctions that were found to present the most clear classificatory patterns were identified and listed. An example of the proposed methodology combining AI/ML models to graphical correlations is also presented.

Artificial intelligence (AI) has increasingly permeated and advanced several fields of study, especially within engineering. As efforts to automate tunneling construction grow in importance and demand, the use of AI will be ever more common. There have been concerns that the more general use of AI/ML tools may result in instances of confirmation bias ¹. Thus, the systematic approach proposed seeks to assist in validating current AI/ML approaches.

To develop my methodology for classifying tunnel rings by analyzing TBM-data in time-series and scatter plots, to establish correlations between geological conditions and ground classes such as rock, soil, rock-like mixed and soil-like mixed. This will improve ground condition predictions. The study also proposes a techno-economic assessment (TEA) to evaluate the effort of AI/ML modeling on cost, schedule, and safety of tunneling projects. Recommendations for future use of AI/ML modeling in tunneling projects.

1.2 Porto Metro Project

The proposed AI/ML methods will be applied to the Porto Metro Project as a case study. Porto Metro or *Metrô do Porto* in Portuguese, is the metro system in the city of Porto (2nd largest city in Portugal) [Metro do Porto, 2010b]. Inaugurated in 2002, it operates throughout the historical city center, reaching the suburbs and

¹The tendency to search for, interpret and record information to confirm preexisting conceptions and hypothesis, while devaluing contradictory evidence [Menardi and Torelli, 2014].

outskirts of the city [Metro do Porto, 2010a]. With 6 lines (lettered from A-F), 82 stations and extending over 67 kilometers (approximately 42 miles), the system serves over 80,000 people every day [Metro do Porto, 2010b].

Functioning both under and above ground, Porto Metro has 7.7 kilometers (4.8 miles) of tunnels over 14 stations [Metro do Porto, 2010b]. Built in a heavily populated urban area, that is also a UNESCO World Heritage Site, the construction of the metro system was a difficult and ambitious endeavor, especially in regard to the construction of tunnels and underground stations [Metro do Porto, 2010a]. The present thesis will look more closely at the construction of the C Line (Green) of the Porto Metro System, accounting for 24 stations, from ISMAI to Campanha (see Figure 1-1), the underground line has little over one mile of tunnels. The figure below Figure 1-3 shows all of the lines and station in Porto Metro system currently.

1.3 Thesis Outline

The present introductory chapter provided a brief overview of the study's background, motivation, research objectives. It also introduced the Porto Metro project and the specific tunneling section that will be evaluated, setting the context for the following chapters. Chapter 2 will provide an extensive bibliographical review on the history of tunneling, the Tunnel Boring Machine (TBM) and the Porto Metro project. The chapter aims to provide a comprehensive understanding of the historical and technical background behind tunneling and the analyzed project, contextualizing the subsequent chapters.

Chapter 3 will focus on the geological and geotechnical conditions in Porto, Portugal. Site investigation methods and results are discussed, as well as the ground classification system used for the project (distinguishing between geomechanical groups numbered from g1-g6, aiming to classify rings between rock, soil and mixed). The chapter will provide a detailed understanding of the geological history of the city of Porto, its most relevant geotechnical aspects and other contributing factors that influenced the tunnel built for Line C of the Porto Metro System. Chapter 4 will present



Figure 1-3: Map of Porto Metro [Metro do Porto, 2010b].

the methodology used to evaluate parameter pairs most relevant for the classification of rings and the relevant pairwise comparisons for finding graphical correlations between TBM parameters that can be potentially translated to ground class predictions. The chapter will then discuss the results obtained from this analysis. Chapter 5 will present an example of the proposed methodology, using scattergrams to identify geologic ground classes and, in parallel, to validate ground-class labels (rock, soil, rock-like mixed and soil-like mixed) obtained from a Confidence Learning ML model. Chapter 6 showcases a techno-economic assessment of the current use of AI/ML modeling for predicting geological conditions ahead of the tunnel face. The chapter will evaluate the effectiveness and efficiency of the proposed technology and conduct a cost-benefit analysis of implementing the technology to future TBM-based tunnel projects. Chapter 7 will present the conclusions and provide suggestions for future research in the field. The chapter will summarize the key findings and contributions of the study, discuss their implications for the Porto Metro project and tunneling in general, and suggest areas for further research and development.

Chapter 2

Background

2.1 Tunneling

2.1.1 Historical Aspects

Tunneling has its roots in prehistoric times. It is hypothesized that tunnels were first used for enlarging caves used as human shelter and for water transport purposes [Caricola et al., 2020]. For the ancient world and its prolific civilizations, tunnels were an indispensable engineering development that contributed to the creation of empires [Goel et al., 2012]. From the Babylonians creating tunnels as early as 2200 BC to the Egyptians, ancient civilizations used techniques to develop tunneling efforts, redirecting the flow of rivers, creating aqueducts, new irrigation systems, passageways, temples and flooding infrastructure [Balasubramanian, 2014]. With the expansion of both the Greek and Roman empires, tunnels became an essential structure for development [Castellani and Dragoni, 1997]. From the use of aqueducts to drain lakes and marshland to 4,000 feet long road tunnels, tunnels became the backbone of the empires' expansion throughout Europe. Below is an image (Figure 2-1) of the Pausilippo tunnel that connected Naples and Pozzuoli, built in 36 B.C [Munfakh, 2003].

By then, tunnels were mainly constructed within rock, that was broken off using methods like fire quenching, where the rock was heated and subsequently cooled then pieces could be more easily removed [Oleson, 2008]. These structures were prefer-



Figure 2-1: Pausilippo tunnel as depicted by Louis-Jean Desprez (1781-1784). The tunnel, built by the Romans was 4,800-foot-long, 25-foot-wide and 30-foot-high [Renard, 2020].

ententially built in materials like limestone and sandstone [Hodge, 1992, Pollio, 2011]. Throughout the Middle Ages, tunneling was mainly used for mining and military purposes, returning to its uses for transportation and basic infrastructure only in the 17th century [Lane, 2019]. Europe restarted building large scale tunneling projects to address its cities growing transportation demands. By 1681, France had finished building the *Canal du Midi* (shown in Figure 2-2), a 515 feet long tunnel with a cross section of 22 by 27 feet, which saw the first extensive use of explosives for tunnel

construction [Mukerji, 2021].



Figure 2-2: Canal du Midi, France [Grand Site Canal du Midi, 2020].

The following two centuries saw the rise of tunnel construction both in Europe and North America, initially with canal tunnels, as most of the logistical operations were conducted through waterways and later for rail [Lane, 2019]. By the mid 1800's the establishment of railroads as the main form of transport for people and goods was well underway, and tunnels became commonplace as tracks disseminated in quickly industrializing nations [Curley et al., 2011]. The Allegheny Portage Railroad, built in 1833, saw the implementation of the first tunnel for rail in the US [Harper, 2011] (see Figure 2-3).

As railroads continued expanding across the United States and Europe, ambitious tunneling projects, that introduced new technologies and revolutionized the industry were under way [Curley et al., 2011]. In the USA, the Hoosac Tunnel, connecting Boston to Albany, was completed in 1876 after 21 years of construction [Curley et al., 2011, Brierley, 1976]. The project introduced new methods of tunneling through hard rock, especially with the use of explosives and power drills [Brierley, 1976, Kirkland, 1947]. Around the same time, even more ambitious projects



Figure 2-3: Allegheny Portage Railroad tunnel [National Parks Service, 2022].

were being executed in the Alps in Europe. The Mont Cenis Tunnel, a 14 year long endeavor, also introduced new methods that would contribute to the advancement of the industry [O'Reilly, 2002]. Most notable were the use of rail-mounted drill carriages, air compressors, air drills and the use of fully catered workers camps, complete with housing, schools, hospitals, recreation centers and repair shops [O'Reilly, 2002, Dal Piazz and Argentieri, 2021]. As also experienced in historical endeavors (Romans, Babylonians, etc.), tunnel ventilation became an increasingly pernicious issue [Amato et al., 2000]. Thus, the development of forced air systems [Curley et al., 2011]. Below, Figures 2-4, 2-5 and 2-6 show the Hoosac and Mont Cenis tunnels respectively, and a schematic of the boring machine used in the Alps.

As transportation through the Alps continued to be an important priority for politicians and engineers in Europe, the Saint Gotthard tunnel, built from 1872 to 1882, continued the endeavor of expanding the Alpine railroads [West, 2005], followed by Simplon (1898-1906) and *Lötschberg* (1906-1911) tunnels [Ring, 2011]. Enduring challenging conditions, such as high *in-situ* stresses and weak material (gypsum and schist), swelling, incomplete geological surveying and accidents, the tun-



Figure 2-4: Hoosac Tunnel, Massachusetts, 1908 [Burns, 2022].



Figure 2-5: Mont Cenis tunnel, France [Cottet Dumoulin and Schueler, 2020].

nels also brought innovations like compressed-air locomotives and the development of better geological and geotechnical surveying methods [Dal Piaz and Argentieri, 2021,

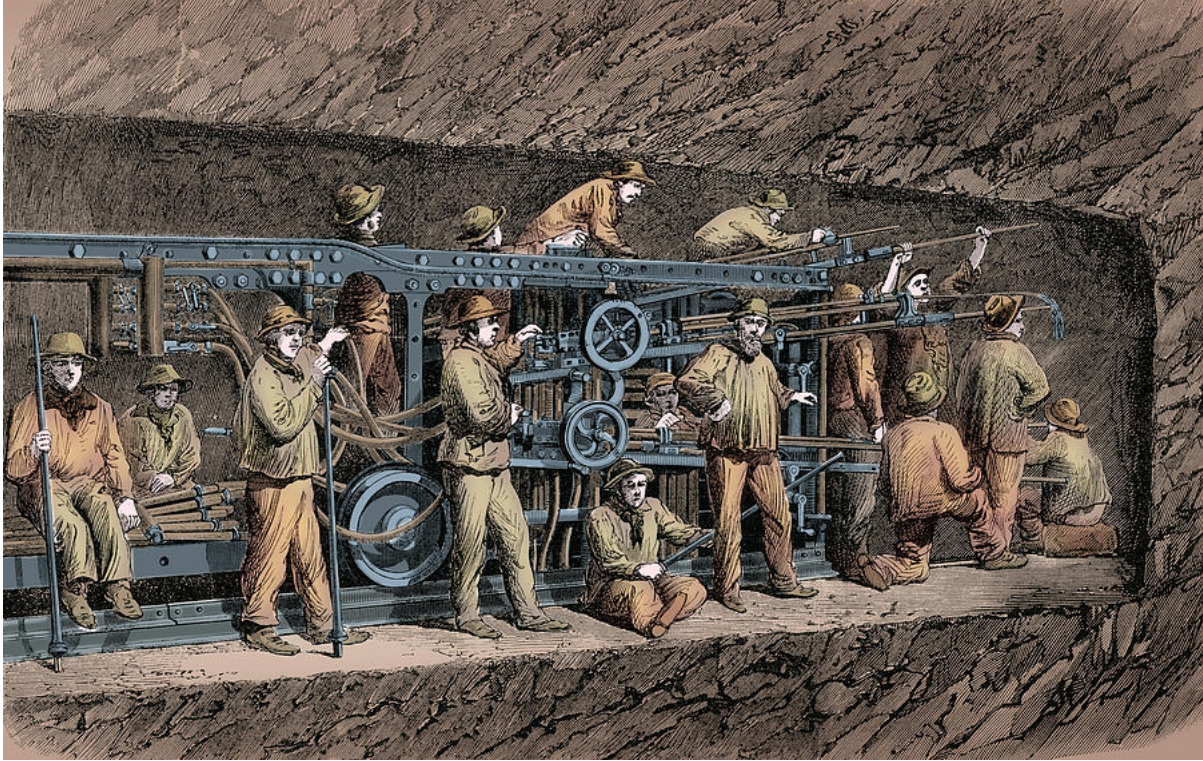


Figure 2-6: Scheme of boring machine used in the construction of the Mont Cenis tunnel [Routledge, 1903].

Gradenwitz, 1913]. Below is an image on the Simplon Tunnel while under construction (Figure 2-7).

One of the most important and transformative contributions of tunneling was underwater construction [Beaver, 1972]. Considered impossible for centuries, boring under riverbeds only became a reality in 1825 with the construction of the Wapping-Rotherhithe Tunnel [Long, 2014]. The tunnel used novel technology (development of the protective shield), envisioned by the French-British engineer Marc Brunel [Mathewson and Kentley, 2006, Place and Cox, 2008]. Wapping-Rotherhithe was built through the clayey material that composed the Thames riverbed, using a horseshoe sections and brick lining [Mathewson and Kentley, 2006]. The tunnel was completed in 1841 after countless mishaps and issues with funding, and delivered the world's first subaqueous tunnel, 1,200 feet long [Mathewson and Kentley, 2006, Long, 2014]. An image of the Wapping-Rotherhithe Tunnel can be seen below (Figure 2-8).



Figure 2-7: Simplon tunnel construction, 1900s [Wonders, 2010].

After the success of the first underwater tunnel, many more followed in the second half of the 19th century [Lane, 2019]. By 1869 a second tunnel was completed under the Thames, a small pedestrian tunnel that introduced circular shield boring (Brunel-Barlow shield) and the use of iron as lining material [Roach and Brunel, 1998]. In 1880, the first tunnel to be built under the Hudson River started [Spielmann, 1880]. They attempted to build using the Brunel-Barlow shield and combining air compression techniques, however, it failed and killed more than 20 workers after less than two thousand feet had been built [Hansen, 2010]. Six years later, London achieved the incredible feat of constructing an underwater tunnel more than seven miles long, using the same technique, for the city's subway system, without losing any lives [Wolmar, 2009]. Combining circular shields with air compression was refined and became ubiquitous in subaqueous tunnels throughout most for the 1900's. This technique, known as the Greathead shield is represented below (Figure 2-9).

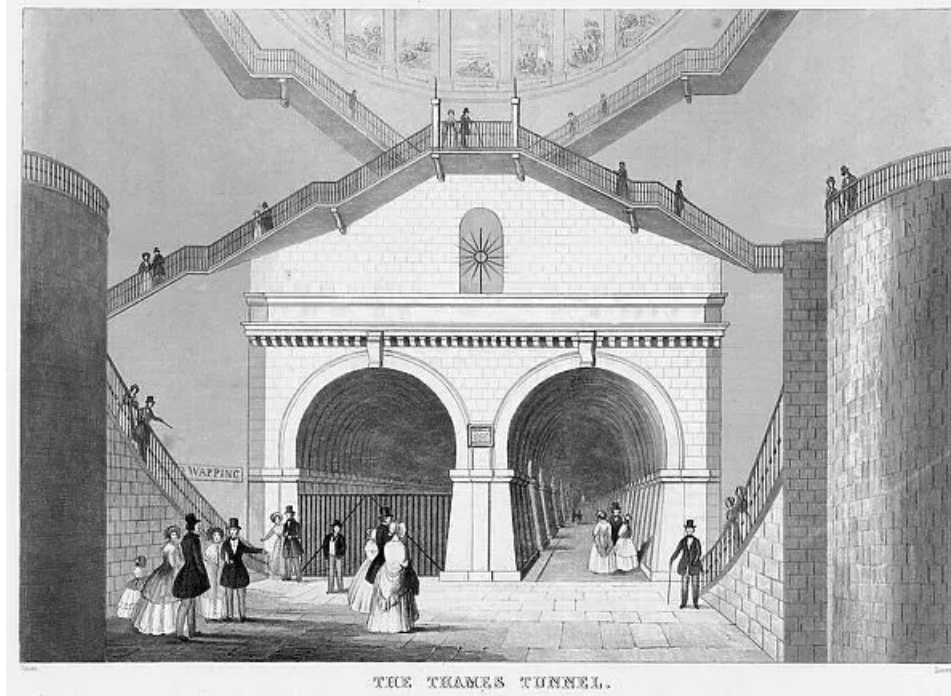


Figure 2-8: Wapping-Rotherhithe Tunnel, horseshoe section of 22 ft by 37 ft. London, 1841 [Mediastorehouse, 2019].

As cities expanded in Europe and North America, demand for more robust transportation systems surged [Rodrigue, 2020]. As cars became a synonym of city life, they introduced harmful gases that prompted better ventilation systems in tunnels [Kolymbas, 2005, Lewis, 2013]. As the first vehicular tunnel was built under the Hudson river in New York City in 1927, engineers struggled to resolve the ventilation issue [Fein, 2012]. Clifford Holland, an American civil engineer involved in the project, resolved the matter with the introduction of large-capacity industrial fans placed at each end of the tunnel [Fein, 2012, Gillespie, 2011]. The forced-air system substantially improved ventilation and served as an important case for similar subsequent projects, such as the tunnel in Queens and the Lincoln tunnel, as well as the Sumner and Callahan tunnels built in Boston [Gillespie, 2011]. To this day the Holland tunnel is a crucial part of New York City's infrastructure, transporting more than 35 million people annually [Cuny University, 2021]. Figure 2-10 shows the Holland Tunnel in its first operating year, when more than 8 million vehicles travelled through it [The Port Authority, 2016].

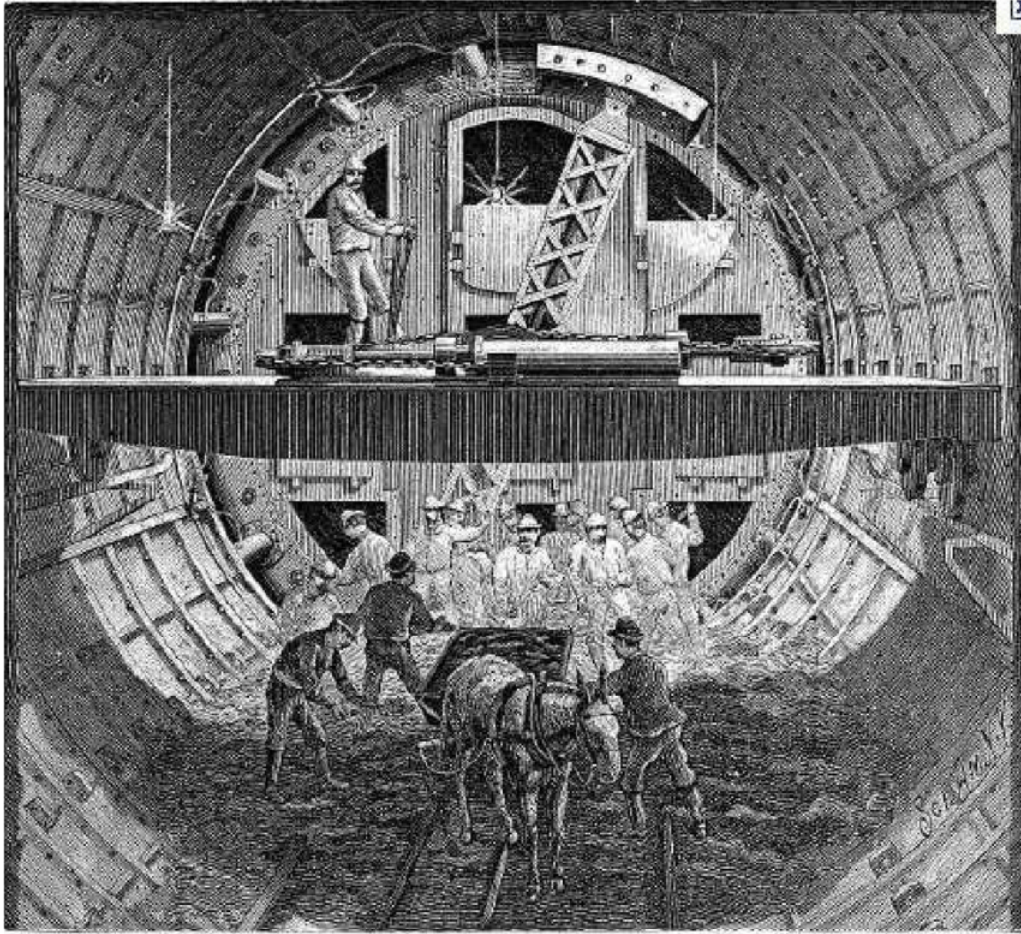


Figure 2-9: Greathead tunneling technique, joining shields and air compression [Diamond and Kassel, 2018].

Currently, underwater tunnels are built mostly using immersed tube construction, where prefabricated concrete or steel sections are placed and subsequently merged to previous sections, having the water pumped out [Grantz, 1997, Shaw, 2022]. This method, developed to build the Michigan Central Railway Tunnel (1910) (Figure 2-11), is deemed safer and more cost effective than the aforementioned shield and air compression construction [Godfrey, 1910, Gleit, 2016].

2.1.2 Tunnel Construction Methods

Tunnels are a distinct and essential type of infrastructure in modern society. Unlike most engineering structures, tunnels are commonly built in natural materials that have no controlled properties [Diamond and Kassel, 2018]. Therefore, knowledge



Figure 2-10: Holland Tunnel in 1928 [The Port Authority, 2016].



Figure 2-11: Michigan Central Railway Tunnel (also known as Detroit River Tunnel), 1910. [Gleit, 2016].

of geological conditions are crucial throughout the building process [Kolymbas, 2005]. Empirical verification and preliminary site surveys (bore hole coring and other on-site and laboratory testing) are insufficient to determine the underlying geological makeup that will be distressed by construction [Lane, 2019, Sowers and Royster, 1978].

Successful tunnel construction is contingent on the experience and engineering judgement of project engineers and geologists, machine-operators, miners, and construction workers [Goel et al., 2012]. Therefore, there is significant interest in advancing tunneling construction through increased automation [Chen et al., 2018]. With mining and drilling operations expected to increase by 4% (year on year) by 2030, efforts to improve safety and efficiency are paramount [Allied Market Research, 2022].

From soft clay to hard rock, tunnels are dug in a diverse range of materials [Goel et al., 2012, Beaver, 1972]. The method of construction is directly determined both by site and project conditions [Lane, 2019, Beaver, 1972]. Aspects like geological makeup and groundwater conditions as well as tunnel shape, depth, diameter, length, tunnel location and other logistical and safety concerns need to be considered in the project [Goel et al., 2012, Beaver, 1972]. Tunnel construction can be divided into three basic methods: cut-and-cover, tunnel boring and immersed [Balasubramanian, 2014, Shaw, 2022].

The cut-and-cover method, one of the most traditional and oldest tunneling methods, is used for shallow tunnels (commonly 10-12 meters deep (30-40 ft) and usually not exceeding 40 meters (130 ft) from the surface), basically built as a trench [Goel et al., 2012, Balasubramanian, 2014]. Although straightforward, the cut-and-cover method generates considerable surface disturbance, and can thus is only implemented in specific conditions [Diamond and Kassel, 2018, Balasubramanian, 2014, Beaver, 1972]. This method is mainly used for underpasses (both pedestrian and rail), some sections of mined tunnels, metro stations and utility tunnels [Beaver, 1972, Goel et al., 2012]. Below, figures 2-12 and 2-13 show examples of the construction of the Paris metro system and a modern tunnel being constructed through the cut-and-cover method.

Bored tunnels, now usually built with the use of Tunnel Boring Machines (TBMs),



Figure 2-12: Paris Metro, early 20th century [Archives Photographiques, 1906].



Figure 2-13: Section of the SR 99 tunnel, built through the cut-and-cover method. Seattle, 2015 [Washington State Department of Transportation, 2020].

are usually used for deep structures [Zheng et al., 2016]. Significantly automating the tunneling process, increasing productivity while reducing costs, TBMs are widely used in large infrastructural projects, especially transportation (metro systems and

stations) [Ishii, 2017]. Being capable of excavating through most materials, from hard rock to sand and soils, TBMs have been adopted for tunnel boring worldwide [Zheng et al., 2016]. From diameters of up to 16 meters (52 ft) wide, they have replaced traditional drilling and blasting methods of tunnel construction in rock and "hand mining" in soils [Bennett et al., 1985]. As the world has become increasingly urban in the past century, demand for tunneling methods that are both efficient, resilient and minimally disruptive, grew [Beaver, 1972, Chester et al., 2019]. With the TBM considered a significant technological advancement to that aim [Beaver, 1972].

Historically the most ancient type of tunnel construction, boring has been performed since prehistoric times [De Feo et al., 2014]. With all major civilizations from the Babylonians to the Romans developing technology to build underground structures, boring has been an important landmark of human civilizational development [De Feo et al., 2014]. Figure 2-14 shows an ancient Persian tunnel dated from 700 B.C.E. Today, tunnel boring is done *in locus* without removing material above the tunnel (in contrast with the cut-and-cover method) [Crighton et al., 1992]. Usually constructed using a u-shaped (horseshoe) cross-section, this type of tunnel uses novel support systems like prefabricated concrete rings, shotcrete, etc., and can be built systematically without much disruption to the surface [Crighton et al., 1992]. Below, figure 2-15 shows a modern tunnel being constructed through the use of a Tunnel Boring Machine (TBM).

2.2 Tunnel Boring Machines (TBM)

2.2.1 Historical Aspects

The idea of Tunnel Boring Machines began with the French-British engineer Isambard Brunel, who invented the first Tunneling Shield (1818) [Roach and Brunel, 1998]. It is believed that Brunel came up with the idea while observing a ship-worm (*Teredo navalis*), a marine bivalve mollusc that feeds on plant-based materials, burrowing itself within the wooden structures of ships, creating immense tunnels (see Figure



Figure 2-14: Gadhara Aqueduct in Jordan, 90-210 A.D. [Pafnutius, 2023].

2-16) [Chapman et al., 2017, Diamond and Kassel, 2018]. He particularly noted that the animal's morphology, especially their shells, protected their mouths and softer tissue while pushing through timber creating long holes [Mathewson and Kentley, 2006]. Brunel thought to emulate the animal by building a machine that would similarly be able to tunnel through soft soil, in a contemporary case of biomimicry¹.

Although Brunel built the first soft soil shield boring machine (known as the Brunel Shield), going through hard rock was still not possible through mechanized methods [Maidl et al., 2008]. It was only in 1851, more than 35 years later, that the Wilson Patent Stone Cutting Machine was developed (see a model of it in Figure 2-17), an instrument that could tunnel through hard rock [Maidl et al., 2008]. A steam

¹The imitation of natural biological designs or processes in engineering or invention [Merriam-Webster,].



Figure 2-15: Saint Lucia tunnel between Bologna and Florence, 2020 [Formiche, 2020].



Figure 2-16: Shipworm digging through wood, inspiring the creation of Tunnel Boring Machines [Fickling, 2020].

powered engine would go through rock using roller cutters, similar to modern-day Tunnel Boring Machines (TBMs) [Maidl et al., 2008].



Figure 2-17: Model of Wilson Patent Stone Cutting Machine model used in the Hoosac Tunnel construction [Kelley, 2017].

For more than a century after little progress was made, as creating new TBM technology proved highly cost-intensive and technically complex, and tunneling through rock was widely carried out using explosives in the well-known drilling and blasting procedure [Chapman et al., 2017]. Only in the 1950s in the construction project of the Oahe Dam in South Dakota, U.S.A., engineers Jerome Ackerman, James S. Robbins and F. K. Mittry (project contractor) came up with the first designs for what would become the modern TBM [Chappell and Parkin, 2004]. Designing the machine to have frontal cutterheads organized in rows and disc cutters that were successfully used to dig through shale rock [Maidl et al., 2013]. These two main components, a frontal rotating cutterhead and a circular protective shield where the tunnel structure would be supported are the main concepts that developed modern-day TBMs (see Figure 2-18 [Maidl et al., 2013]).

Throughout the 20th century the development of more sophisticated tunnel boring machine technology ensued, still based on the two main concepts employed by

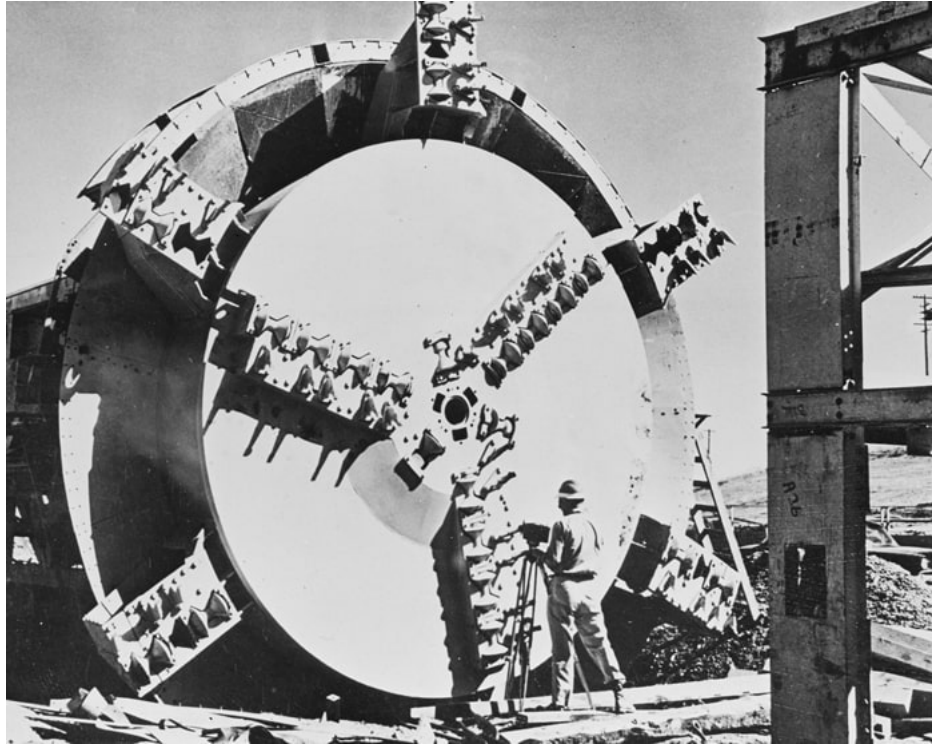


Figure 2-18: First hard-rock TBM, developed in 1952 for the Oahe Dam construction in the Missouri River [Tunnel Business Magazine, 2017].

Ackerman, Robbins and Mittry (cutterhead and shield) [Chappell and Parkin, 2004]. These advancements saw the beginning of diverse machinery designs that were made to cut through specific types of rock and soil, where variations in design allowed for increased productivity and safety in worksites [Chapman et al., 2017]. Following, the main types of TBM designs will be discussed.

2.2.2 Tunnel Boring Machine (TBM) Designs

The "Mittry Mole" as the first TBM became known was absolutely successful, tunneling machines became more available and frequently adopted around the world. Created to automate tunnel construction, TBMs become known as the best, most cost effective and safest way to construct underground structures [Zlatanovic, 2022]. As urbanization flourished, especially after World War 2, tunnels became an important way to add much needed infrastructure to growing cities [Railssystem, 2018]. To cite a few different designs we have the Gripper TBM, Single and Double-Shield TBMs,

Earth-Pressure Machines, Slurry TBM amongst others [Railsystem, 2018].

Different Tunnel Boring Machine designs were developed to address challenges of specific ground conditions. For instance, soft-soil TBMs like earth-pressure balanced machines and bentonite slurry TBMs contain a pressurized cavity in their front shields that allows them to dig through ground underneath the water table [Mair and Taylor, 1997]. Although still facing difficulties, these modified TBMs are still favored over conventional pressurized air and lock/decompression chambers digging methods, that were both more dangerous for workers and moved at a much slower pace [Zhao et al., 2012]. Below is an image depicting a Slurry TBM (Figure 2-19).



Figure 2-19: Slurry TBM [Ugitech, 2019].

The Gripper TBM as its name suggests, is used to tunnel through hard rock [Herrenknecht, 2021]. The TBM advances by gripping the rock surface through the use of 2 main hydraulic jack systems, where one fixes the TBM against the rock surface and the second securing the machine's mobile section (see Figure 2-20) [Herrenknecht, 2021]. In tunneling through hard rock, both the Gripper and shielded

or other open-type TBMs may be used [Maidl et al., 2008]. They all use distinct disc cutters (placed in the TBM cutter head), which create a powerful compressive force to fracture the rock [Maidl et al., 2013]. With open-type TBMs the lack of shield makes room for the machine to support itself on surrounding rock, making it useful for hard rock tunneling [Ugitech, 2019].

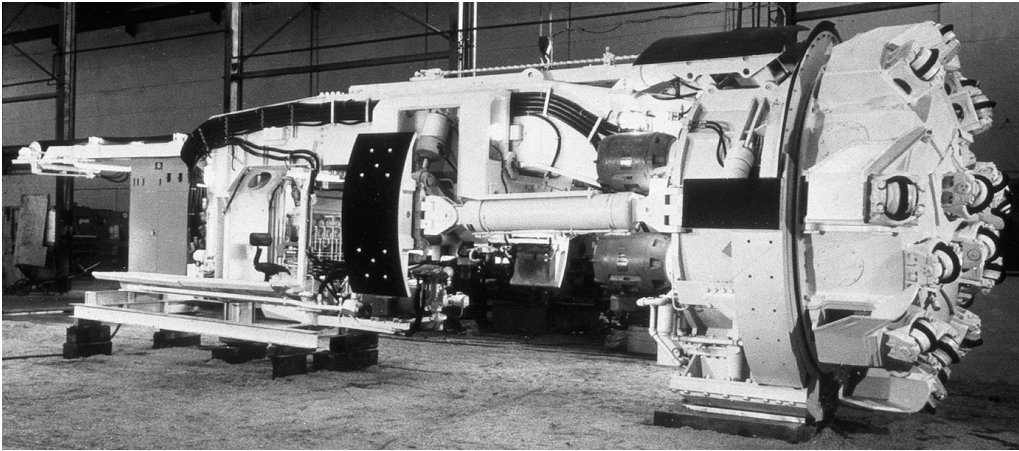


Figure 2-20: Gripper TBM, where both sets of mechanic jacks can be seen in black (Courtesy of Robins).

With single shield TBMs the machine uses thrust force (through modified cylinders) to move forward through the tunnel face (see Figure 2-21). It is used for tunneling through soft ground as it uses each installed concrete ring as support for digging through the next segment [Robbins, 2021]. Double shield TBMs (Figure 2-22) operate similarly to single shield TBMs (using thrust cylinders) but have a retractable additional front shield that aides and extends the reach of the shield-face cutter-heads [Stack, 1995]. They also operate in two forms, gripping tunnel walls when the ground is stable and using thrust against the liner to tunnel through less stable ground [Stack, 1995].

All Tunnel Boring Machines have support decks extending behind the tunnel-face, trailing through completed segments of the project [Chapman et al., 1992]. These back-up systems usually contain long conveyor belts for muck removal, slurry pipelines for softer soils, alongside central control rooms and places for electrical systems management, dust removal and ventilation, TBMs carry diverse sensors and measuring systems that record thrust force, weight and volume of excavated material, pressure



Figure 2-21: Single-shield TBM [Robbins, 2021].

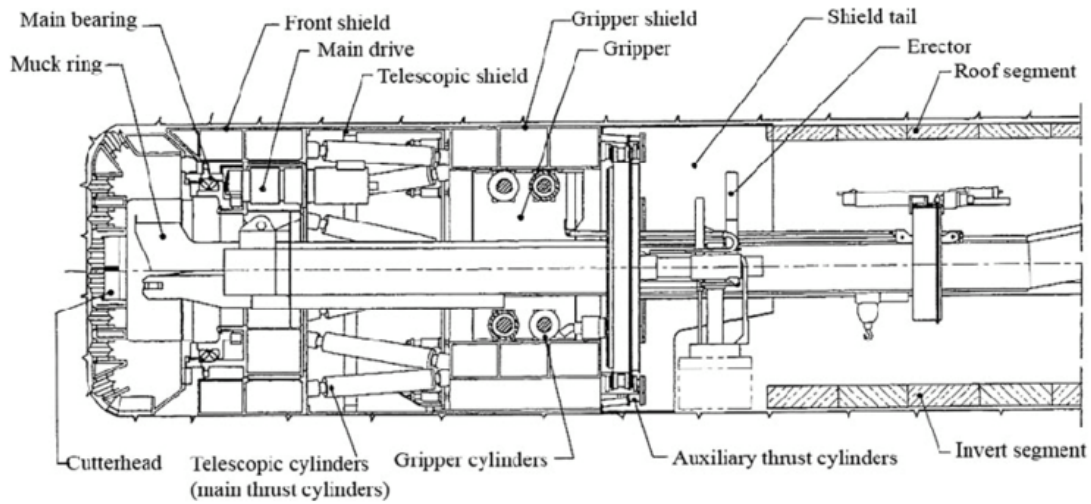


Figure 2-22: Cross-section of a double-shield TBM [Zhao et al., 2012].

and a multitude of other parameters [Chapman et al., 1992, Stack, 1995]. Figure 2-23 below compares various TBM designs. And the following image (Figure 2-24) shows a cross section of a TBM with its main components.

2.3 Porto Metro

The Porto Metro, a component of the mass transport system in the city of Porto

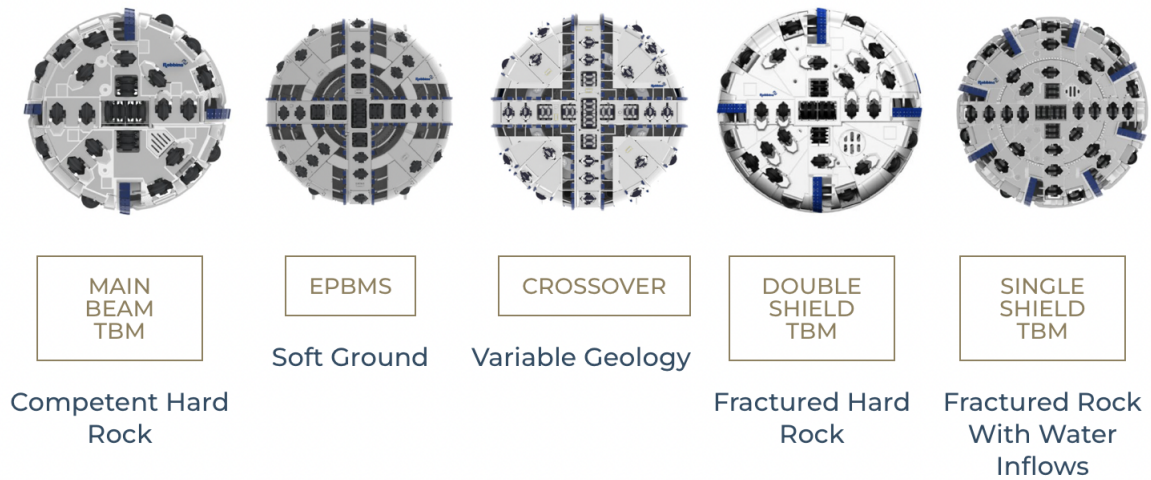


Figure 2-23: Comparison between different TBM shields and the ground-types they are employed in [Robbins, 2021].

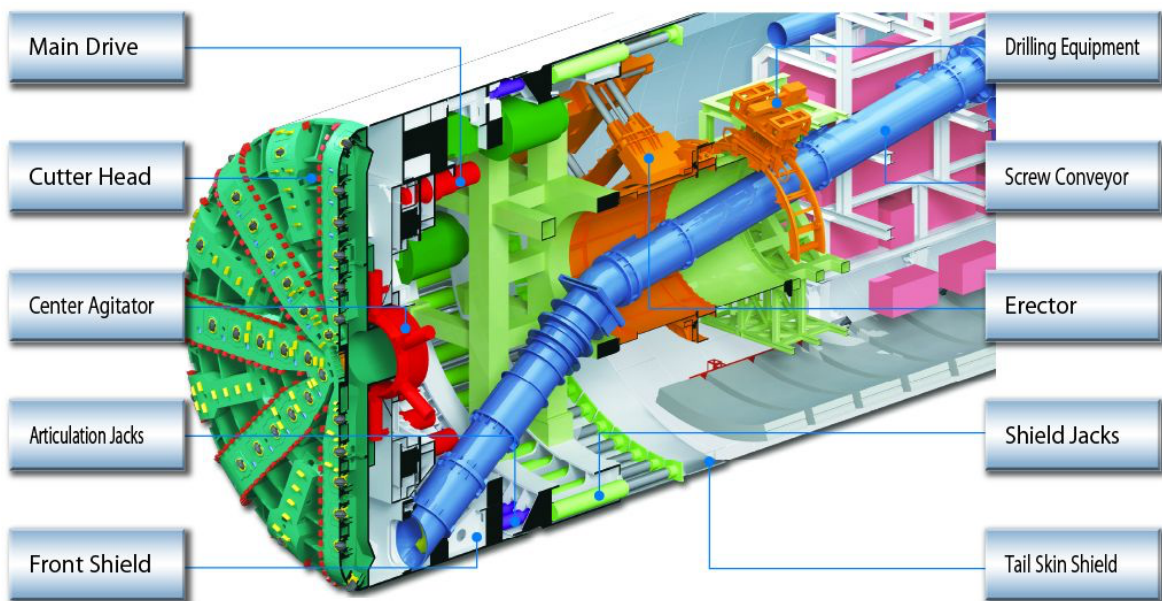


Figure 2-24: Cross-section of TBM with parts highlighted and identified. In the image we can see the machine's main digging and thrust components [Ugitech, 2019].

in Portugal, operates on a network of light rail that runs throughout the historical city center and it's outskirts [Metro do Porto, 2010a]. With more than five miles of underground tunnels and a total of 42 miles, the metro has 82 stations, both above and below ground [Metro do Porto, 2010b]. Founded in 1993 the Metro do Porto S.A., which runs the system is a publicly owned enterprise with both municipal, state, and

federal shareholders [Metro do Porto, 2010a].

Starting operations in 2002, the Porto Metro system has been expanding to a total of six lines functioning today [Metro do Porto, 2010a]. The mass transport structure reaches seven different municipalities amongst Porto's metropolitan area, being the city of Porto, Matosinhos, *Póvoa de Varzim*, Vila Nova de Gaia, Maia, Gondomar, and Vila do Conde [Bombardier, 2003]. Currently operated by ViaPORTO, a private operator company owned by Portugal's Grupo Barraqueiros [Railway Technology, 2008]. Responsible for the transport of more than 9000 people an hour, with over 102 metro cars, six operating lines and more than 500 staffers, Porto Metro is the second largest metro system in Portugal (behind only Lisbon) [Railway Technology, 2008].

Its 6 lines are lettered (from A-F) with Line A (also known as the blue line) being completed in 2002, for the 2004 Euro Football Championship [Metro do Porto, 2010a, Metro do Porto S.A., 2006]. Followed by Line B (red), inaugurated in 2005, and alongside Line A took advantage of the extinct narrow-gauge railway systems that operated there since 1875 [Metro do Porto, 2010a, Metro do Porto S.A., 2006]. Line C (green), which is the focus of this study, started running in 2005 right after Line B, and reached the municipal center of Maia, in Porto's suburbs [Metro do Porto, 2010a, Metro do Porto S.A., 2006]. Followed by Line D (yellow) in 2005, which faced considerable setbacks in construction (particularly in crossing the Douro River), having some of its stations closed until April, 2006 due to safety concerns [Metro do Porto, 2010a, Metro do Porto S.A., 2006]. After being cleared, the line was expanded further into the city in 2011 [Metro do Porto, 2010a].

Line E (purple) was launched in 2006, being the first to connect the city of Porto's Airport to the center, later expanding to the local football (soccer) stadium [Metro do Porto, 2010a, Metro do Porto S.A., 2006]. Finally, the newest expansion of the network, Line F (orange line) began operating in 2011 connecting the city of Porto to nearby Gondomar [Metro do Porto, 2010a, Metro do Porto S.A., 2006]. Below (Figure 2-25) is a map of the full system.



Figure 2-25: Porto Metro full system map throughout the city of Porto’s metropolitan area [Mapa Metro, 2010].

2.3.1 The Project

Talks of updating Porto’s public transport infrastructure were well underway throughout the 1990s [Metro do Porto, 2010a]. City planners and the government intended to relieve the usage of cars in Porto, especially throughout the historical city center, while also providing a comprehensive transport link between Porto and its surrounding metropolitan area [Metro do Porto, 2010a]. They finally decided on a 45-mile long train network system that began works by the late 1990s and was inaugurated in the early 2000s (as mentioned above) [Metro do Porto, 2010a, Metro do Porto, 2010b, Metro do Porto, 2019].

Out of the total 45 miles, 12.5 run through the city centre, incorporating the sub-urban railway lines and creating a comprehensive and fully integrated network that reaches most of Greater Porto [Mapa Metro, 2010]. By 1998, the government had awarded the Normetro Consortium the project, from conception to construction and full operations for five years [Metro do Porto, 2010a]. The consortium encompassed Bombardier Transportation (responsible for supplying power, electrical and mechanical systems and telecommunications), Soares da Costa and Semaly (which worked on project coordination and construction), ABB Sadelmi (employing all the fixed installations) and Transdev (coordinating operations and maintenance of the system) [Metro do Porto, 2010a].

2.3.2 Infrastructure

As the 5 miles of underground tunnels projected below the historical city center began development, great caution was exerted to minimally disrupt the surface [Metro do Porto, 2010b, Metro do Porto, 2010a]. This avoided damaging historic buildings and streets [Metro do Porto, 2010b]. With stations built every 750 meters, the system aimed to ensure quick access and user comfort [Metro do Porto, 2010a, Metro do Porto S.A., 2006]. Figure 2-26 shows an underground station amongst the tunnels of line D.

Porto Metro uses novel Eurotrams, a low-floor articulated wagon train, alongside Flexity Swift Light Rail Vehicles (LRVs), that are used in lines B and C reaching up to 60 mph [Railway Technology, 2008]. The LRVs contain a larger number of seats and function with modern mechanical motors that can recover up to 30% of consumed energy during breaking [Railway Technology, 2008].

Most services run with two LRVs coupled together [Metro do Porto, 2010b]. The Eurotram has of four compartments, two in each carriage joined together by small corridors and an articulation system to join carriages [Railway Technology, 2008]. They have a capacity of 80 seated and 134 standing passengers (see Figure 2-27) [Railway Technology, 2008].



Figure 2-26: Marquês Underground Station (Line D)[Guedes, 2017].



Figure 2-27: Eurotram used in the Porto Metro system [Guedes, 2017].

2.3.3 Ticketing

The Porto Metro system uses the "Andante" ticketing system (represented in Figure 2-28), which functions as an all-encompassing cross-networking ticket for both metro and bus lines, as well as the railway [Transportes Publicos de Portugal, 2015]. Designated stations provide both single-use (blue ticket) and multiple-use cards (gold ticket) that can be bought and topped up [Transportes Publicos de Portugal, 2015]. Validated tickets allow unlimited trips for an hour, which can increase depending on the zone of entrance [Transportes Publicos de Portugal, 2015].



Figure 2-28: Andante Ticketing stations in a Porto Metro station [Guedes, 2017].

During peak traffic hours, an additional fee is charged, while a reduction in price is offered for off-peak hours [Transportes Publicos de Portugal, 2015]. The system also supplies users with a day pass (called Andante 24), especially used by tourists [Transportes Publicos de Portugal, 2015]. The fare gates are located within the metro stations and ticketing is verified by random inspections carried out by staff members [Transportes Publicos de Portugal, 2015].

The city of Porto and the greater metropolitan area is divided by counties which are subsequently reached into sub-zones [Marchesi, 2019]. This organization greatly improved the city's public transport system, as it suffered for many years from inadequate supply and convoluted integration between bus and train lines [Marchesi, 2019]. Being a major commercial and touristic city, Porto has long required a rehabilitation

of its transport system, which came through the creation of the city’s metro system [Marchesi, 2019].

2.3.4 Communication Systems

As aforementioned, within the Normetro consortium, Bombardier is responsible for communication systems, which include power supply, radio communications, keeping depot equipment and rail signalling [Bombardier, 2003, Bombardier, 2012]. Porto Metro uses traditional light rail signalling, wherein the metro system is monitored remotely from a central command center and drivers have the autonomy to make real-time decisions [Intelligent Transport, 2019, Bombardier, 2012].

2.3.5 Financial considerations

Despite being regarded as a crucial and effective means of transportation, the Porto Metro public transportation system has incurred a cost of over 3.5 billion euros to the public funds since 2007 [Metro do Porto, 2010b]. This amount is equivalent to over 1% of Portugal’s annual GDP² [Metro do Porto S.A., 2006].

According to sources such as [Metro do Porto S.A., 2006] and [Bombardier, 2003], the first phase of the Porto Metro project (Lines A-D) was a joint venture between the city of Porto and Greater Porto area. However, the cost of the project ended up being over twice the originally estimated amount, resulting in a surcharge of over 1.5 billion euros, which is 140% higher than the initial projection. The Porto Metro system has not been profitable since its inception, which is a common occurrence for mass transit systems worldwide, with reported losses every year. In 2006, the deficit was at its lowest point, reaching 122 million euros [Metro do Porto S.A., 2006, Intelligent Transport, 2019].

²Gross Domestic Product, meaning the sum of all market value generated by the development of goods and services within a particular country’s borders measured in a specific amount of time (usually a year) [U.S. Bureau of Economic Analysis (BEA), 2022].

This page intentionally left blank.

Chapter 3

Geological and Geotechnical Aspects

3.1 The Geomorphology of Portugal

Despite being one of the smaller countries of the European continent, Portugal, with an area of 35,603 square miles, is vastly diversified in terms of geomorphological landscapes [Central Intelligence Agency, 2022]. This is the result of a protracted and intricate geological evolution process that include two Wilson Cycles ¹ and many significant changes especially since the Paleozoic [Vieira et al., 2020, Feio and Daveau, 2004]. Its geographical placement along the Eurasian boundary as well as strong climatic fluctuations shaped its distinct morphogenetic environment [Vieira et al., 2020, Ferreira, 2005]. Figure 3-1 shows the lithological characteristics of Portugal.

The well known Iberian Massif, that is the result of the flattening of the extinct Variscan Cordillera (see Figure 3-2) was the result of the first Wilson cycle (Variscan cycle) [Feio and Daveau, 2004]. The second cycle, known as the Tethys or Atlantic cycle defined the other three main morphostructural units that constitute the Portuguese territory today: the Meso-Cenozoic Basins, Cenozoic Basins and the formation of the marine archipelagos of Azores and Madeira [Dias, 2013, Dias R., 2013]. These three main morphostructural components of the country are currently classified

¹Geologic concept that relates the cyclical opening and closing of ocean basins as an important aspect of the formation and breakup of super-continent [Wilson, 2019].

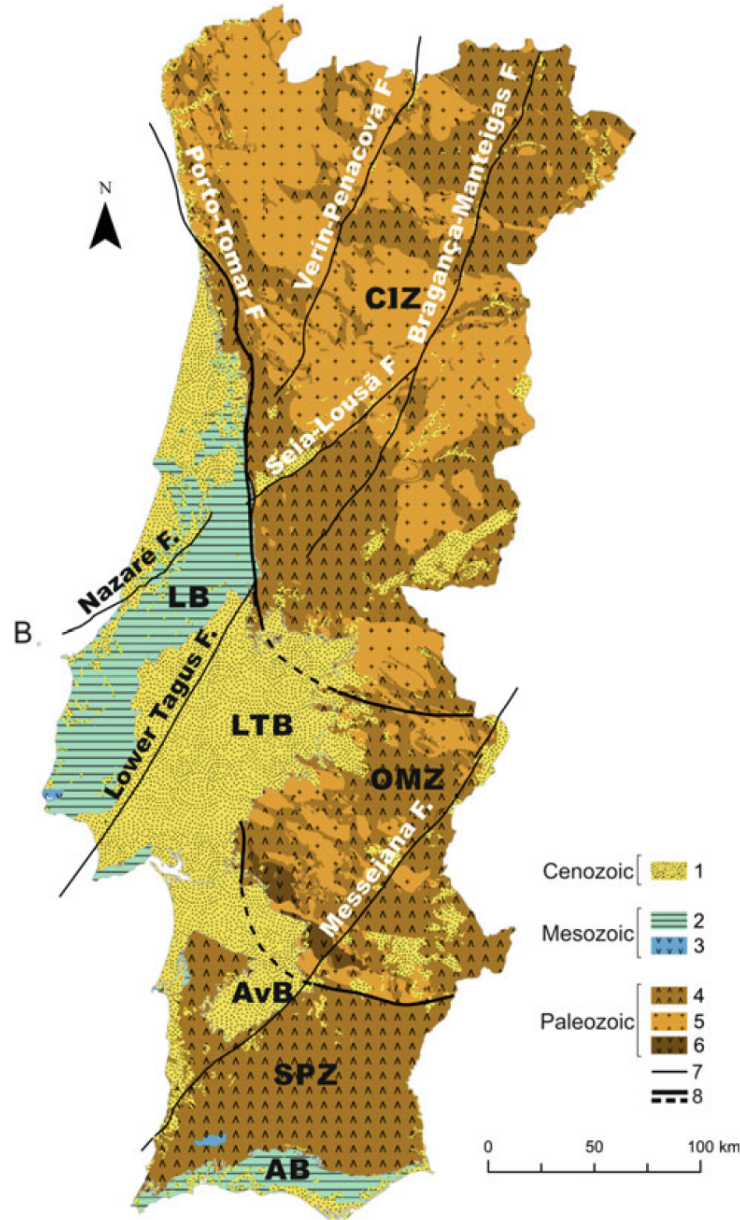


Figure 3-1: General lithology of Portugal. In the legend, 1, 2 and 4 are sedimentary formations; 3 represents igneous rocks; 5 shows the intrusive formations; 6 the porphyrys; the continuous line (7) shows the main geologic faults present in the country while the dashed line (in 8) gives the limits of the Iberian Massif [Vieira et al., 2020]).

amongst 10 regional geomorphological subdivisions [Vieira et al., 2020].

The consecutive incidence of wet and dry climate phases resulted in comprehensive weathering of bedrock and the severe erosion that led to soil formation [Ferreira, 2005]. These cyclical climatic changes were the main drivers of the vast planation structures formed in the region during the pre-Quaternary [Feio and Daveau, 2004]. Portugal's

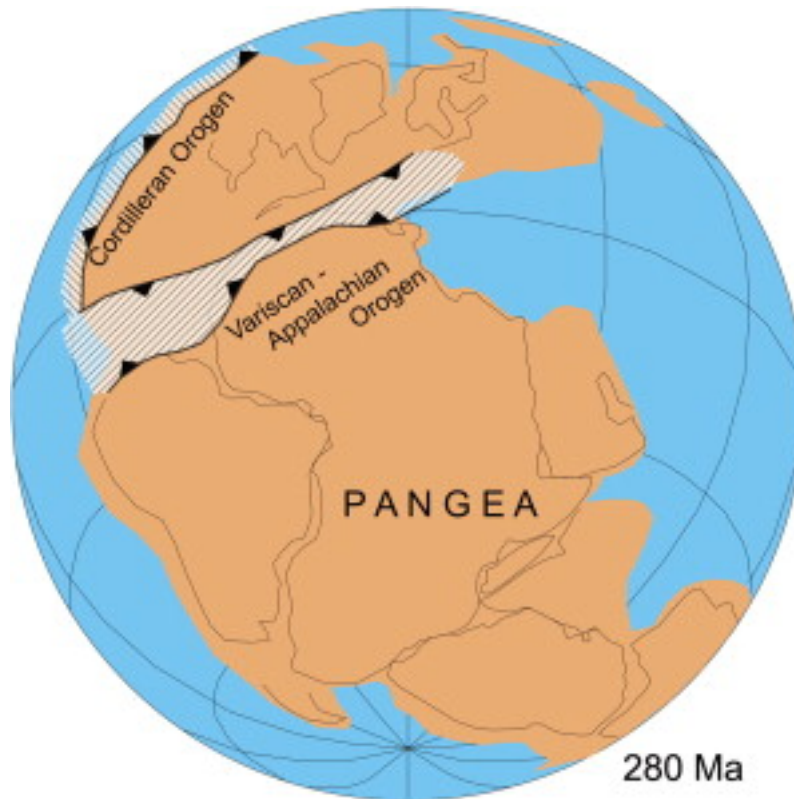


Figure 3-2: Schematic image showing the formation process of the Variscan Cordillera [Johnston and Gutierrez-Alonso, 2010]).

interior much less affected by tectonic activity, saw the development of polygenetic landforms² and stepped planation formations that created the mountains seen today [Vieira et al., 2020]. Figure 3-3 below show the Eurasian tectonic plate and Portugal's positioning within it.

The cold climate of the Quaternary period contributed to the lowering of sea level and the deterioration of planation surfaces which helped entrench rivers and elevate the relief throughout the European landmass [Feio and Daveau, 2004]. The period is also responsible for the formation of the volcanic islands of Azores and Madeira [Vieira et al., 2020]. Portugal is a very geomorphologically diverse country, the result of the lithological response to both tectonic movement and climatic alterations [Ferreira, 2005]. This unique and interesting geologic history formed the landforms we see today, comprised mainly of volcanic, granitic, schist and karst formations

²Landscapes that are the result of several endogenetic and exogenic geological processes [Kamp and Owen, 2013].

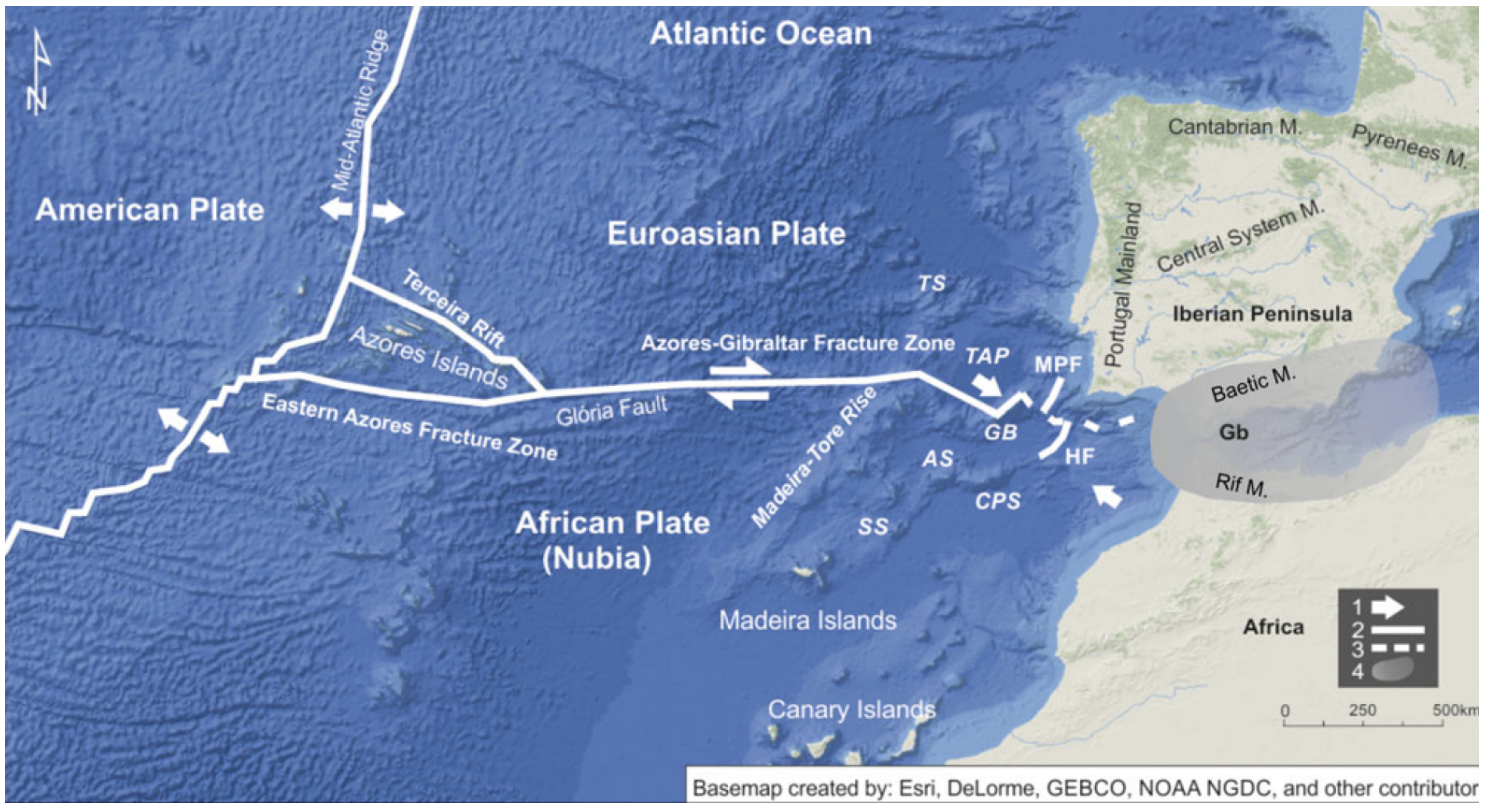


Figure 3-3: Tectonic placement of Portugal. In the image, the white arrows (1 in the legend) represent the movement of coinciding tectonic plates; the continuous (2) and dashed (3) white lines show the known and approximate locations of geologic faults, respectively. Finally the blurred segment (4) between the Iberian Peninsula and African continent shows the region where continental plates collide [Vieira et al., 2020]).

[Pereira, 1997]. Figure 3-4 shows Portugal’s landmass relief [Vieira et al., 2020].

3.2 The City of Porto

Porto, which was declared a World Heritage Site by UNESCO in 1996 is one of the oldest cities in Portugal (dating back 900 years to the Bronze Age) [Vieira et al., 2020]. With a population of 237,559 residents and 1.6 million visitors every year it is one of the most important tourist destinations in Europe [World Population Review, 2022]. Porto dealt with rapid urban expansion during the 19th century which alongside challenging natural conditions like floods, slope stability issues and coastal erosion made the city a difficult building site [Patatas et al., 2011]. Figure 3-5 shows an early depiction of Porto.

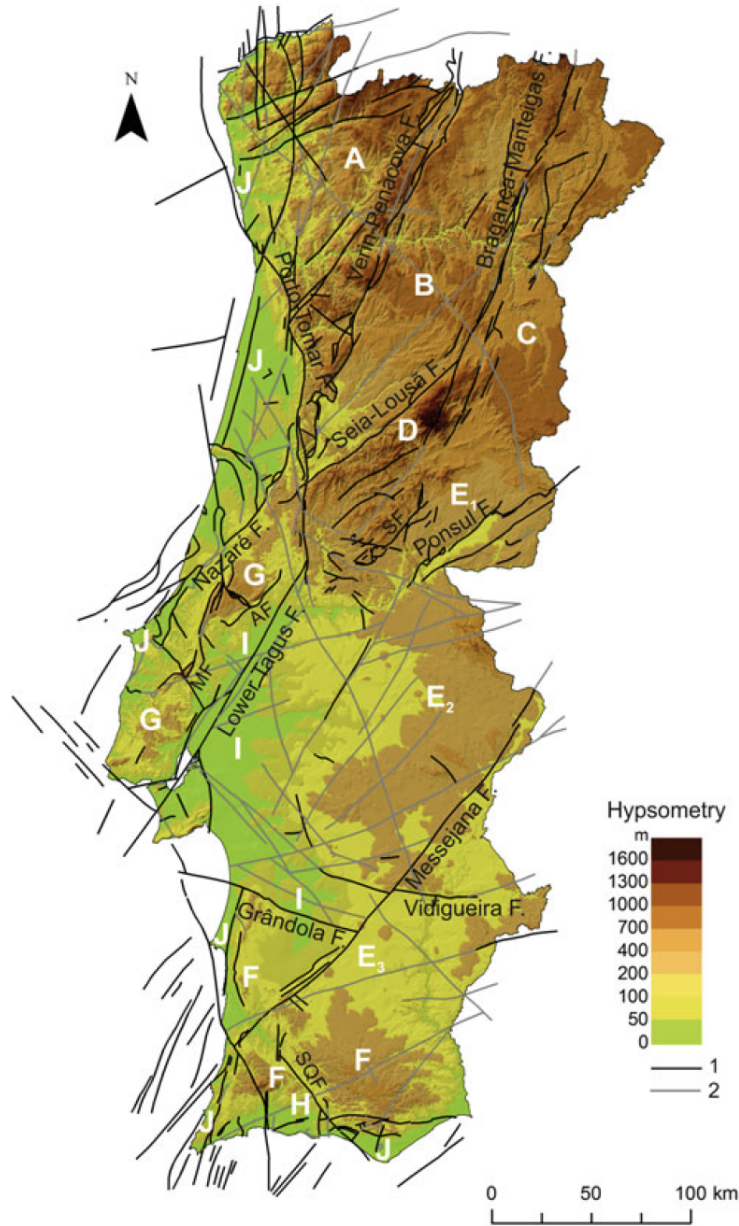


Figure 3-4: Topographic map of Portugal. Where the darker lines (represented by 1 in the legend) show the currently active geological faults within the territory and the faded lines (2) represent the geologic lines that may conform to active faults [Vieira et al., 2020]).

Placed between the Douro river and the sea, Porto was initially used as a defensive city, placed in the granitic hill of Pena Ventosa [Ribeiro da Silva, 2004]. After Roman occupation and use of the city as an important port, known as "Portus Cale" (which originated the name Portugal), the city kept expanding alongside the river bank [Disney, 2009]. It served as an economically relevant city throughout the Portuguese



Figure 3-5: Porto. Depicted by H. Duncalf and William Henry Toms, English royal envoys sent to the city in 1736 [Arquivo Municipal do Porto, 2022]).

"Discoveries" of the 15th and 16th centuries, especially due to wine and other exports [Disney, 2009]. Figure 3-6 below shows part of Porto's historical city center.



Figure 3-6: Porto's historical city center today [Vieira et al., 2020]).

3.2.1 Geological Conditions

Placed along the Iberian Massif, Porto has complex geological conditions. Directly located in the PTFASZ shear zone (Porto-Tomar-Ferreira do Alentejo) the city is placed in a lithological region formed during the Precambrian [Dias and Ribeiro, 1995, Romão et al., 2008]. Comprised mainly of sedimentary rock (sandstone, limestone) alongside metamorphic formations (gneiss, amphibibolite) and post-tectonic granites, the city has even been known as "Porto Granite" [Noronha and Leterrier, 1995, Noronha and Leterrier, 2000]. Porto is a geologically diverse city, being formed by stepped planes formed in the Pliocene-Quaternary period, covered by fluvial and marine deposits dating back to the last Ice Age [Araújo, 1984]. Figure 3-7 shows the geomorphology of Portugal's northeast region, where Porto is located.

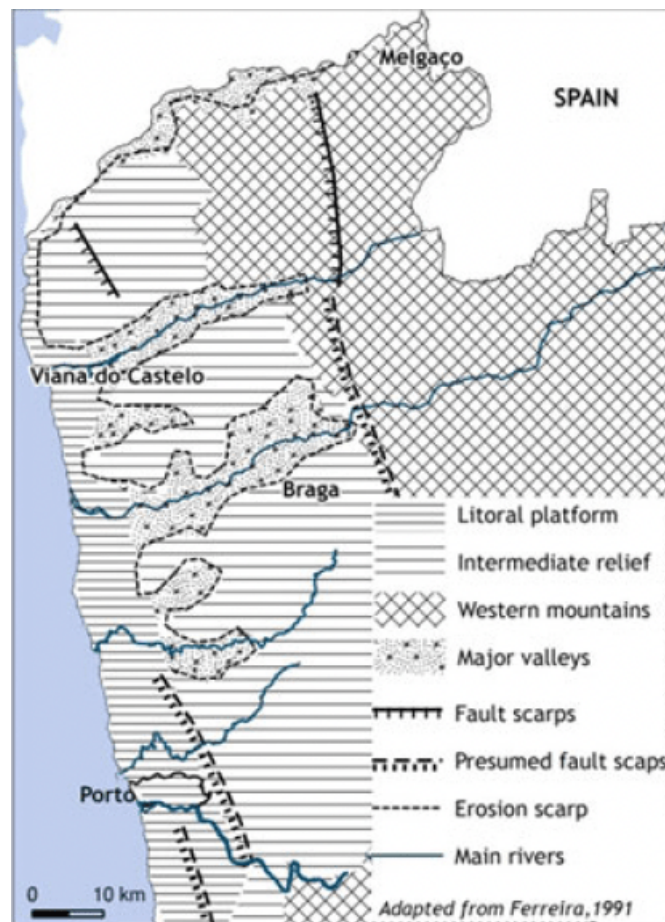


Figure 3-7: Partial geomorphological map of Portugal. The city of Porto is located in the bottom-left corner, where the main rivers flowing by the city can be seen. Also notable is that Porto is located well within the Portuguese litoral platform [Vieira et al., 2020].

Affected by strong weathering, the bedrock in Porto was shaped by changes in climate [Araújo, 2014]. Above the bedrock, sandstone blocks and alluvial formations are followed by coarse material that has been deposited (up to 160 feet) [Araújo, 2014]. By the coast, marine deposits are associated with an interglacial period and its sand-silt composition spreads across the Douro river valley [Araújo, 2004, Ribeiro et al., 2010]. The following map Figure 3-8 shows the topography of the region around Porto and its main geologic faults.

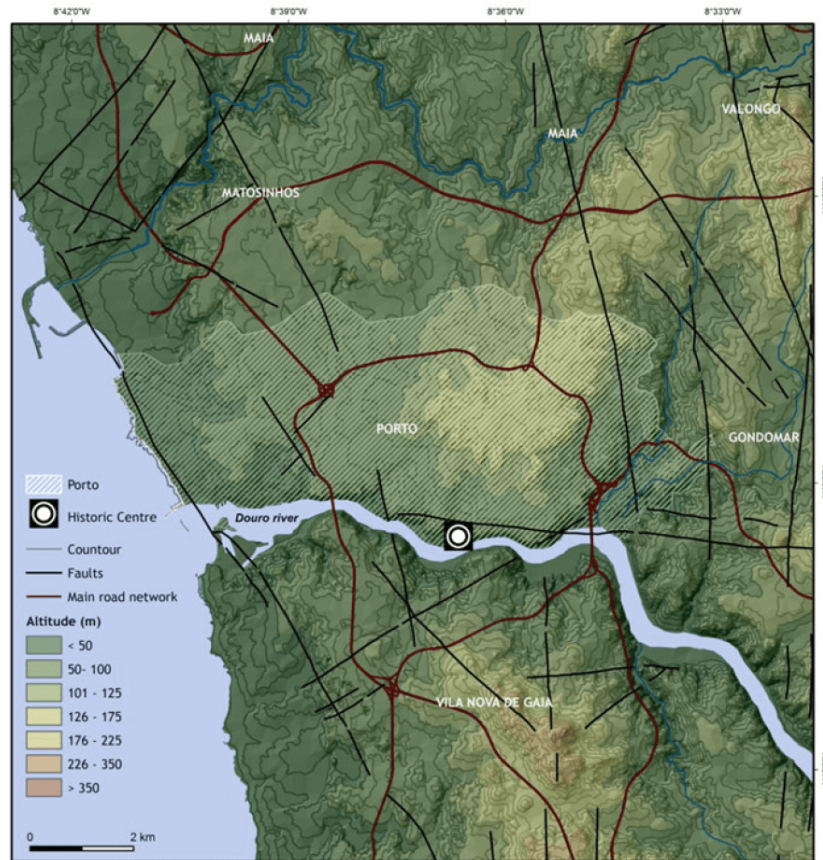


Figure 3-8: Topographical map of the Porto region and main geologic faults. Where the main road networks are represented by the red lines and geologic faults in black. The historic city center is shown by the black and white circle, located in the margins of the Douro River [Vieira et al., 2020]).

Between the city of Porto and neighboring Vila Nova de Gaia, lies the Douro river estuary, which includes the biggest drainage basin in the Iberian Peninsula (shared by Portugal and Spain) [Vieira et al., 2020]. Modified by sea-level retraction and subsequent rise in the Quaternary period, the Douro river valley and its outlet to the ocean has been one of the most important natural aspects to drive the human

occupation of Porto [Araújo et al., 2013]. Determining many boundaries and changes of the urban landscape as well as building social and cultural alignment along the river, Porto was the site of important developments in military and naval engineering, helping Portugal reach its centuries-long prominence in navigation and development of maritime trading routes [Dias et al., 2000]. Below is a map (Figure 3-9) depicting the main geologic composition of the city of Porto and its surrounding area.

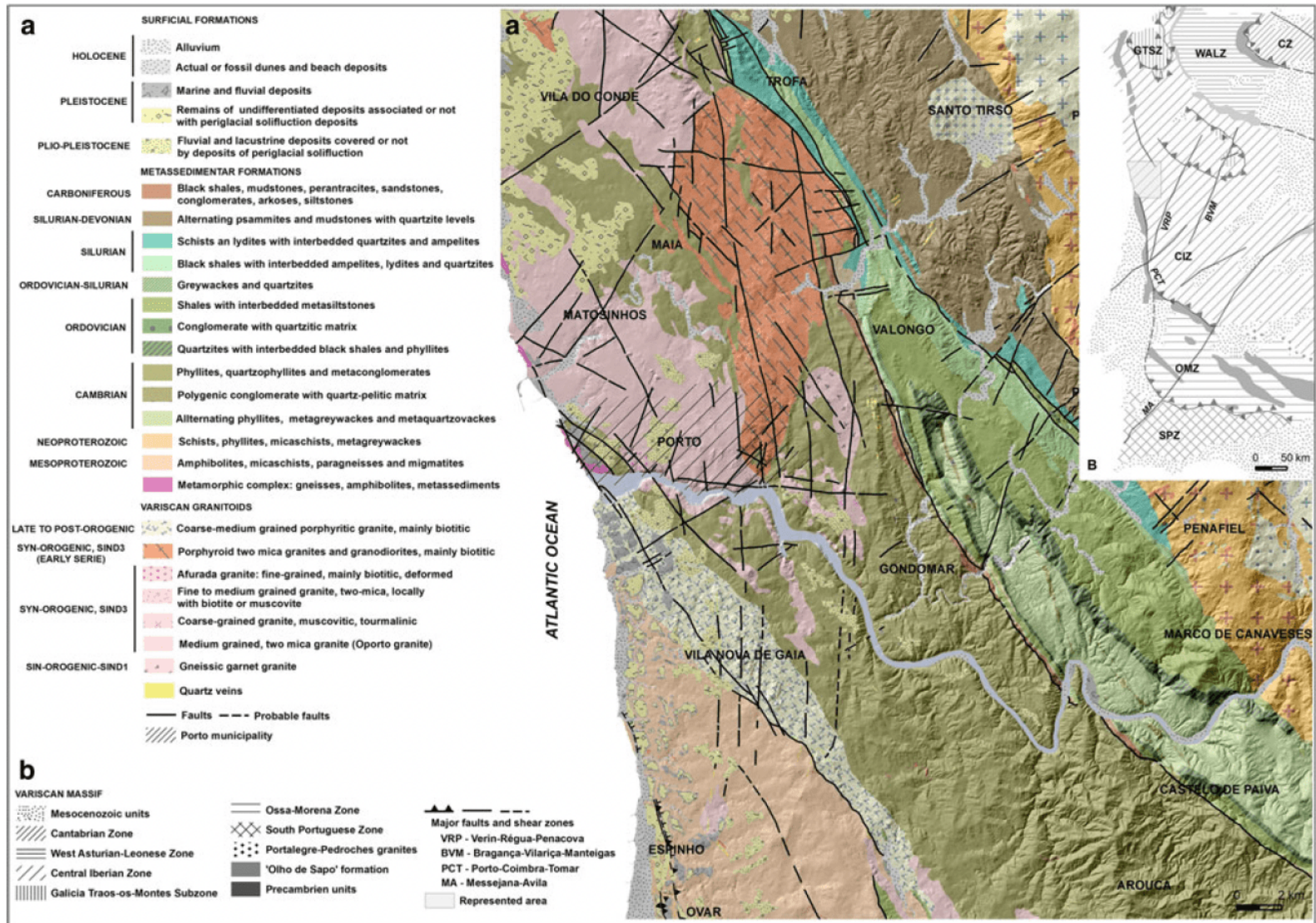


Figure 3-9: Main geological subdivisions around the city of Porto. From the map it is clear that the Porto regions is composed mainly of medium grained, two mica granite, named Oporto Granite (represented in light pink). There is also presence of fluvial and lacustrine deposits from the Douro River basin (light green) [Vieira et al., 2020]).

Constructing several coastal harbors, river dams, military bases and the early

riverbed dredging for navigation purposes, led to significant sediment carrying and loss, contributing greatly to coastal erosion [Dias et al., 2000]. As these issues become graver and seeing that Porto still harbors important portuary infrastructure, there have been recent (2000-2005) engineering interventions (e.g. jetties, break-water systems, etc.) aiming to mitigate the loss of landmass [Vieira et al., 2020, Bastos et al., 2012]. The infrastructure placed increased navigable pathways for ships and aided in decreasing coastal erosion especially in flood-prone areas around the city, including beaches that had been losing land since the 1950s [Vieira et al., 2020, Bastos et al., 2012, Instituto Portuário e dos Transportes Marítimos, 2009]. However, it also generated strong sediment accumulation in other localities (like the Sao Paio Bay), gravely impacting the aquatic ecosystem [Dias, 1993, Bastos et al., 2012]. Although abating coastal erosion in some regions of the city, flooding and sea-level rise due to anthropogenic-led climate change is expected to continue challenging the city of Porto must be considered in the building of new infrastructure or new developments in the city [Araújo, 2014]. Figure 3-10 shows the geomorphological map of the city of Porto.

3.3 Porto Metro Project

As aforementioned (see section 3.2.1), the city of Porto has a diverse geologic history and thus formations. Regarding the Porto Metro project (Line C) the region is mostly comprised of igneous formations especially the Oporto Granite (abundant in the city - see Figure 3-11). The encountered geological profile is typical of intensely weathered regions, with joints and faults along the tunnel line [Sousa, 2010]. This extremely irregular formation leads to considerable uncertainty in the projected geologic profile generated from boring holes and other geologic information gathered before tunnel construction [Sousa, 2010].

Extreme weathering leads not only to unpredicted conditions on-site but also intense discrepancies in material density, permeability, strength amongst other geomechanical parameters [Sousa, 2010]. The highly weathered Oporto granite produces

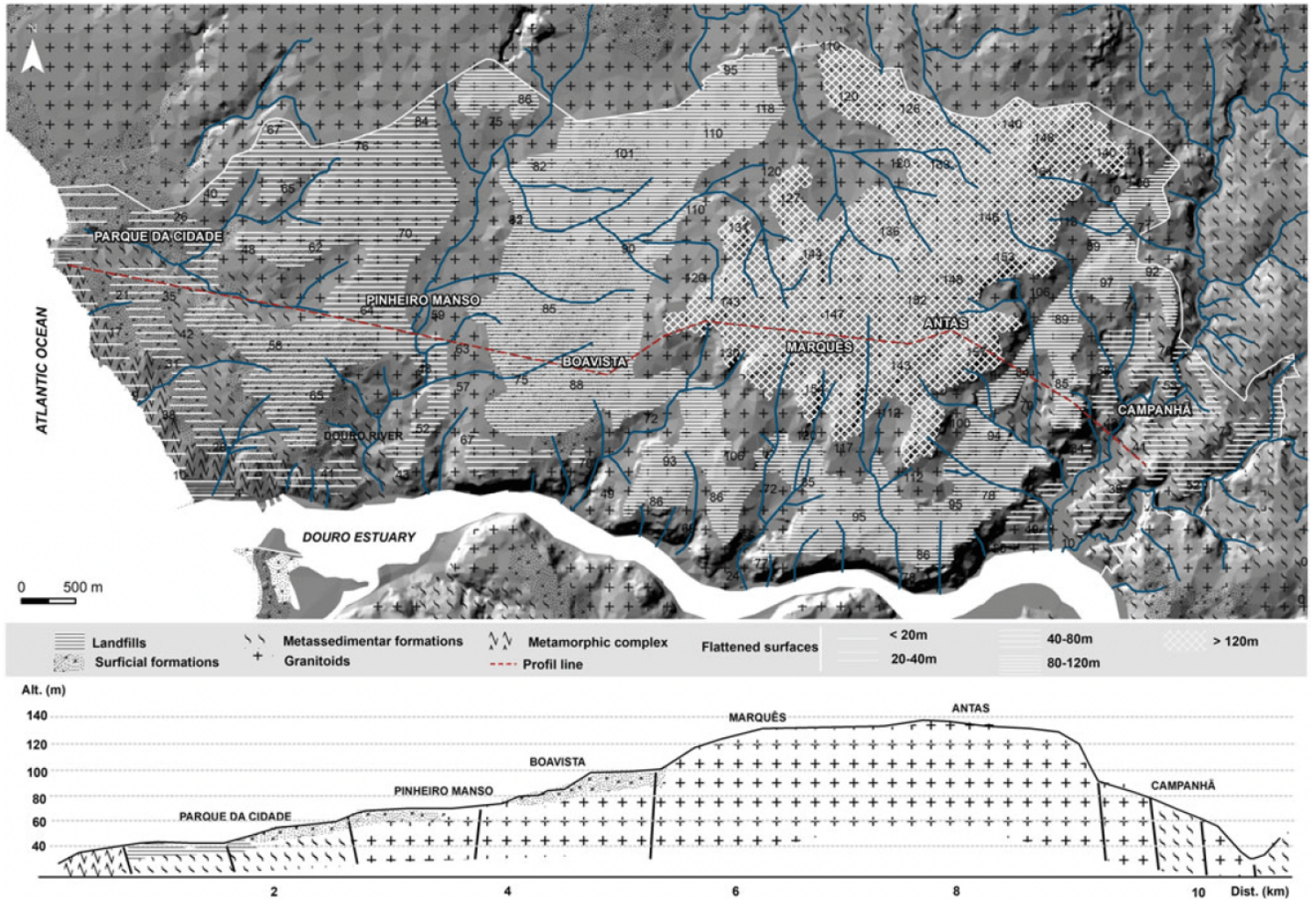


Figure 3-10: The top map shows Porto's geomorphology while the bottom represents the city's relief cross-section. Varying from 40 to 140 meters above sea level, Porto is mostly composed of granitoid formations (represented by the crosses from Pinheiro Manso to Campanhã), followed by metasedimentary formations (slashes) in Parque da Cidade and after Campanhã. Some landfills, metamorphic and superficial formations are also present along the city [Vieira et al., 2020].

different hydrological patterns and water-flow paths, leading to highly uncertain geologic conditions, which can be a considerable source of accidents, stoppages and delays in an infrastructure project of this magnitude [Sousa, 2010]. Figure 3-12 below shows the tunnel section evaluated in this thesis, alongside the relevant borings conducted throughout the alignment.

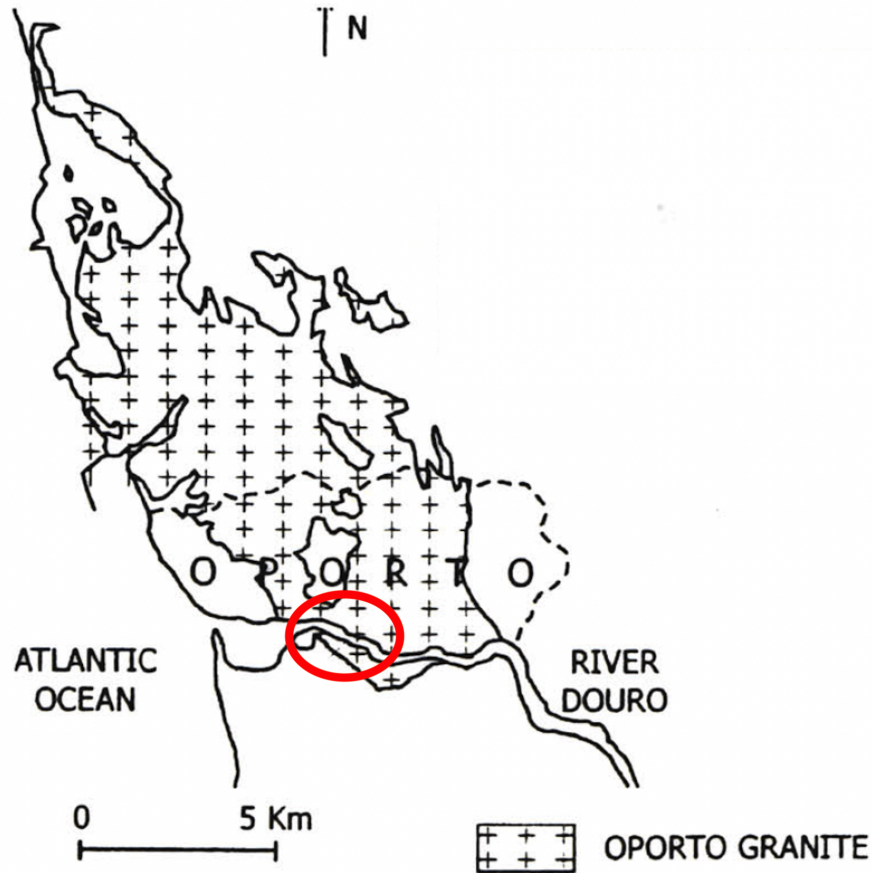


Figure 3-11: Distribution of Oporto Granite amongst the Douro River valley. The metropolitan area of the city of Porto is indicated in red [Sousa, 2010].

3.3.1 Projected Geological Profile

Below, Figures 3-13, 3-14, 3-15, 3-16 showcase the projected geological profile determined by Line C's designers. As the scale of the profile does not allow for it to be presented in a single sheet, the evaluated tunnel sections will be presented as cuts from the main section. Firstly the stretch from Ring 533 to Ring 610 (Figure 3-13) followed by Rings 611-689 (Figure 3-14), Rings 690-814 (Figure 3-15) and Rings 815-942 (Figure 3-16).

3.3.2 Encountered Geology

It is clear that there were significant discrepancies between predicted and encountered geological conditions [Sousa, 2010]. This section will present these differences

through the geological profiles and a graphical comparison of what was projected and what was found on site (Figures 3-17, 3-18, 3-19, 3-20).

3.3.3 Face mappings

The present section will show the estimated geologic profile based on the face mappings executed throughout the construction of the tunnel. It is important to note that the grey sections of the face mappings corresponds to the hidden section of the face. Table 3.1 lists the location of all the face mappings available from Rings 533 to 942 (see Figures 3-21, 3-22, 3-23, 3-24). Following the order presented above, the face mappings and corresponding profiles will be presented in sections (Rings 533 - 610; 611 - 689; 690 - 814; 815 - 942).

The ring's face mappings were closely looked at and mapped alongside the geologic profile. Both projected and encountered ground conditions will be important to determine the validity of machine learning models aiming to predict geology ahead of the tunnel face and further automate TBM operations. In the present study models that aim to classify rings between rock, soil, rock-like mixed and soil-like mixed using machine-generated data to find patterns that could potentially indicate changes in upcoming ground conditions.

Rings	Start point (m)	Face Map Locations (m)
533-615	906.7	907.4; 941.0; 959.2; 983.0; 998.4; 1019.4; 1022.5
616-653	1024.0	1027.8; 1033.4; 1043.2; 1050.2; 1054.4; 1071.2
654-689	1075.0	1093.6; 1102.0; 1117.4
690-756	1025.0	1158.0; 1175.0; 1184.0; 1193.0; 1195.0; 1211.0; 1218.0
757-812	1220.0	1230.0; 1240.0; 1258.0; 1271.0; 1288.0
813-868	1298.0	1299.0; 1305.0; 1328.0; 1340.0; 1352.0; 1366.0
869-942	1375.0	1389.0; 1401.0; 1414.0; 1435.0; 1437.0

Table 3.1: Location of face mappings (in meters) along Rings 533 - 942.

GEOTECHNICAL LONGITUDINAL SECTION

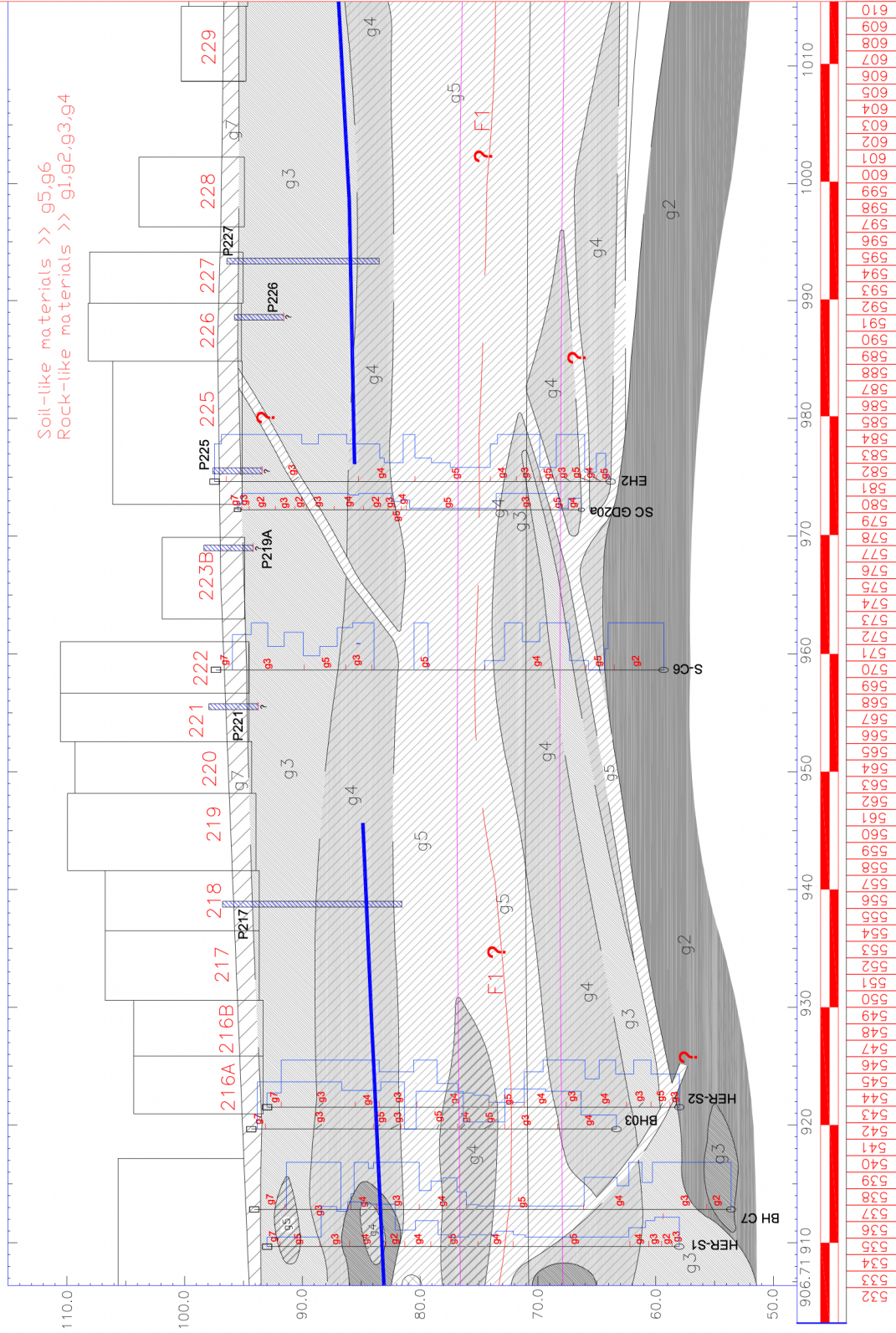


Figure 3-13: Geotechnical Profile Rings 533-610. Where the x axis shows the longitudinal distance and y the altitude (both measured in meters). The distance between two consecutive rings is 1 meter. This complete profile is based on several boring holes (represented in the figure alongside boring logs). Where g1, g2, g3 and g4 are rock-like materials and g5 represents soils. Courtesy of Normetro.

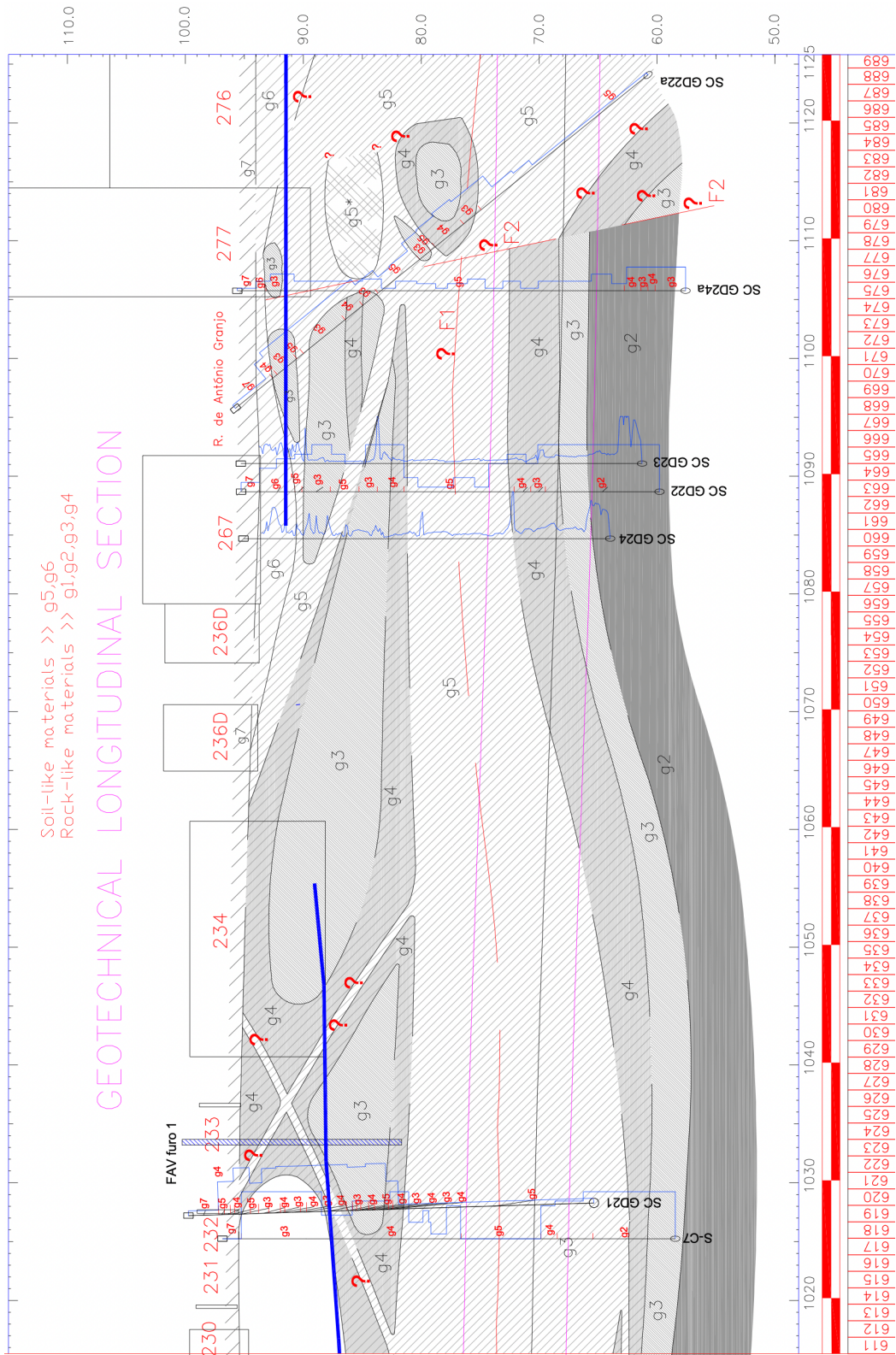


Figure 3-14: Geotechnical Profile Rings 611-689. Distance and altitude are represented by the x and y axis respectively (both measured in meters). The distance between two consecutive rings is 1 meter. This complete profile is based on several boring holes (represented in the figure alongside boring logs) and other geotechnical investigations. Where g1, g2, g3 and g4 are rock-like materials and g5 represents soils. Courtesy of Normetro.

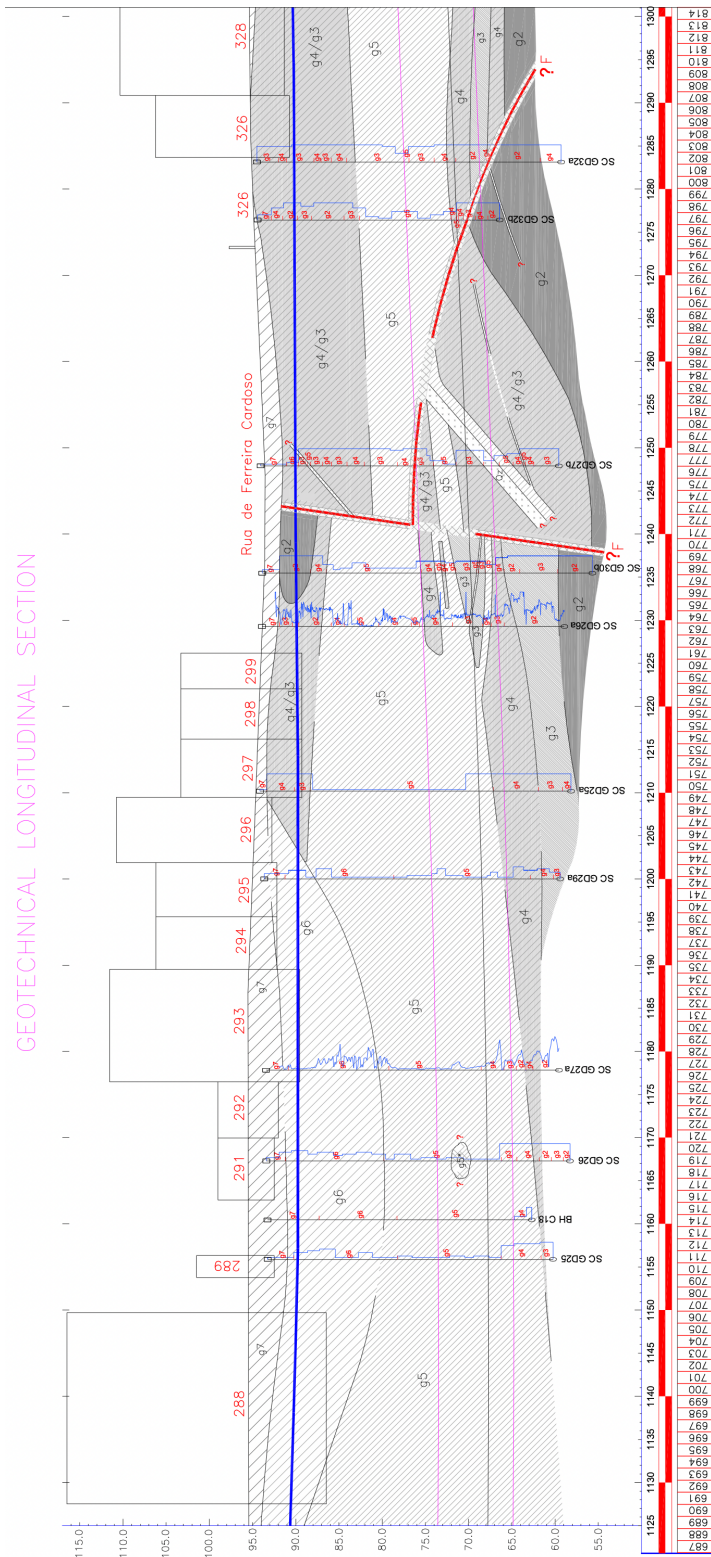


Figure 3-15: Geotechnical Profile Rings 690-814. Distance and altitude are represented by the x and y axis respectively (both measured in meters). This complete profile is based on several boring holes (represented in the figure alongside boring logs) and other geotechnical investigations (distance between two consecutive rings is 1 meter). Where g1, g2, g3 and g4 are rock-like materials and g5 represents soils. Courtesy of Normetro.

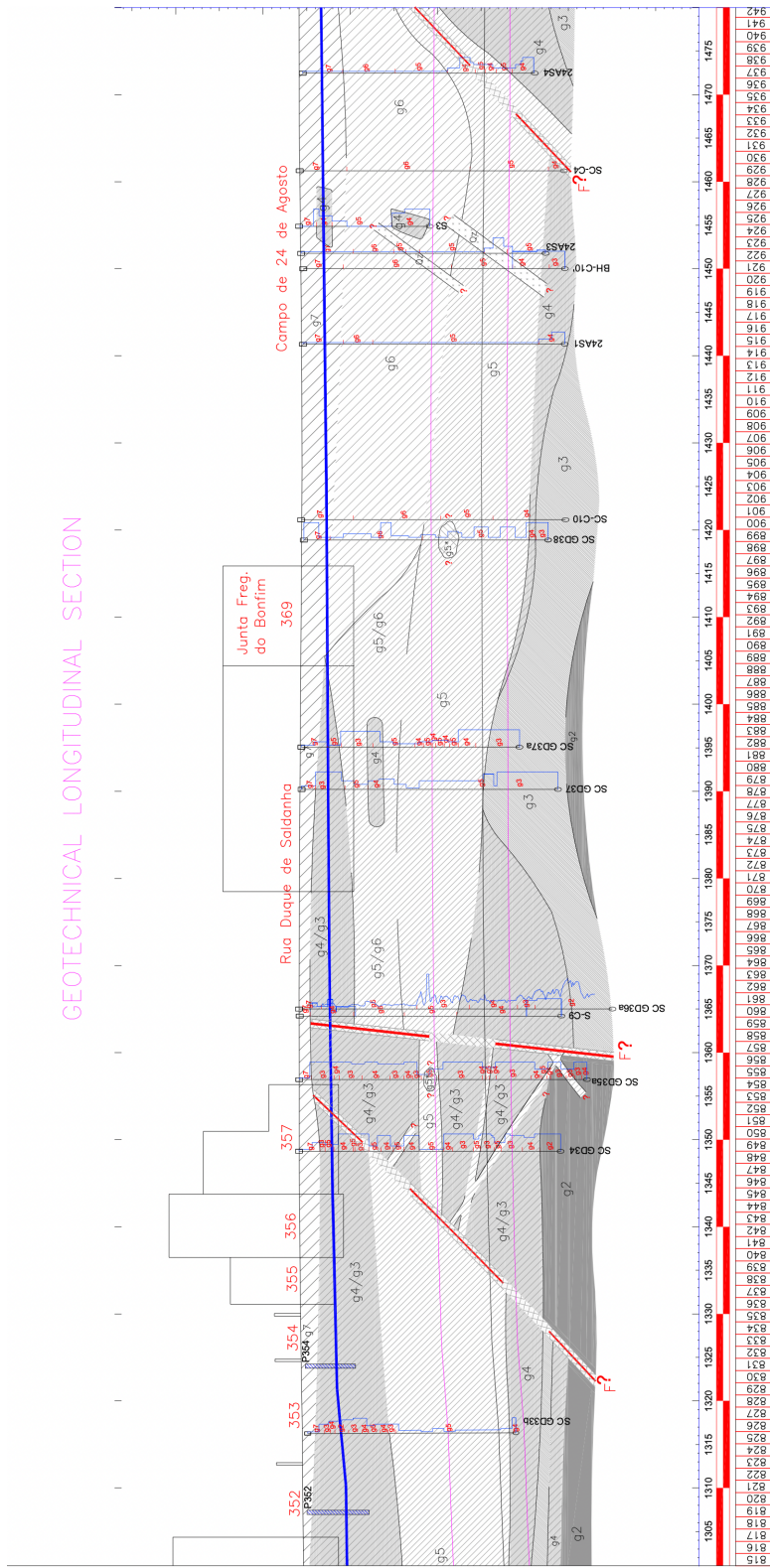


Figure 3-16: Geotechnical Profile Rings 815-942. Distance and altitude are represented by the x and y axis respectively (both measured in meters). The distance between two consecutive rings is 1 meter. This complete profile is based on several boring holes (represented in the figure alongside boring logs) and other geotechnical investigations. Where g1, g2, g3 and g4 are rock-like materials and g5 represents soils. Courtesy of Normetro.

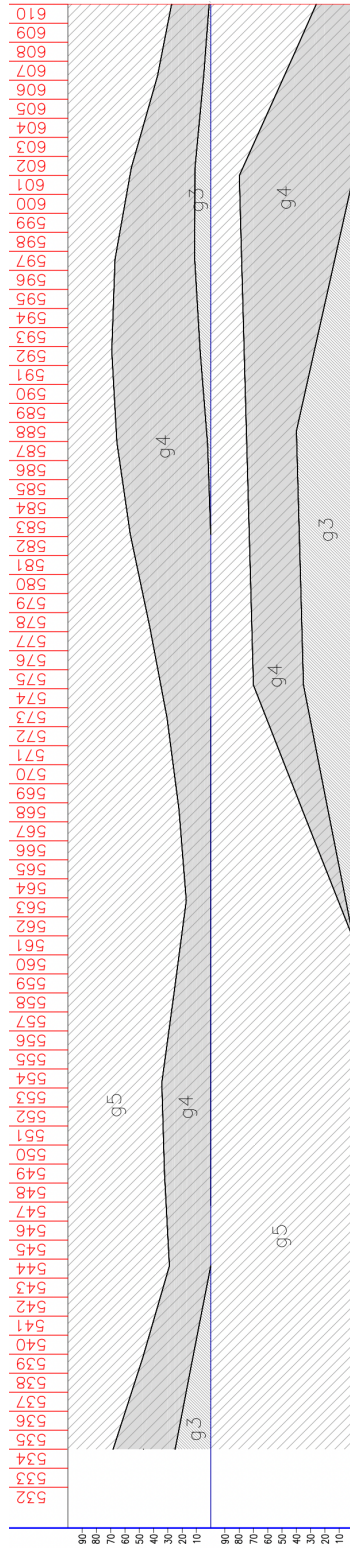


Figure 3-17: Predicted geomechanical conditions (top) versus encountered geomechanical (bottom) conditions for Rings 533-610. Where g1, g2, g3 and g4 are rock-like materials and g5 represents soils. As seen in the image, from Rings 535 to 561 they encountered only soil-like material (g5) different from what was predicted. This pattern is followed by the section between rings 561 and 610, where g3 and g4 sections were different from what was predicted. Courtesy of Normetro.

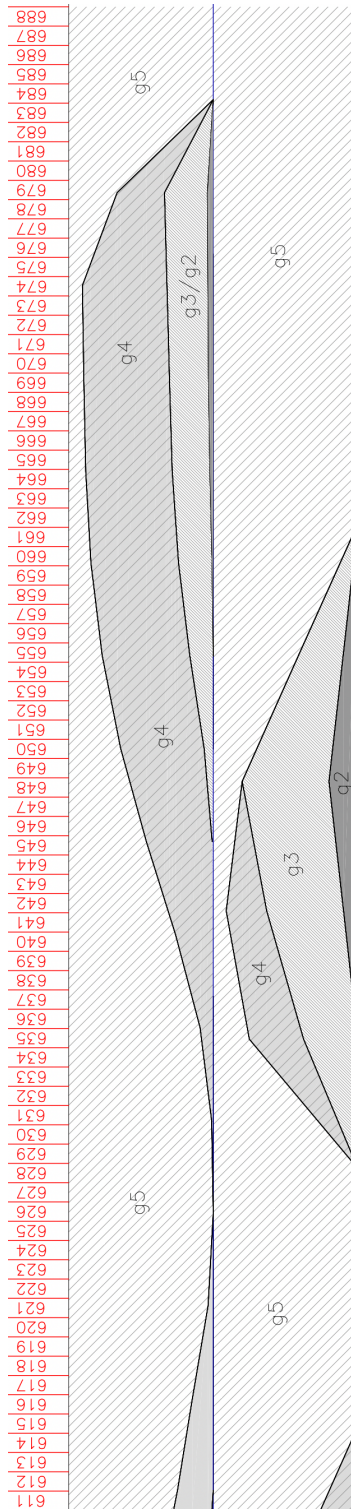


Figure 3-18: Predicted geomechanical conditions versus encountered geomechanical conditions for Rings 611-689. Where g1, g2, g3 and g4 are rock-like materials and g5 represents soils. As seen in the image, from Rings 535 to 561 they encountered only soil-like material (g5) different from what was predicted. This pattern is followed by the section between rings 630 and 661, where g3 and g4 sections were different from what was predicted and g2 material was found. Also, from rings 661 to 688 predicted and encountered geology diverged, with soil-like material (g5) more abundant than originally imagined. Courtesy of Normetro.

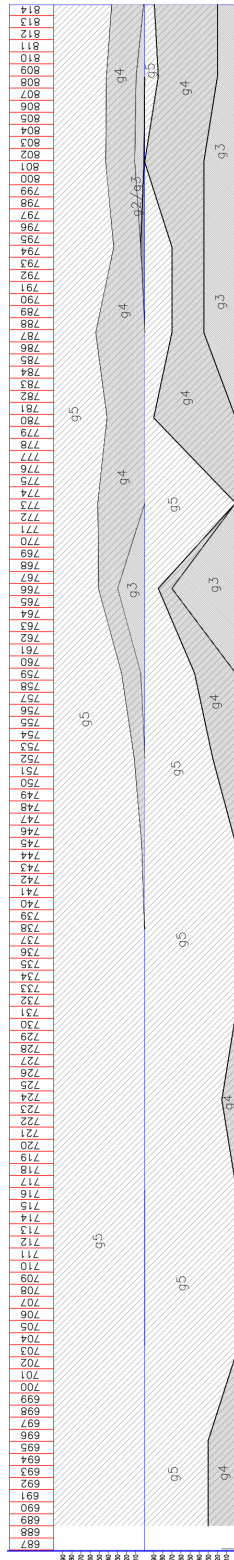


Figure 3-19: Predicted geomechanical conditions versus encountered geomechanical conditions for Rings 690-814. Where g1, g2, g3 and g4 are rock-like materials and g5 represents soils. From rings 690 to 745 they encountered unexpected rock-like material (g4). From rings 746 - 814 they found similar patterns to what was predicted but different concentrations, coming across more rock-like material (g3, g4) than what was expected. Courtesy of Normetro.

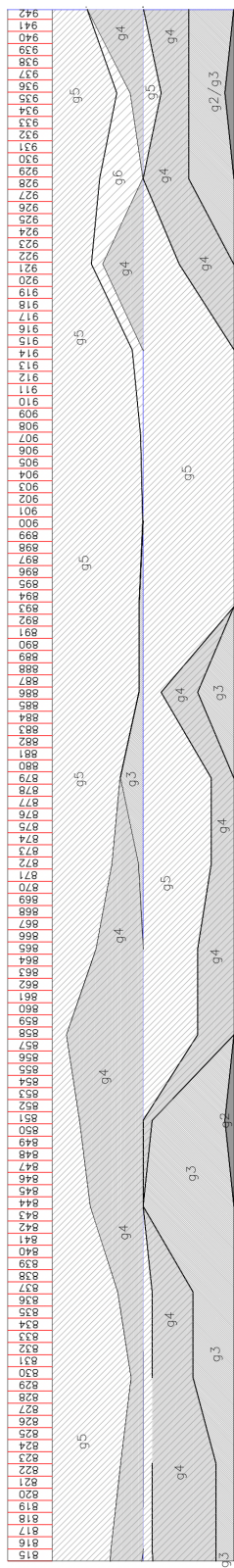


Figure 3-20: Predicted geomechanical conditions versus encountered geomechanical conditions for Rings 815-942. Where g1, g2, g3 and g4 are rock-like materials and g5 represents soils. Expected geology contrasted widely with conditions confronted in the construction process. Soil-like material (g5) was greatly overestimated especially from rings 815 - 850. Location of rock-like ground (g3, g4) was also uncertain and diverged from the encountered geology throughout most of the section. Courtesy of Normetro.

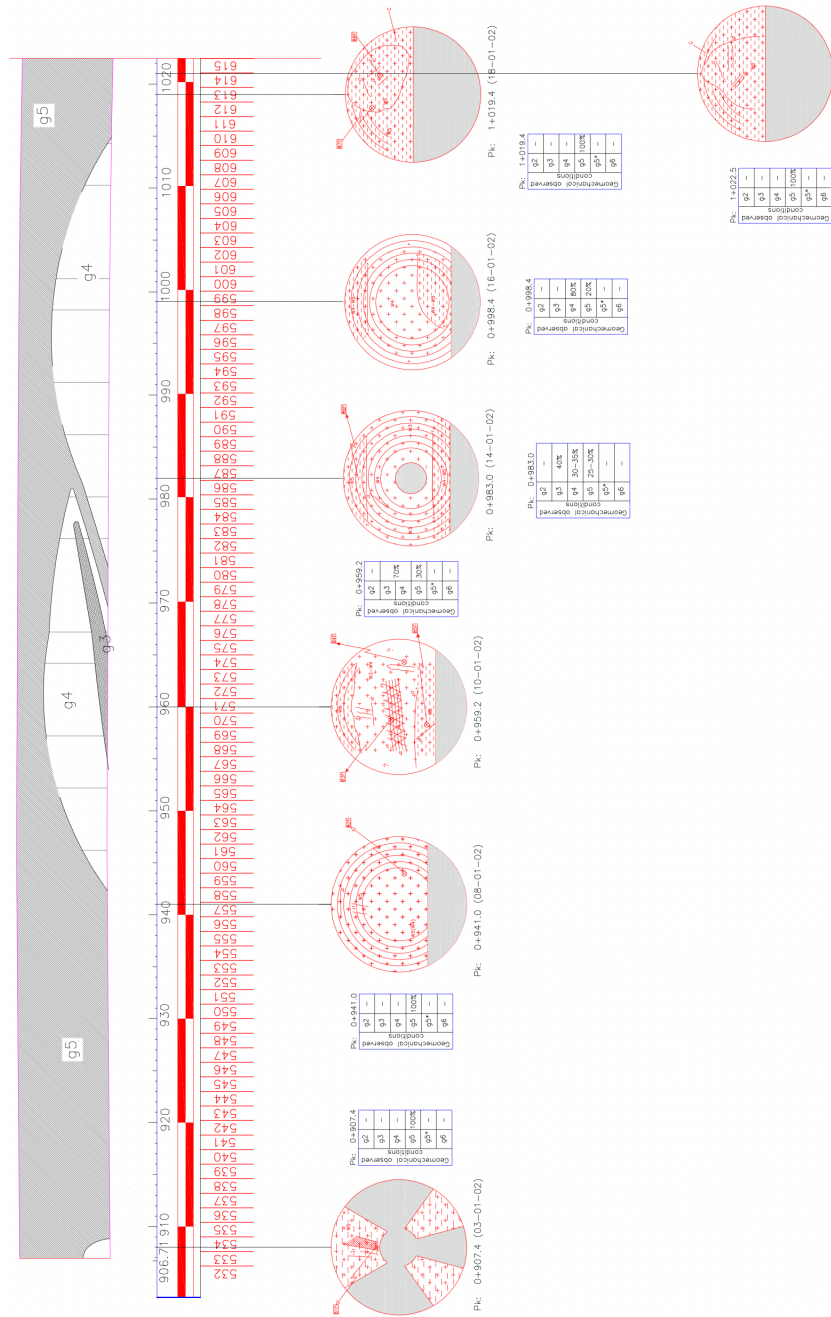


Figure 3-21: Face mappings and corresponding geologic section: Rings 533-610. Courtesy of Normetro.

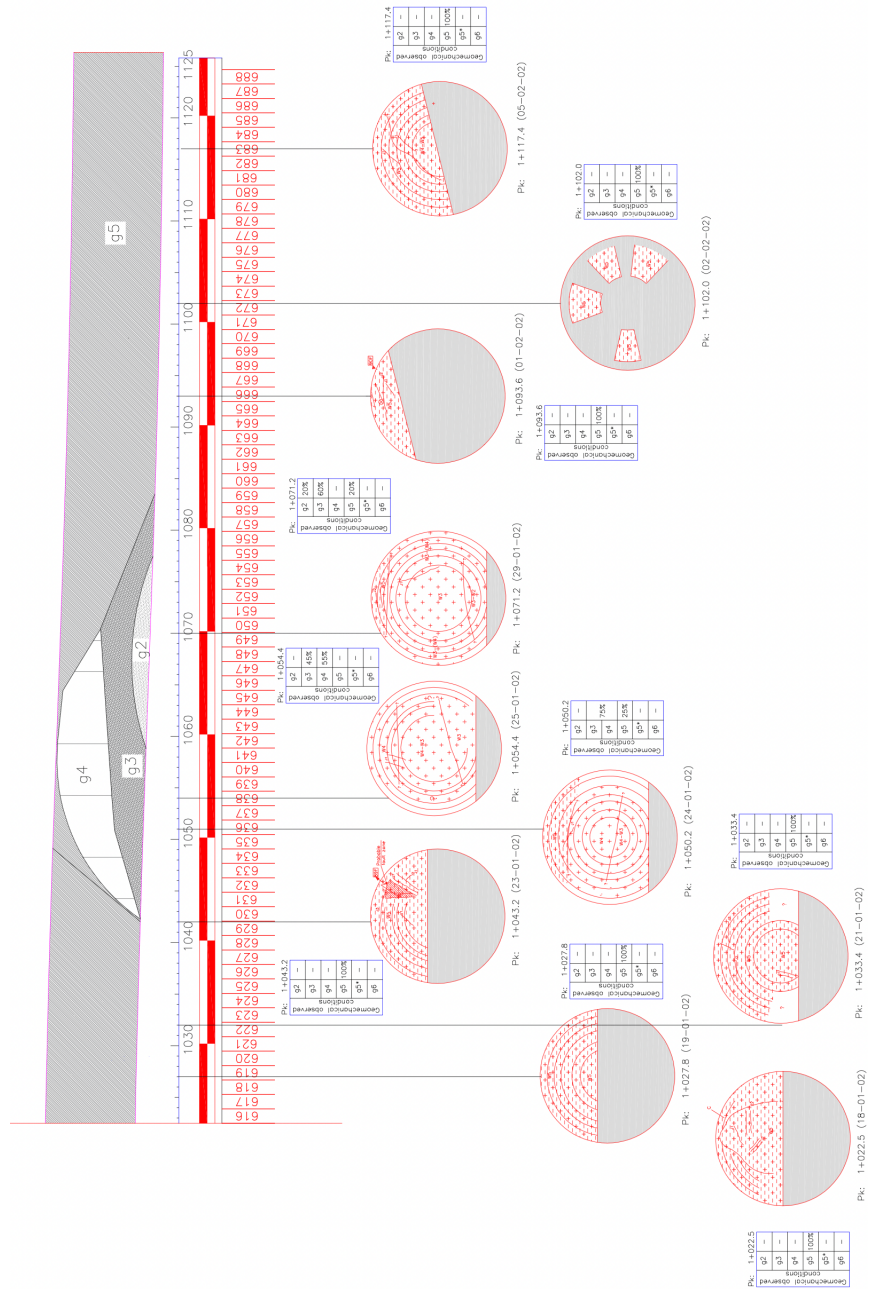


Figure 3-22: Face mappings and corresponding geologic section: Rings 611-689. Courtesy of Normetro.

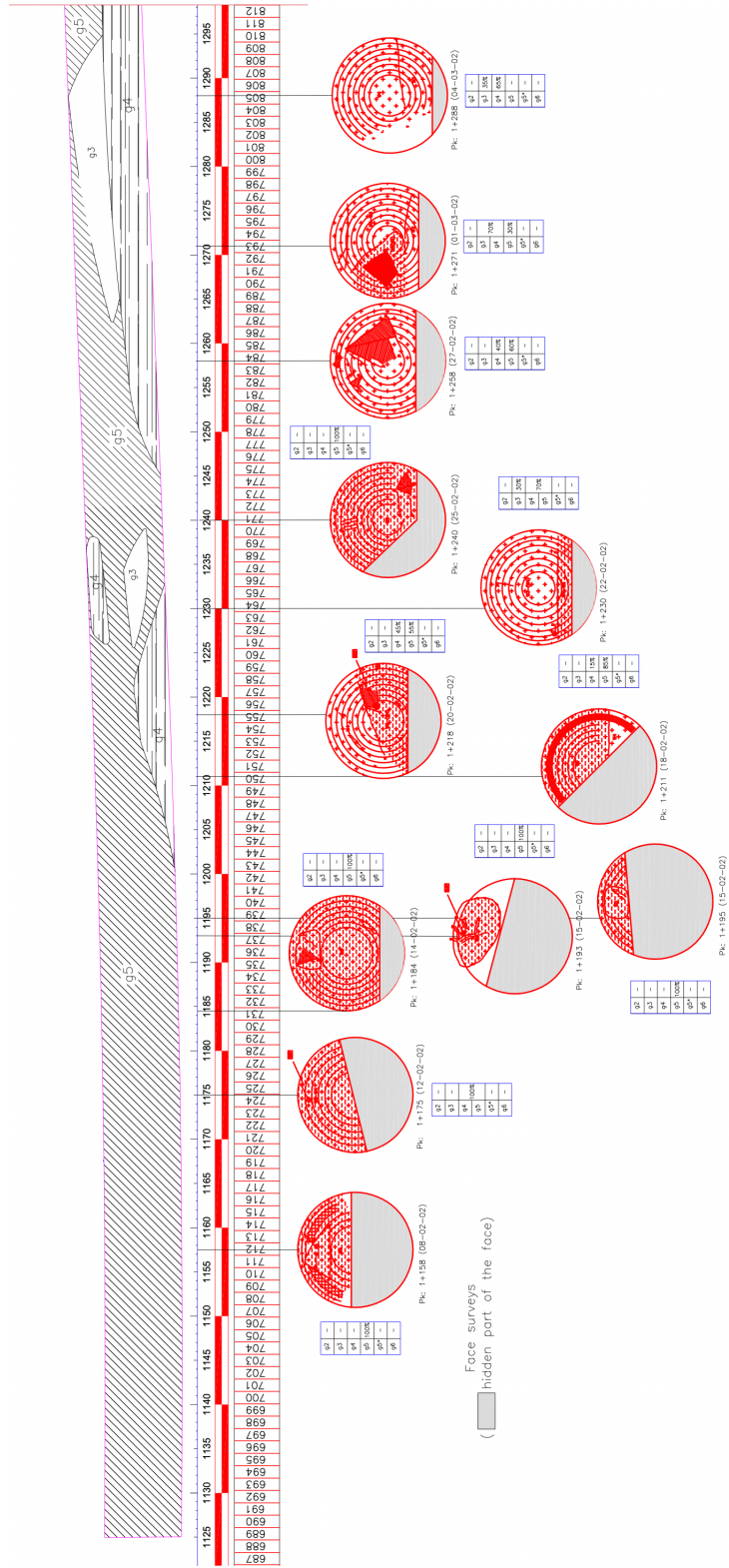


Figure 3-23: Face mappings and corresponding geologic section: Rings 690-814. Courtesy of Normetro.

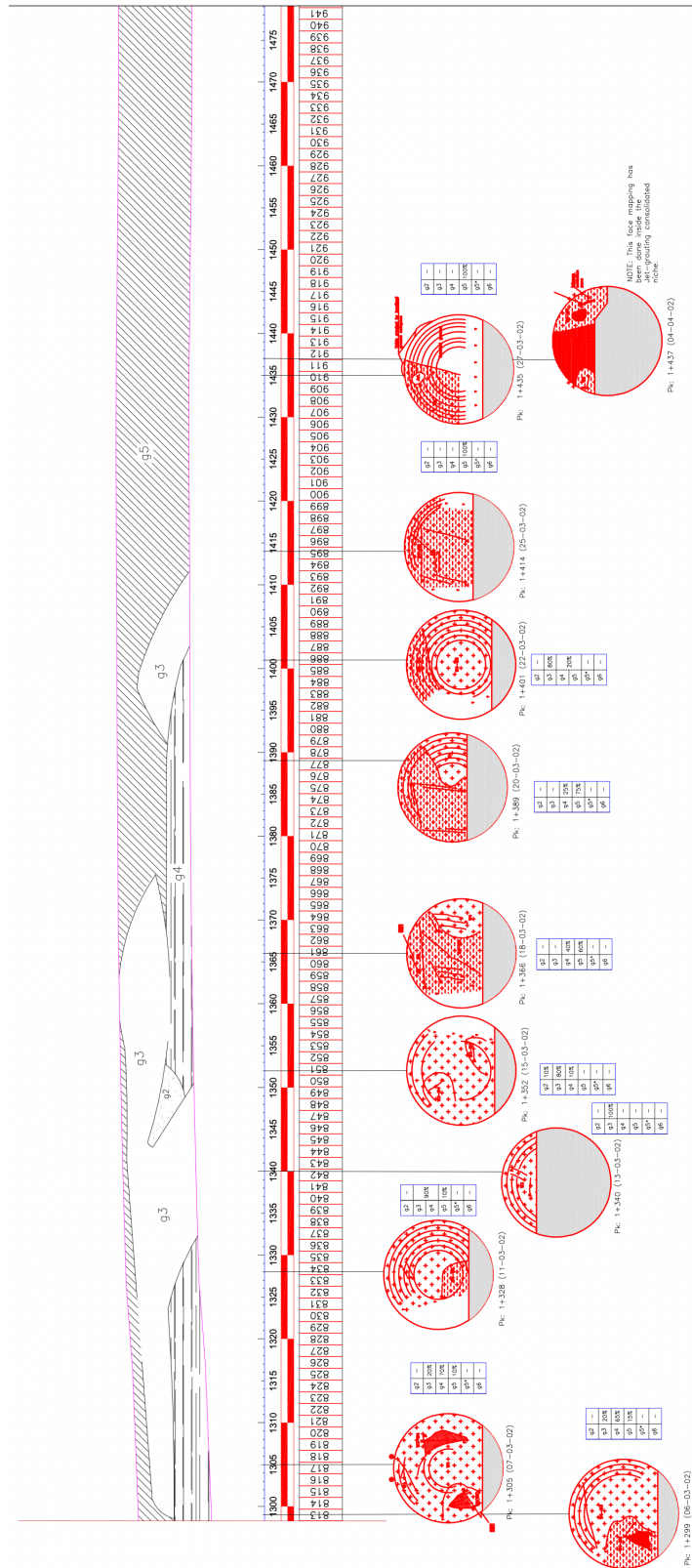


Figure 3-24: Face mappings and corresponding geologic section: Rings 815-942. Courtesy of Normetro.

Chapter 4

Methodology & Results

The purpose of this chapter is to explore the different methods and models used for ground forecasting in TBM tunneling that are advancing automation efforts. While geotechnical site investigations are highly important, they are insufficient to determine a comprehensive geological profile of the tunnel alignment, which is only fully developed on site. Therefore, the use of data-driven geologic predictions are becoming increasingly necessary to improve real-time decision-making in mechanized tunneling.

The chapter will highlight the potential of time series plots and scattergrams in identifying relevant patterns that can be correlated to geology, potentially informing on ground conditions ahead of the tunnel face. The TBM generates a massive data-set on more than 150 parameters at ten-second intervals, but are rarely used to proactively adapt machine operation in real-time. By leveraging machine learning and AI algorithms, it is possible to predict geology a few meters ahead of the tunnel face, which can aid machine operators, prevent accidents, and minimize delays. Ultimately, the chapter aims to demonstrate how the use of these techniques alongside the proposed methodology can improve TBM tunneling efficiency, reduce risks, and increase automation.

4.1 Contextual Aspects of Mechanized Tunneling Automation

Tunneling in urban areas requires minimal surface intrusion due to high population density [Bobet et al., 2019]. To avoid ground subsidence, traditional tunneling projects focus on maintaining ground pressure during and after construction, which can be particularly challenging when dealing with mixed ground or saturated soils [Rostami, 2016, Hencher, 2004]

The unpredictability of real-time geological conditions is a significant challenge in modern tunnelling, despite the development of specific TBMs for such purposes (see section 2.2.2) [Fu et al., 2023]. Illustrating this, a TBM accident in Sao Paulo, Brazil in 2022 was caused by unforeseen geological conditions, resulting in the need for a modified tunnel lining which, subsequently, burst into sewage pipes, ultimately contributing to the collapse of a busy highway (See Figure 4-1) [Garcia, 2022].

TBMs and related systems have significantly reduced tunnel construction costs and time, contributing to the increasing trend of urbanization [Bobet et al., 2019]. With 68% of the world’s human population expected to live in cities by 2050 and indices as high as 90% in OECD countries ¹, tunneling projects are expected to increase [Szabo, 2016]. As a consequence, research into automating tunnel construction is growing, including the use of AI models to predict upcoming ground conditions based on TBM sensor data [Fu et al., 2023, Sun et al., 2018, Xu et al., 2019, Jung et al., 2019]. This development is seen as potentially game-changing. Figure 4-2 displays global expectations of urbanization.

4.1.1 TBM Data

TBMs are equipped with intricate sensors that measure various data-points throughout the cutterhead and body during tunnel construction [Mooney et al., 2012].

¹Organisation for Economic Co-operation and Development, an organization of mostly rich, developed countries dating back to the 1960s. With 38 members the OECD was created to dynamize economic progress and world trade [OECD, 2019].



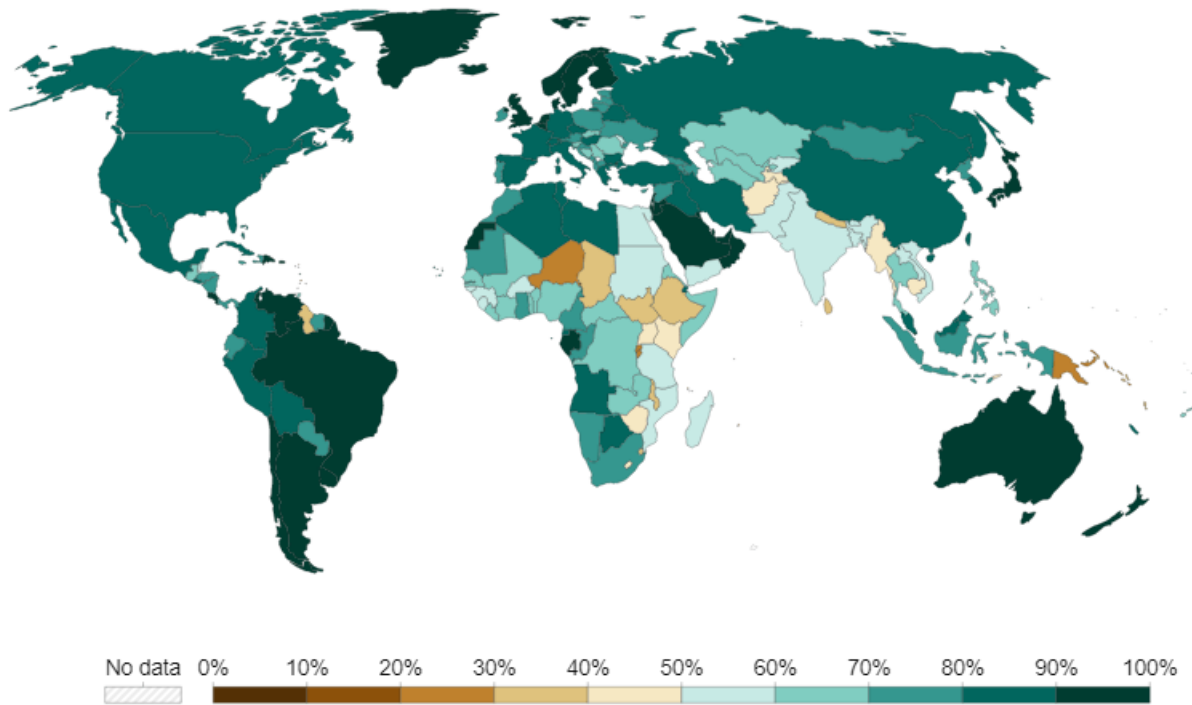
Figure 4-1: Images showing an accident that occurred in the construction of a new metro line in Sao Paulo, Brazil. The accident was caused by unforeseen geological conditions encountered by the TBM (left-hand side) during tunnel construction. A slight course modifications led by adverse ground conditions along the original tunnel line, made the machine's vibration felt on the surface, collapsing a nearby highway and bursting sewage pipes [Garcia, 2022].

Refer to Table 4.1 for the main types of data collected by the machine.

TBM data modeling involves not only collecting and recording sensor data but also analyzing, organizing, and validating it throughout the tunneling process to improve safety and productivity in real-time [Zhang et al., 2019a, Koopialipoor et al., 2019, Guo et al., 2022]. As AI and Machine Learning become more prevalent in data-driven technology, their use in tunneling is starting to emerge, mainly in modeling applications for real-time ground-condition predictions ahead of the tunnel face [Sheil et al., 2020a]. Due to its complexity, numerous variables and unpredictable conditions, efforts to improve tunneling through data-driven decision-making are still in their infancy.

Share of the population living in urban areas, 2050

Share of the total population living in urban areas, with UN urbanization projections to 2050.



Source: OWID based on UN World Urbanization Prospects 2018 and historical sources (see Sources) OurWorldInData.org/urbanization • CC BY
Note: Urban areas are defined based on national definitions which can vary by country.

Figure 4-2: Graph showing the UN’s prediction on urbanization rates by 2050 [Ritchie and Roser, 2018]).

4.1.2 The Future of Tunneling

In seeking to improve tunnel construction, stakeholders are increasing operational speed and cost-effectiveness, given the growing need for transport and space in cities [National Research Council, 2009, Vertovec, 2015]. However, the protracted pace of conventional TBM operations has led to challenges in meeting increasing demand. To illustrate this, Figure 4-3 shows the projected growth of the global TBM market over the next decade.

Efforts to improve tunnel construction aim to reduce time spent underground, with increased productivity approaches ranging from full autonomous operation of the machine to incremental improvements like reducing the need for installing supporting

Data Type	Description	Examples
Location	Information on the machine's location	Geo-location, position, heading and orientation, etc
Speed/Progressing	Information on TBM speed	Velocity, Advance rates, etc.
Performance	Data on the machine's performance rates	Power consumption, torque screw, thrust force, amongst other operational parameters.
Geology	Data on ground conditions	Rock/soil type and sometimes composition, groundwater data and subsurface conditions.
Safety	Data on machine and operator safety	Temperature, humidity, air quality, etc.
Maintenance	Information regarding the need for machine maintenance	Wear and tear of cutterheads and other components, operating status of machine components.

Table 4.1: General classification of TBM-output data.

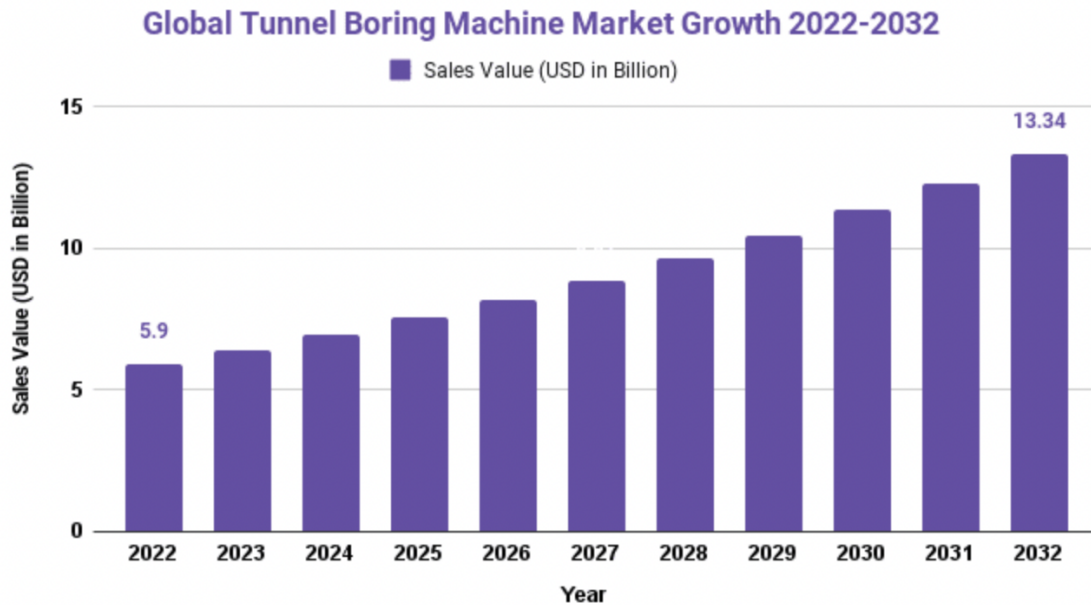


Figure 4-3: Graph showing the predicted growth of the Tunnel Boring Machine (TBM) Market [Pasalkar, 2023]).

concrete rings [Sebbeh-Newton et al., 2021]. These improvements are critical as the need for underground infrastructure increases due to urbanization and global climate change [Cedergren, 2013].

At the forefront of this contemporary age of tunneling, Malaysia's contributions to tunneling include the variable density Tunnel Boring Machine (see Figure 4-4), which can modify the density of excavated material by varying slurry pressure in the cutterhead [Mass Rapid Transit Corporation, 2013]. This TBM can be used in unpredictable or frequently altering ground conditions as well as in contaminated soil [Herrenknecht, 2013].

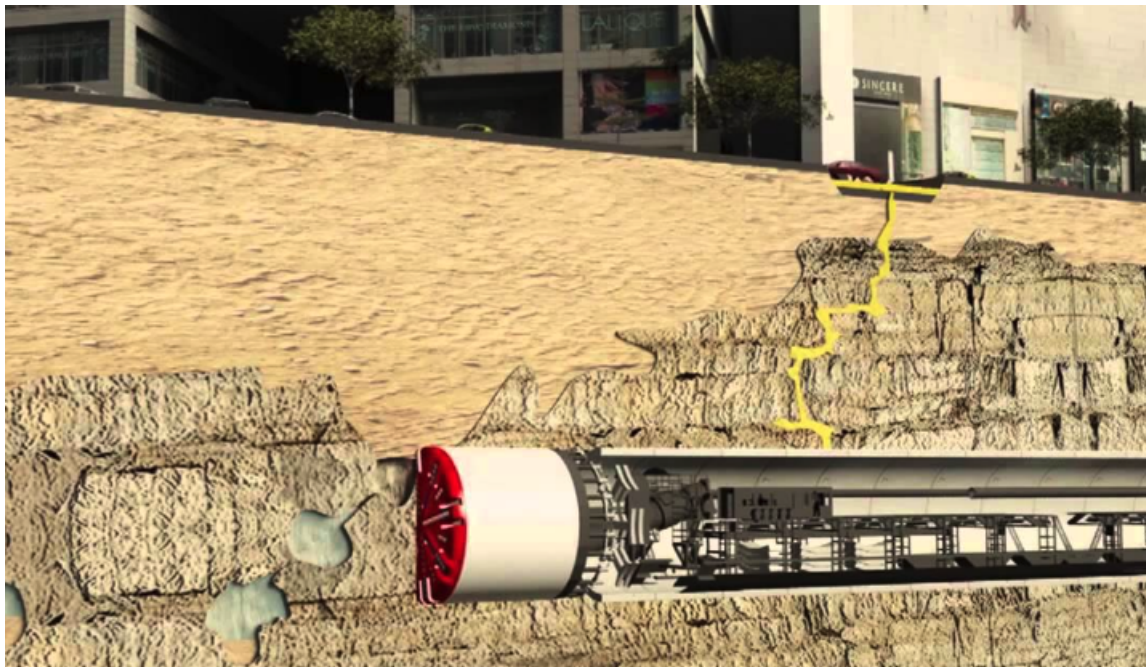


Figure 4-4: A computational rendering of the variable density TBM operating in Malaysia [Mass Rapid Transit Corporation, 2013]).

Malaysia deployed the first fully Autonomous Tunnel Boring Machine (ATBM) system (Figure 4-5), controlled by an Artificial Intelligence (AI) system to increase productivity, precision and worksite safety [Byrd, 2016, Berhad, 2019]. Further research and development is needed to better integrate AI systems and the TBM's constant data output, but have shown promising results .



Figure 4-5: Image of the ATBM being setup in a large public transport infrastructure construction site in Malaysia, 2018 [Byrd, 2016]).

4.2 An Introduction to Artificial Intelligence and Machine Learning

AI refers to machine-generated simulations of human thought and intelligence [Nilsson, 1982]. Machine Learning (ML) is focused on producing statistical models and algorithms that allow for computational systems to automatically increase performance through experience [Girasa and Girasa, 2020, Alzubi et al., 2018]. Three main types of machine learning are supervised learning, semi-supervised learning, and unsupervised learning. The present study will focus on a semi-supervised ML algorithm, known as Confidence Learning (explained in further detail in section 5.2).

Data labeling in machine learning refers to the process of assigning predefined tags or categories to data to make them understandable and usable for ML algorithms [Nilsson, 1982]. It involves manual or automated annotation of data, which

simplifies the recognition process for ML models, making it easier for the model to recognize patterns and make predictions [Alzubi et al., 2018]. Specifically, data labeling adds metadata to raw data, allowing them to be used as an input for ML models [Nilsson, 1982, Alzubi et al., 2018]. Refer to Table 4.2 for characteristics and commonly used algorithms for each type of machine learning [Suthaharan, 2016, Rajoub, 2020].

Machine Learning Type	Description	Algorithms
Supervised Learning	Most commonly used. Trains a model based on data that were previously labeled.	Linear Regression, Decision Trees, Neural Networks, k-Nearest Neighbors, Support Vector Machines (SVMs)
Unsupervised Learning	Combines supervised and unsupervised learning using some labeled data and a large amount of unlabeled data.	Self-training, Co-training, Multi-task learning, Generative Adversarial Networks (GANs).
Semi-Supervised Learning	Trains a model based on unlabeled data-sets, where the outcome is not known.	Clustering, Principal Component Analysis (PCA), Autoencoder, Single Value Decomposition (SVD).

Table 4.2: Machine Learning classification and examples [Dasgupta and Nath, 2016].

4.2.1 Previous work in Geology Prediction using TBM Data

Tunnel Boring Machines (TBMs) are a safe and efficient method of tunnel construction, especially in densely populated areas, offering advantages over conventional drilling and blasting [Singh and Singh, 2006]. However, the uncertainty of ground conditions can lead to delays, increased costs, and accidents, emphasizing the need for better geotechnical investigation [Ruwanpura et al., 2004, Záruba, 2012].

Geotechnical site investigations are important but insufficient to determine a comprehensive geological profile of tunnel alignment [Soldo et al., 2019]. Data-driven

geological predictions can improve real-time decision-making in TBM operations, advancing tunnel automation technology [Sebbeh-Newton et al., 2021]. TBM activity is highly dependent on trained operators to monitor generated parameter data [Garcia et al., 2021]. The main operational thresholds observed by the operator are predetermined, which can be uncertain or incoherent with real-world conditions [Sun et al., 2018].

Currently, TBM data are rarely used to proactively adapt machine operation despite having sensors that generate data on more than 150 parameters at ten-second intervals [Sun et al., 2018]. Adverse ground conditions are responsible for most occurrences of machine jamming and damage, over-excavation and cost increases in TBM operations [Sousa and Einstein, 2012, Sousa and Einstein, 2021]. With more than 30% of incidents directly related to human error, efforts to increase automation have the potential to revolutionize the industry [Hammerer, 2015].

Machine Parameter Information

TBM performance depends on the machine’s ability to adapt to subsurface changes [Yu et al., 2022]. However, geological variations and machine intermittence can make the acquired data inconsistent and inefficient [Yu et al., 2022]. Mathematical models that predict ground conditions and forecast geology in real-time can reduce risks and improve decision-making [Liu et al., 2020]. Artificial Intelligence can aid machine operators by predicting geology a few meters ahead of the tunnel face, minimizing delays and accidents [Zheng et al., 2023].

To mitigate risks and uncertainties associated with tunnel construction, mathematical models that predict ground conditions and forecast geology in real-time can be used [Liu et al., 2020]. These models can improve the decision-making process and prevent accidents by predicting geology a few meters ahead of the tunnel face, which makes Artificial Intelligence a useful tool to aid machine operators and minimize delays [Zheng et al., 2023]. As cities grow alongside demand for tunneling, it is becoming increasingly essential to focus on the risks associated with this infrastructure [Flyvbjerg, 2010].

Use of Data-Driven Modeling in Geology Prediction

Studies spanning over several decades have aimed to improve prediction of ground conditions in tunneling construction. Earlier research focused on using TBM penetration rates to estimate costs and construction time [Li et al., 2017]. Recently, models based on TBM data focus on risk reduction, such as predicting ground subsidence and other accident indicators [Liu et al., 2023].

AI techniques have improved data-driven modelling by making models more reliable, given enough data to train machine learning algorithms [Reichstein et al., 2019]. As the TBM generates huge data-sets stemming from more than 200 sensors, it is an ideal use case for training AI/ML models [Sheil et al., 2020b].

ML algorithms analyze and detect patterns in the data without explicit knowledge of physical interactions or mathematical relationships in the system being studied [Carleo et al., 2019], making data-driven modeling particularly useful for problems with uncertainty and complexity where detailed modeling can be computationally costly or unfeasible [Zhang et al., 2019b]. However, as will be presented with the proposed methodology, aligning these computational methods to physical interpretation of data can improve the quality and validity of AI/ML models.

Recent Studies

Table 4.3 below shows some of the most recent studies on geology prediction in tunnel operations using TBM-generated machine learning models.

Table 4.3: Papers on use of Machine Learning (ML) algorithms for geology prediction using TBM-generated data.

Source	ML Type	Model	Data (Parameters Used)
Cao et. al., 2019	Unsupervised	Concept Drift	331
Zhang et. al., 2019	Unsupervised	K-means Clustering	5
Shi et. al., 2019	Supervised	Deep Neural Network (DNN)	53
Zhao et. al., 2019	Supervised	Artificial Neural Network (ANN)	72
Liu et. al., 2020	Supervised	AdaBoost-CART	10
Kim et. al., 2020	Supervised	Deep Neural Network (DNN)	10
Nagresha et. al., 2020	Supervised	Recurrent Neural Network (RNN)	5
Sebbeh-Newton et. al., 2020	Supervised	Random Forest (RF)	-
Wang et. al., 2020	Supervised	XGBoost	155
Liu et. al., 2021	Supervised	Long-Short Term Memory (LSTM)	12
Bai et. al., 2021	Supervised/ Unsupervised	LR, DTR, SVR, GBR	25
Continued on next page			

Table 4.3 – Continued from previous page

Source	ML Type	Model	Data (Parameters Used)
Gong et. al., 2021	Computer Vision	Convolution Neural Network (CNN)	3
Hou et. al., 2021	Supervised	Stacking Ensemble Classifier	10
Wu et. al., 2021	Unsupervised	Spectral Clustering	10
Yu et. al., 2021	Semi-Supervised	Sparse Autoencoder	20
Zhang, 2022	Semi-Supervised	Generative Adversarial Network (GAN)	69
Yu et. al., 2022	Semi-Supervised	Convolution Dense Autoencoder	177
Yin et. al., 2022	Unsupervised	Gaussian Mixture Model (GMM)	5
Jin et. al., 2022	Supervised	Long-Short Term Memory (LSTM)	-
Yang et. al., 2022	Unsupervised	K-means Clustering	6
Fu et. al., 2022	Unsupervised	Shared Nearest Neighbor (SNN)	-
Pan et. al., 2022	Supervised	Deep Neural Network (DNN)	-

Continued on next page

Table 4.3 – Continued from previous page

Source	ML Type	Model	Data (Parameters Used)
Wang et. al., 2023	Supervised	Reccurent-unit Neural Network (C-GRU)	-
Fu et. al., 2023	Supervised	Long-Short Term Memory (LSTM)	12
Liu et. al., 2023	Supervised	Deep Neural Network (DNN)	5

4.2.2 Porto Metro Data

In this study, TBM-data from the construction of Line C of the Porto Metro project were utilized. The data consisted of 182 parameters recorded every ten seconds over an approximately one-mile length (Rings 354 - 1611). Data pre-processing involved removing instances where the Advance Rate was zero, to focus on patterns and correlations between ground conditions and TBM-generated data. The machine is typically stopped due to the installation of structural concrete rings placed every meter of excavation, or the occurrence of technical difficulties, accidents. Figure 4-6 below shows a diagram of the EPBM TBM used in the Porto Metro project studied in this thesis.

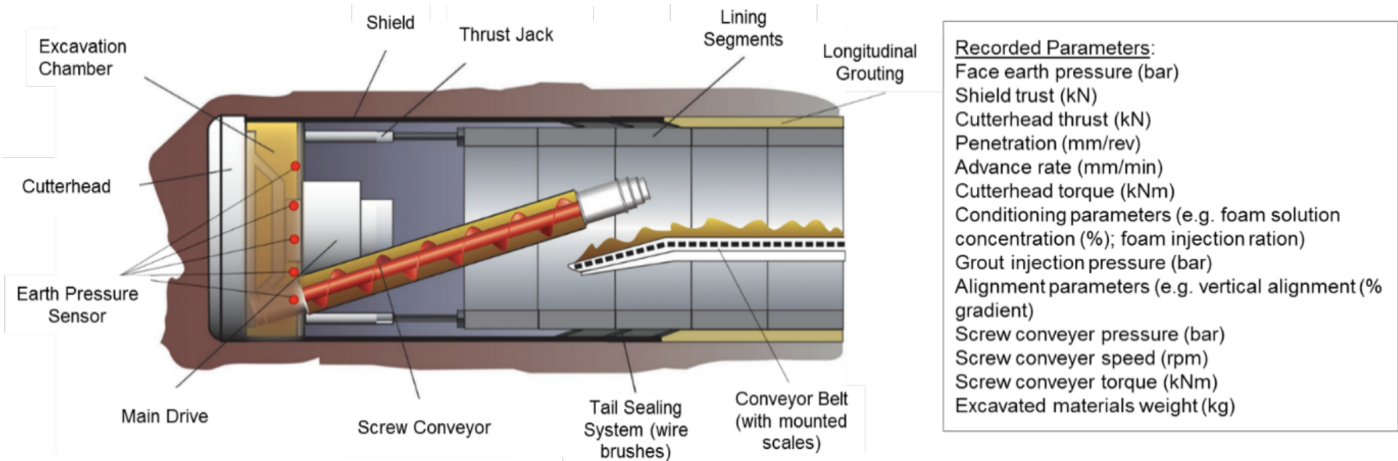


Figure 4-6: Diagram of the EPBM TBM used during the excavation of the Line C tunnel of the Porto Metro project [Guglielmetti et al., 2008].

Unnecessary data can be removed to improve the accuracy of AI/ML models and graphical visualizations, as well as to focus on correlations. Figure 4-7 shows a sample of a ring's data-set where machine parameter data is recorded. MATLAB version R2022b was used to generate results.

DATE	TIME	RING	ST	W0001	W0002	W0003	W0004	W0005	W0011	W0012	W0013	W0014	W0019	W0020	W0102	W0103	W0104	W0105	W0106	W0107
20.03.2002	03:10:15	877	2	2.676	4.750	5099.000	20403.000	-2.930	1	0	1	0	1	0	9.000	11.000	14.000	27.000	34.000	79.000
20.03.2002	03:10:25	877	2	7.107	4.910	5589.000	23447.000	9.370	1	0	1	0	1	0	10.000	13.000	12.000	27.000	32.800	79.000
20.03.2002	03:10:35	877	2	6.749	5.430	6283.000	24531.000	9.000	1	0	1	0	1	0	9.000	12.000	14.000	27.000	32.600	79.000
20.03.2002	03:10:45	877	2	8.584	5.940	6804.000	25128.000	11.410	1	0	1	0	1	0	10.000	12.000	13.000	27.000	32.000	79.000
20.03.2002	03:10:55	877	2	7.680	6.460	7577.000	25600.000	13.980	1	0	1	0	1	0	10.000	12.000	14.000	28.000	32.200	80.000
20.03.2002	03:11:05	877	2	8.185	7.030	8296.000	26012.000	12.570	1	0	1	0	1	0	9.000	11.000	13.000	28.000	31.700	79.000
20.03.2002	03:11:15	877	2	7.799	7.230	8819.000	26598.000	13.630	1	0	1	0	1	0	10.000	13.000	12.000	28.000	31.600	79.000
20.03.2002	03:11:25	877	2	7.918	7.670	9139.000	26661.000	14.730	1	0	1	0	1	0	9.000	11.000	14.000	28.000	32.000	79.000
20.03.2002	03:11:35	877	2	9.155	8.000	9484.000	27022.000	15.470	1	0	1	0	1	0	11.000	13.000	13.000	28.000	32.200	80.000
20.03.2002	03:11:45	877	2	7.461	8.280	9482.000	26480.000	16.390	1	0	1	0	1	0	10.000	12.000	15.000	28.000	31.500	79.000
20.03.2002	03:11:55	877	2	7.433	8.370	9484.000	26449.000	9.570	1	0	1	0	1	0	9.000	11.000	13.000	29.000	32.100	79.000
20.03.2002	03:12:05	877	2	6.758	8.130	9607.000	27653.000	9.260	1	0	1	0	1	0	10.000	13.000	12.000	29.000	31.700	79.000
20.03.2002	03:12:15	877	2	6.932	8.260	9698.000	28211.000	17.380	1	0	1	0	1	0	9.000	11.000	14.000	29.000	32.100	80.000
20.03.2002	03:12:25	877	2	8.264	8.620	9806.000	27741.000	13.520	1	0	1	0	1	0	11.000	13.000	12.000	29.000	31.800	80.000
20.03.2002	03:12:35	877	2	7.836	8.580	9934.000	27422.000	16.610	1	0	1	0	1	0	10.000	12.000	15.000	29.000	31.600	80.000
20.03.2002	03:12:45	877	2	6.625	8.650	10061.000	27288.000	15.480	1	0	1	0	1	0	9.000	11.000	13.000	30.000	32.000	79.000
20.03.2002	03:12:55	877	2	7.619	8.580	10308.000	27458.000	16.380	1	0	1	0	1	0	10.000	13.000	13.000	30.000	31.400	79.000
20.03.2002	03:13:05	877	2	7.069	8.360	10255.000	27503.000	16.060	1	0	1	0	1	0	9.000	12.000	14.000	30.000	31.700	79.000
20.03.2002	03:13:15	877	2	6.767	8.150	10227.000	27619.000	14.520	1	0	1	0	1	0	11.000	13.000	12.000	30.000	31.100	79.000
20.03.2002	03:13:25	877	2	6.845	8.260	10520.000	28148.000	14.440	1	0	1	0	1	0	10.000	12.000	15.000	30.000	31.500	79.000
20.03.2002	03:13:35	877	2	6.897	8.360	10512.000	28019.000	14.270	1	0	1	0	1	0	9.000	11.000	13.000	31.000	31.900	79.000
20.03.2002	03:13:45	877	2	5.789	8.010	10325.000	28207.000	15.760	1	0	1	0	1	0	10.000	12.000	14.000	31.000	31.300	79.000
20.03.2002	03:13:55	877	2	5.837	8.270	10529.000	28714.000	12.050	1	0	1	0	1	0	9.000	11.000	14.000	31.000	31.300	79.000
20.03.2002	03:14:05	877	2	5.536	8.470	10635.000	28784.000	12.790	1	0	1	0	1	0	11.000	13.000	12.000	31.000	31.500	80.000
20.03.2002	03:14:15	877	2	5.536	8.470	10457.000	28768.000	13.190	1	0	1	0	1	0	9.000	12.000	14.000	31.000	30.900	79.000
20.03.2002	03:14:25	877	2	5.374	8.170	10678.000	29124.000	12.980	1	0	1	0	1	0	10.000	11.000	13.000	31.000	31.200	79.000
20.03.2002	03:14:35	877	2	4.608	8.710	10841.000	29049.000	12.690	1	0	1	0	1	0	10.000	13.000	13.000	31.000	31.900	79.000
20.03.2002	03:14:45	877	2	5.522	8.560	10628.000	28739.000	13.600	1	0	1	0	1	0	9.000	11.000	14.000	31.000	31.400	79.000
20.03.2002	03:14:55	877	2	5.942	8.380	10577.000	28993.000	15.460	1	0	1	0	1	0	10.000	13.000	12.000	32.000	31.100	79.000
20.03.2002	03:15:05	877	2	6.181	8.610	10906.000	29007.000	15.670	1	0	1	0	1	0	9.000	12.000	14.000	32.000	31.400	79.000
20.03.2002	03:15:15	877	2	4.581	8.690	10678.000	28562.000	17.270	1	0	1	0	1	0	10.000	11.000	13.000	32.000	31.300	79.000
20.03.2002	03:15:25	877	2	5.562	8.490	10608.000	28633.000	14.210	1	0	1	0	1	0	10.000	13.000	13.000	32.000	31.200	79.000
20.03.2002	03:15:35	877	2	4.702	8.920	10913.000	28658.000	18.170	1	0	1	0	1	0	9.000	11.000	14.000	32.000	30.800	79.000
20.03.2002	03:15:45	877	2	4.718	8.970	10856.000	28512.000	18.310	1	0	1	0	1	0	11.000	13.000	12.000	32.000	30.900	80.000
20.03.2002	03:15:55	877	2	6.206	8.650	10515.000	28317.000	17.100	1	0	1	0	1	0	9.000	12.000	14.000	33.000	31.500	79.000
20.03.2002	03:16:05	877	2	5.681	8.600	10909.000	28391.000	18.080	1	0	1	0	1	0	10.000	11.000	13.000	33.000	31.100	79.000
20.03.2002	03:16:15	877	2	5.731	8.840	11055.000	28305.000	18.380	1	0	1	0	1	0	10.000	12.000	14.000	33.000	31.300	79.000
20.03.2002	03:16:25	877	2	6.044	8.540	10498.000	27515.000	20.160	1	0	1	0	1	0	9.000	11.000	13.000	33.000	30.900	79.000
20.03.2002	03:16:35	877	2	4.529	8.600	10371.000	27289.000	16.610	1	0	1	0	1	0	10.000	13.000	12.000	33.000	31.200	79.000
20.03.2002	03:16:45	877	2	7.102	8.490	10493.000	27814.000	13.130	1	0	1	0	1	0	9.000	12.000	14.000	33.000	31.300	79.000
20.03.2002	03:16:55	877	2	7.023	8.580	10657.000	29502.000	16.160	1	0	1	0	1	0	10.000	12.000	13.000	33.000	31.100	79.000
20.03.2002	03:17:05	877	2	6.304	8.840	10966.000	30514.000	17.000	1	0	1	0	1	0	10.000	12.000	15.000	34.000	30.700	79.000
20.03.2002	03:17:15	877	2	6.876	9.010	11317.000	30691.000	20.150	1	0	1	0	1	0	9.000	11.000	14.000	34.000	30.800	79.000
20.03.2002	03:17:25	877	2	7.836	9.030	11540.000	31095.000	19.660	1	0	1	0	1	0	10.000	13.000	13.000	34.000	31.000	79.000

Figure 4-7: Sample data-set for a soil tunnel section (Ring 877). Where W0001-W107 represent different parameters.

4.3 Relating Ground Conditions to Machine-Generated Data

4.3.1 Proposed Approach

Results from this study aimed to evaluate the validity of machine learning models in determining ground classes from TBM-generated parameter data. The goal was to assign each ring to either rock, soil, and mixed ground classes using a systematic framework, which is presented below.

1. Studied the parameters recorded by the machine and their physical implications.
2. Determined parameters that offer insight into ground conditions.
3. Plotted these parameters against time and machine status (linear plots).
4. Established which pairs of parameters are important to compare through the use of scatter-plots.
5. Plotted these pairwise parameters in scatter-plots and 3-D histograms.
6. Checked most significant correlations and parameter pairs.
7. Labeled (rock, soil or mixed) each evaluated ring based on graphical representations.
8. Verified label accuracy and cross-referenced to available geological and geotechnical information as well as face-mappings carried out during construction.

4.3.2 Evaluated Parameters

Out of 182 parameters recorded by the TBM, 26 were selected for analysis based on their physical implications and possible correlation to geological conditions. Tables 4.4 and 4.5 display the parameters plotted against time and machine status and those plotted against each other in scattergrams, respectively. The selection process of each

parameter is explained, and an evaluation of its accuracy in determining the potential ground class of the ring (rock, soil, or mixed) is provided. A coefficient ranging from one to ten is used to assess the relevance of each parameter in AI/ML models aimed at predicting geology using TBM-generated data.

Parameters Plotted Against Time
Thrust Force x Cutting Wheel Speed of Rotation
Pressure Force Cutting Wheel x Thrust Force
Torque Cutting Wheel x Pressure Force Cutting Wheel
Penetration x Torque Screw
Penetration x Thrust Force
Penetration x Advanced Speed
Penetration x Actually Excavated Material Flow Belt, Quantity of Excavated Material (Advance), Quantity of Excavated Material (Total)
Actually Excavated Material x Quantity Excavated Material 1
Cutting Wheel Speed of Rotation x Cutting Wheel High Pressure, Thrust Pressure
Penetration x Torque Cutting Wheel, Pressure Force Cutting Wheel, Thrust Force, Torque Screw, Actually Excavated Material, Quantity of Excavated Material
Thrust Pressure x Thrust Pressure Groups A, B, C, D, E, F
Thrust Pressure Groups A, B, C, D, E, F

Table 4.4: Time-series plots.

Scatter Plots
Torque Cutting Wheel x Pressure Force Cutting Wheel
Thrust Force x Pressure Force Cutting Wheel
Penetration x Torque Screw
Penetration x Actually Excavated Material
Penetration x Advance Speed
Penetration x Thrust Force
Penetration x Screw Conveyor Speed Measuring
Penetration x Screw Conveyor Pressure
Penetration x Earth Pressure 1
Penetration x Quantity Excavated Material 1 (Total)
Penetration x Quantity Excavated Material 2 (Advance)
Penetration x Quantity Excavated Material 2 (Total)
Advance Speed x Screw Conveyor Speed Measuring
Thrust Force x Cutting Wheel Speed of Rotation

Table 4.5: Scatter plots.

4.3.3 Importance of Chosen Parameters

The parameters evaluated were selected based on existing literature and physical understandings of their correlation to ground conditions.

"Thrust force", which indicates the pressure exerted on the ground during tunneling, is a widely used indicator of geological conditions. Studies on squeezing ground have assessed thrust force, as shown in previous works [Mohammadzamani et al., 2019, Ramoni and Anagnostou, 2010, Hasanpour et al., 2018]. Zhou et al. (2015) have demonstrated the use of thrust force in predicting total thrust in mechanical models, which can reflect global trends and geological conditions [Zhou et al., 2015]. Thrust force, measured in kilo-Newtons (kN), is a crucial parameter for analyzing TBM operations.

"Pressure force cutting wheel" evaluates the force applied to the TBM's cutterhead while digging. It, along with other related parameters such as cutting wheel speed of rotation and torque, have been used to verify or understand geological conditions during tunneling. Studies have looked at using the pressure force cutting wheel to improve cutterhead design [Entacher et al., 2012], improve performance in breaking through hard-rock [Pan et al., 2018, Wang et al., 2020], and predict penetration rates [Li et al., 2022].

Also related to TBM cutterheads, "Torque cutting wheel" measures the rotational force exerted in TBM cutterheads. This important metric has been widely used to improve cutterhead design and inform machine operators and project stakeholders on the impact of the digging process on the machine [Li et al., 2022, Liu et al., 2015]. As cutterhead damage and replacement can cause significant TBM stoppages and repairs, it is crucial to evaluate and understand this metric in order to enhance tunneling productivity. The torque cutting wheel transmits torque from the TBM's drive system to its cutterheads for excavation [Gehring, 2009]. The cutters are designed to fracture the ground and remove excavated material, and the torque cutting wheel applies the necessary force to the cutters [Cigla et al., 2001].

"Penetration rate" provides valuable information about ground conditions encoun-

tered during tunneling and have been widely explored in efforts to automate tunnel construction. Studies such as Gao et al. (2021) using ML [Gao et al., 2021], Jain et al. (2015) correlating ground conditions to machine-generated data in Mumbai [Jain et al., 2015], and Sousa (2010) exploring automation and prediction of ground conditions [Sousa, 2010] have all utilized penetration rates. By monitoring changes in penetration rate, machine operators can optimize the excavation process and adjust relevant TBM parameters to ensure maximum efficiency [Mahdevari et al., 2014]. Additionally, penetration rate data can be used to calibrate geological models and refine geotechnical understanding, reducing the risk of construction delays, cost overruns, and safety issues [Gong et al., 2007]. Correlation with geology is critical, making penetration rate one of the most important TBM parameters [Benato and Oreste, 2015].

Within the TBM, torque screw, controls the speed and force of the cutting head and machine advancement [Girmscheid, 2003]. It is usually measured through torque sensors installed on the drive motors and/or gearboxes powering the TBM (typically at the rear of the machine) [Girmscheid, 2003]. The torque screw is a long, threaded rod that is driven into rotation by the drive motor, using it to push the cutterhead forward [Girmscheid, 2003].

As torque screw serves as a better indicator of the resistance encountered by the TBM as it advances, it produces a more direct and accurate measure of ground reactionary forces [Sutcliffe, 1996]. Which in turn can be translated into useful information on geological conditions. It is measured in kilo-newtons-meter [kNm].

Thrust force, measured by pressure sensors on hydraulic jacks, is an important TBM parameter that can help correlate geology and predict ground conditions [Girmscheid, 2003, Farrokh and Rostami, 2008]. It is the force exerted by the TBM on the tunnel face to advance and is influenced by factors such as ground geology, TBM type and design, and pre-established operating parameters [Girmscheid, 2003]. Hydraulic pressure, advance rate, and torque cutting wheel can also provide information on thrust force [Girmscheid, 2003].

"Advance speed", measured in millimeters per minute [mm/min], is a crucial parameter in TBM operations, representing the rate at which the machine progresses

through the ground. Sensors throughout the machine's body, including those measuring cutting wheel rotation, cutterhead movement, and machine displacement, are used to monitor advance speed [Sutcliffe, 1996]. While not widely explored in the literature as a means of predicting geology, real-time monitoring of advance speed can provide valuable insights into the geological conditions being encountered and inform machine operators and project engineers to adjust the TBM's operating parameters, optimizing performance and ensuring safe and efficient tunnel excavation [Eftekhari et al., 2010, Girmscheid, 2003, Cigla et al., 2001].

The "Actually excavated material flow belt" informs on the conveyor system used to transport excavated material out of the tunnel [Girmscheid, 2003]. Through the analysis of the material being excavated and transported, operators can gain insight into the geology of the surrounding material. Thus identify potential hazards and changes in ground conditions that may affect the excavation process. Quantity of Excavated Material (Advance) refers to the amount of material excavated during a given time period [Sutcliffe, 1996]. This measure can provide information on the efficiency of the TBM and effectiveness of the excavation process [Girmscheid, 2003]. Similarly, quantity of excavated material (Total) is a cumulative measure referring to the total material excavated by the TBM [Girmscheid, 2003].

"Cutting wheel speed of rotation" measures the speed of the cutterhead, which directly impacts the rate of excavation [Wu et al., 2021]. Cutting wheel high pressure measures the pressure of the slurry (or water) used to remove excavated material from the tunnel face [Wu et al., 2021]. Lastly, thrust pressure measures the force being applied by the machine to advance into the rock or soil [Hasanpour et al., 2018].

Thrust pressure, as aforementioned, represents the pressure exerted by the TBM against the tunnel face in advancing. Thrust pressure groups A-F refer to different levels of thrust pressure that are used by the TBM to excavate through different geological formations [Bilgin, 2016]. These parameters are typically recorded at the machine's hydraulic jacks or cylinders [Entacher et al., 2012].

4.3.4 Correlating Graphical Data to Ground Conditions

Through physical understanding of machine parameters and the results we have obtained, it has become clear that comparing specific parameters and plotting them against each other produces interesting graphical patterns that can be attributed to specific ground classes. These patterns provide valuable insight into the geological conditions that the tunneling machine is operating in, and can be used to optimize the tunneling process.

Time series plots of TBM performance parameters, such as thrust, torque, cutter-head speed, and advance rate, demonstrate cyclical patterns that are characteristic of different ground classes. For example, in soft soil conditions, the TBM will typically encounter a smoother and more consistent cycle than in harder rock conditions, where the cycle is more irregular and erratic, which can be identified graphically. By analyzing these patterns, it may be possible to predict changes in geological conditions and adjust TBM operation accordingly.

Similarly, scattergrams show correlations between different variables that output characteristic patterns that can be attributed to either soil, rock, or mixed ground conditions. By analyzing these correlations, it is possible to identify changes in geological conditions that affect TBM performance, such as the transition from soft ground to hard rock.

The use of time series plots and scattergrams can be a powerful tool for correlating TBM-generated data with geology, allowing for a better understanding of ground conditions and the ability to adjust TBM operations accordingly. These techniques can aid in predicting changes in geological conditions and optimizing the tunneling process, ultimately leading to more efficient and effective tunnel construction.

4.3.5 Tunnel Sections Analyzed

Parameter data from over 20 rings were plotted for 26 different parameter combination comparisons. Below, Table 4.6 lists the rings evaluated in this study.

Ring Section	Selected Rings
Up to 533	461, 477, 513
533 - 610	552, 557, 598
611 - 689	613, 615, 619, 623, 630, 650
690 - 814	720, 784
815 - 942	816, 834, 842, 851, 853, 877, 886
After 942	1134, 1233, 1310

Table 4.6: Rings analyzed in the present study, from Ring 461 to 1310.

4.4 Results

As for each parameter combination there are 20 rings with the same number of plots, the presented results will display a sample of all the generated plots. This section will present, for all proposed parameters, a ring classified as rock, soil, rock-like mixed and soil-like mixed.

4.4.1 Time-series Plots

Time-series plots can help analyze TBM operational data and ground class designation for accurate geology prediction in real-time. By tracking machine parameters over time, it is possible to identify changes in geology and TBM performance, as well as the evolution of ground classes along the tunnel rings. This information can be used to adjust excavation strategies, refine geological predictions, leading to more accurate tunnel designs and better risk management. This section will provide examples of these plots for rock, soil, and mixed ground classes, offering a physical interpretation for each parameter pair comparison.

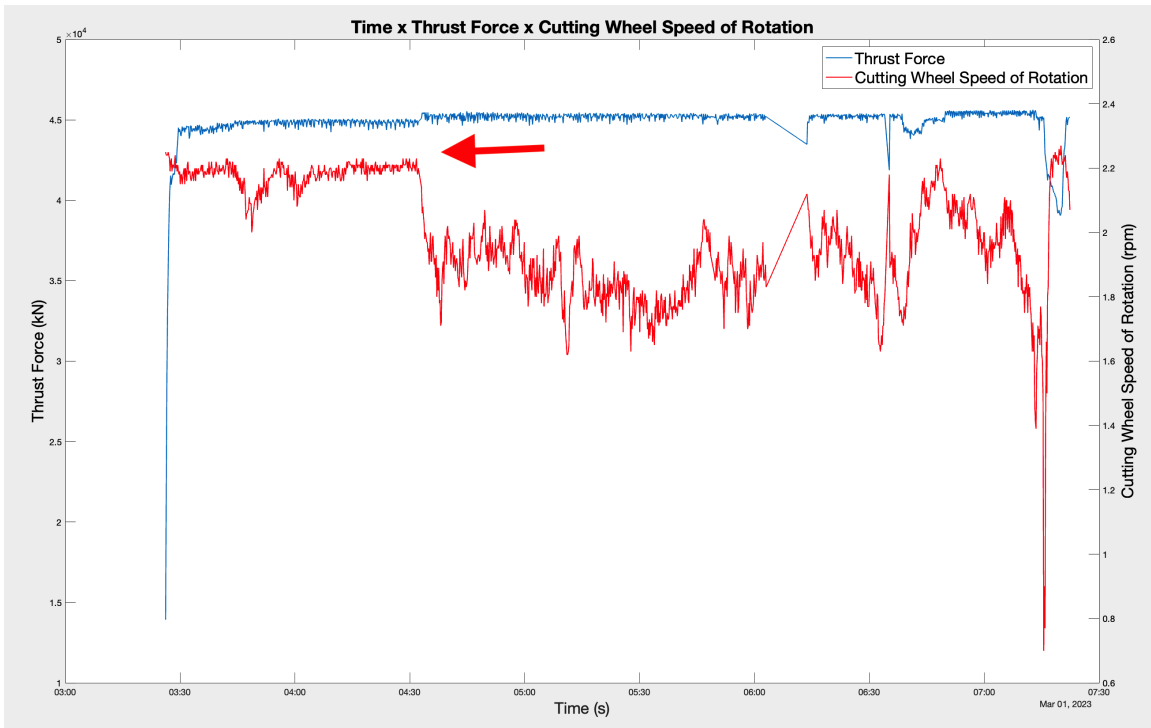
Time x Thrust Force x Cutting Wheel Speed of Rotation

The speed at which the cutting wheel rotates is an important parameter that can provide information about the type of ground being excavated. By comparing the thrust force and the speed of rotation, distinct patterns can be observed between different types of ground.

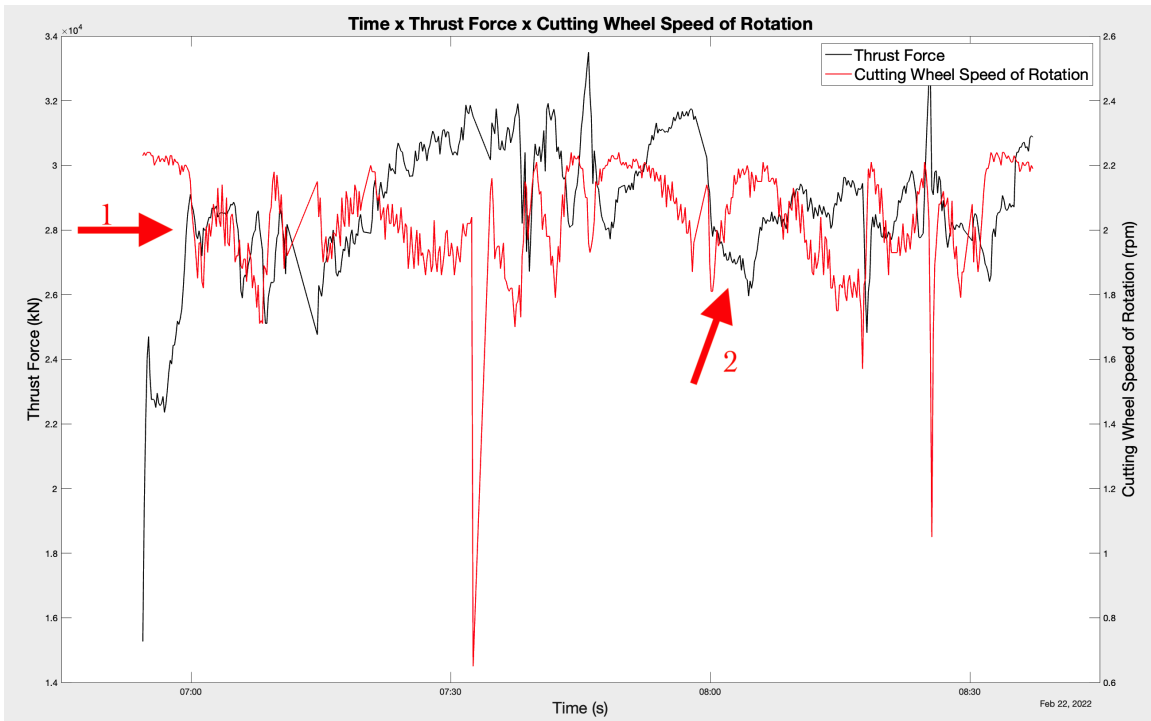
For example, if the speed of rotation increases, it suggests the presence of harder

material like rock, which requires the machine to work harder and advance at a slower speed. Conversely, if the speed is more consistent, it indicates the potential presence of soils. Figures 4-8 and 4-9 illustrate examples of rock, rock-like mixed, soil, and soil-like mixed rings.

This page intentionally left blank.

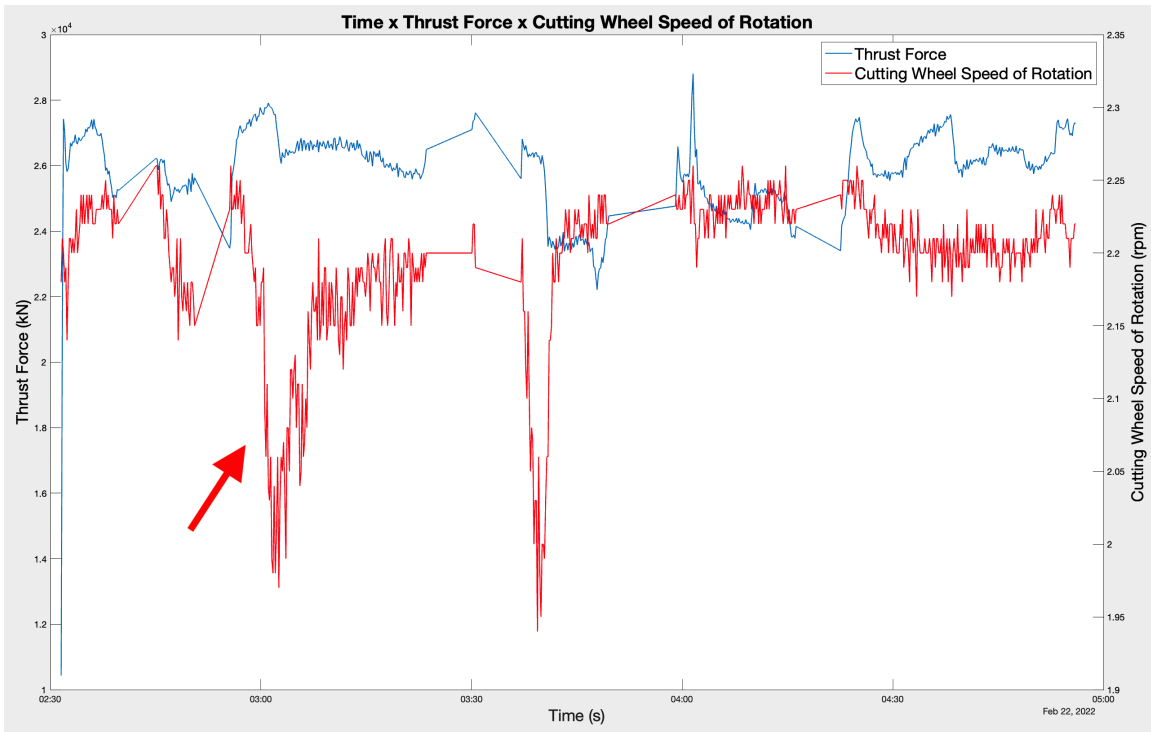


(a) Ring 842: Rock. Very concentrated "peaks" and "valleys" can be noted. The red arrow indicates the specific patterns seen in both variables in harder, rock-like material.

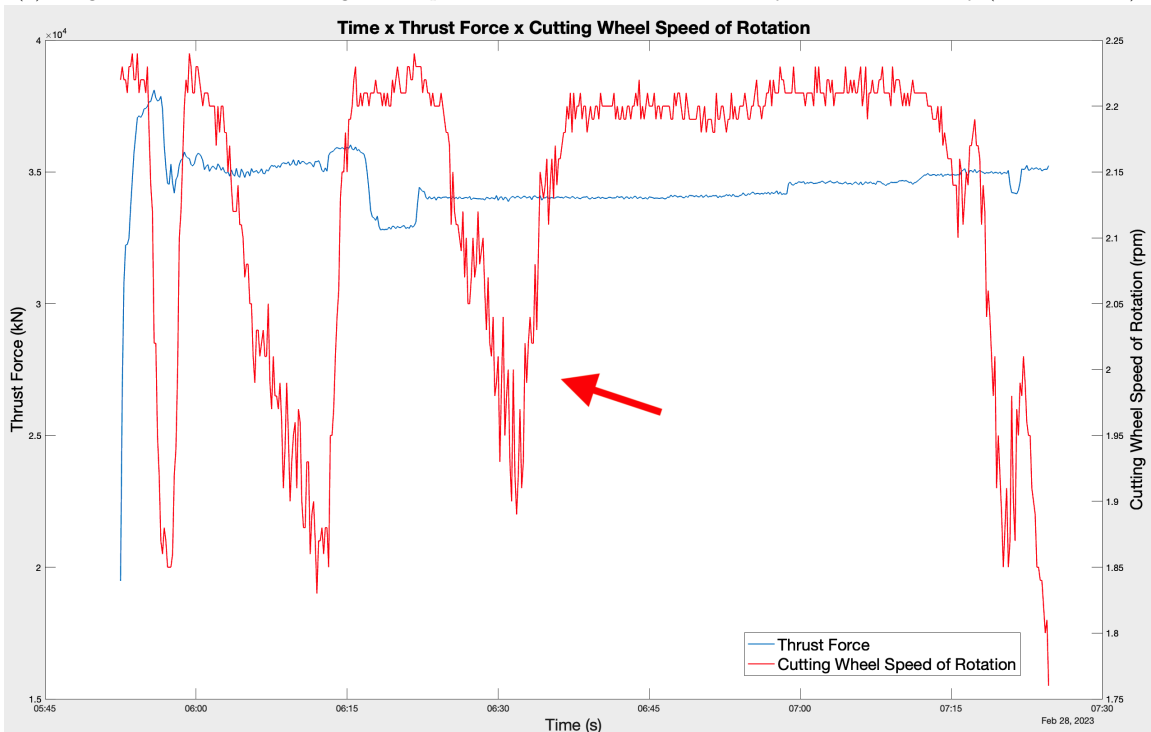


(b) Ring 598: Rock-like mixed. Where both rock-like and soil-like patterns can be observed. Arrow 1 indicates a positive correlation between the parameters, and Arrow 2 shows negative correlation between parameters.

Figure 4-8: Time series plots relating Thrust Force and Cutting Wheel Speed of Rotation for rock and rock-like mixed.



(a) Ring 557: Soil. Where cutting wheel speed of rotation can be seen to vary much more starkly (see indication).



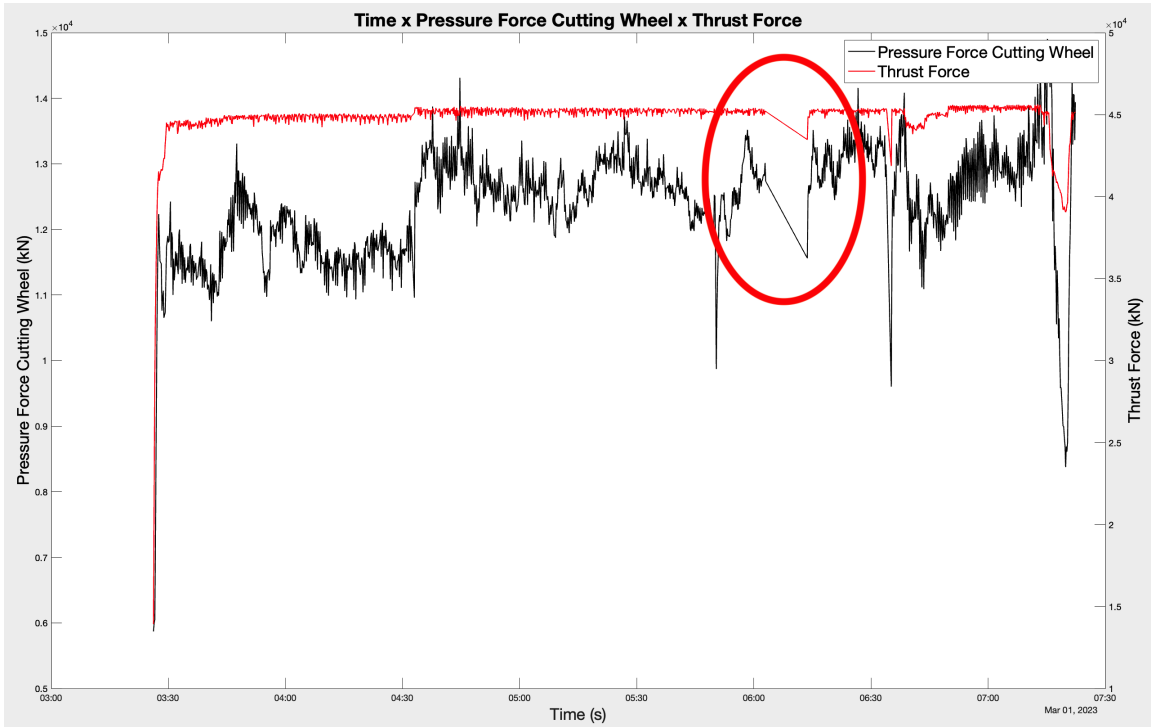
(b) Ring 613: Soil-like mixed. Again variability is present. As soil-like material is much more heterogeneous, the machine must constantly adapt to keep running at consistent speeds.

Figure 4-9: Time series plots relating Thrust Force and Cutting Wheel Speed of Rotation for soil and soil-like mixed.

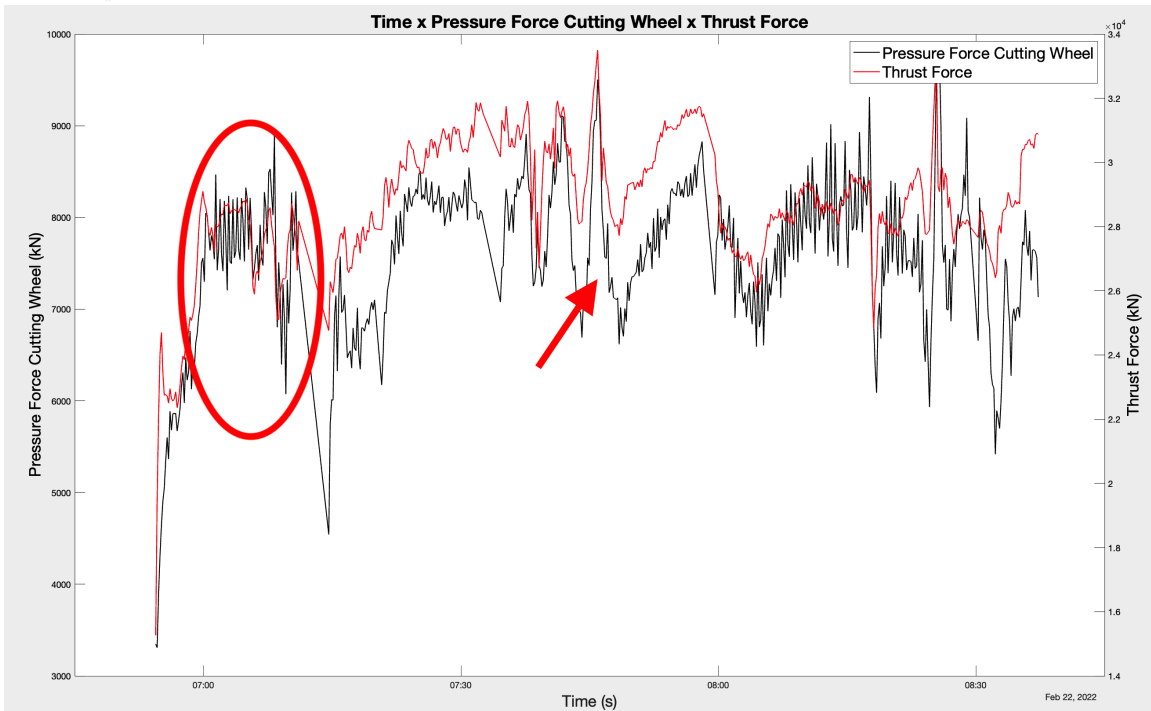
Time x Pressure Force Cutting Wheel x Thrust Force

Thrust force is an important parameter that can predict the total thrust on Tunnel Boring Machines (TBMs) and potentially relate it to surrounding ground conditions. To better correlate machine-generated data to ground class classification, comparing thrust force to pressure force cutting wheel can reveal distinct patterns, especially between rock and soil. The pressure force cutting wheel is expected to follow similar patterns to the thrust force. Sample plots for rock, soil, and mixed rings are illustrated in Figures 4-10 and 4-11.

This page intentionally left blank.

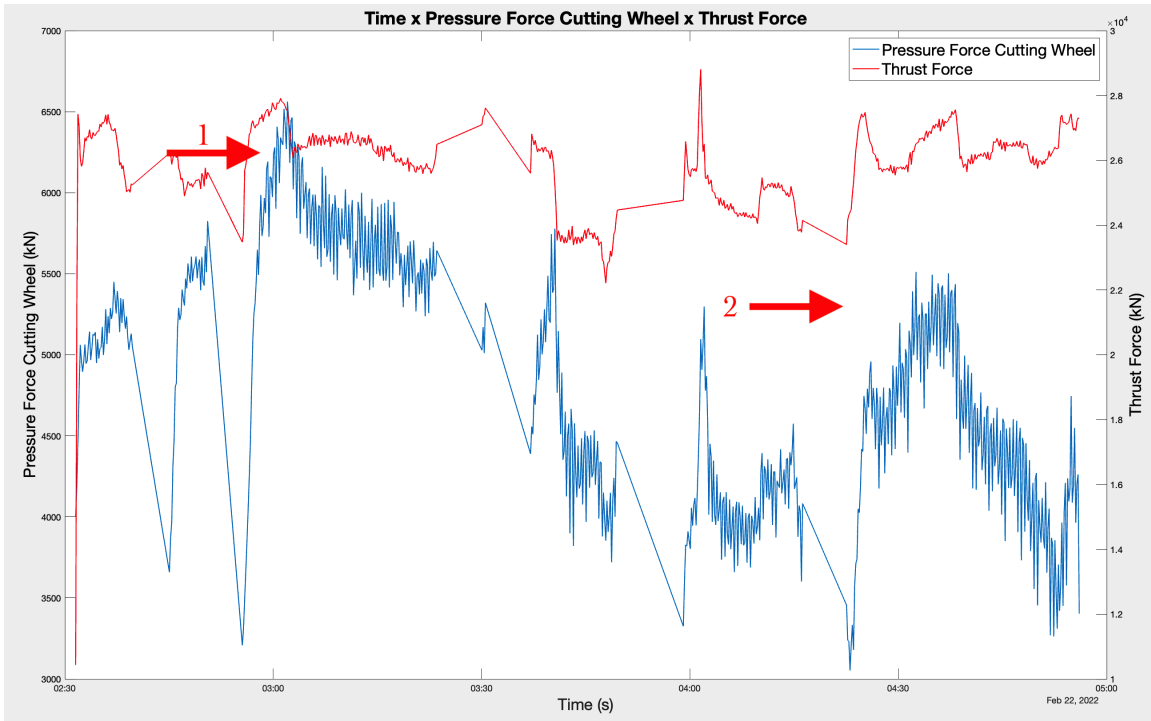


(a) Ring 842: Rock. Again one can see significant variation in both parameters, where the "up" and "down" movement of the curves is prevalent. The red circle indicates a region where one can see similar behavior patterns in both evaluated parameters.

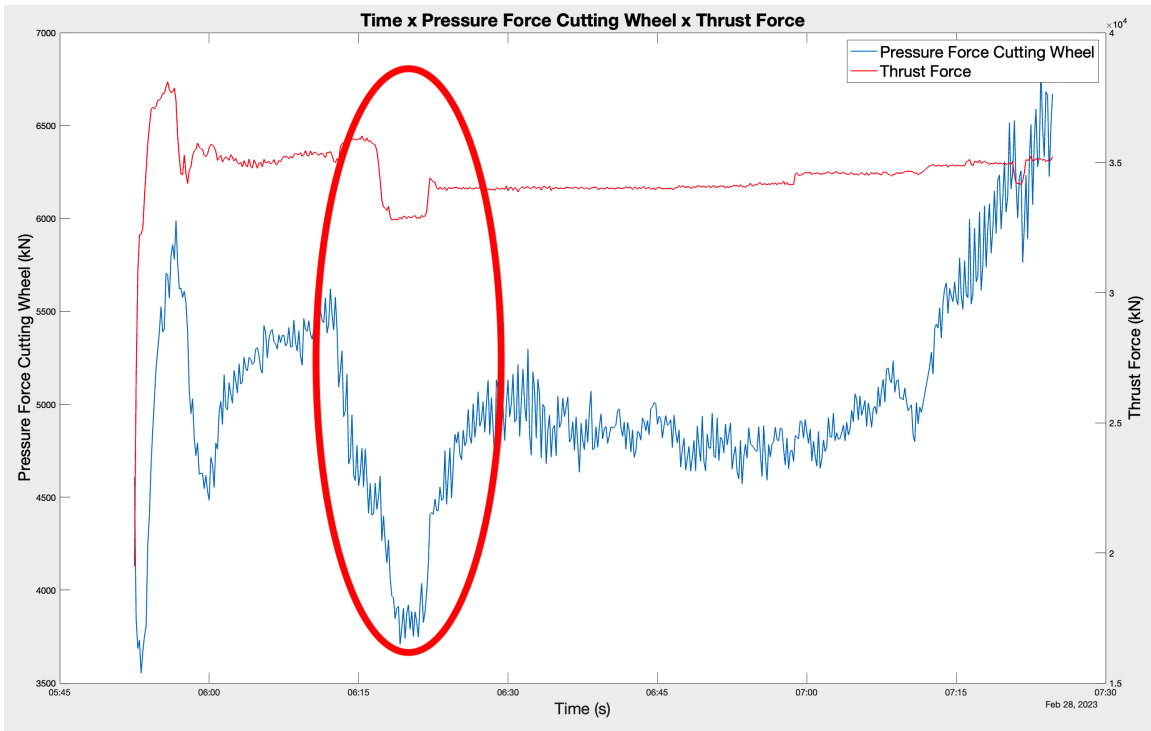


(b) Ring 598: Rock-like mixed. The red circle indicates a region where one can see overlap between parameters. While the arrow indicates a region where both pressure force cutting wheel and thrust force are following the same pattern.

Figure 4-10: Time series plots relating Pressure Force Cutting Wheel and Thrust Force for rock and rock-like mixed.



(a) Ring 557: Soil. Arrow 1 indicates a region where parameters show overlap, indicating the positive relationship between them. Arrow 2 shows that both parameters have similar patterns throughout the ring.



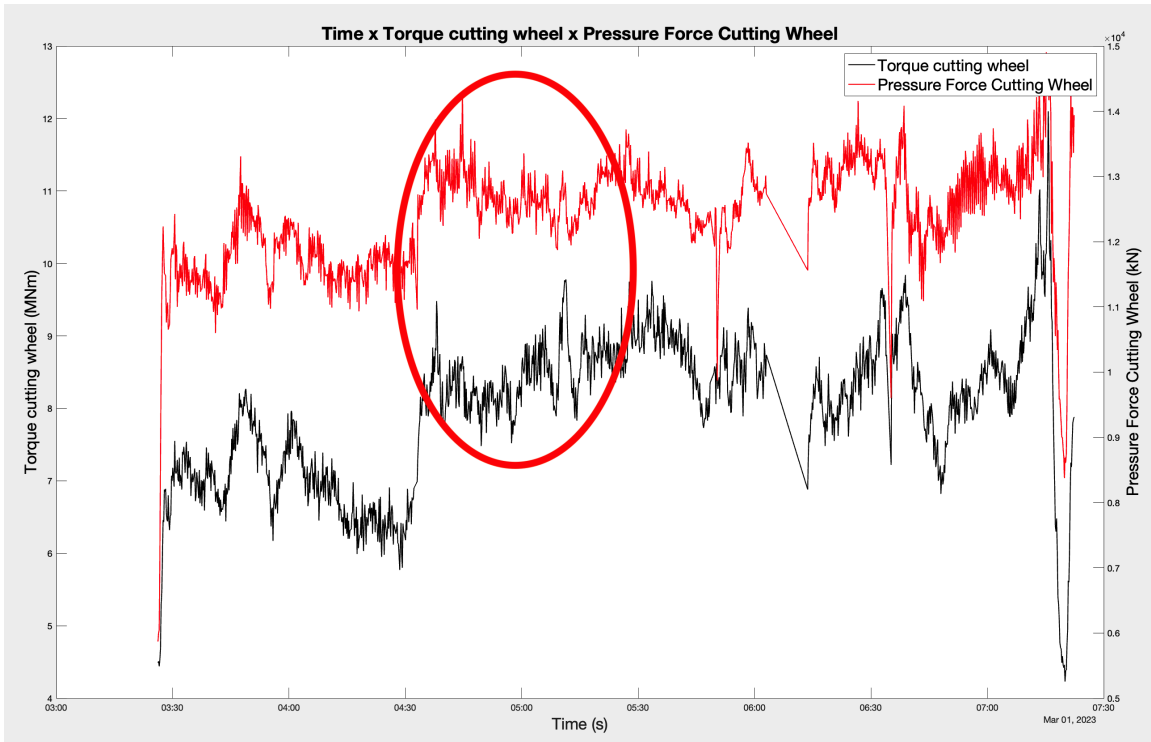
(b) Ring 613: Soil-like mixed. The red circle indicates a sample region where both parameters follow similar patterns.

Figure 4-11: Time series plots relating Pressure Force Cutting Wheel and Thrust Force for soil and soil-like mixed.

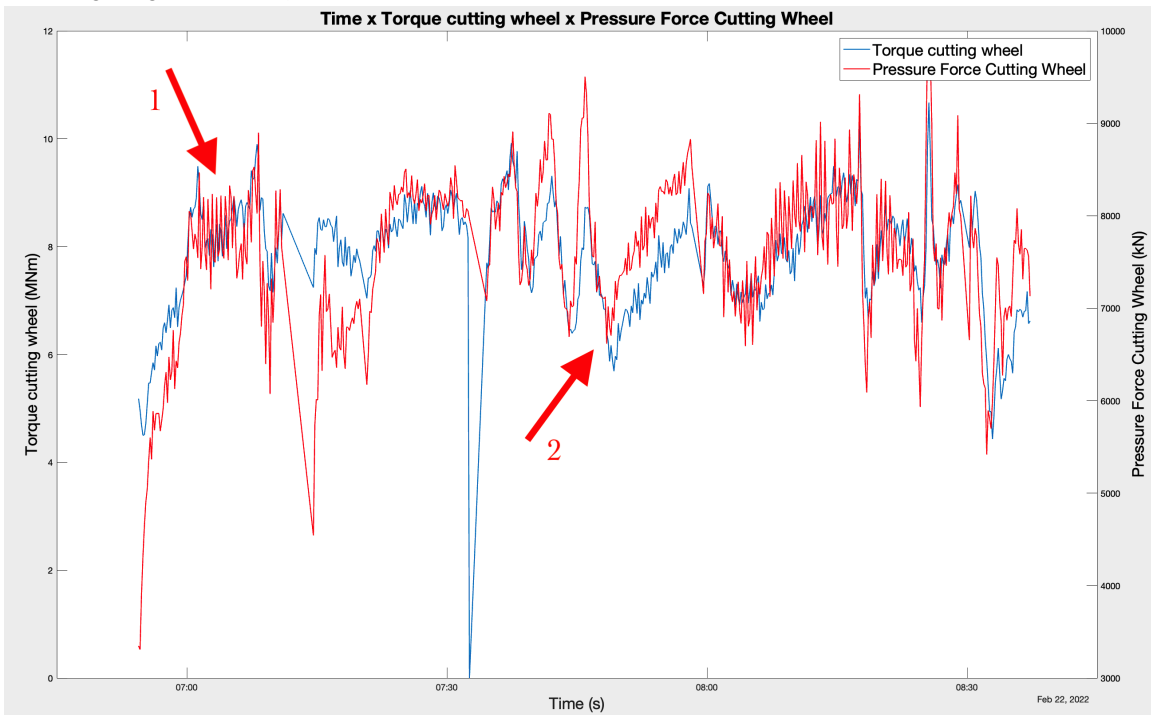
Time x Torque Cutting Wheel x Pressure Force Cutting Wheel

The combination of torque cutting wheel and pressure force cutting wheel can be a useful metric for predicting geology by correlating machine data to ground conditions. Both parameters relate to forces applied on the cutterheads. Figures 4-12 and 4-13 demonstrate the correlations for rock and soil-like material.

This page intentionally left blank.

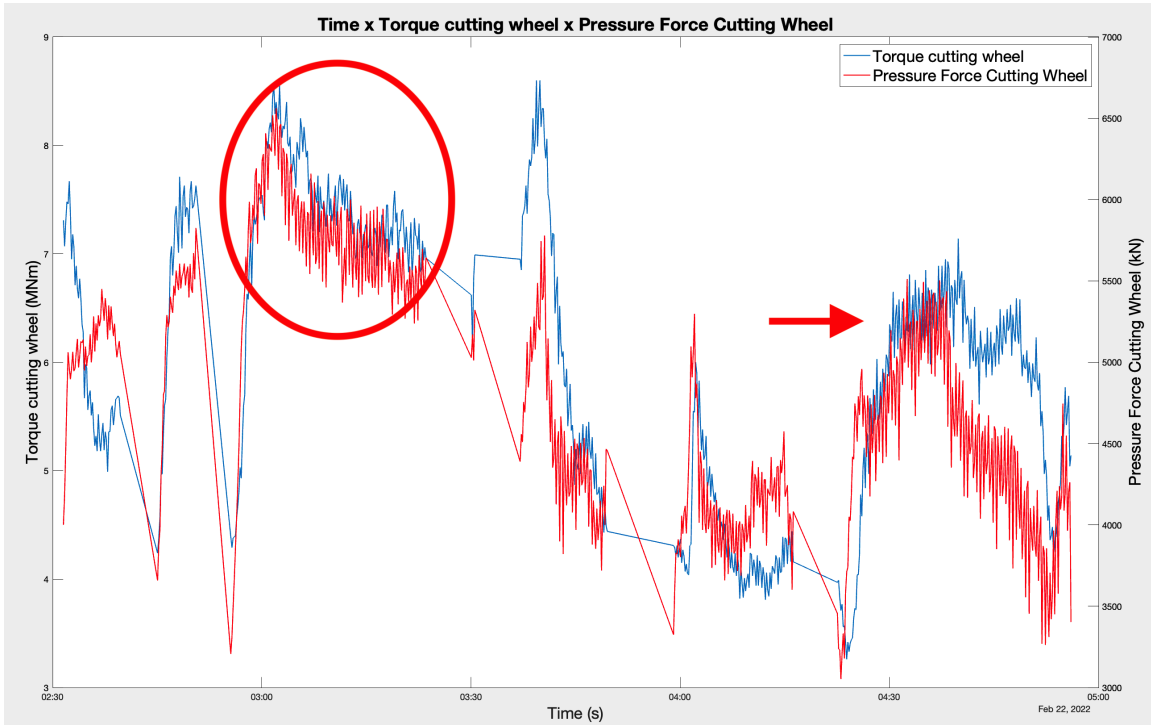


(a) Ring 842: Rock. The red circle indicates a sample region where parameter graphs follow the same pattern, indicating a region of harder, rock-like material.

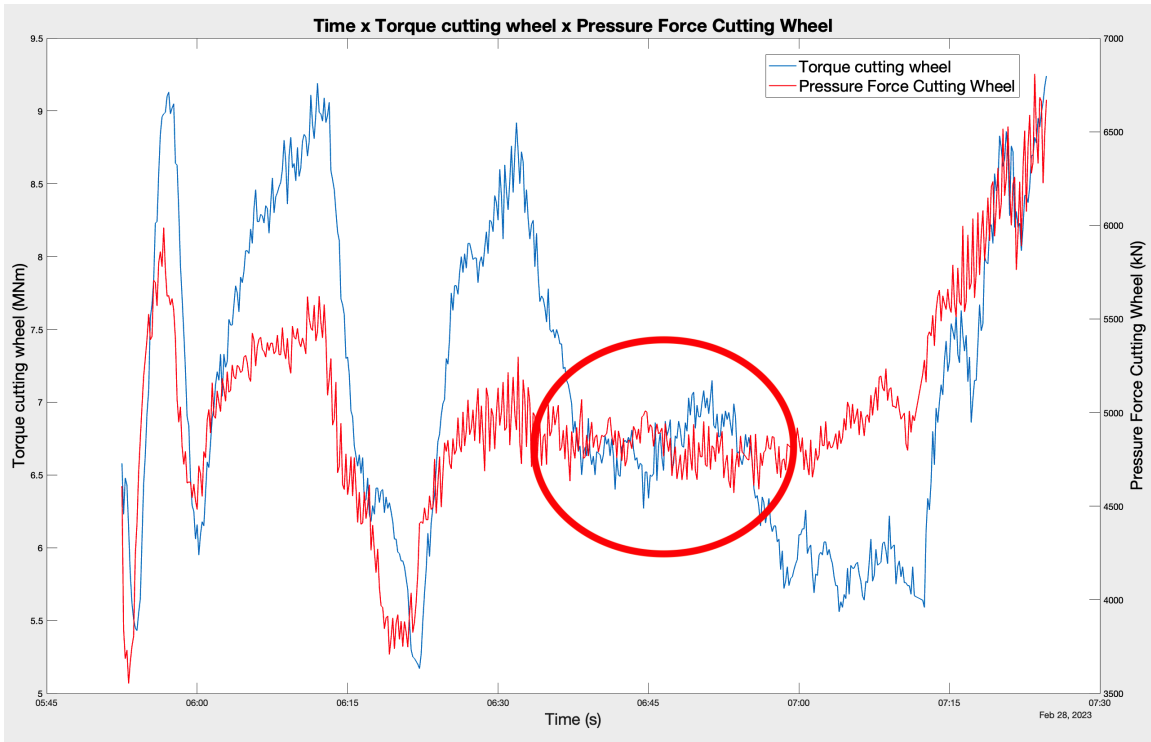


(b) Ring 598: Rock-like mixed. Arrow 1 indicates parameter overlap, where parameters are strongly positively correlated. Arrow 2 indicates a sample region where parameter graphs follow the same pattern, without overlap.

Figure 4-12: Time series plots relating Torque Cutting Wheel and Pressure Force Cutting Wheel for rock and rock-like mixed.



(a) Ring 557: Soil. Both the red circle and arrow indicate regions of significant parameter overlap, indicative of a strong positive correlation and softer material.



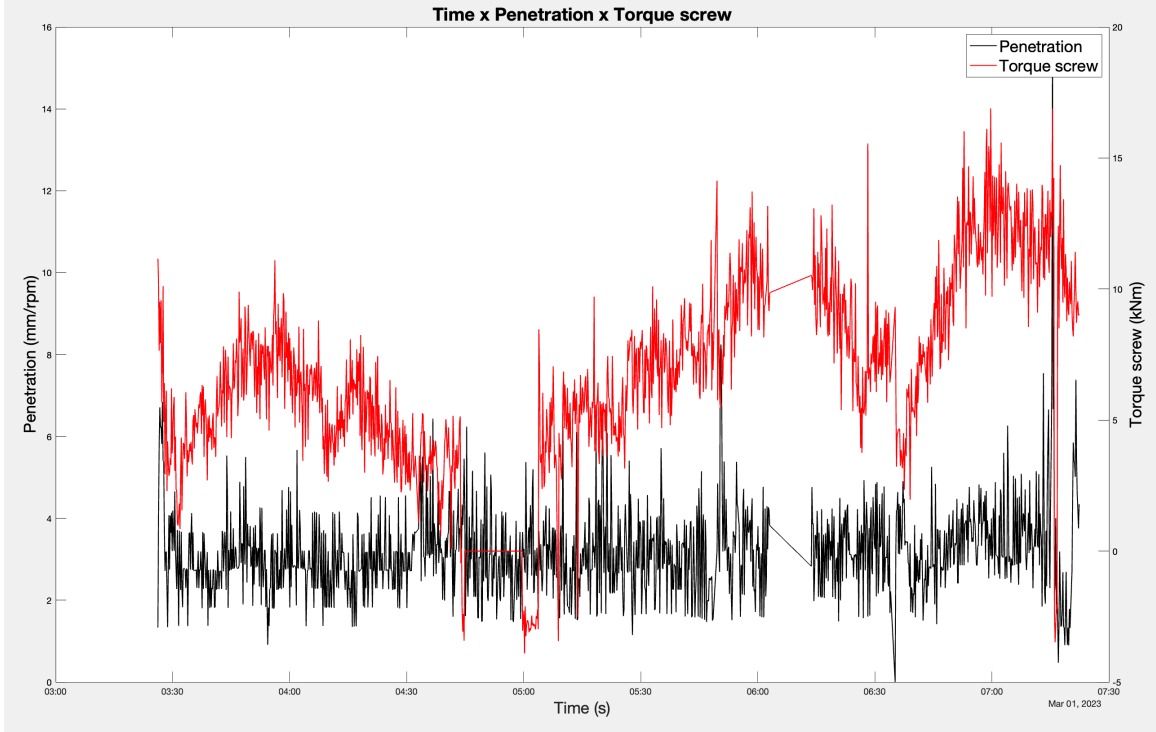
(b) Ring 613: Soil-like mixed. Here throughout the ring both parameters display a similar pattern and positive correlation. The red circle indicates a region where parameters overlap and have negative correlations.

Figure 4-13: Time series plots relating Torque Cutting Wheel and Pressure Force Cutting Wheel for soil and soil-like mixed.

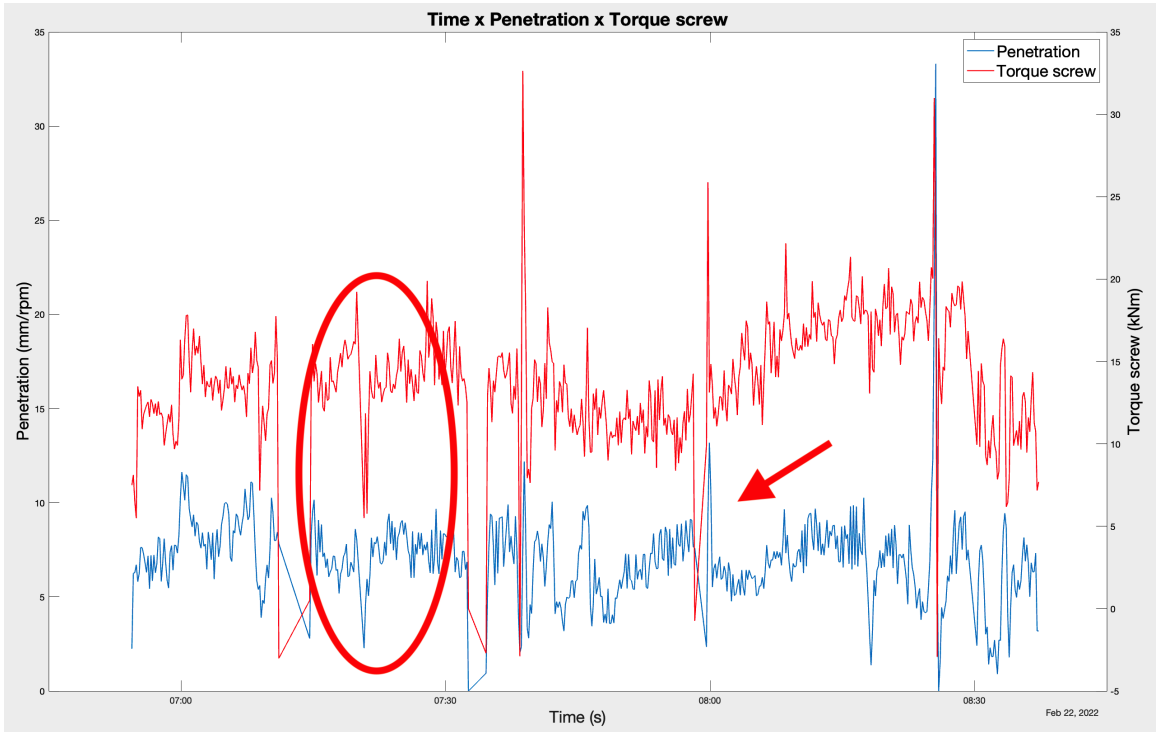
Time x Penetration x Torque Screw

Torque cutting wheel and penetration/torque screw play distinctive roles in the excavation process and operate in different sections of the machine. The results obtained for this parameter comparison will be presented in Figures 4-14 and 4-15.

This page intentionally left blank.

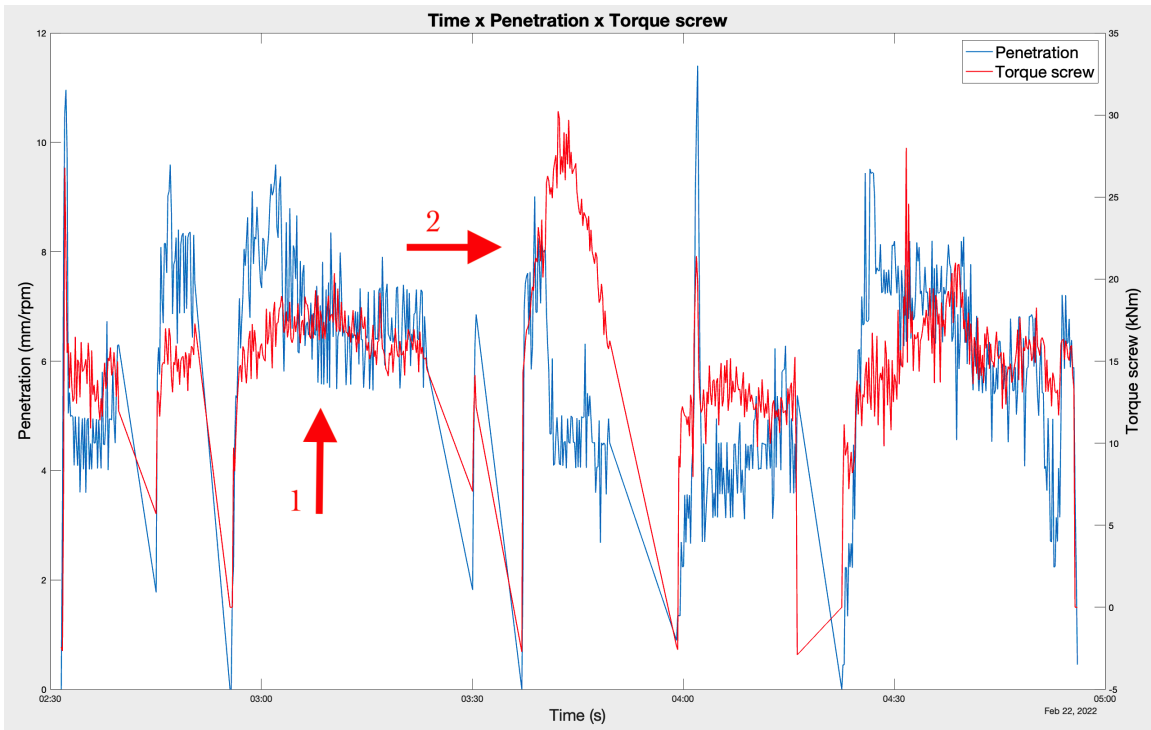


(a) Ring 842: Rock. Observations are highly variable for both parameters.

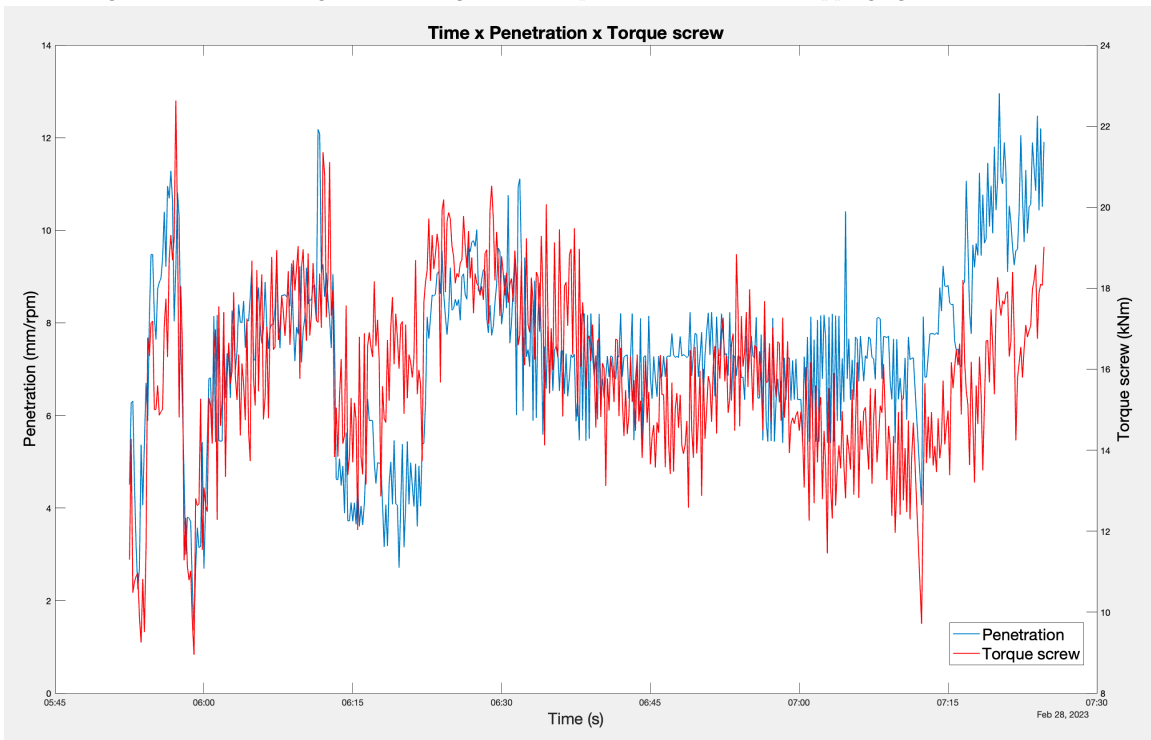


(b) Ring 598: Rock-like mixed. The red circle indicates a sample region where parameters follow the same patterns.

Figure 4-14: Time series plots relating Penetration and Torque Screw for rock and rock-like mixed.



(a) Ring 557: Soil. Parameters can be seen to overlap as indicated by Arrow 1 and throughout the ring. Arrow 2 shows a region where there is significant changes between parameters before overlapping again.



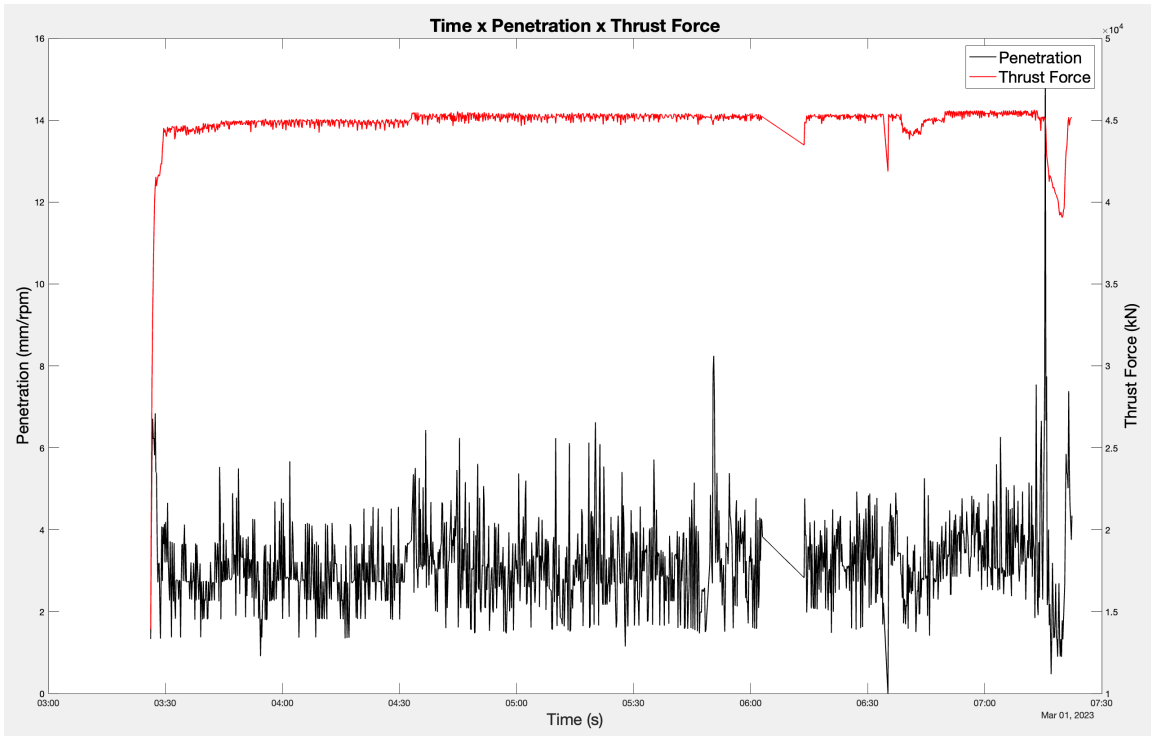
(b) Ring 613: Soil-like mixed. Throughout the ring, the parameters are strongly correlated and follow an overlapping distribution.

Figure 4-15: Time series plots relating Penetration and Torque Screw for soil and soil-like mixed.

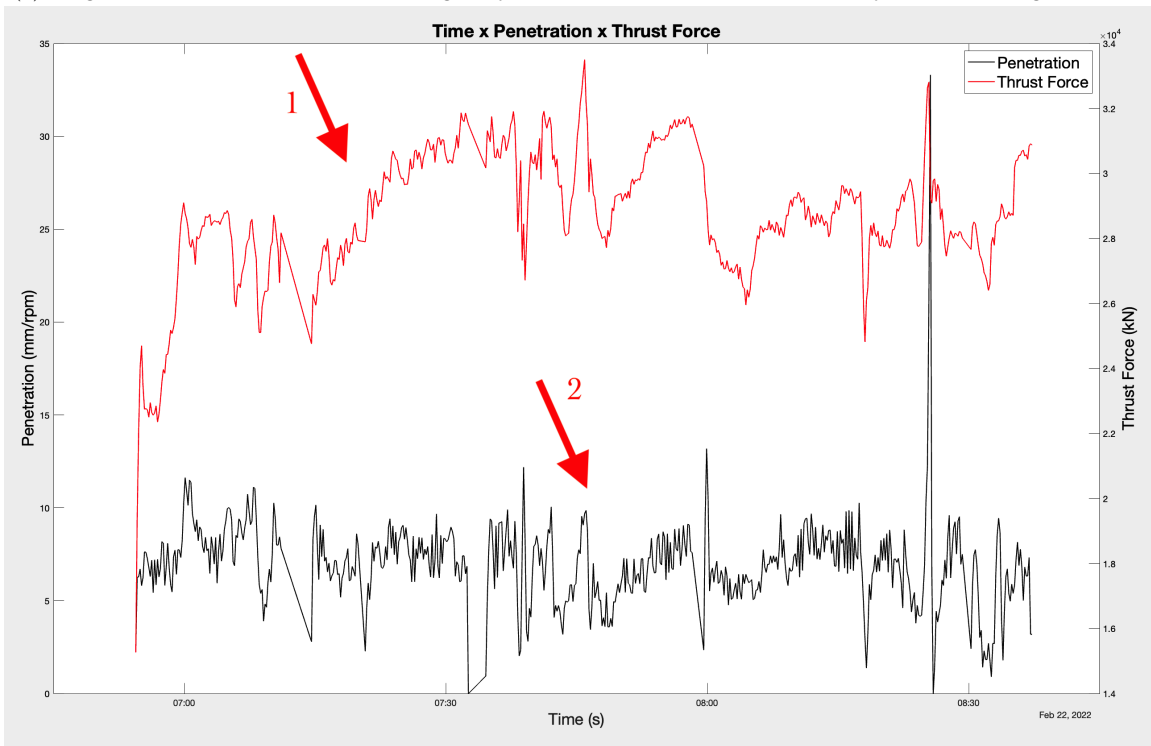
Time x Penetration x Thrust Force

In attempting to correlate thrust force with geology, the basic principle is that harder rock formations will call for greater thrust force for the TBM to advance. Conversely, softer and weaker ground formations will require less thrust force. This parameter relationship has not been widely explored in the literature and results obtained in this thesis will be presented in the following figures (4-16, 4-17).

This page intentionally left blank.

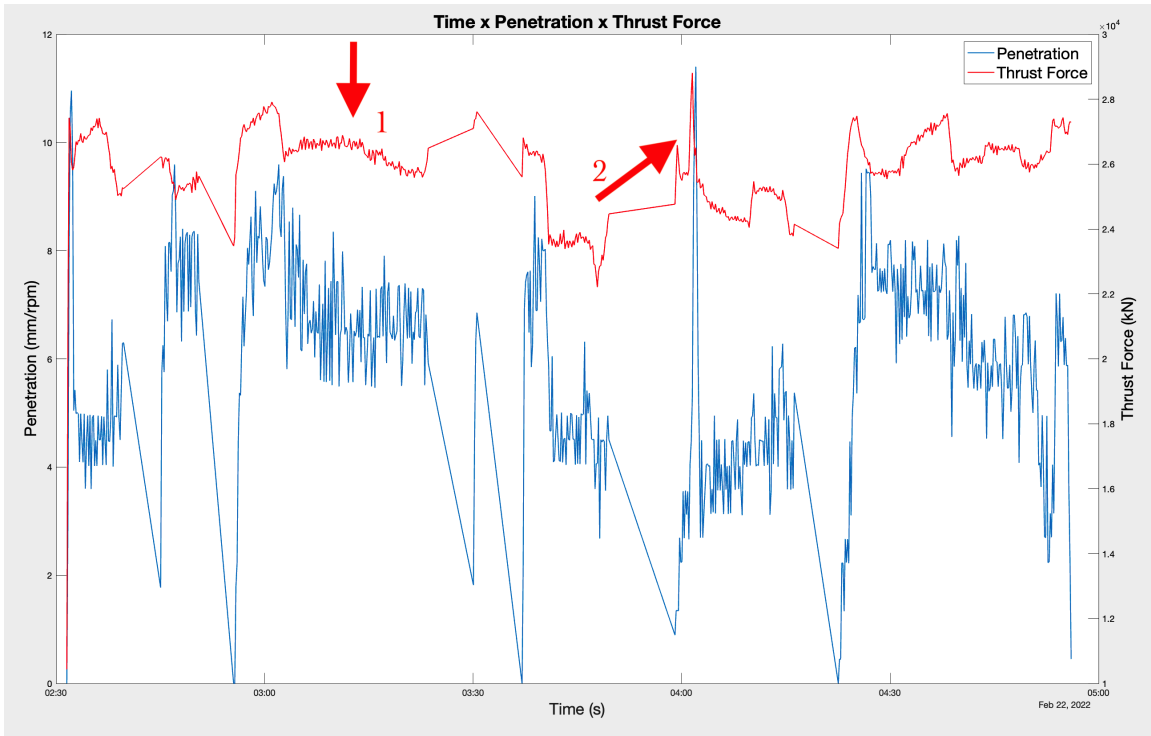


(a) Ring 842: Rock. Penetration is seen to greatly fluctuate. Thrust force remains fairly constant at higher values.

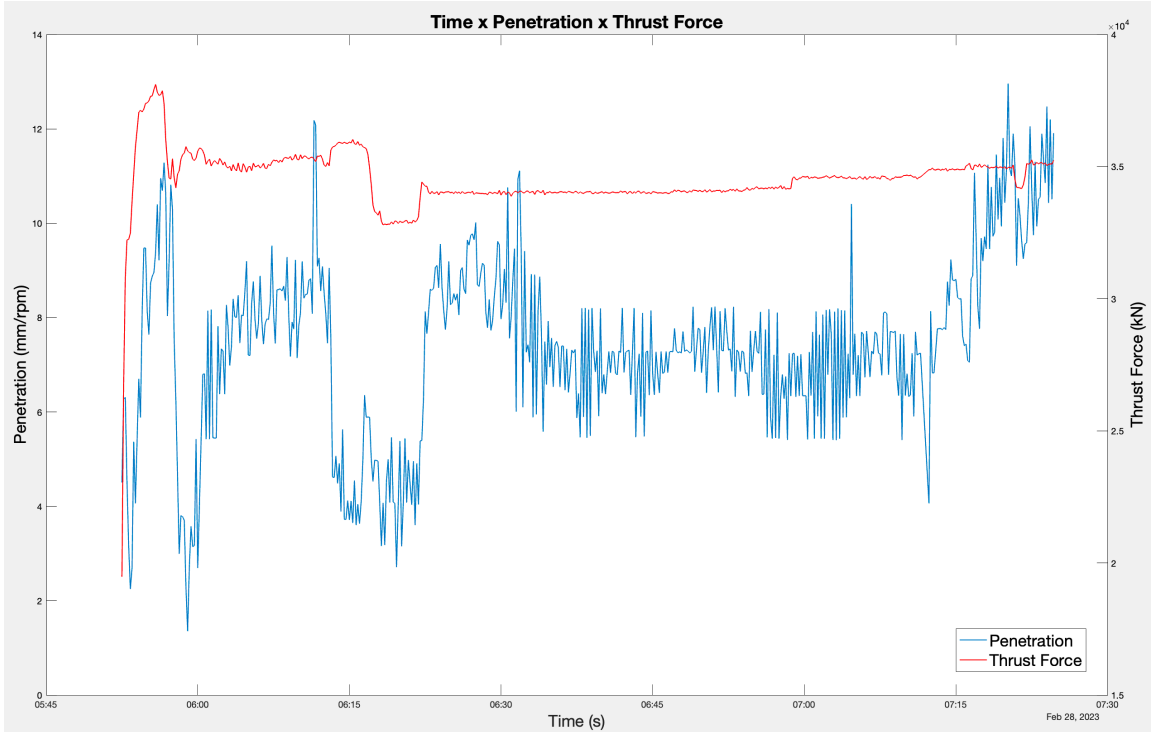


(b) Ring 598: Rock-like mixed. Penetration and thrust force follow similar parameters to rock material. Where both vary significantly at higher values of thrust pressure and lower penetration rates. Arrows 1 and 2 show the changes in thrust force as penetration increases and decreases.

Figure 4-16: Time series plots relating Penetration and Thrust Force for rock and rock-like mixed.



(a) Ring 557: Soil. Penetration and thrust force are highly variable, however, follow similar patterns (see arrow 1). Penetration remains at higher values, sometimes peaking (as indicated in Arrow 2), with thrust force varying.



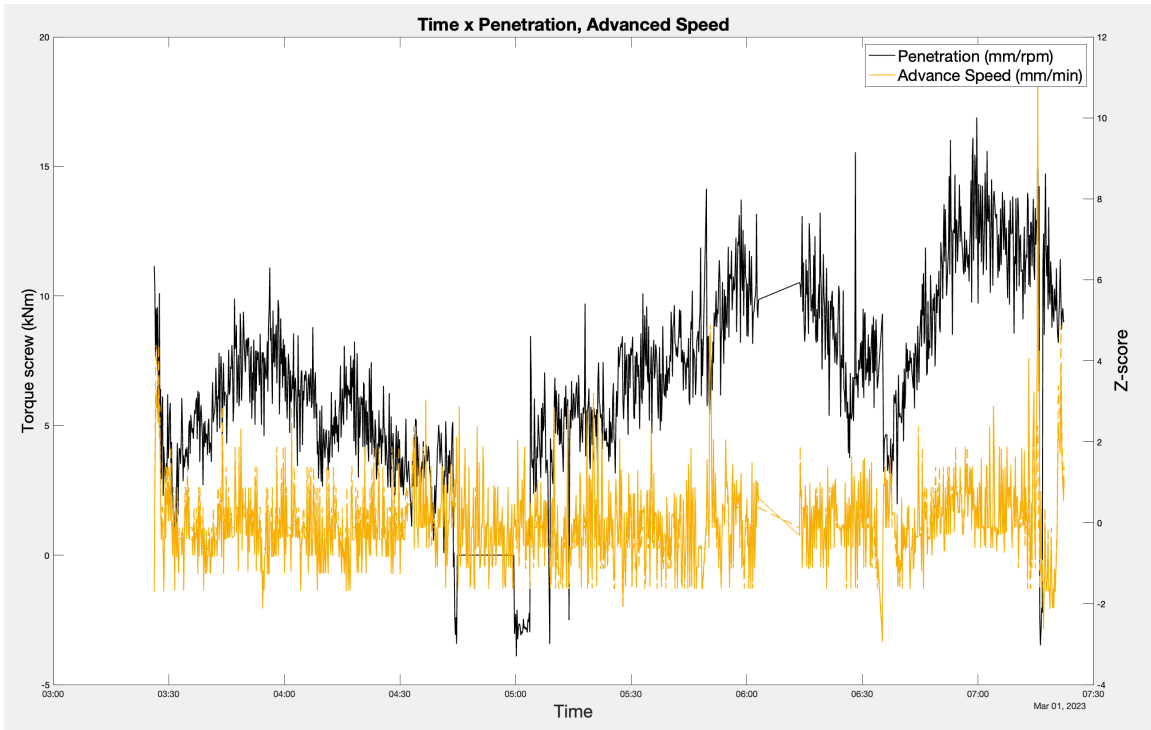
(b) Ring 613: Soil-like mixed. Penetration varies significantly while thrust force remains fairly constant.

Figure 4-17: Time series plots relating Penetration and Thrust Force for soil and soil-like mixed.

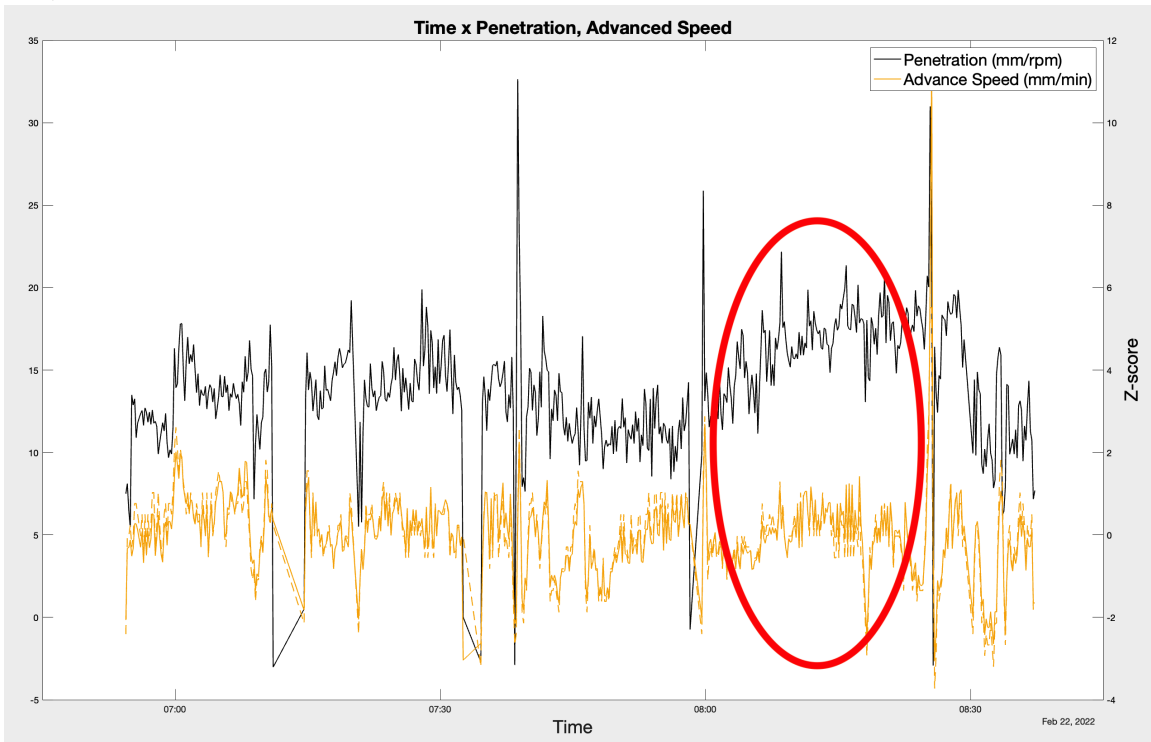
Time x Penetration x Advance Speed

Penetration and torque screw can offer insights into geological conditions by identifying changes in ground conditions, such as the presence of harder or softer rock layers or changes in soil consistency. A decrease in penetration rate with constant machine advance speed may indicate the machine has encountered a layer of hard rock, while an increase in penetration rate with constant advance speed may indicate a softer soil layer. Sample results for rock, soil, rock-like mixed, and soil-like mixed rings are presented in Figures 4-18 and 4-19.

This page intentionally left blank.

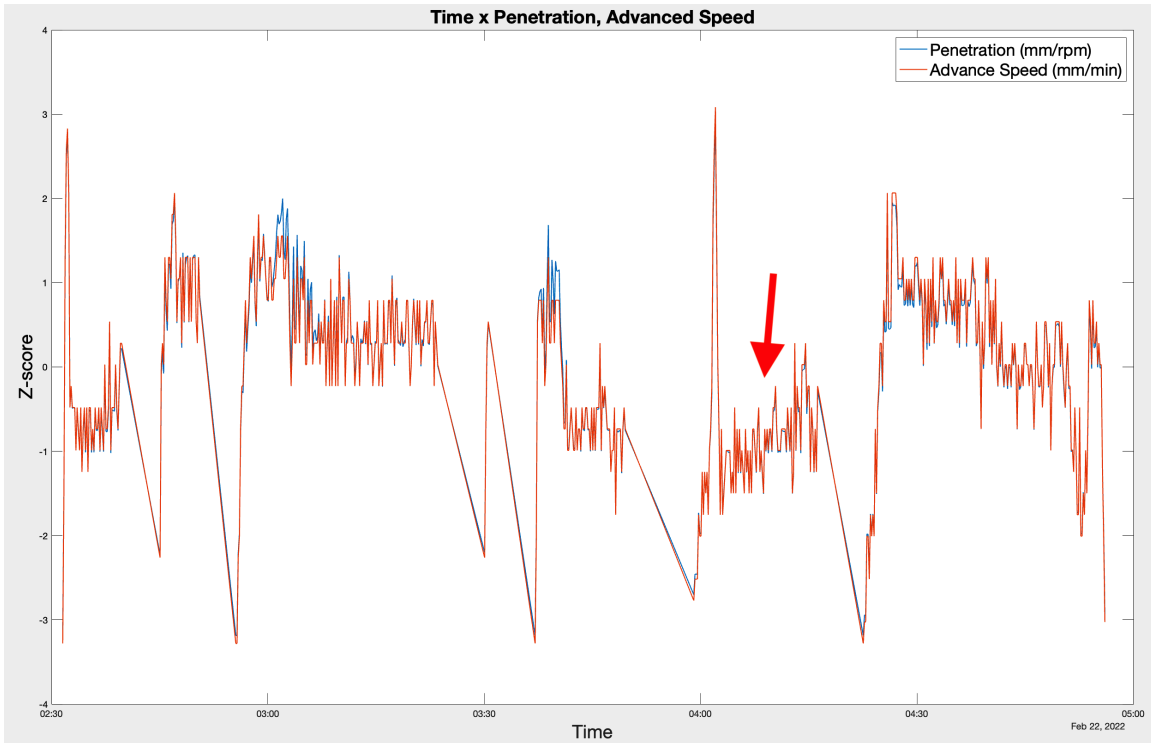


(a) Ring 842: Rock. Fluctuations in penetration are observed. Again, the characteristic density and short "up"/"down" variations can be seen. Meanwhile, advance speed also varies considerably at lower values.

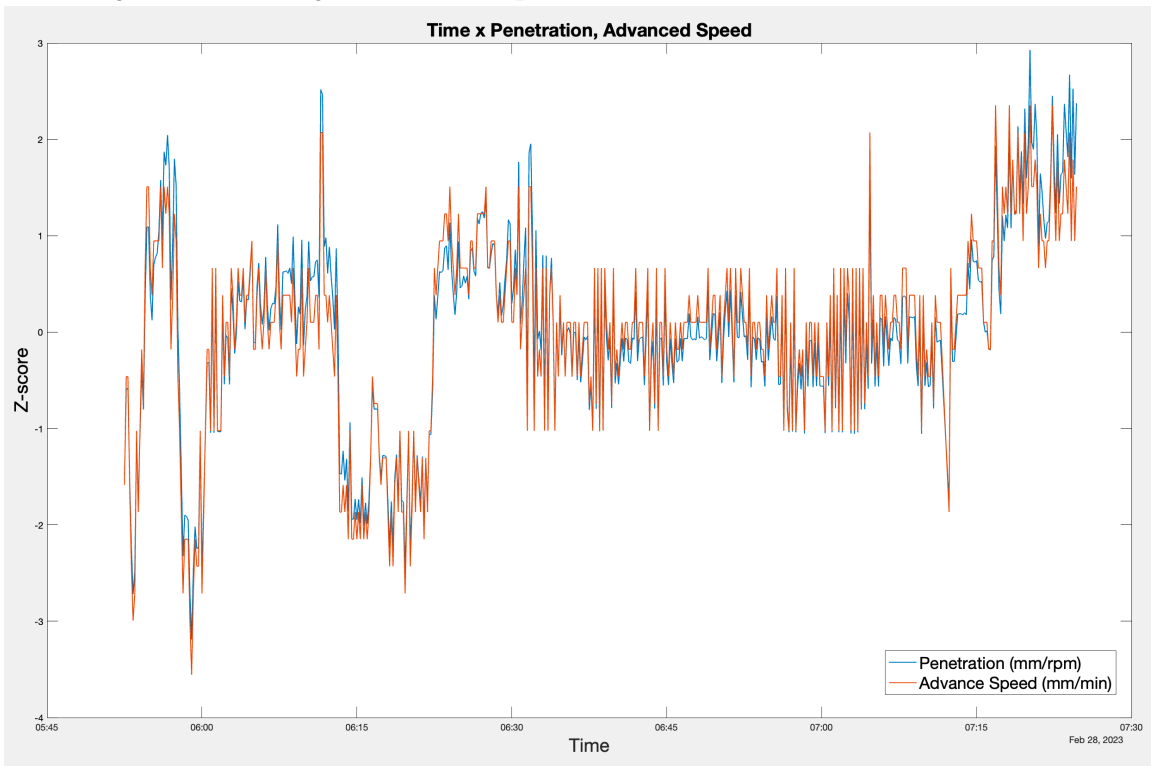


(b) Ring 598: Rock-like mixed. Penetration and thrust force exhibit analogous patterns in rock-like material, with both parameters exhibiting notable fluctuations at lower advance speed and penetration rates, yet following similar patterns (as highlighted in red).

Figure 4-18: Time series plots relating Penetration and Advance Speed for rock and rock-like mixed.



(a) Ring 557: Soil. The overlapping of penetration and advance speed (perfect overlap shown by the red arrow) indicates a correlation between the two parameters, commonly observed in softer soil-like materials. Here the TBM is advancing faster without a significant increase in penetration rates.



(b) Ring 613: Soil-like mixed. The intermingling of penetration and advance speed reflects a relationship between the two parameters. Almost complete overlap between parameters.

Figure 4-19: Time series plots relating Penetration and Advance Speed for soil and soil-like mixed.

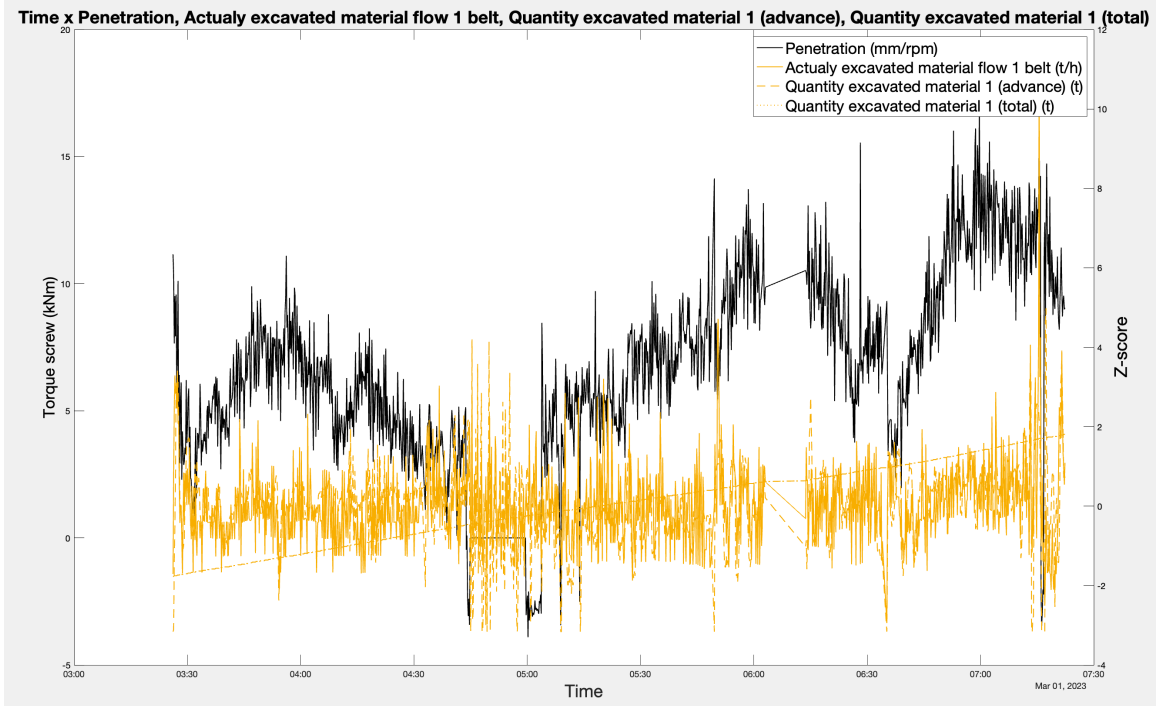
Time x Penetration, Actually Excavated Material Flow Belt, Quantity of Excavated Material (Advance), Quantity of Excavated Material (Total)

The parameters chosen: Penetration, Actually Excavated Material Flow Belt, Quantity of Excavated Material (Advance), and Quantity Excavated Material (Total) are all measurements that can provide valuable insights into encountered ground conditions. As explained above, penetration measures the distance the TBM advances into the material in front of the tunnel face. By comparing the total amount of material excavated with other data, such as borehole logs or geological surveys, a more accurate picture of ground conditions can be obtained.

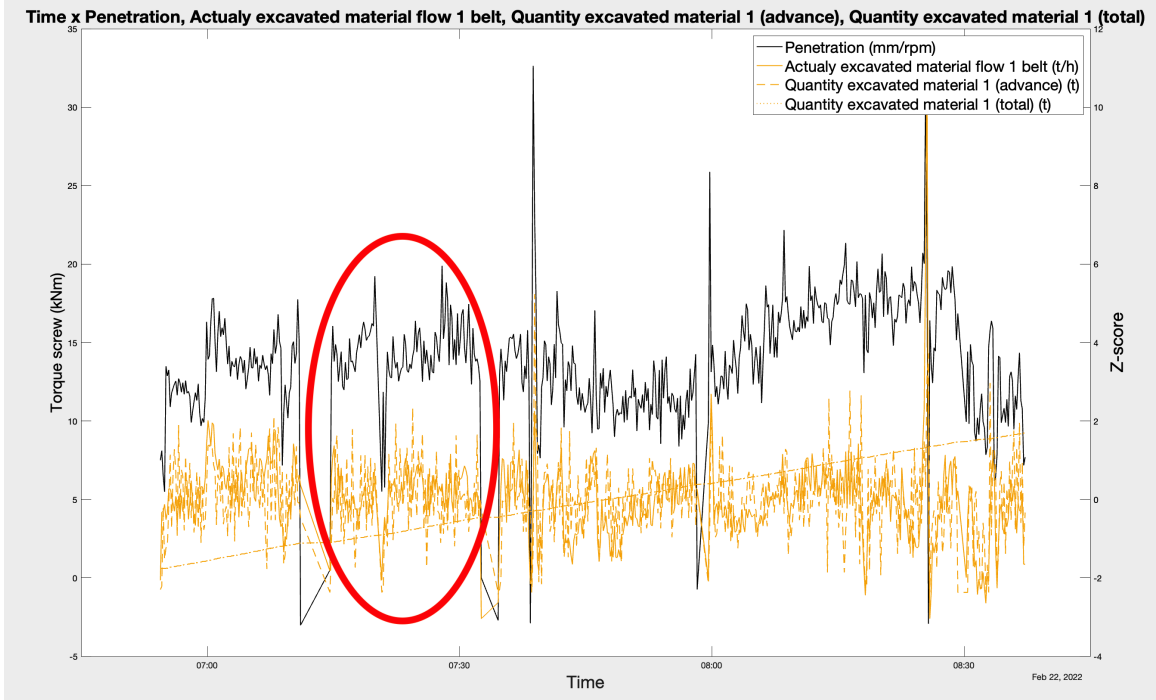
Analyzing these parameters together can provide a more complete understanding of the geological conditions encountered during excavation. For example, if the penetration rate is decreasing while the rate of advance is also decreasing, it may indicate that the TBM is encountering harder or more challenging geological conditions (i.e. rock). By analyzing the actually excavated material flow belt, operators can gain insight into the characteristics of the material being excavated, which can help in identifying changes in geological conditions.

Overall, by analyzing these parameters together, TBM operators can gain a better understanding of the geological conditions and make necessary adjustments to the excavation process. The following graphs will show this relationship for both soil, rock and mixed rings (see Figures 4-20, 4-21).

This page intentionally left blank.

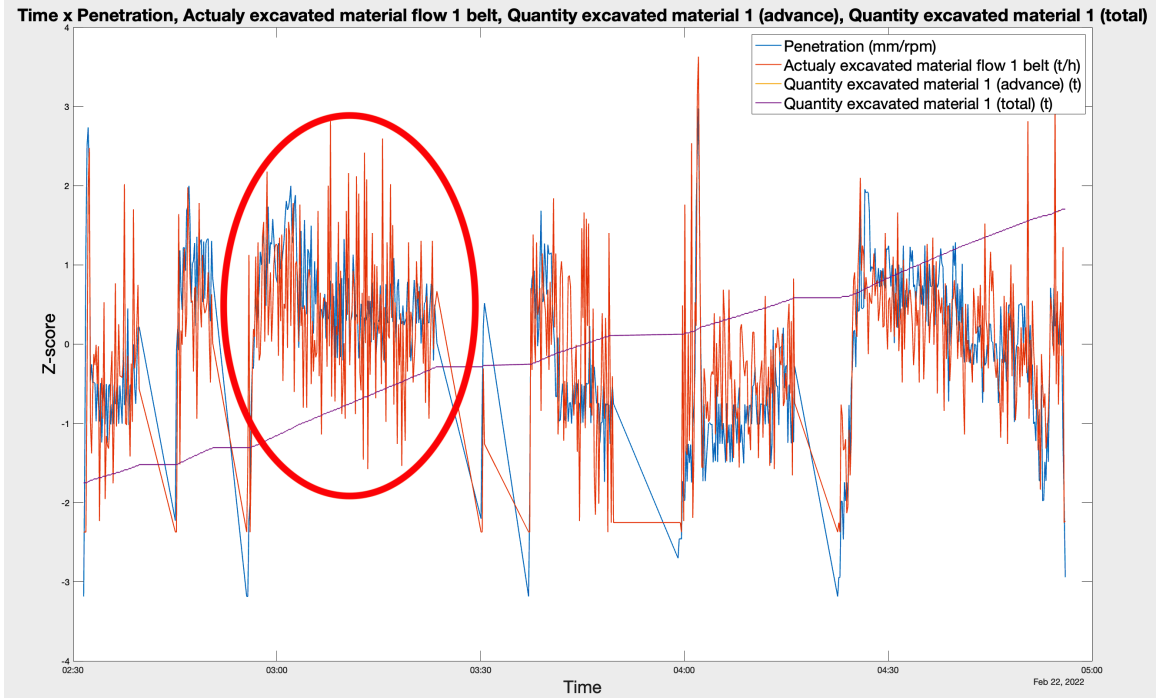


(a) Ring 842: Rock. Here penetration rates are highly variable and do not follow the pattern seen in the other evaluated parameters.

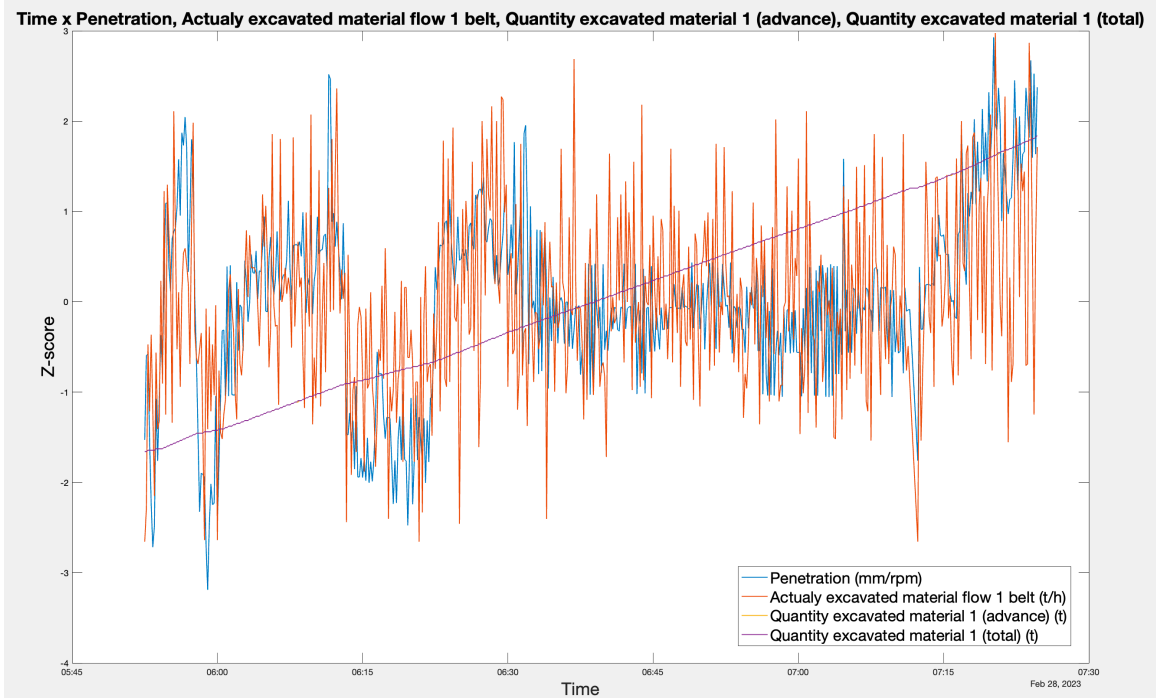


(b) Ring 598: Rock-like mixed. Penetration rates do not behave in tandem with other parameters (as indicated in red). However, it is presented in a graphical pattern similar to what is being recorded in the other parameters.

Figure 4-20: Time series plots relating Penetration, Actually Excavated Material Flow Belt, Quantity of Excavated Material (Advance) and Quantity of Excavated Material (Total) for rock and rock-like mixed.



(a) Ring 557: Soil. Here penetration and actually excavated material present similar patterns, almost completely overlapping.



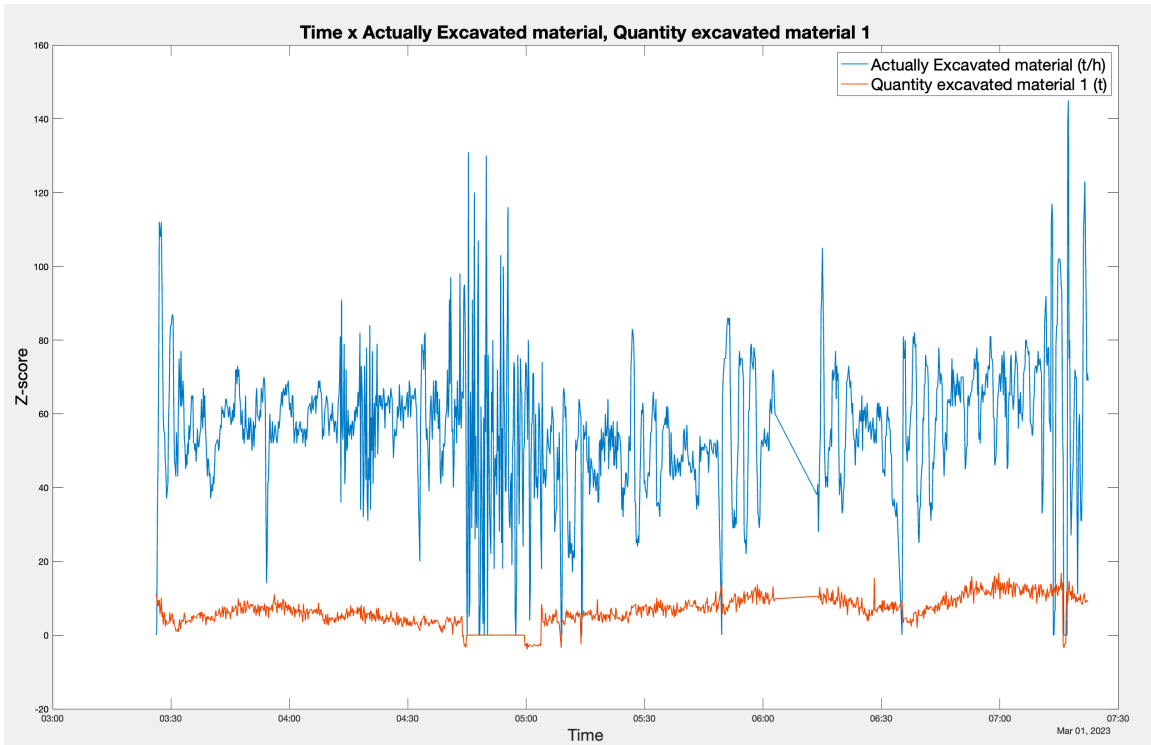
(b) Ring 613: Soil-like mixed. An overlap can be seen between penetration rates and actually excavated material (see the indicated circle). However, penetration varies significantly more than in the previous ring.

Figure 4-21: Time series plots relating Penetration, Actually Excavated Material Flow Belt, Quantity of Excavated Material (Advance) and Quantity of Excavated Material (Total) for soil and soil-like mixed.

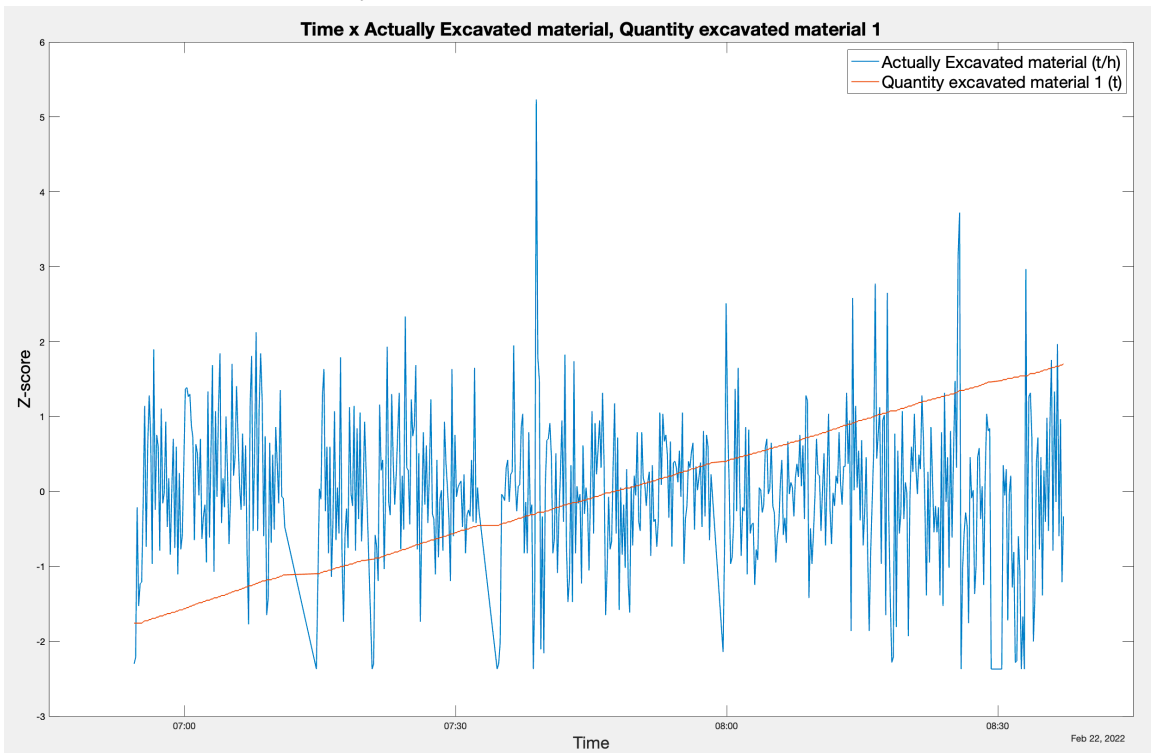
Time x Actually Excavated Material x Quantity of Excavated Material 1

By analyzing only these two parameters together, in contrast to the previous example, it is possible to gain clearer insight into the efficiency of the excavation process, as well as encountered geology. Next, figures 4-22, 4-23 will show an example for rock, soil, rock-like mixed and soil-like mixed rings respectively.

This page intentionally left blank.

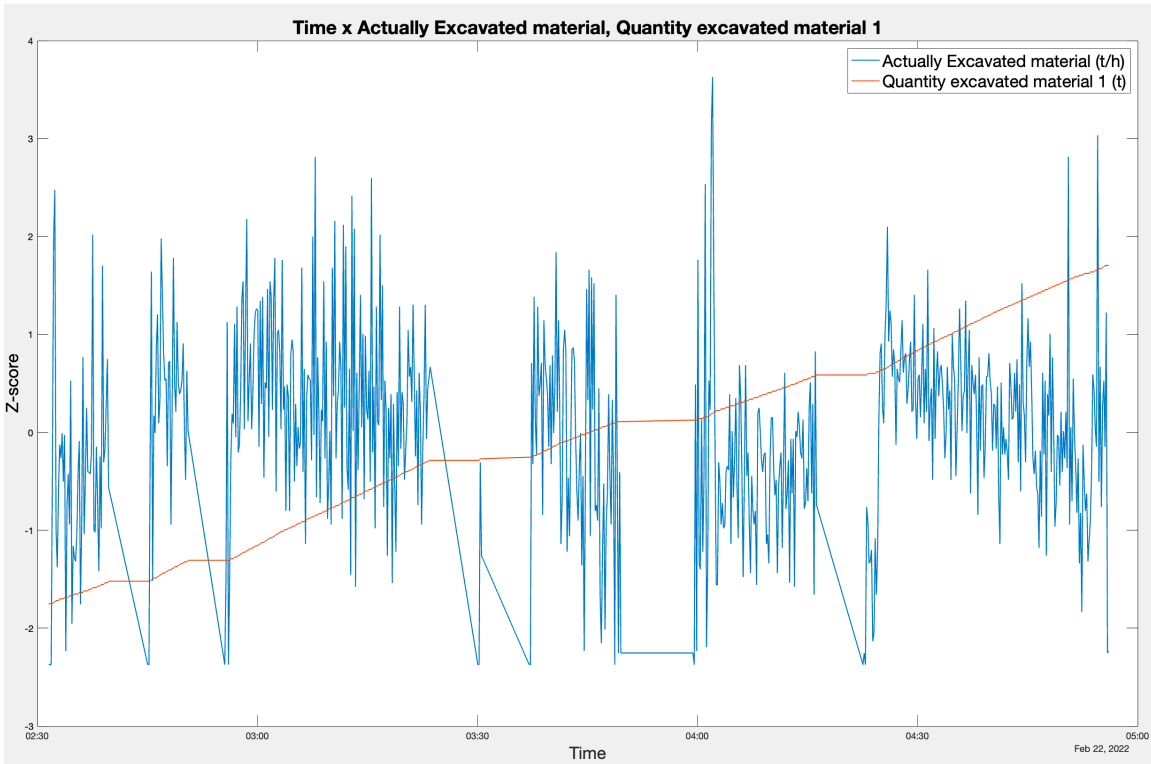


(a) Ring 842: Rock. From the graph it is notable that actually excavated material varies widely, while quantity of excavated material remains relatively constant and low.

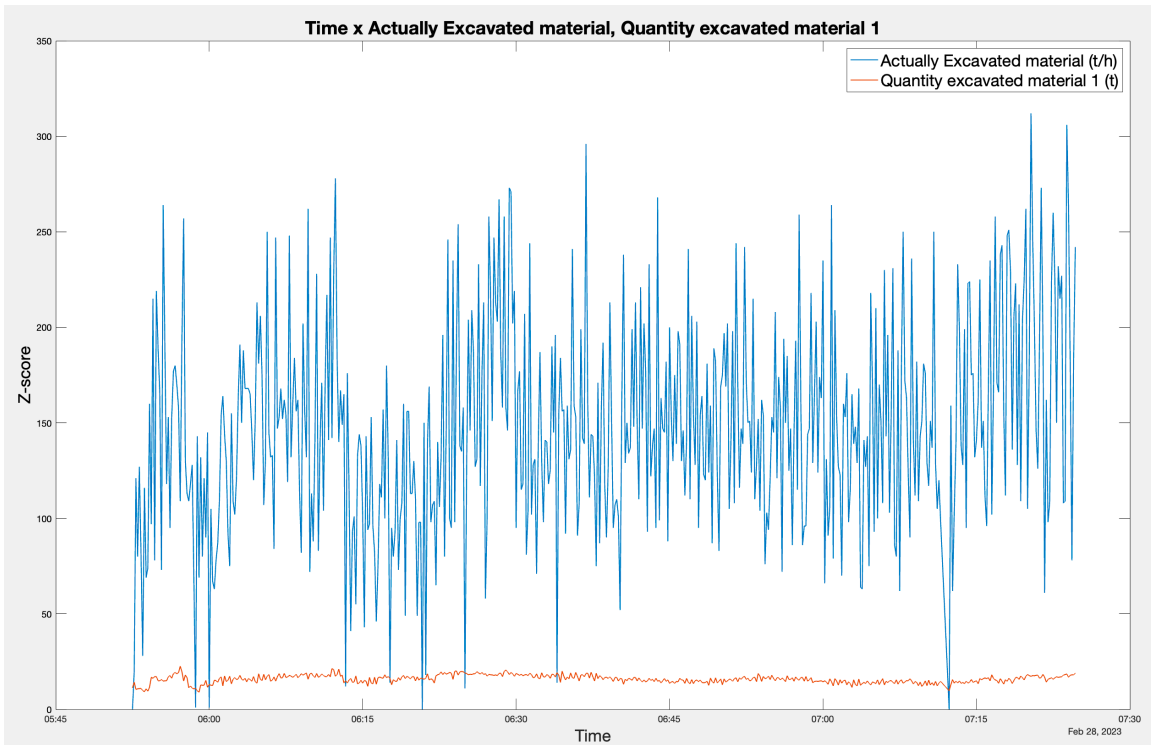


(b) Ring 598: Rock-like mixed. Here actually excavated material varies although less than what was seen in rock, while the quantity of excavated material rises throughout the ring.

Figure 4-22: Time series plots relating Actually Excavated Material and Quantity of Excavated Material 1 for rock and rock-like mixed.



(a) Ring 557: Soil. Actually excavated material varies significantly throughout the ring, while quantity of excavated material rises.



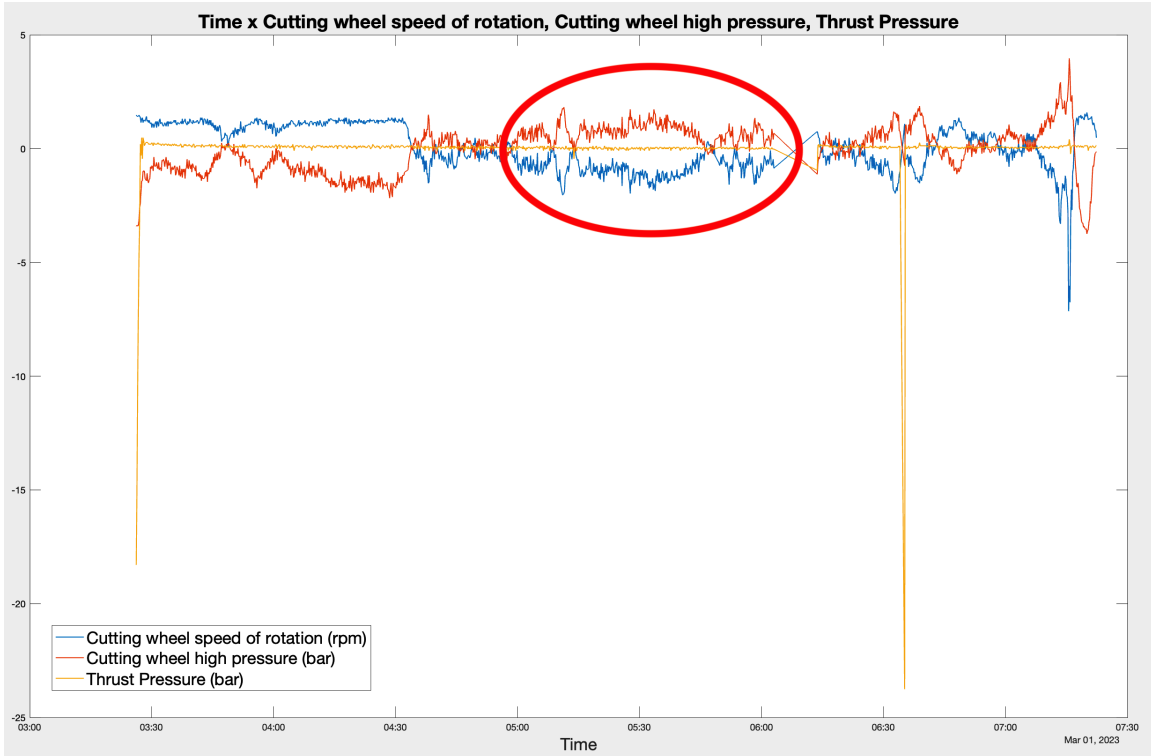
(b) Ring 613: Soil-like mixed. Variation occurs in actually excavated material. Quantity of excavated material remains fairly low.

Figure 4-23: Time series plots relating Actually Excavated Material and Quantity of Excavated Material 1 for soil and soil-like mixed.

Time x Cutting Wheel Speed of Rotation, Cutting Wheel High Pressure, Thrust Pressure

Cutting Wheel Speed of Rotation, Cutting Wheel High Pressure, and Thrust Pressure are all critical parameters for TBM operations. Based on aforementioned physical characteristics, variation in thrust pressure and cutting wheel high pressure can potentially inform variations in rock or soil conditions, while changes in cutting wheel speed may indicate alterations in hardness and abrasiveness of the excavated material. Below this relationship is demonstrated through figures 4-24, 4-25.

This page intentionally left blank.

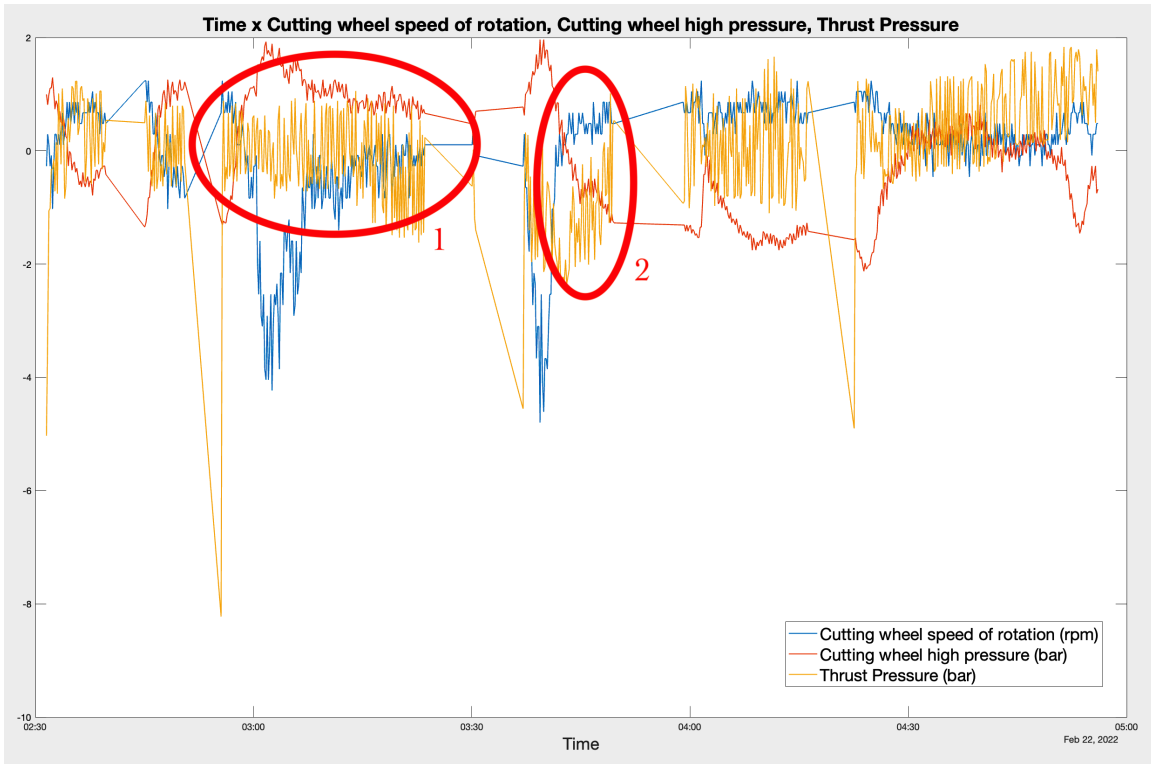


(a) Ring 842: Rock. Parameters vary slightly but remain fairly constant throughout the ring. The red circle indicates a sample region where both cutting wheel speed of rotation and cutting wheel high pressure is mirrored.

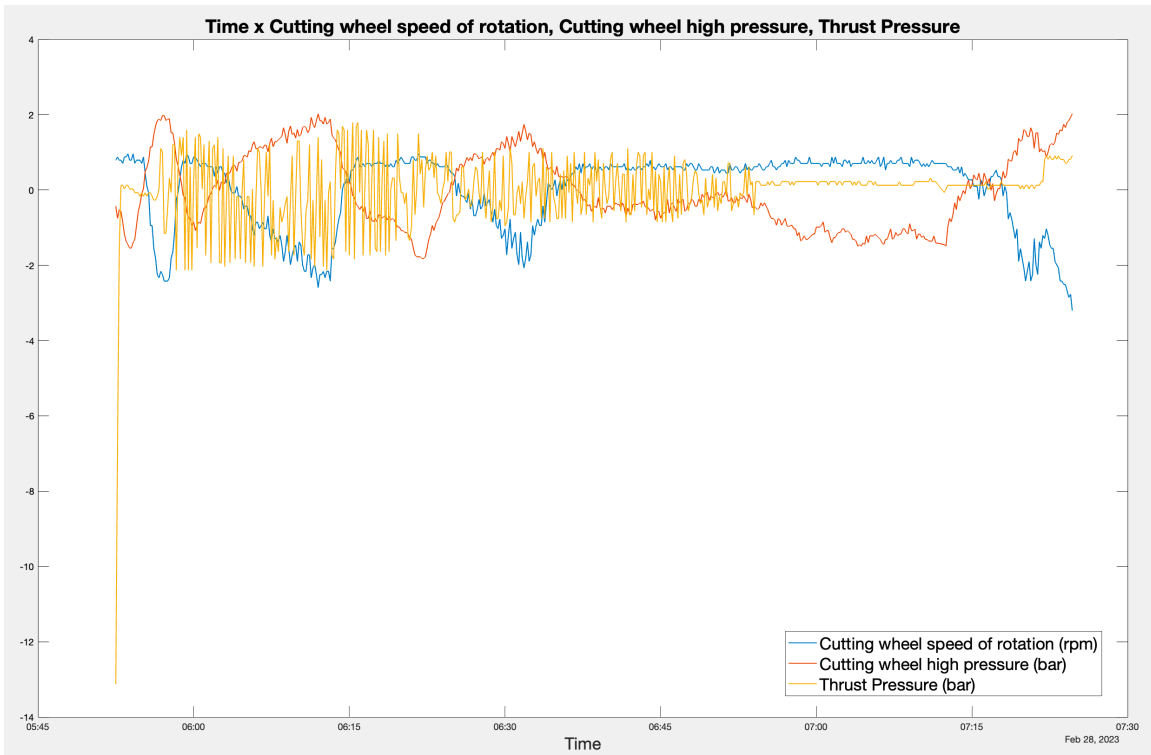


(b) Ring 598: Rock-like mixed. Here a lot of variation can be observed, especially in thrust pressure. The red circle and arrow indicate regions where there is positive and negative correlation between cutting wheel speed of rotation and cutting wheel high pressure.

Figure 4-24: Time series plots relating Cutting Wheel Speed of Rotation, Cutting Wheel High Pressure and Thrust Pressure for rock and rock-like mixed.



(a) Ring 557: Soil. Variation in parameters can be seen, especially in thrust pressure, consistent with softer material. Circles 1 and 2 showcase this variability in thrust pressure and the mirroring occurring between cutting wheel speed of rotation and cutting wheel high pressure.



(b) Ring 613: Soil-like mixed. Cutting wheel speed of rotation and cutting wheel high pressure vary mirroring each other, while thrust pressure varies significantly.

Figure 4-25: Time series plots relating Cutting Wheel Speed of Rotation, Cutting Wheel High Pressure and Thrust Pressure for soil and soil-like mixed.

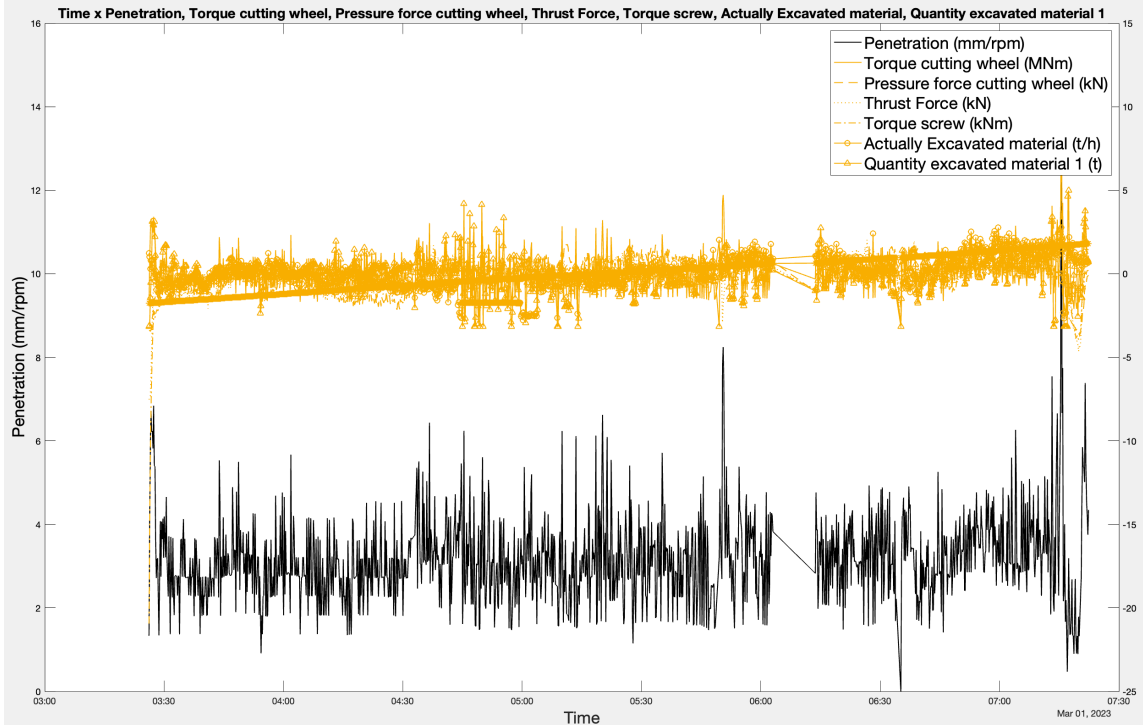
Time x Penetration x Torque Cutting Wheel, Pressure Force Cutting Wheel, Thrust Force, Torque Screw, Actually Excavated Material, Quantity of Excavated Material

Torque cutting wheel, pressure force cutting wheel, and thrust force, alongside penetration are also measured on the TBM's cutterhead and inform on the torque pressure and force applied to the cutterhead, moving it forward. Torque screw, measured on the machine's screw conveyor, is responsible for recording material removal from the tunnel. Actually excavated material indicates the amount of material excavated and transported away from the tunnel face, while quantity of excavated material represents to the total amount of material excavated, cumulatively, during the entire tunneling process.

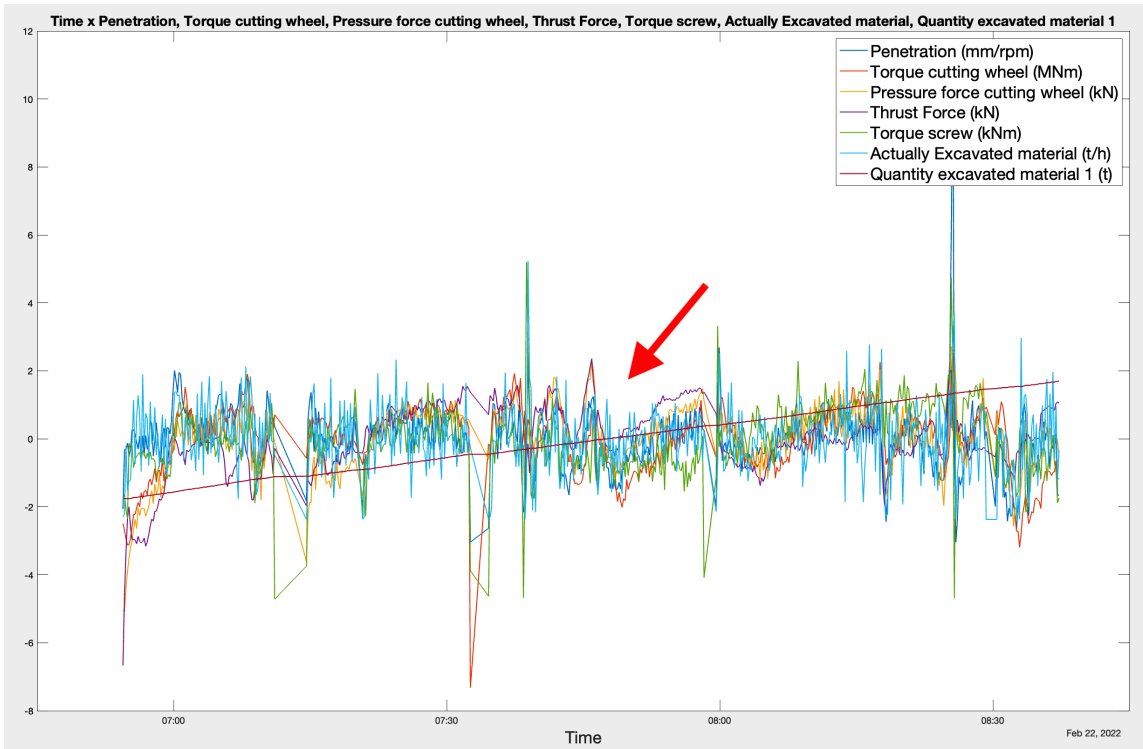
As all of these parameters relate either to machine advancement or the material being excavated out of the tunnel, analyzing them together was expected to provide insights on the geological conditions encountered by the TBM. For instance, penetration rates can correlate directly to ground conditions being harder or softer, while torque cutting wheel and pressure force cutting wheel represent the resistance of the material being excavated. Thrust force can help identify high ground stress or difficult geological conditions, while torque screw can indicate the efficiency of the TBM's excavation and transport processes.

Overall, these parameters are already used to optimize the tunneling process and adjust excavation techniques in real-time to the geological conditions encountered by the TBM. Next, figures 4-26, 4-27 will show the resulting graphs.

This page intentionally left blank.



(a) Ring 842: Rock. Here the graphs are very meshed into each other making it difficult to distinguish specific behavior. However, as seen in previous parameter comparisons, penetration varies significantly and is separated from the other parameters.

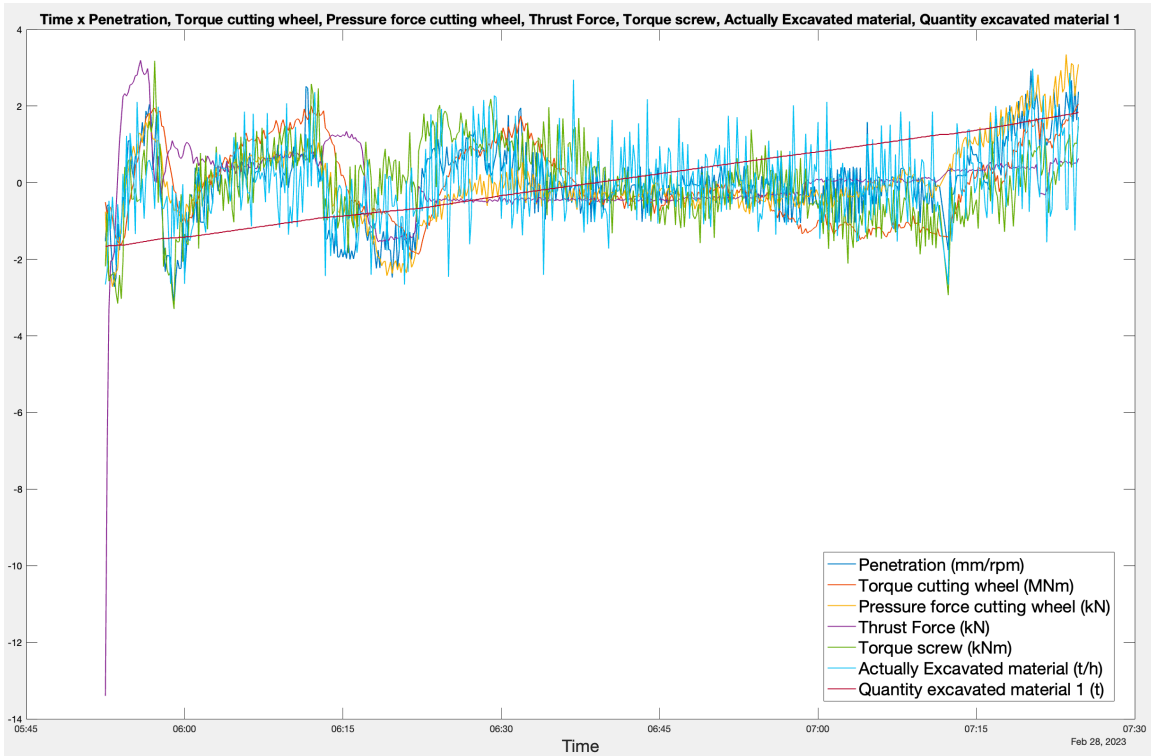


(b) Ring 598: Rock-like mixed. Parameters follow a similar pattern than what was observed in rock, with penetration reaching higher values. As indicated by the red arrow, all parameters are following similar patterns.

Figure 4-26: Time series plots relating Penetration, Torque Cutting Wheel, Pressure Force Cutting Wheel, Thrust Force, Torque Screw, Actually Excavated Material and Quantity of Excavated Material for rock and rock-like mixed.



(a) Ring 557: Soil. The parameters follow similar distributions, rising and falling in tandem. Circles 1 and 2 show how penetration and torque screw are intimately related, where they rise and fall together.



(b) Ring 613: Soil-like mixed. Here behavior similar to soils can be observed, where all parameters seem to follow a similar pattern throughout the ring.

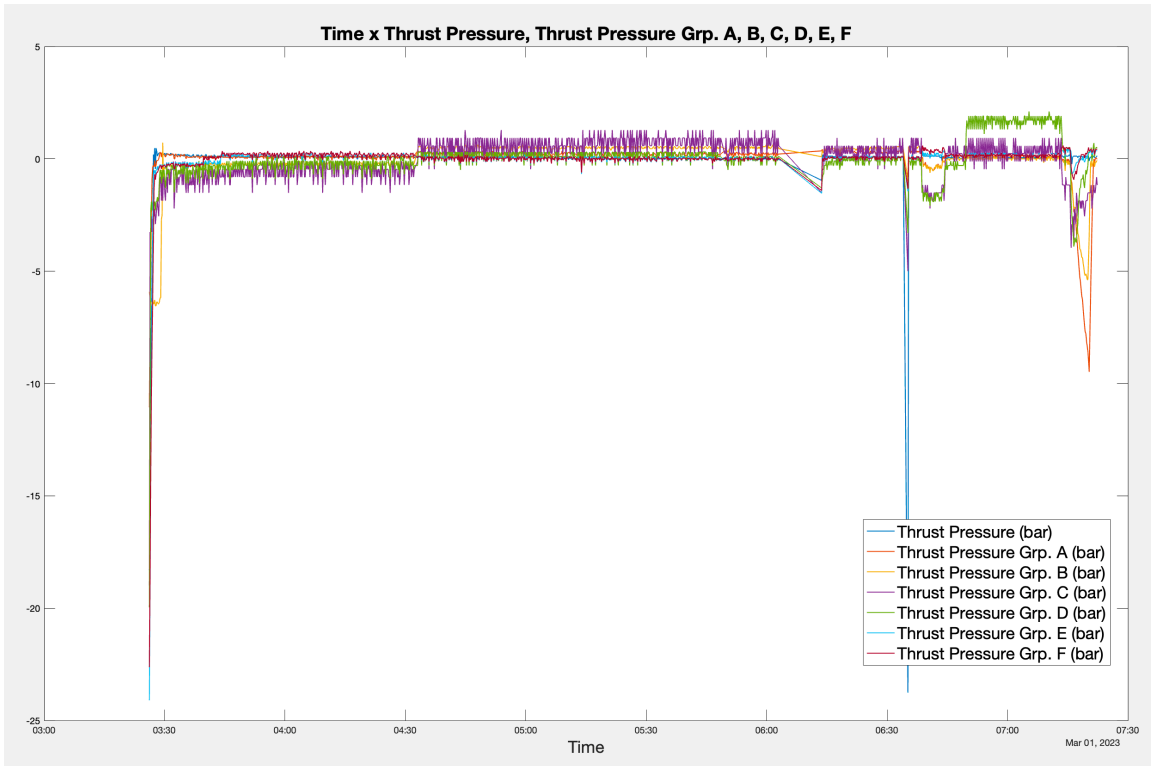
Figure 4-27: Time series plots relating Penetration, Torque Cutting Wheel, Pressure Force Cutting Wheel, Thrust Force, Torque Screw, Actually Excavated Material and Quantity of Excavated Material for soil and soil-like mixed.

Time x Thrust Pressure x Thrust Pressure Groups A, B, C, D, E, F

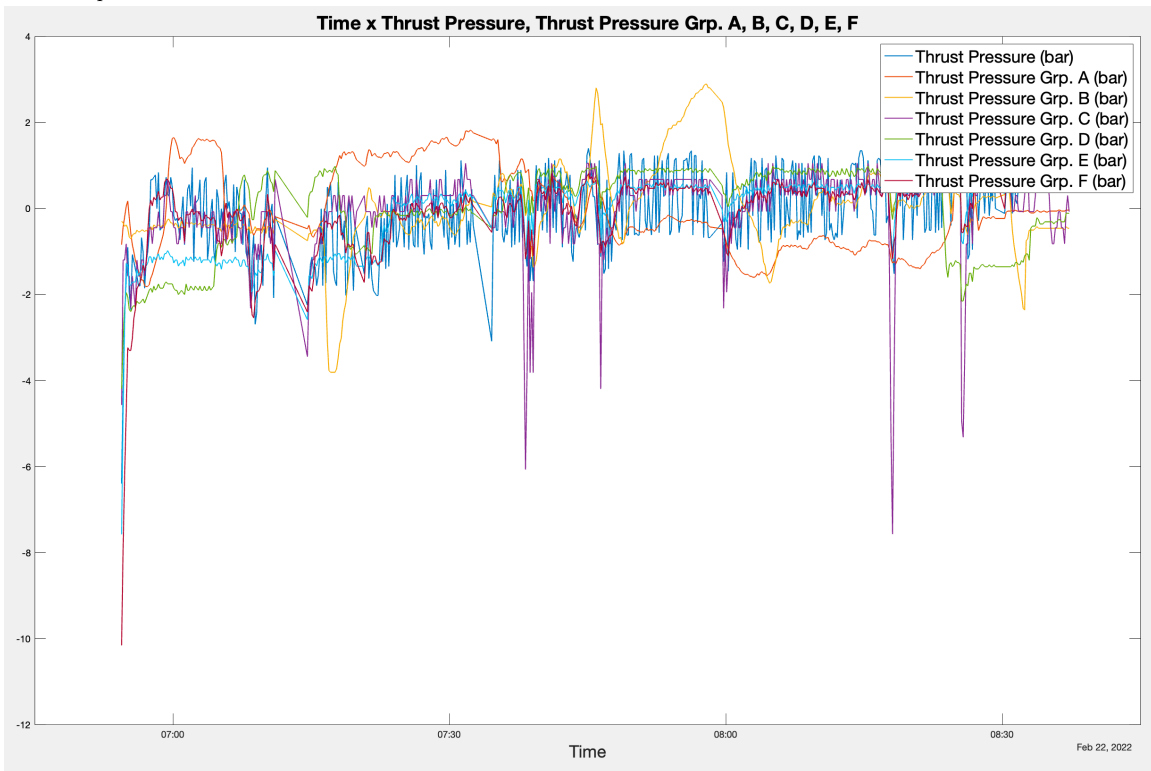
Analyzing thrust pressure alongside corresponding thrust pressure groups (A-F) can provide insights into the geological conditions encountered by the TBM. For instance, if the machine is using a higher thrust pressure group, it may indicate that the geological formation is more resistant to excavation, such as harder rock or mixed ground conditions. The distinction between thrust pressure groups A through F can vary based on the machine manufacturer, however, Group A commonly represents the lowest and Group F the highest thrust forces. Conversely, if the machine is using a lower thrust pressure group, this may indicate that the geological formation is softer and easier to excavate.

By analyzing the relationship between thrust pressure and the corresponding pressure groups, alongside thrust pressure, it is possible to gain a better understanding of the geological conditions and adjust the excavation process accordingly. Below, figures show the results obtained for this parameter 4-28, 4-29 comparison.

This page intentionally left blank.

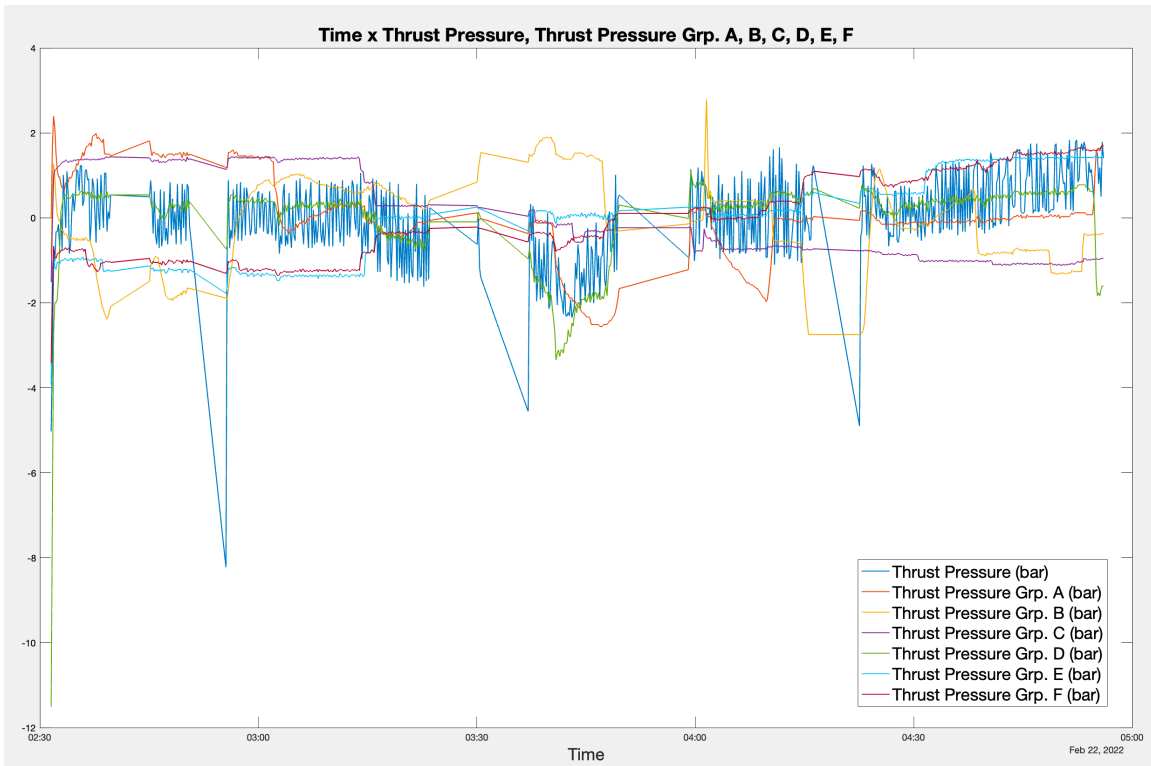


(a) Ring 842: Rock. Thrust pressures are varying very little, with observations seen to be concentrated at higher values of pressure.

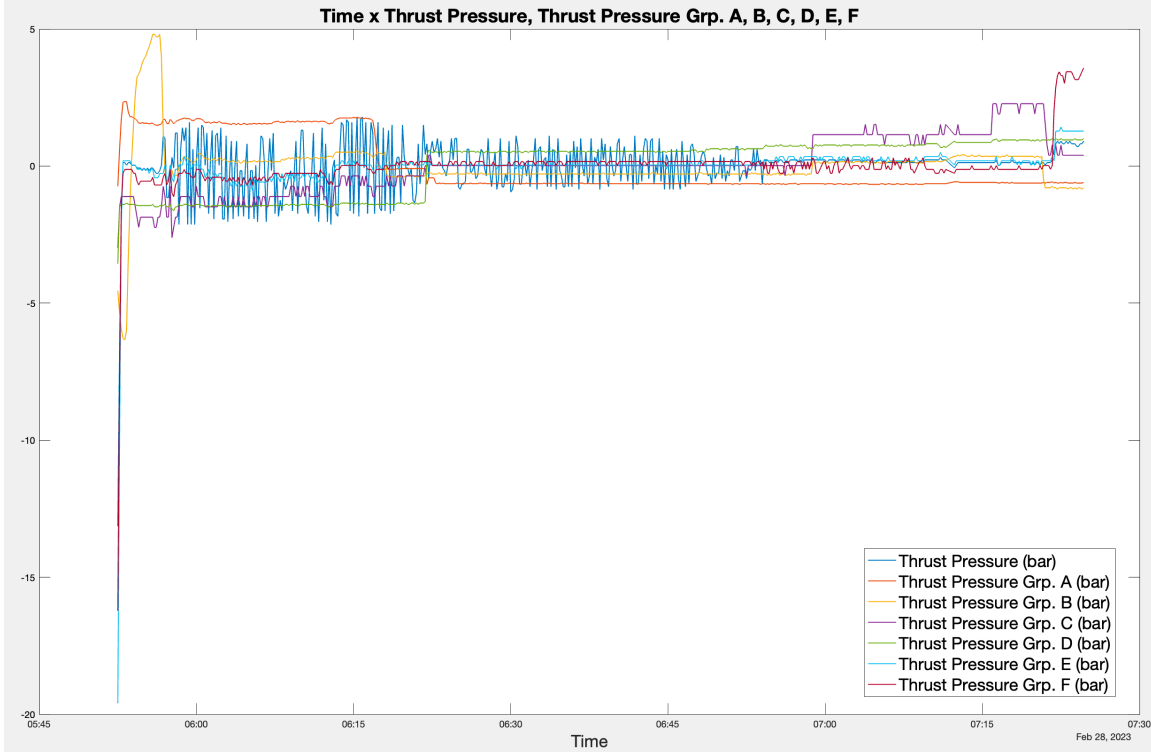


(b) Ring 598: Rock-like mixed. Thrust pressure varies significantly while remaining constant at higher values of thrust pressure groups A-F.

Figure 4-28: Time series plots relating Thrust Pressure and Thrust Pressure Groups A, B, C, D, E, F for rock and rock-like mixed.



(a) Ring 557: Soil. Thrust pressure groups vary significantly. While thrust pressure varies around a certain threshold.



(b) Ring 613: Soil-like mixed. All thrust pressure groups vary together, reducing variability towards the end of the ring.

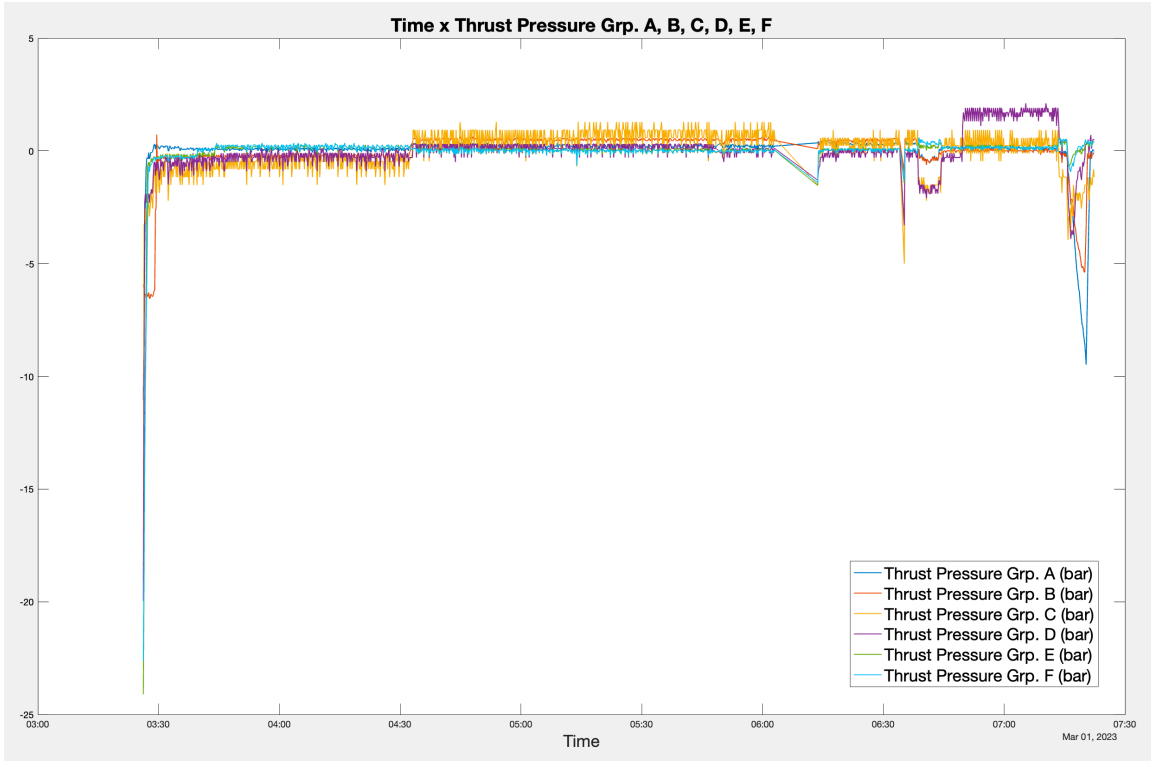
Figure 4-29: Time series plots relating Thrust Pressure and Thrust Pressure Groups A, B, C, D, E, F for soil and soil-like mixed.

Time x Thrust Pressure Groups A, B, C, D, E, F

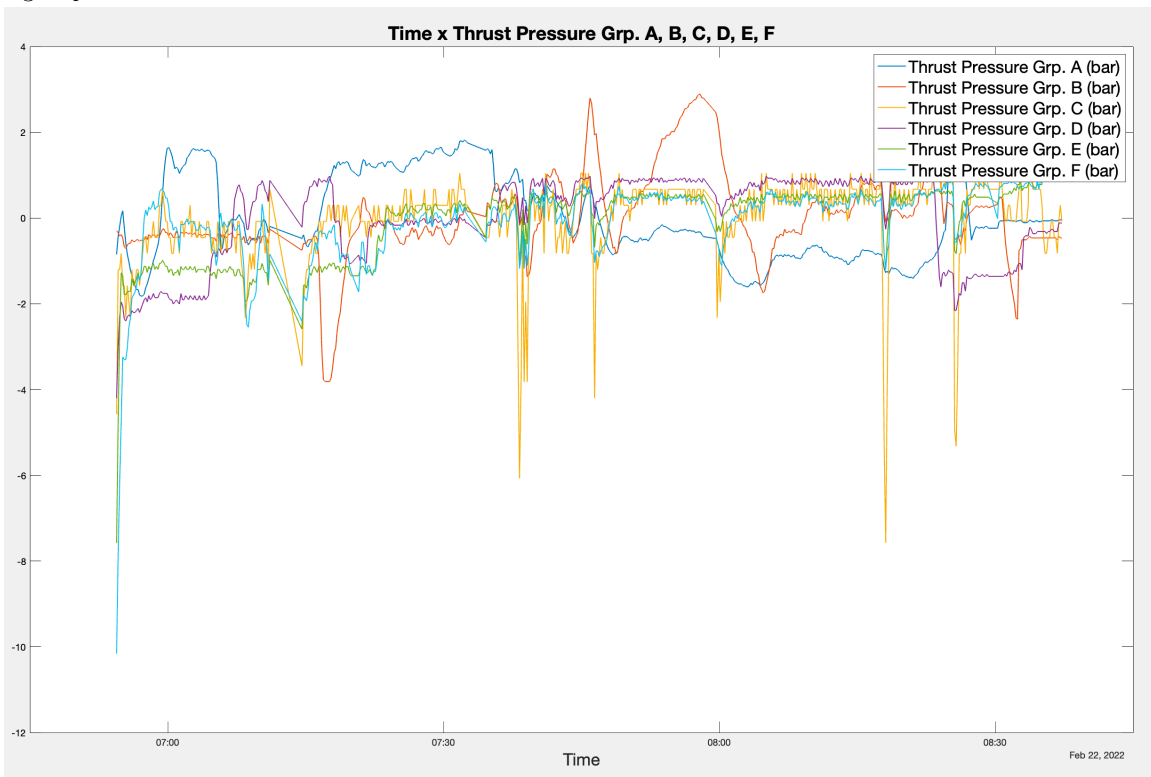
Thrust pressures in tunnel boring machines (TBMs) are classified into different groups, namely A, B, C, D, E, and F. These groups correspond to different levels of pressure that the TBM can exert on the tunnel face during excavation. Group A TBMs are typically used in soft ground conditions and exert a low thrust pressure, while Group F TBMs are used in hard rock conditions and can exert the highest thrust pressure. The selection of the appropriate thrust pressure group depends on the geological conditions of the tunnel being excavated, as well as the size and power of the TBM being used.

Thrust pressure groups A through F as mentioned above, are the different levels of thrust pressure used to excavate through different ground conditions. They are chosen based on anticipated geological conditions, with harder or more heterogeneous formations requiring higher thrust pressure groups and softer or more homogeneous ground requiring lower thrust pressure groups. Below a sample from rock, soil, rock-like mixed and soil-like mixed rings is presented (see Figures 4-30 and 4-31).

This page intentionally left blank.

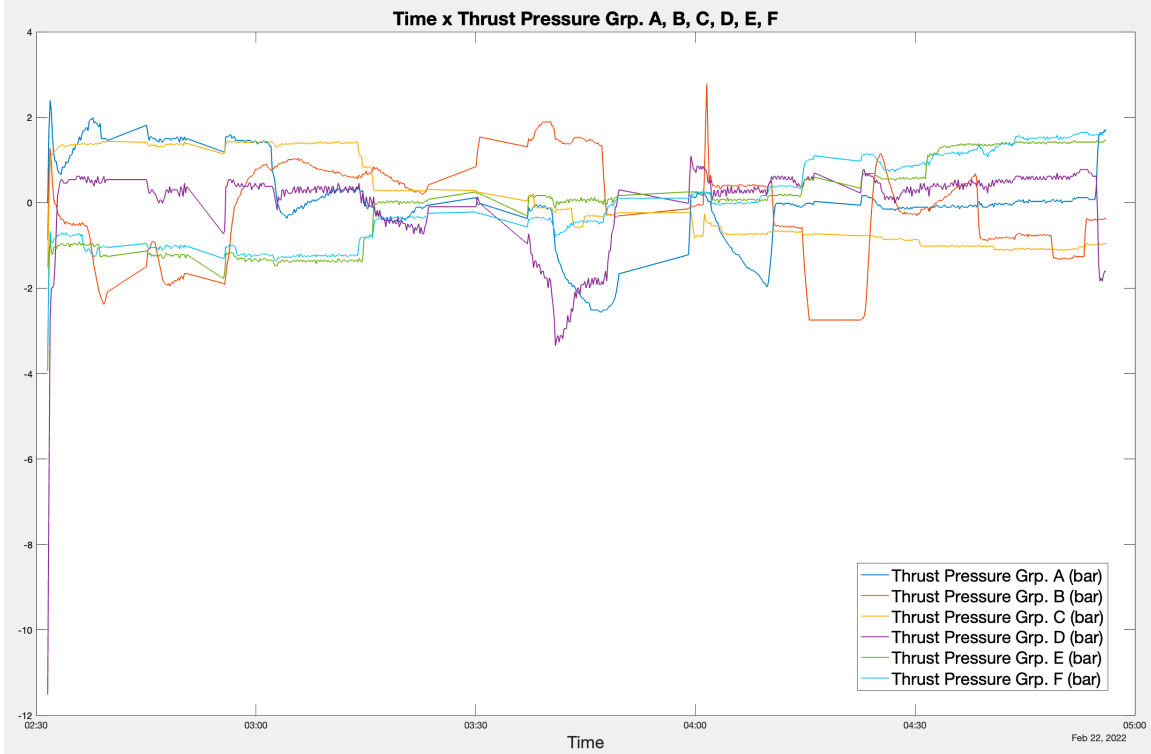


(a) Ring 842: Rock. There is minimal variation in the thrust pressure groups, and most of the observations indicate higher pressure values.

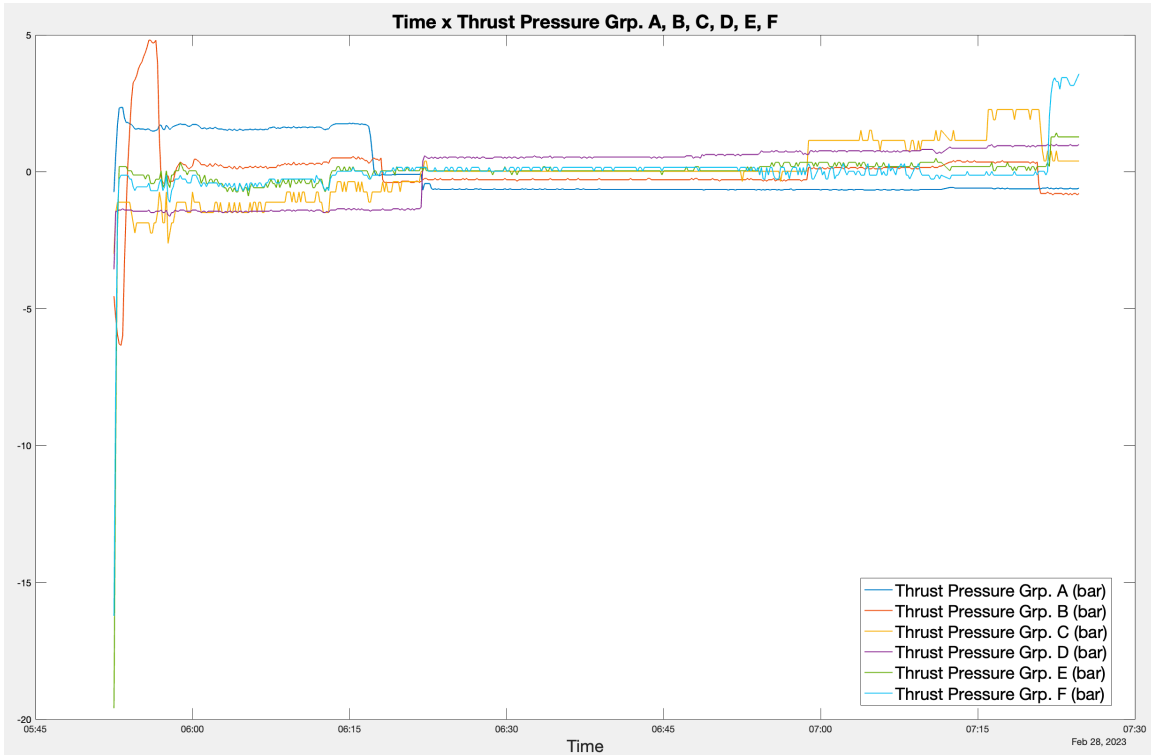


(b) Ring 598: Rock-like mixed. Thrust pressure groups show a considerable degree of variation but remains consistent at higher pressure levels.

Figure 4-30: Time series plots relating Thrust Pressure Groups A, B, C, D, E, F for rock and rock-like mixed.



(a) Ring 557: Soil. There is notable variability among different groups of thrust pressure.



(b) Ring 613: Soil-like mixed. All groups of thrust pressure exhibit similar patterns of variation, resulting in reduced variability towards the middle and end of the ring.

Figure 4-31: Time series plots relating Thrust Pressure Groups A, B, C, D, E, F for soil and soil-like mixed.

4.4.2 Scatter Plots

Scattergrams are crucial in predicting geology and classifying ground conditions for TBM operations. By plotting variables against each other, they enable pattern observation and outlier identification. This aids in making informed decisions about operating parameters.

The section includes illustrations of the selected ground classes, including both rock-like and soil-like mixed rings. Each of the 17 proposed scattergrams, as well as histogram pairings for each parameter, will be presented. For each comparison of parameter pairs, graphs for rock, soil, and mixed ground classes will be displayed, in that order. Additionally, physical interpretations for each graph are proposed.

To clarify the terminology used to describe the main characteristics of data points in a scattergram, Table 4.7 is presented. This table defines outlier, cluster, and correlation, which are important terms to understand when interpreting scattergrams. By understanding these terms, we can better analyze and interpret the relationships between variables represented in scattergrams.

Torque Cutting Wheel x Pressure Force Cutting Wheel

A positive correlation between torque cutting wheel and pressure force cutting wheel can indicate more resistant geological formations that require increased torque and pressure to advance the TBM, while a negative correlation may suggest less resistant ground formations such as soil. Visual representations of these correlations for each ground class can be found in Figures 4-32 and 4-33.


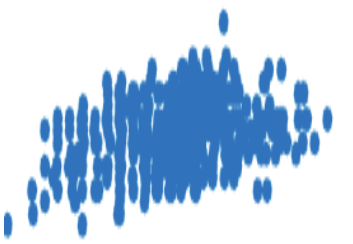


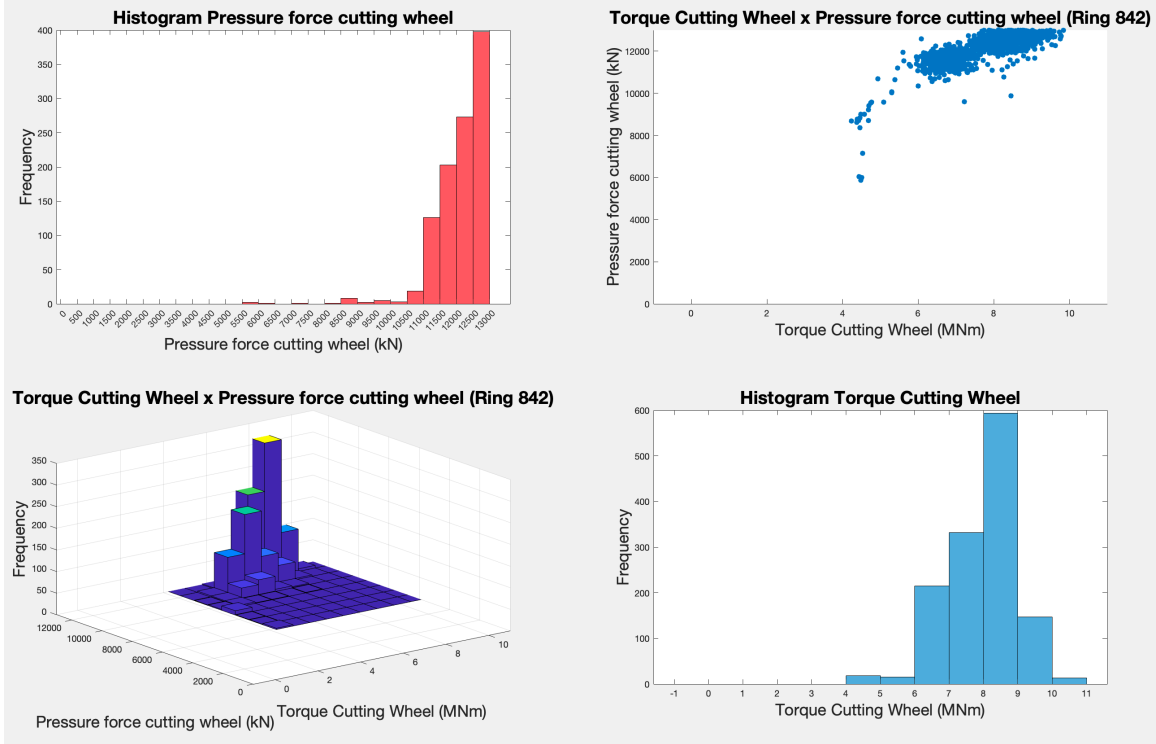
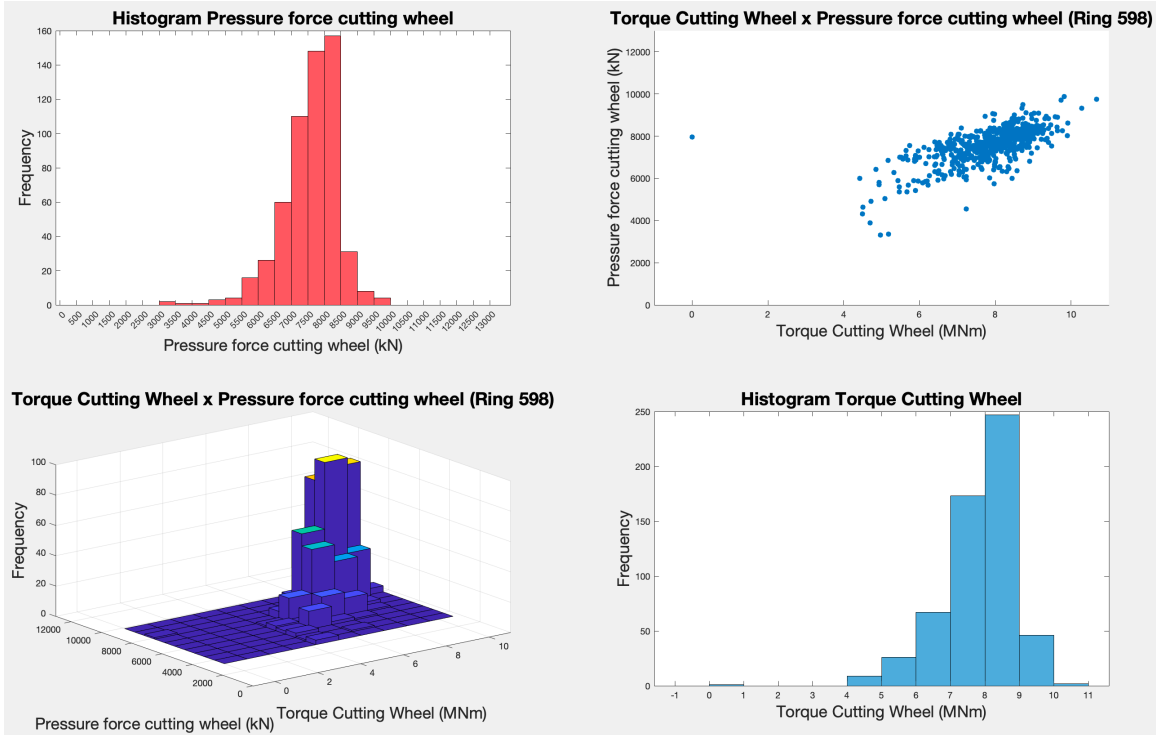
Representative Image	Terminology
	Highly concentrated
	Concentrated
	Somewhat spread-out
	Spread-out

Table 4.7: Terminology used to describe characteristics of data-points.

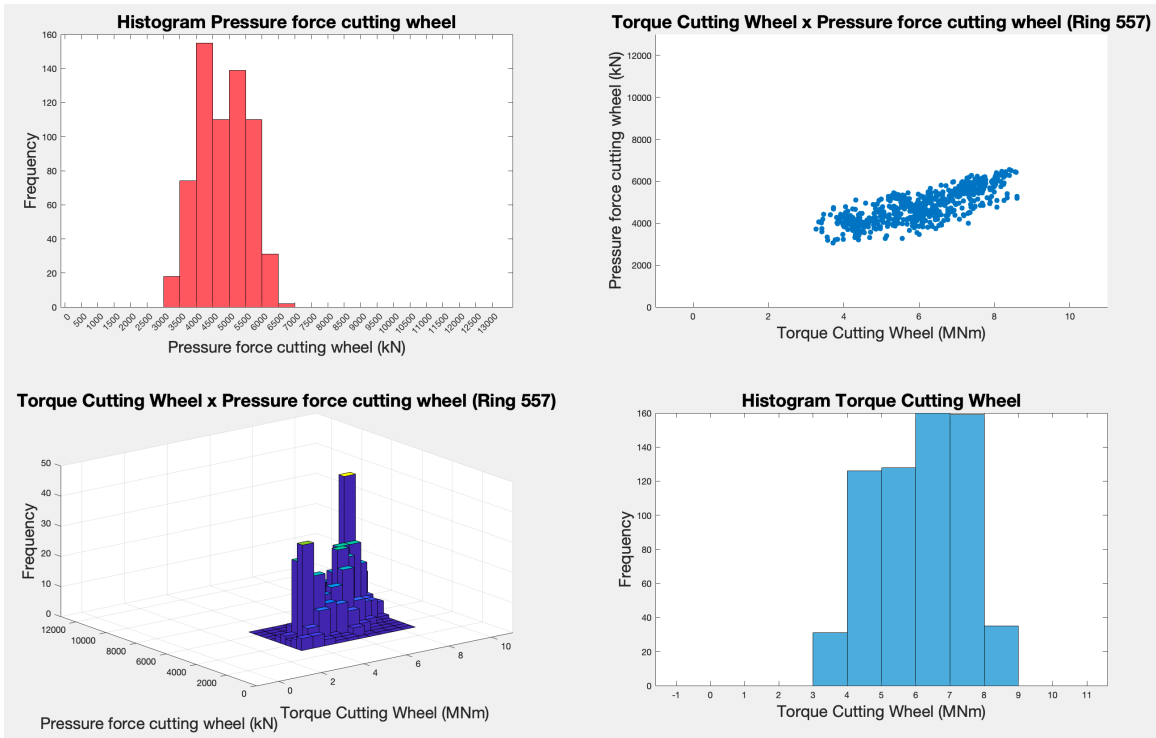


(a) Ring 842: Rock. Data-points are highly concentrated at high values of pressure force cutting wheel and torque cutting wheel. Also, considerable variability can be observed, with sparse data-points around the edges of data clusters.

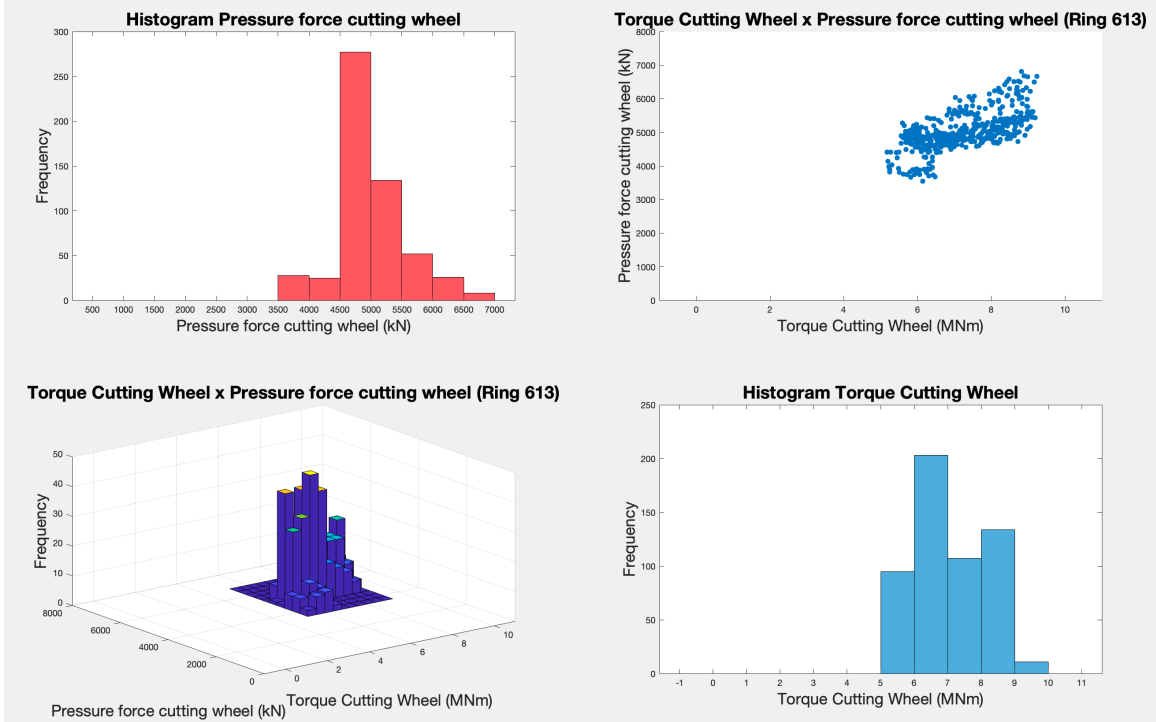


(b) Ring 598: Rock-like mixed. The data-points are concentrated around higher values of pressure force cutting wheel and torque cutting wheel.

Figure 4-32: Scatter plots and histograms relating Torque Cutting Wheel and Pressure Force Cutting Wheel for rock and rock-like mixed.



(a) Ring 557: Soil. Data-points are concentrated at a smaller range of torque cutting wheel, with a defined oval shape.



(b) Ring 613: Soil-like mixed. The data are concentrated within a specific range of torque cutting wheel, without recording of outlier values.

Figure 4-33: Scatter plots and histograms relating Torque Cutting Wheel and Pressure Force Cutting Wheel for soil and soil-like mixed.

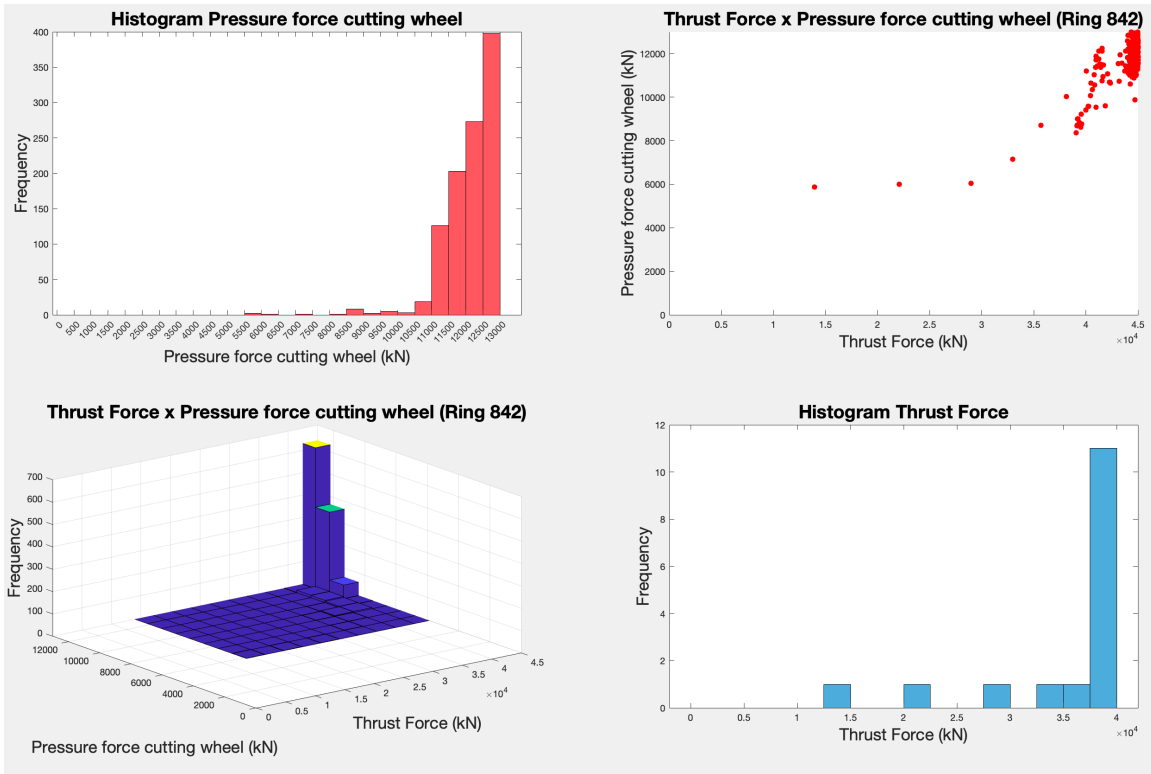
The data-point concentration observed in rock indicates that geological formation is relatively consistent in resistance to excavation, outputting highly concentrated data points around higher values of both parameters.

On the other hand, the more spread-out data points in the scattergram for soil suggest that the geological formation is highly variable, requiring fluctuating levels of torque and pressure to excavate. Analyzing the relationship between torque cutting wheel and pressure force cutting wheel can provide valuable insights into the geological conditions and potentially inform a ground class distinction system.

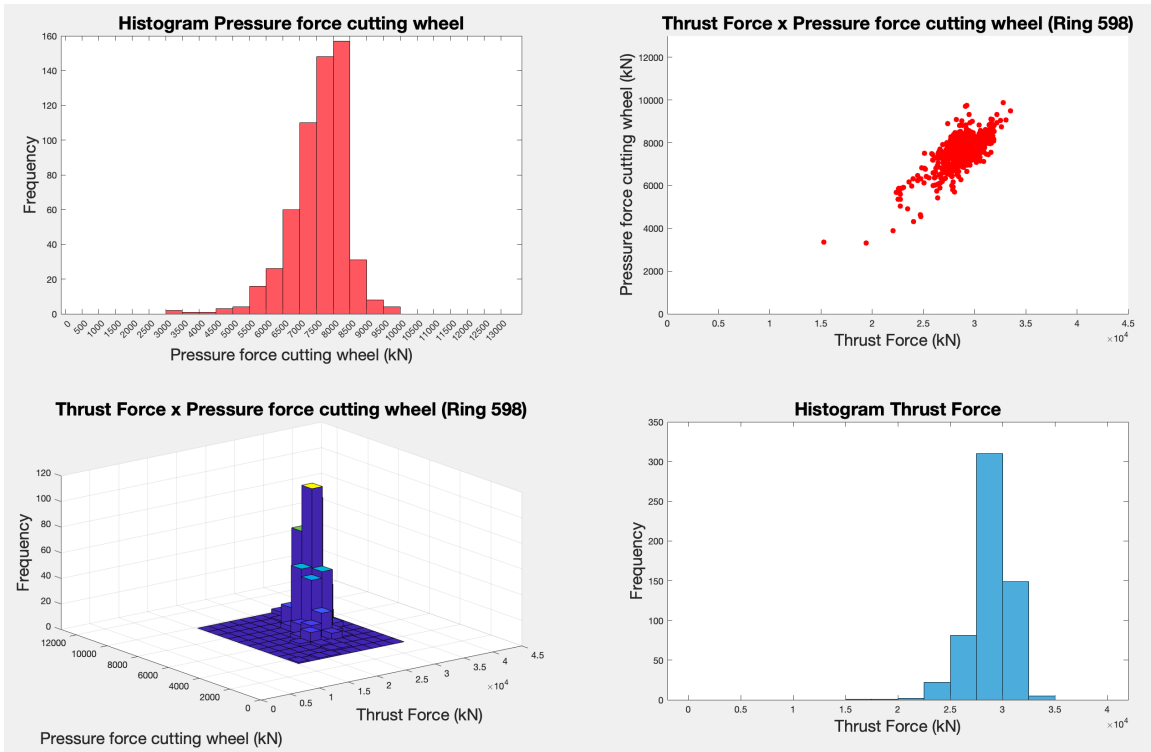
Thrust Force x Pressure Force Cutting Wheel

As previously discussed, higher pressure force cutting wheel indicates resistant material while the contrary would indicate softer geological formation. Below a sample from rock, soil, rock-like mixed and soil-like mixed rings is presented (see Figures 4-34, 4-35).

This page intentionally left blank.

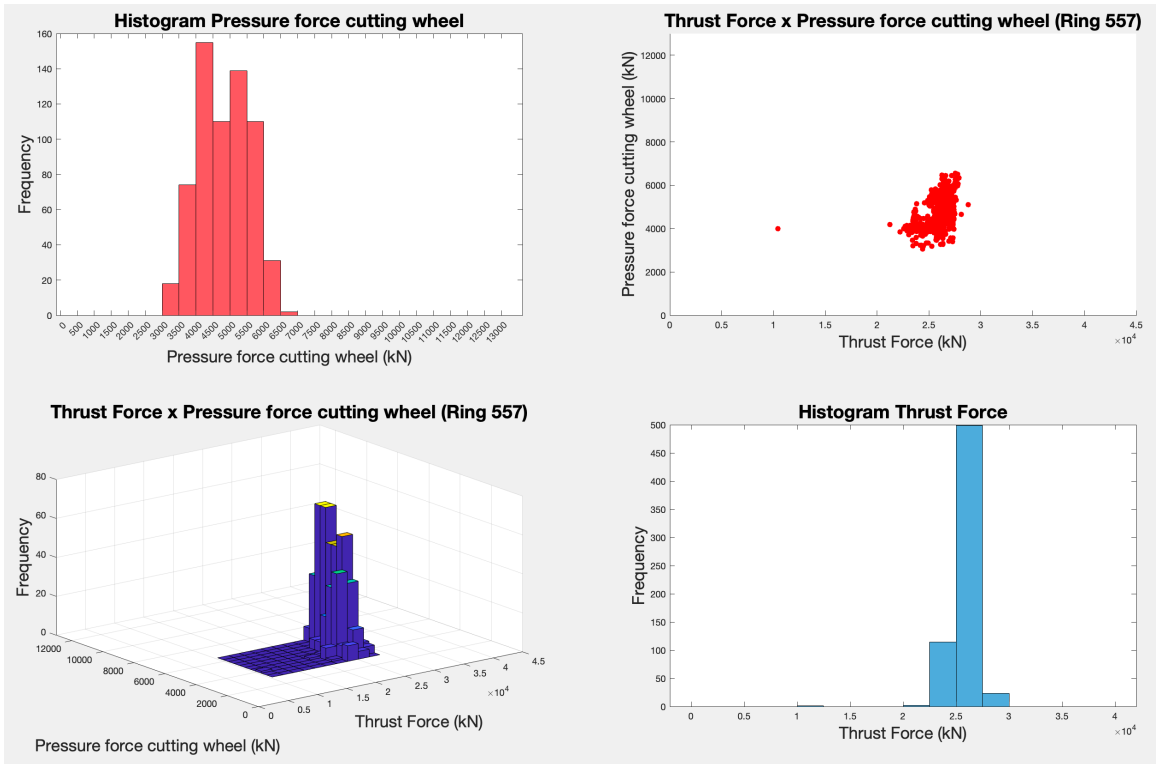


(a) Ring 842: Rock. Data are highly concentrated around higher values of thrust force.

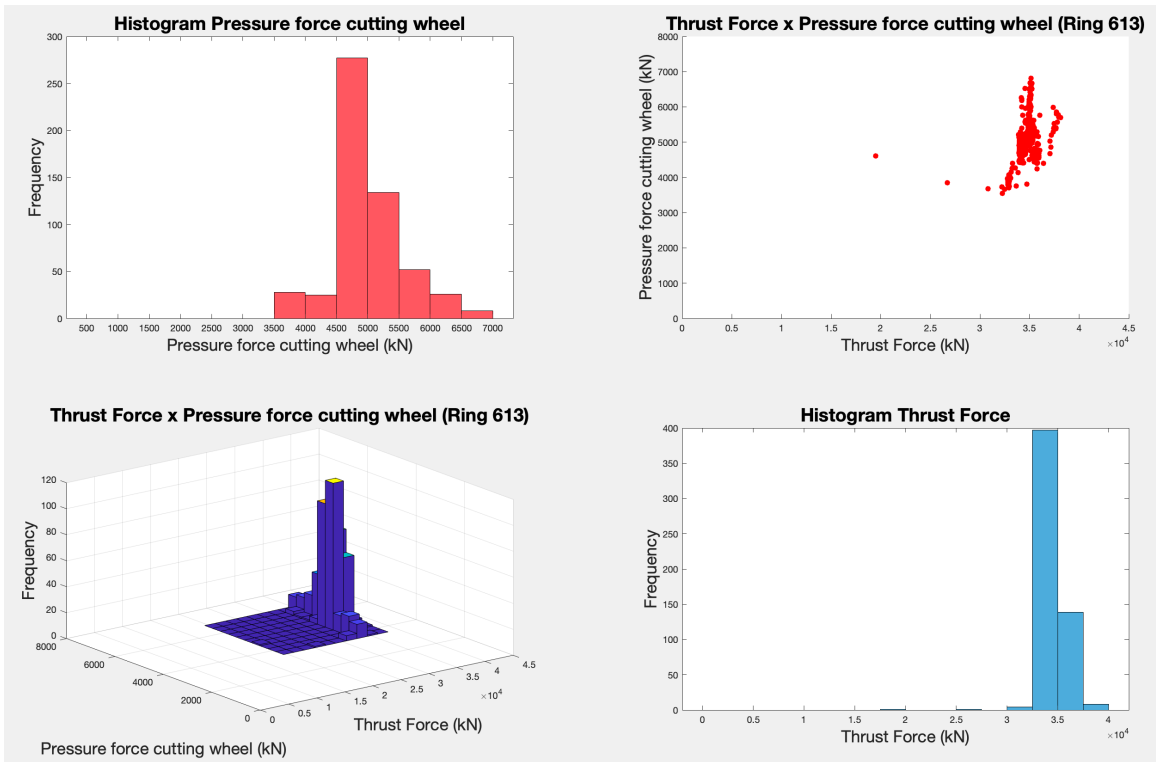


(b) Ring 598: Rock-like mixed. Concentration can be seen at lower thrust-force, while pressure force cutting wheel remains high.

Figure 4-34: Scatter plots and histograms relating Thrust Force and Pressure Force Cutting Wheel for rock and rock-like mixed.



(a) Ring 557: Soil. Data-points are highly concentrated around lower values of both thrust force and pressure force cutting wheel.



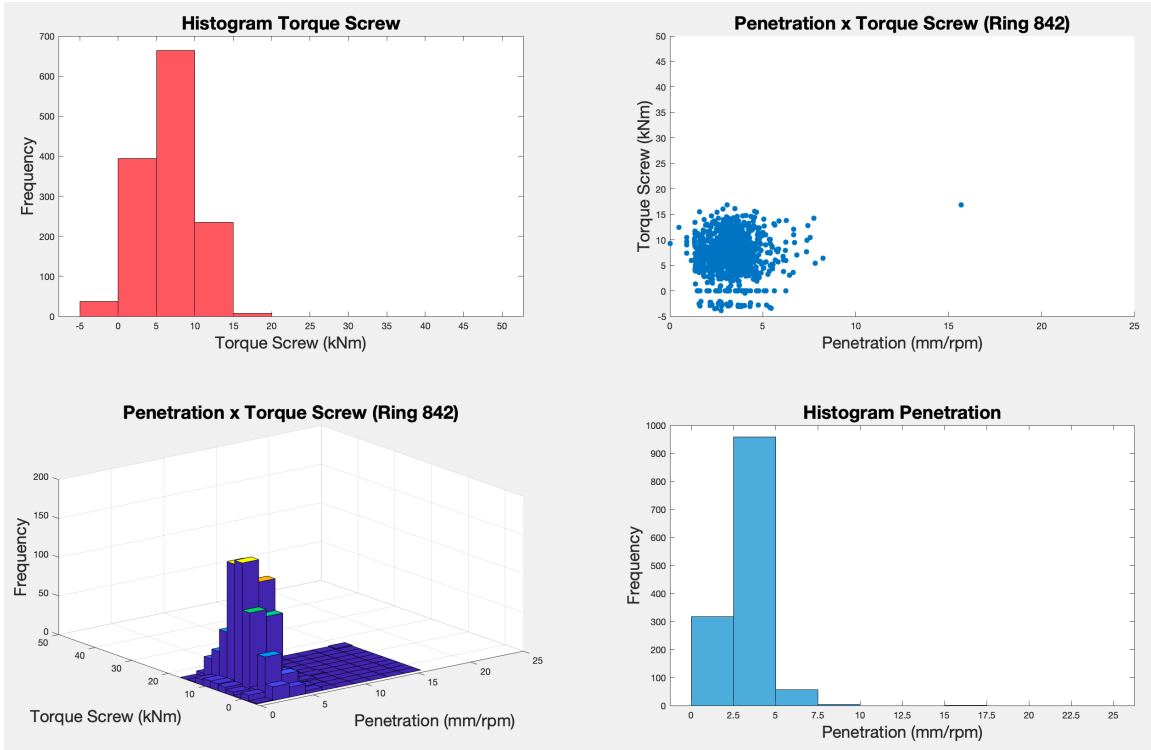
(b) Ring 613: Soil-like mixed. Data-points are concentrated around a wide range of pressure force cutting wheel values.

Figure 4-35: Scatter plots and histograms relating Thrust Force and Pressure Force Cutting Wheel for soil and soil-like mixed.

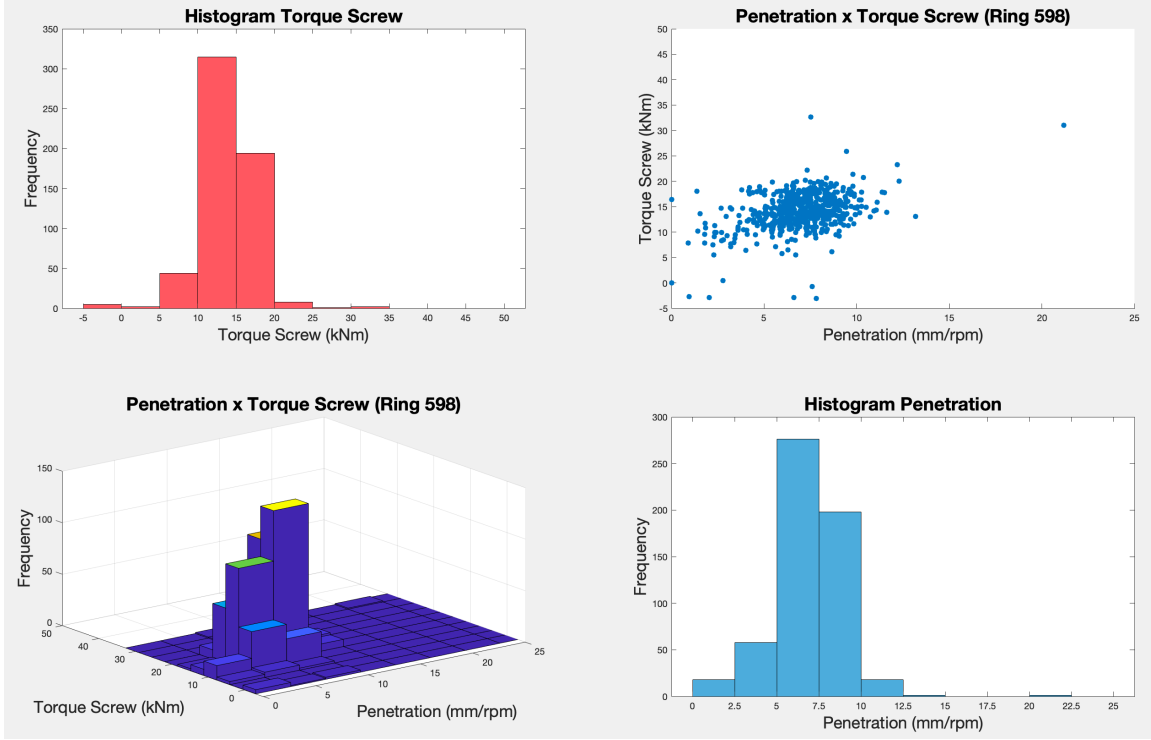
Penetration x Torque Screw

It has been noted that if penetration rate is raised against low torque screw values, this may indicate that the material being excavated is softer and easier to move through (i.e. soil, soil-like mixed rings). Conversely, if penetration is low and torque screw is high, the indication is that the material would be harder and more difficult to excavate. If there is a strong positive correlation between penetration and torque screw, this may suggest that the TBM is encountering consistent and homogeneous geology (typically rock). However, if the scattergram shows a lot of variation or no clear pattern, it may indicate that the geological conditions are more complex and heterogeneous (typically soils). The following images will show a sample of this relationship for each chosen ground class (Figures 4-36, 4-37).

This page intentionally left blank.

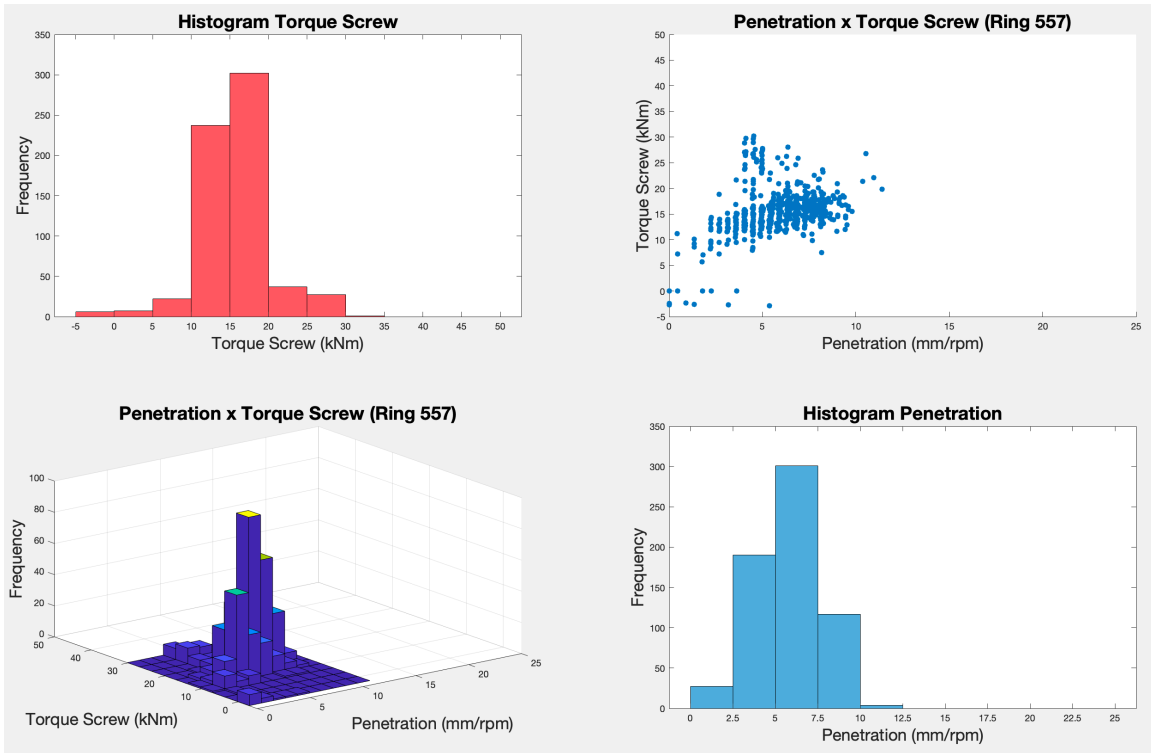


(a) Ring 842: Rock. Observations are highly concentrated at lower values for both torque screw and penetration.

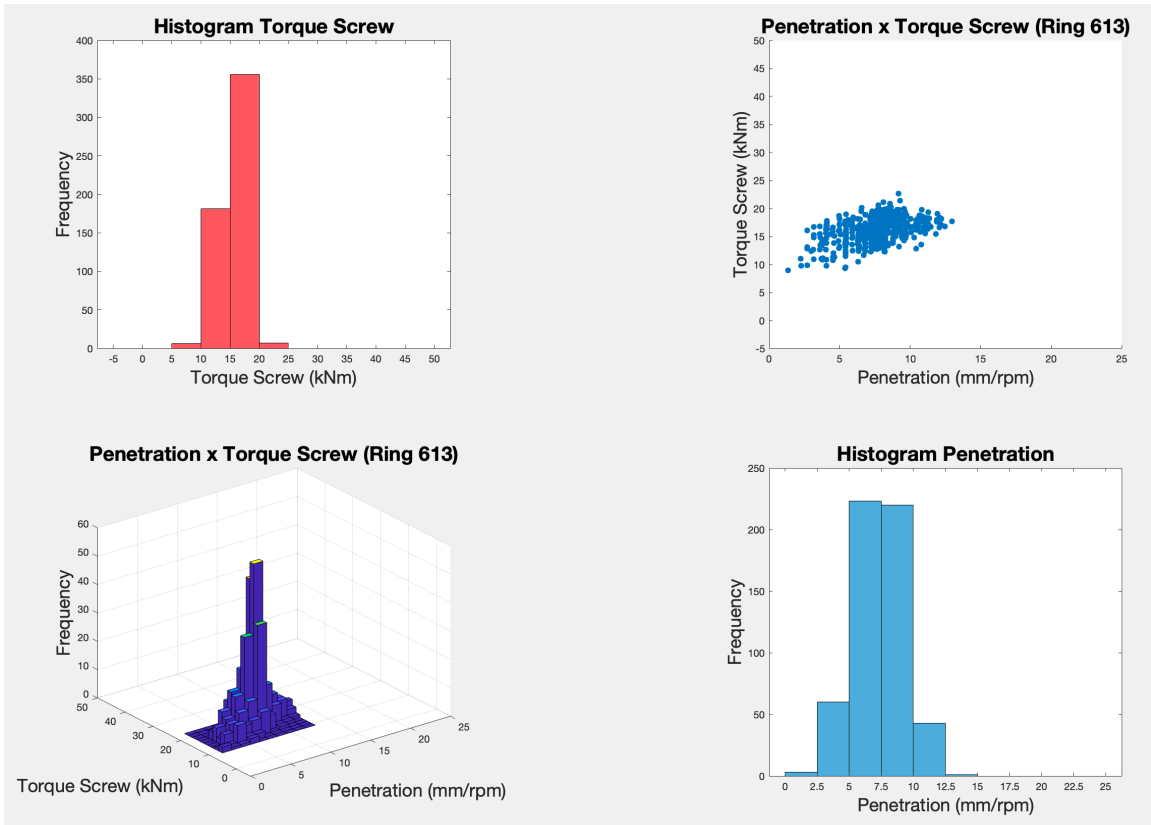


(b) Ring 598: Rock-like mixed. Data-points are concentrated at lower values of torque screw and penetration, however more sparse when compared to rock rings.

Figure 4-36: Scatter plots and histograms relating Penetration and Torque Screw for rock and rock-like mixed.



(a) Ring 557: Soil. Distinct vertical lines can be seen, typical of soil rings where there are fixed penetration rates, determined by the machine operator. Data-points are concentrated around higher values of penetration and lower torque screw values.



(b) Ring 613: Soil-like mixed. The vertical lines, where penetration rates were fixed can still be seen, indicating that there is soil-like material. Data-points are highly concentrated at higher penetration and lower torque screw values.

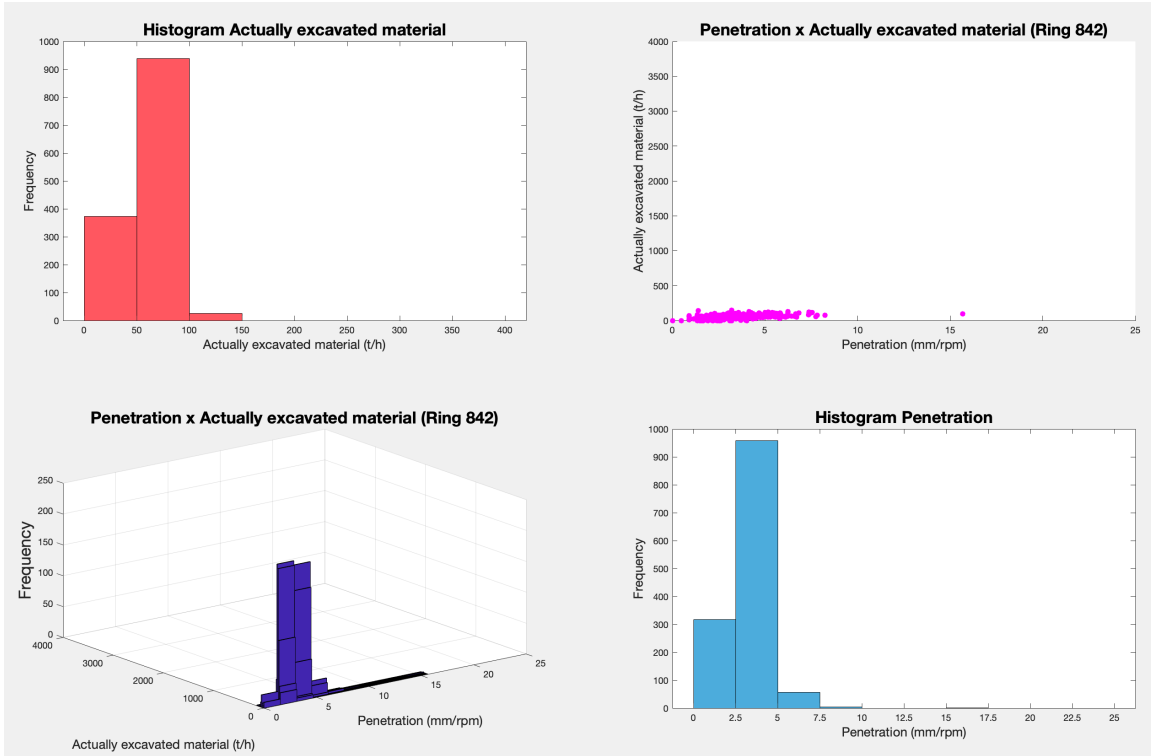
Figure 4-37: Scatter plots and histograms relating Penetration and Torque Screw for soil and soil-like mixed.

Penetration x Actually Excavated Material

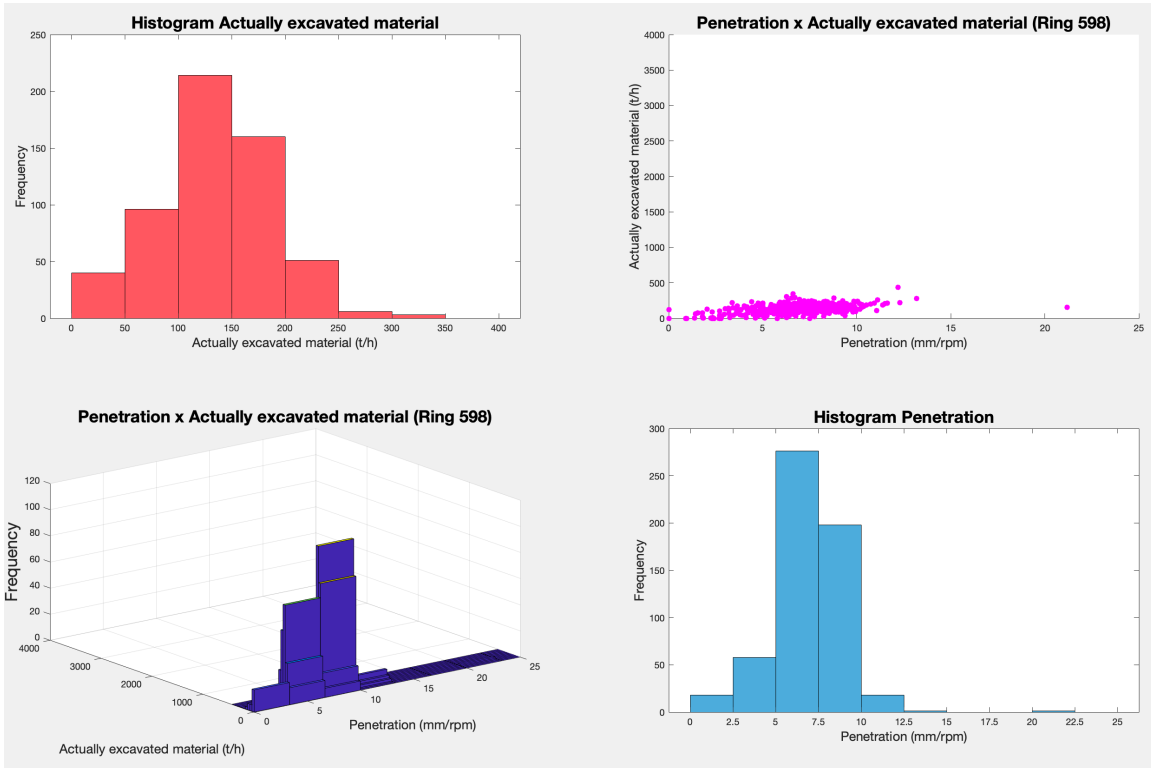
Penetration as was just mentioned is measuring the machine advancement in millimeters per rotation. Actually excavated material relates to material being removed and transported out of the tunnel face, measured in cubic meters (m³).

Both are measured through sensors, with penetration measured in the cutterhead and actually excavated material measured using load cells or pressure sensors on the conveyor system transporting material out of the tunnel. The resulting graphical representations are as presented below (figures 4-38, 4-39).

This page intentionally left blank.

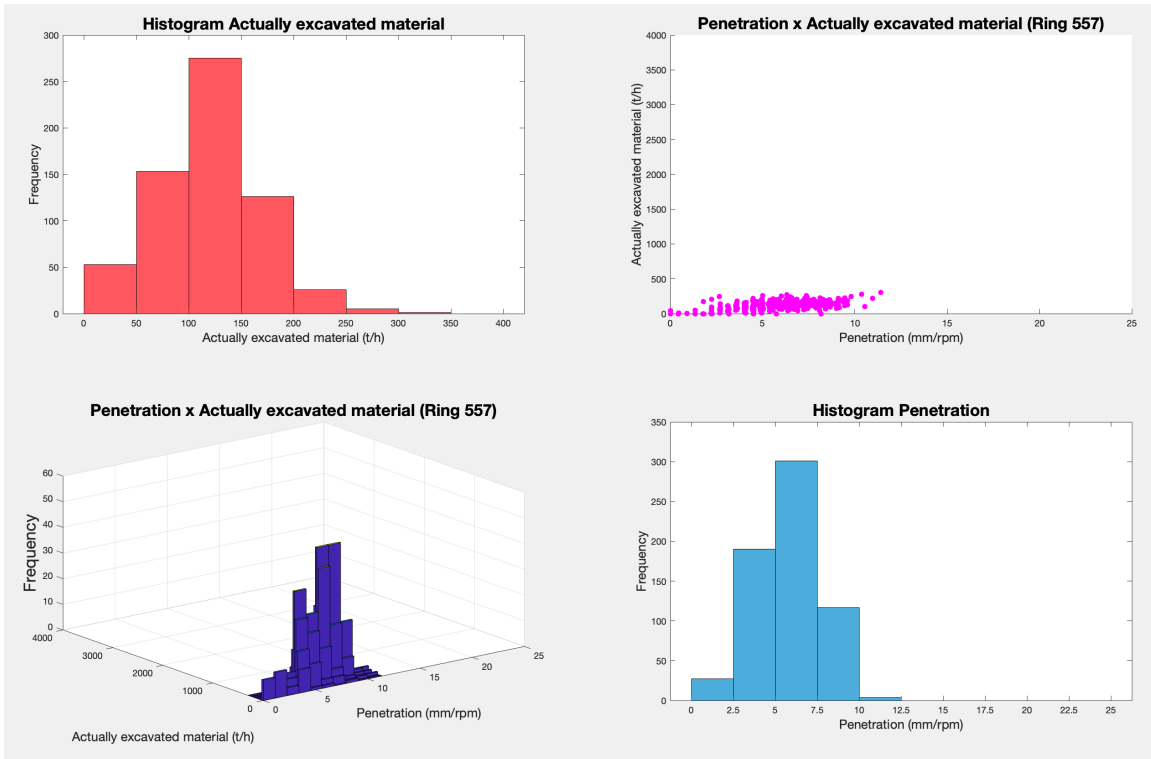


(a) Ring 842: Rock. Data-points are highly concentrated around low values of both penetration and actually excavated material.

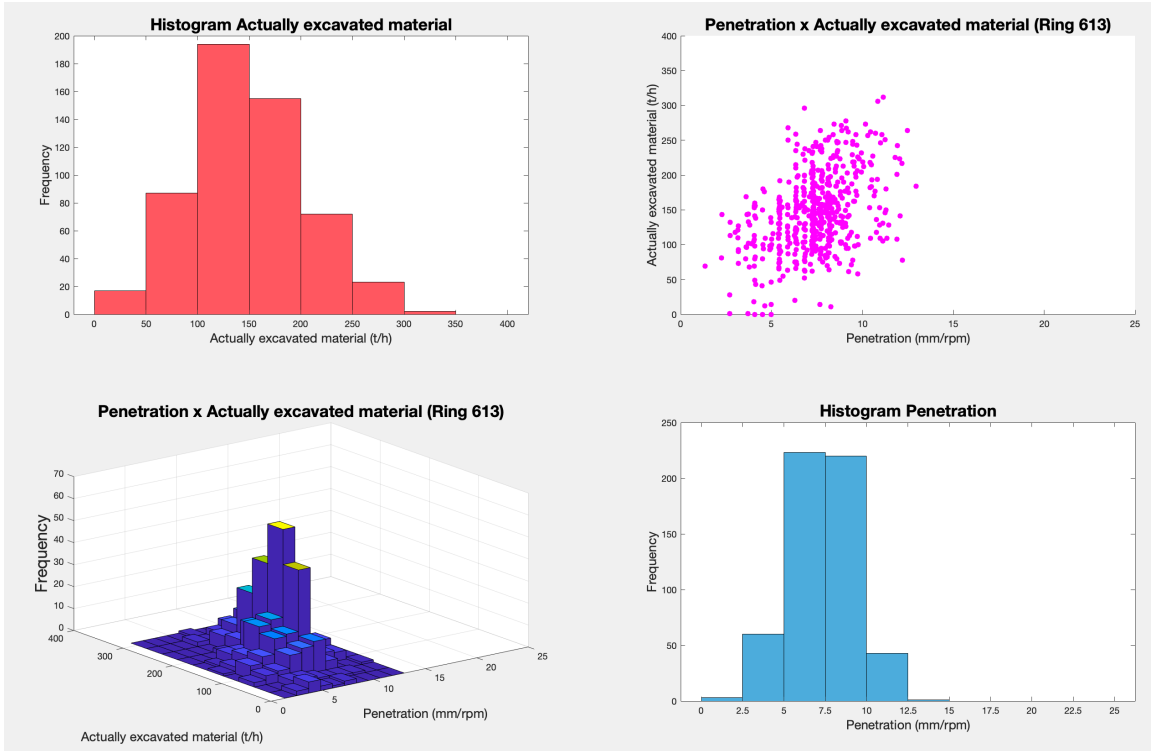


(b) Ring 598: Rock-like mixed. Concentration is seen at low values for both parameters.

Figure 4-38: Scatter plots and histograms relating Penetration and Actually Excavated Material for rock and rock-like mixed.



(a) Ring 557: Soil. Again vertical lines, suggesting controlled values of penetration rates. Data are highly concentrated at lower values of actually excavated material and higher penetration rates.



(b) Ring 613: Soil-like mixed. Vertical lines can be seen especially around lower values of penetration. The distribution is somewhat spread out.

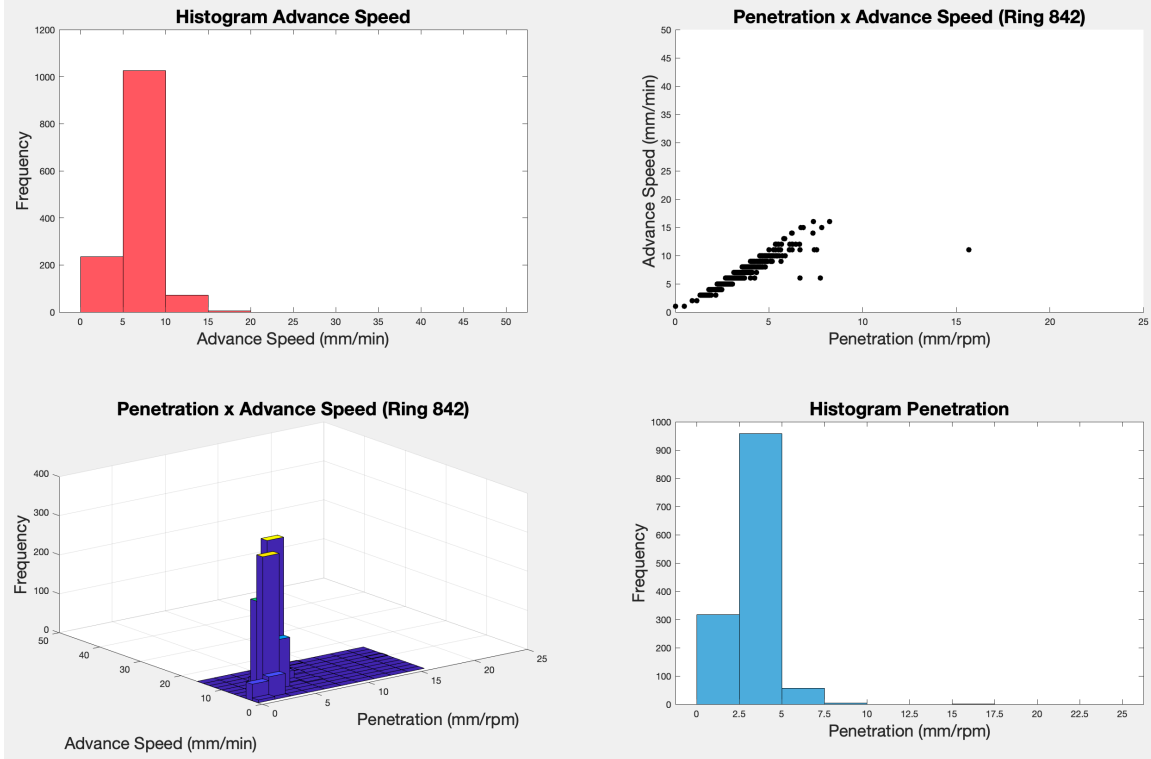
Figure 4-39: Scatter plots and histograms relating Penetration and Actually Excavated Material for soil and soil-like mixed.

Penetration x Advance Speed

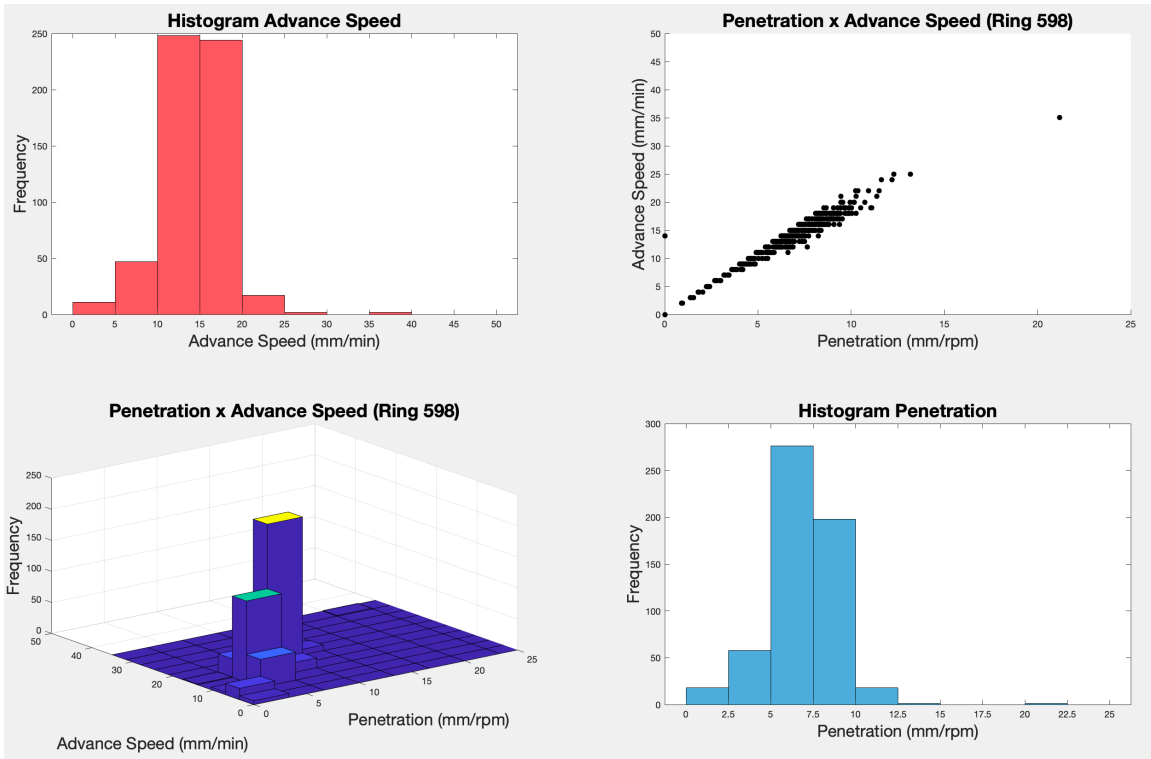
Penetration, as explained before measures the distance that the TBM excavates per revolution of the cutterhead, while advance speed is the rate at which the TBM advances through the tunnel face, measured in meters per minute (m/min). Both parameters are calculated directly on the machine during excavation, where penetration is recorded in the cutterhead and advance speed through several different techniques including lasers and GPS sensors.

As a general rule, rock formations tend to have lower penetration rates and slower advance speed due to high material resistance to excavation. In reverse, soils usually permit for higher penetration rates and faster advance speed based on the lower strength and resistance to excavation. Examining the scattergram distributions (presented in figures 4-40 and 4-41) show tendencies that provide insights into the nature of the ground conditions being excavated.

This page intentionally left blank.

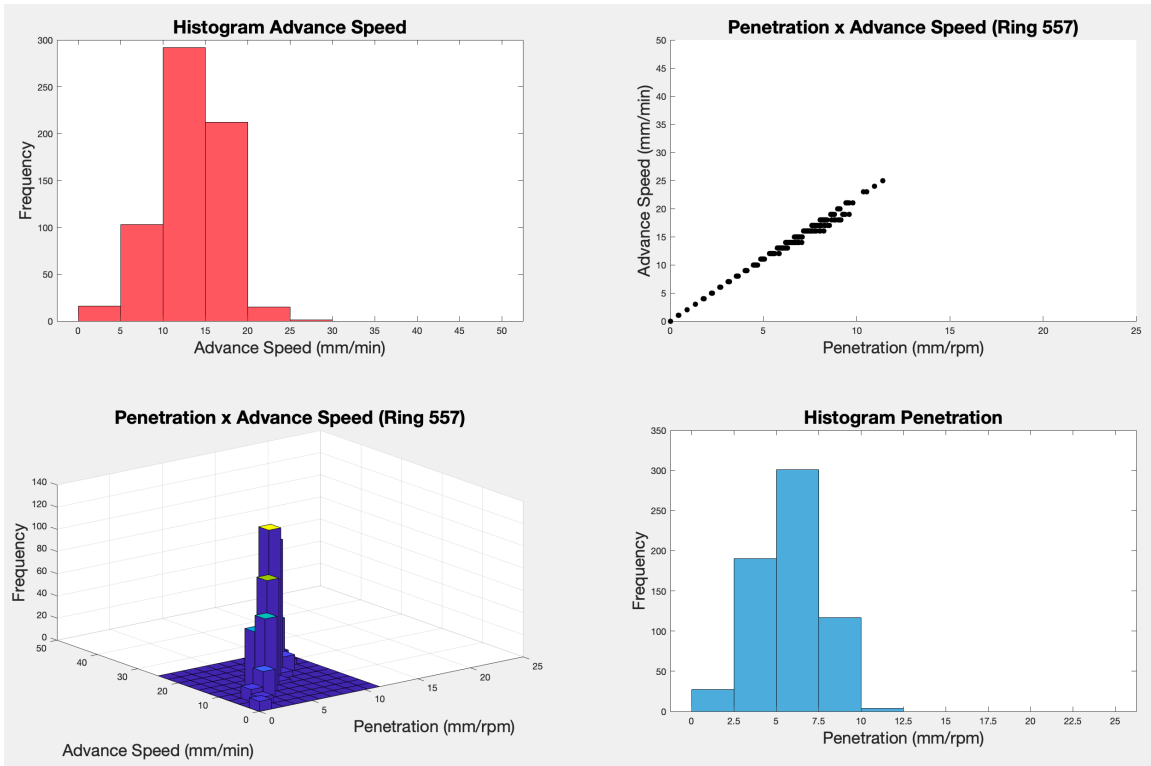


(a) Ring 842: Rock. Data-points are concentrated at lower values of both penetration and advance speed.

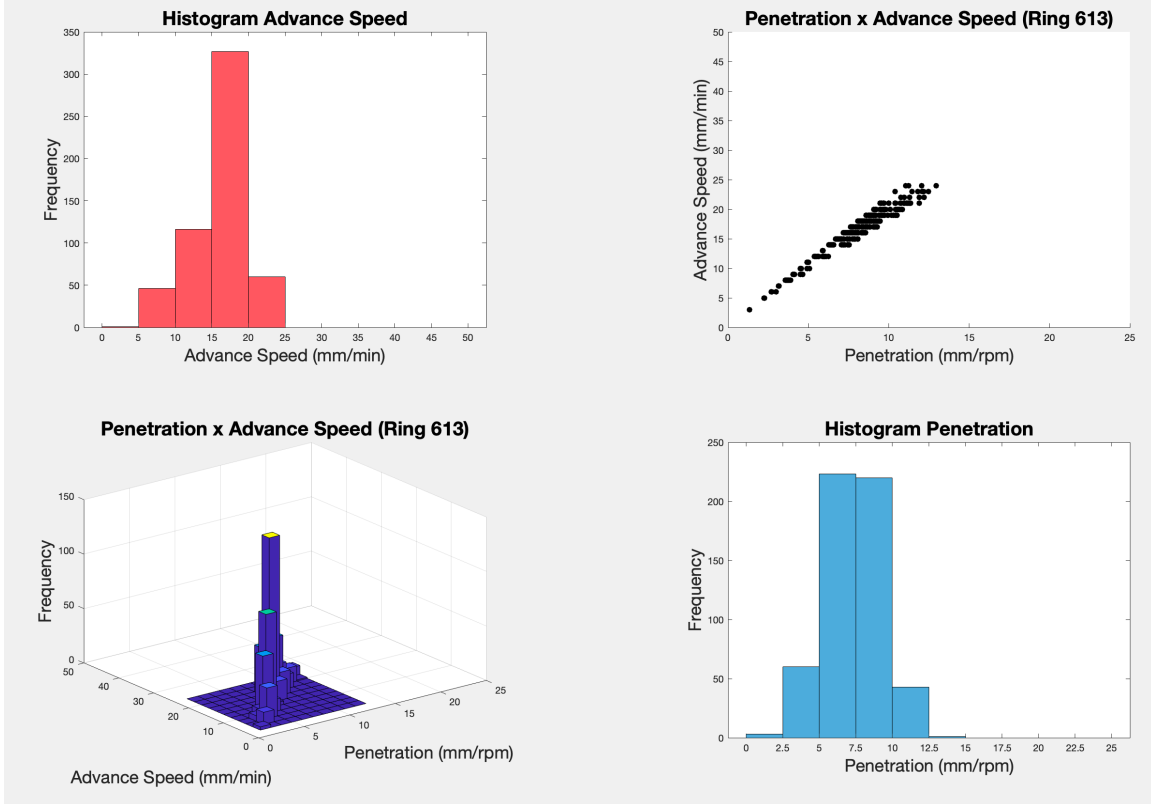


(b) Ring 598: Rock-like mixed. Concentration happens at higher values of penetration and advance speed.

Figure 4-40: Scatter plots and histograms relating Penetration and Advance Speed for rock and rock-like mixed.



(a) Ring 557: Soil. Penetration varies widely and data-points are concentrated around higher values of advance speed.



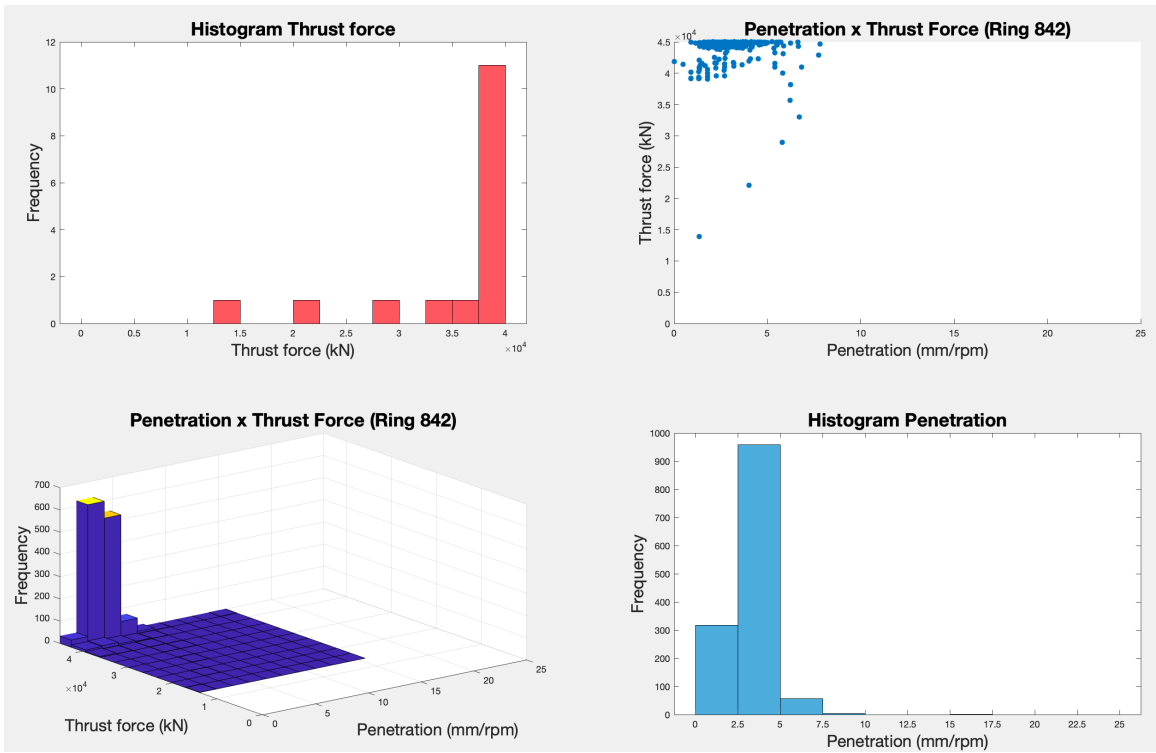
(b) Ring 613: Soil-like mixed. Advance speed and penetration vary significantly and are highly concentrated around higher values for both parameters.

Figure 4-41: Scatter plots and histograms relating Penetration and Advance Speed for soil and soil-like mixed.

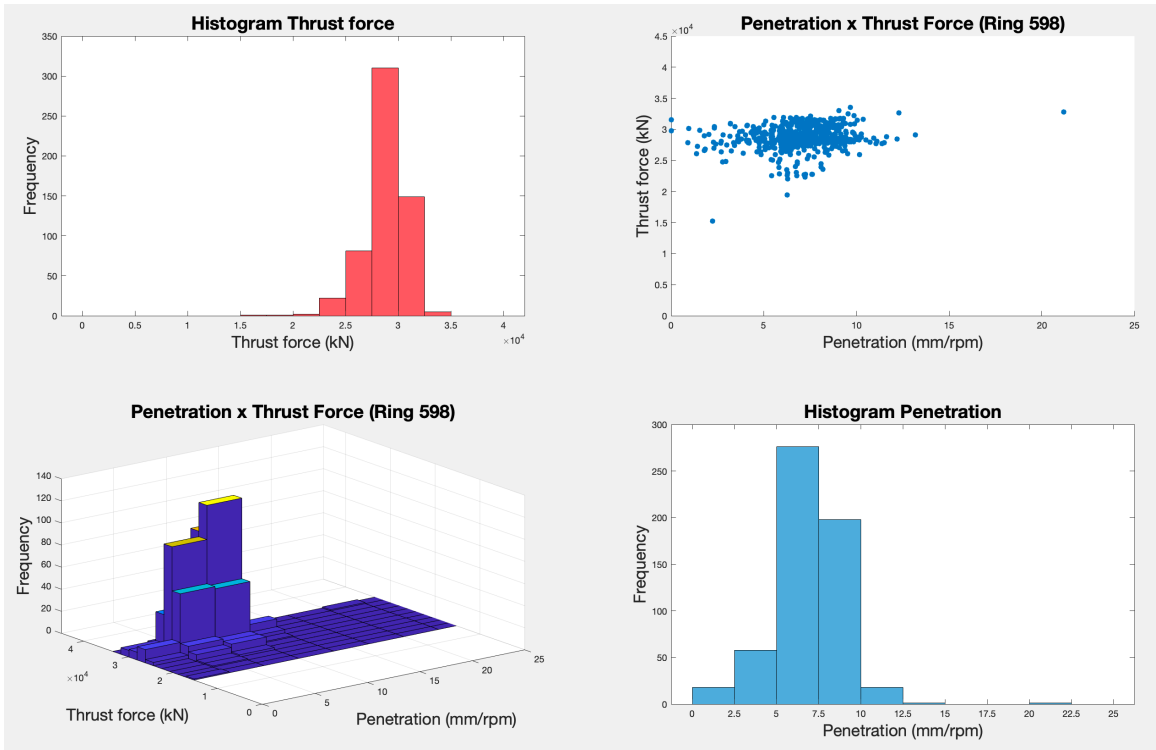
Penetration x Thrust Force

Measuring and analyzing the relationship between penetration and thrust force can assist TBM operators in optimizing the excavation process and identifying areas of the tunnel where geological conditions may require special attention. Below, samples from each studied ground class will be presented in figures 4-42, 4-43.

This page intentionally left blank.

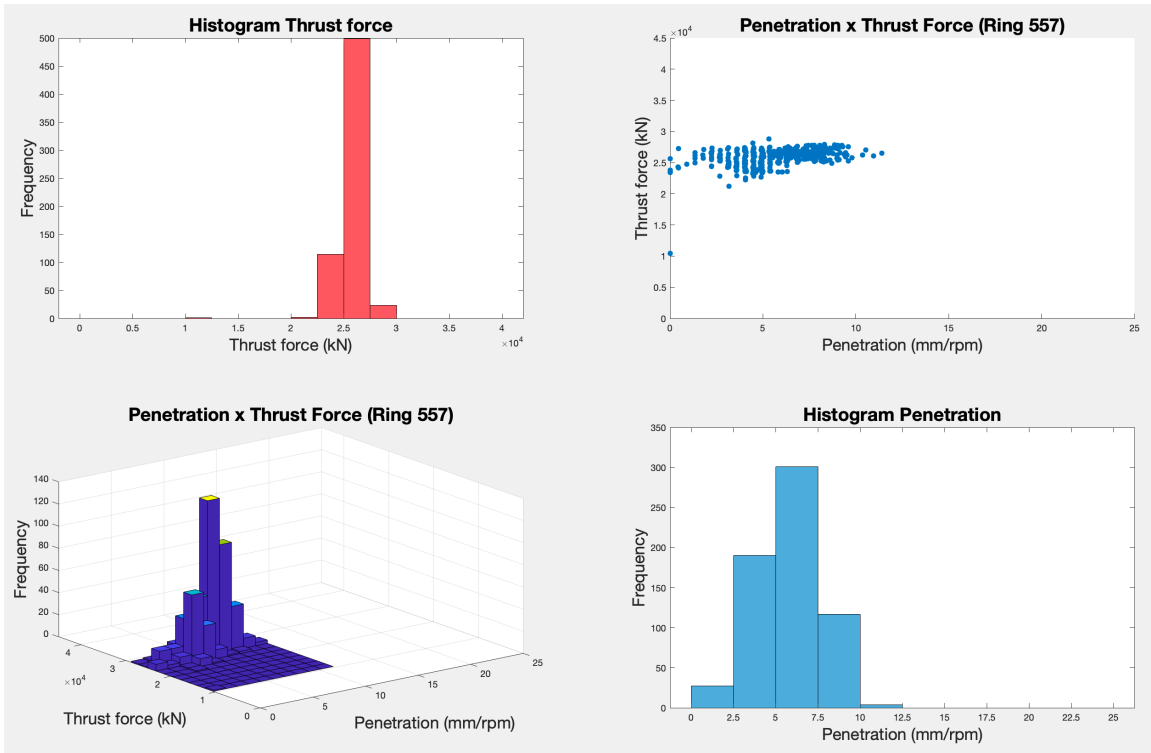


(a) Ring 842: Rock. Data-points are highly concentrated at the highest values of thrust force, while penetration remains low.

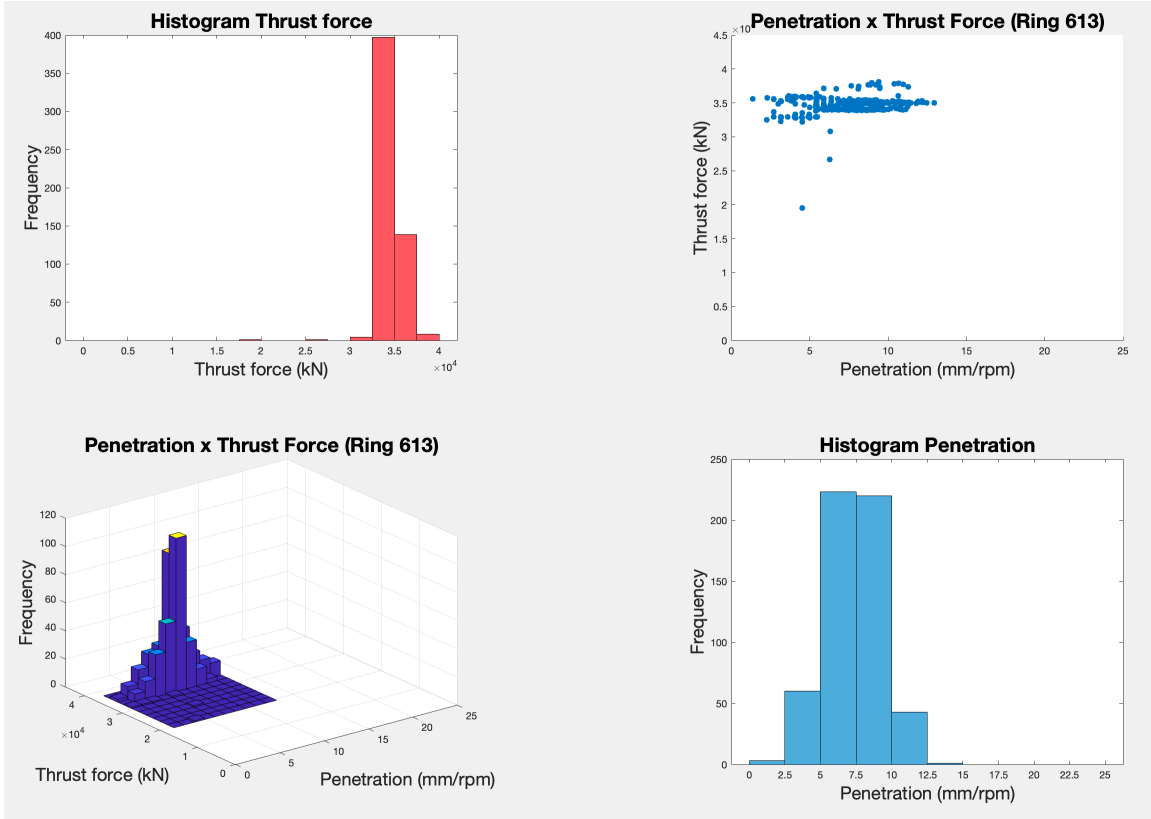


(b) Ring 598: Rock-like mixed. Concentration around mid-high values of thrust force and lower values of penetration. Extremely similar to what was seen in rock.

Figure 4-42: Scatter plots and histograms relating Penetration and Thrust Force for rock and rock-like mixed.



(a) Ring 557: Soil. Distinct vertical lines can be seen suggesting fixed values for penetration. Thrust force remains fairly constant and low throughout the ring.



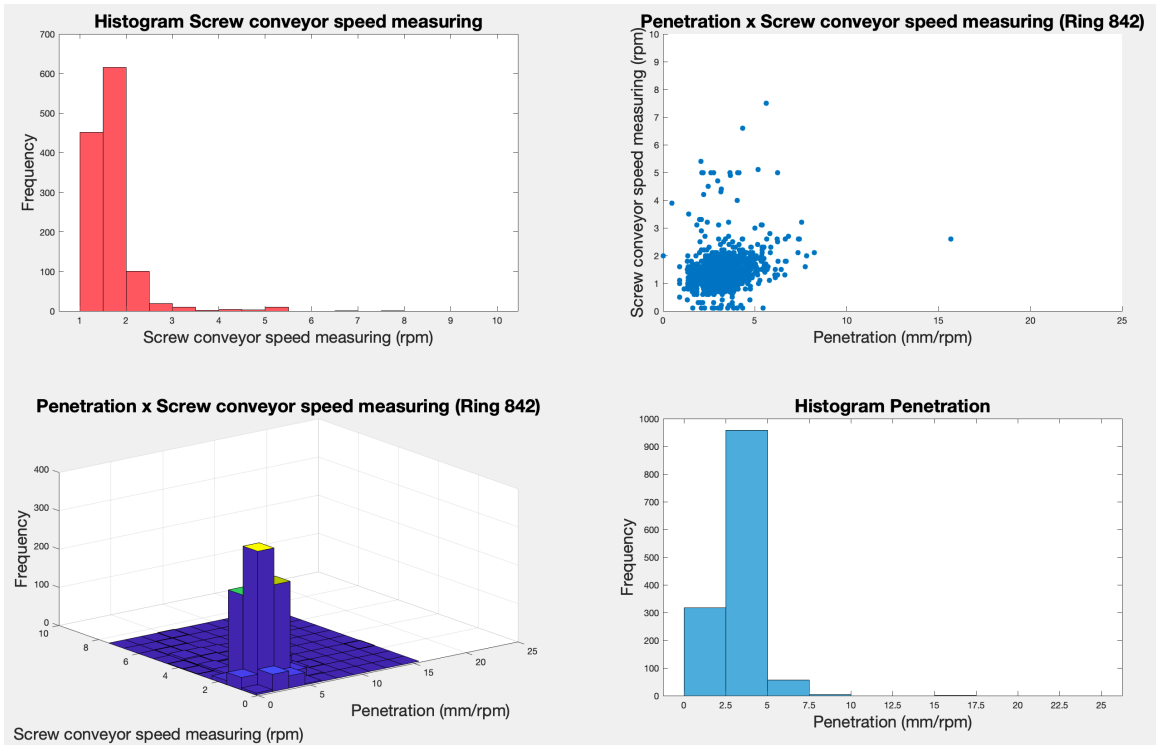
(b) Ring 613: Soil-like mixed. Data-points are highly concentrated around higher values of thrust force and penetration.

Figure 4-43: Scatter plots and histograms relating Penetration and Thrust Force for soil and soil-like mixed.

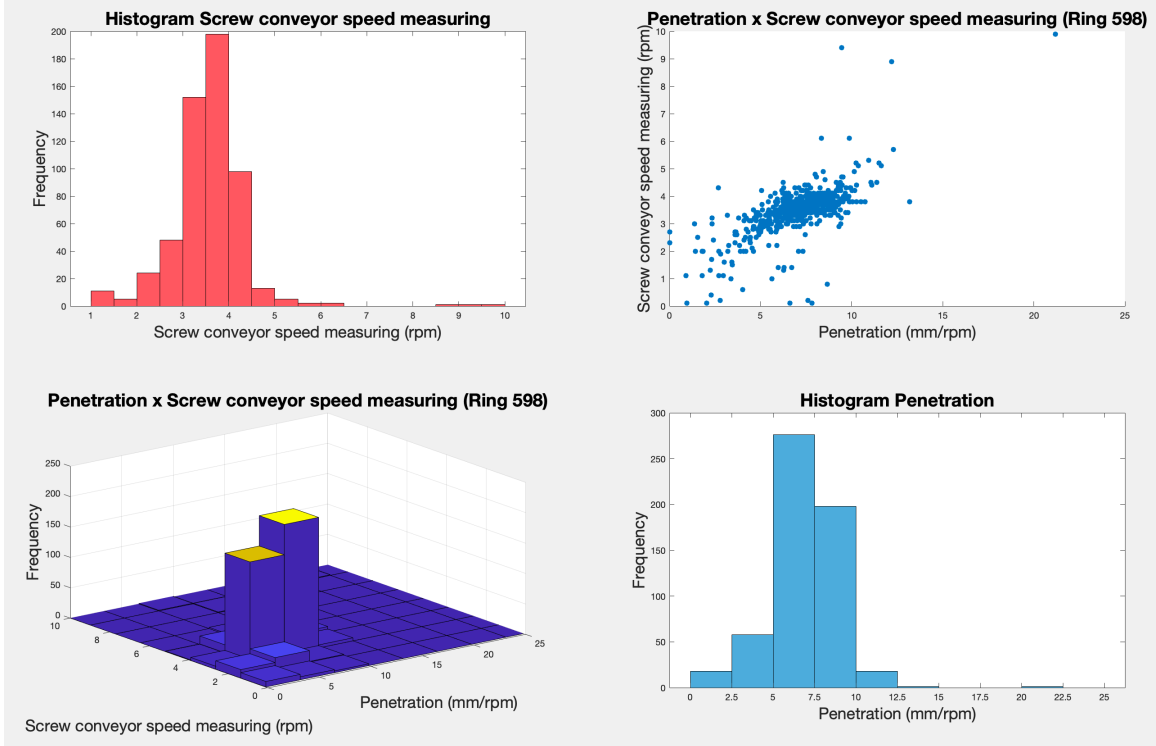
Penetration x Screw Conveyor Speed Measuring

Comparing these two parameters can potentially provide insights on the excavation process, revealing the TBM's efficiency in the excavation process. Generally, higher screw conveyor speed would convey higher rates of excavated material, which, added to higher penetration rates, should indicate a faster excavation progress. The images below show a sample of this parameter comparison for each of the evaluated ground classes (figures 4-44, 4-45).

This page intentionally left blank.

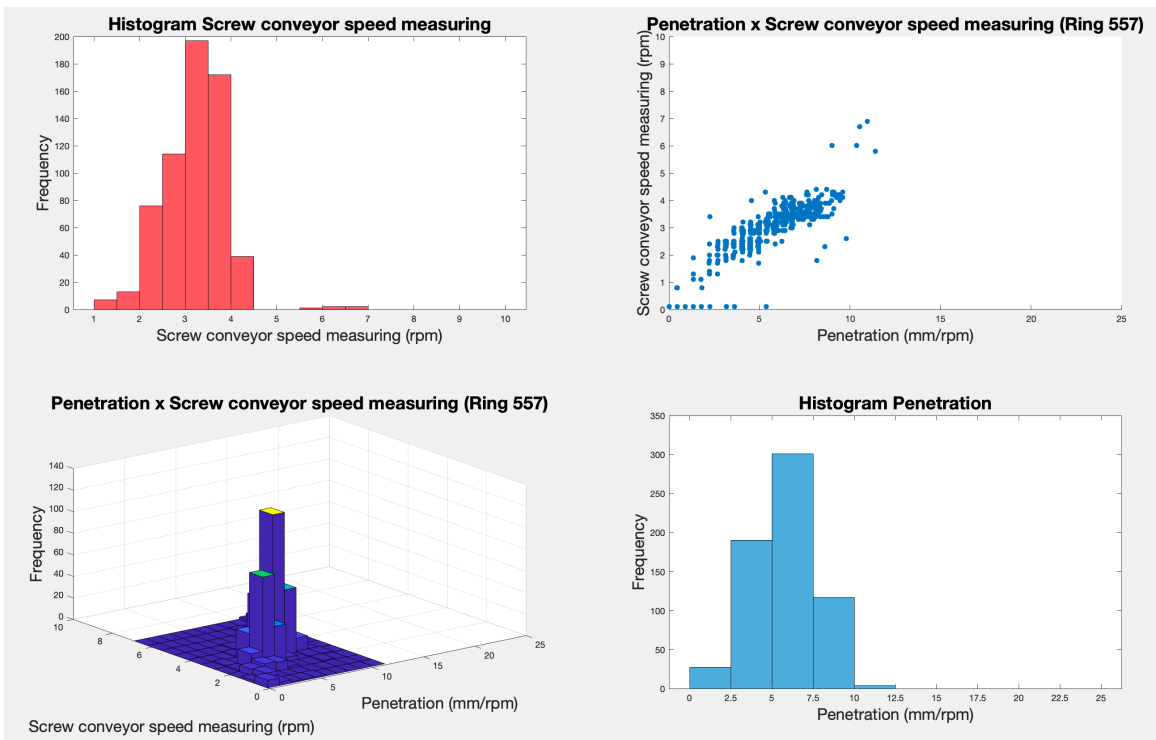


(a) Ring 842: Rock. Data-points are highly concentrated at low penetration and screw conveyor speed measuring.

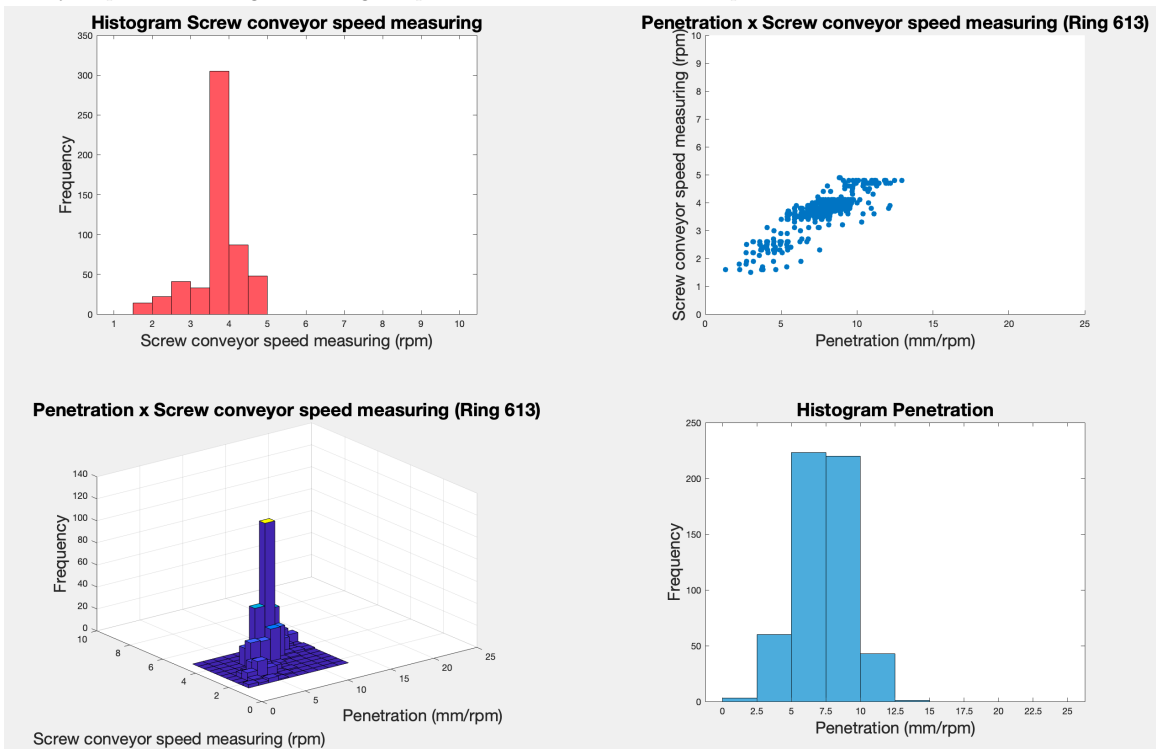


(b) Ring 598: Rock-like mixed. Data-points are concentrated around higher penetration and screw conveyor speed measuring values.

Figure 4-44: Scatter plots and histograms relating Penetration and Screw Conveyor Speed Measuring for rock and rock-like mixed.



(a) Ring 557: Soil. Distinct vertical lines showing that penetration rates are fixed around certain values. Screw conveyor speed measuring rises alongside penetration. Little outlier data-points are observed.



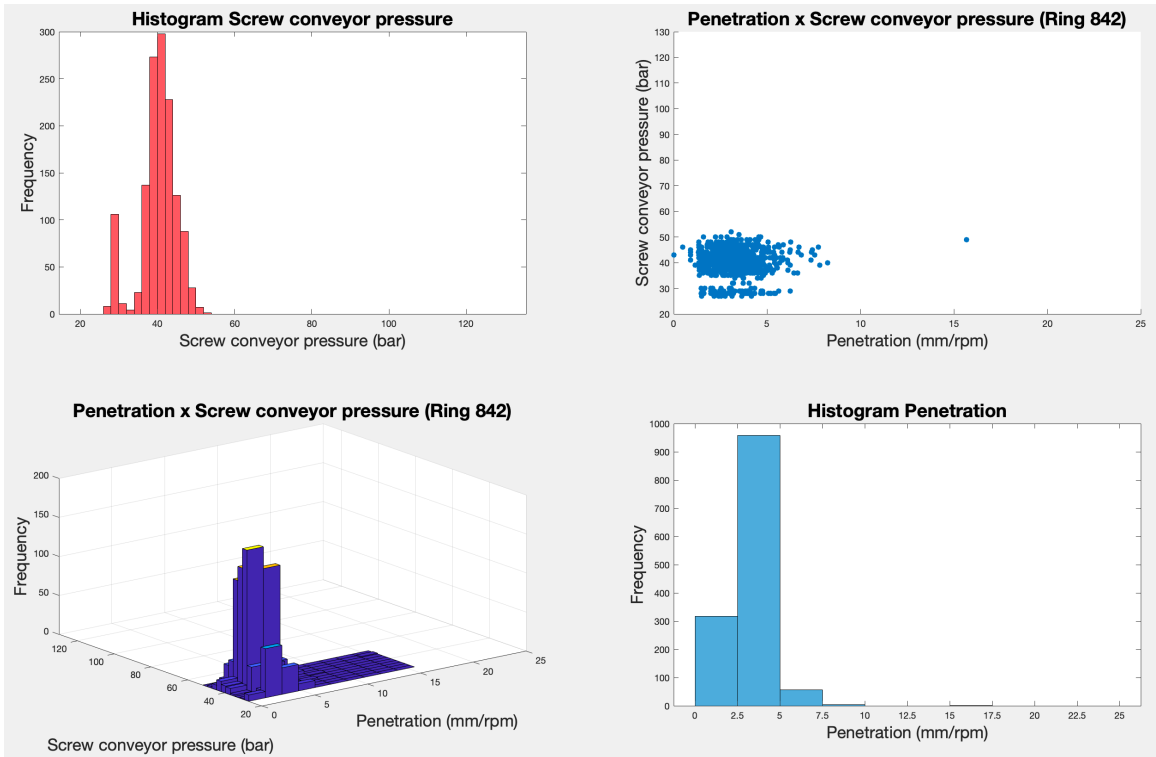
(b) Ring 613: Soil-like mixed. Penetration rates are fixed around certain values while screw conveyor speed measuring rises alongside penetration rates.

Figure 4-45: Scatter plots and histograms relating Penetration and Screw Conveyor Speed Measuring for soil and soil-like mixed.

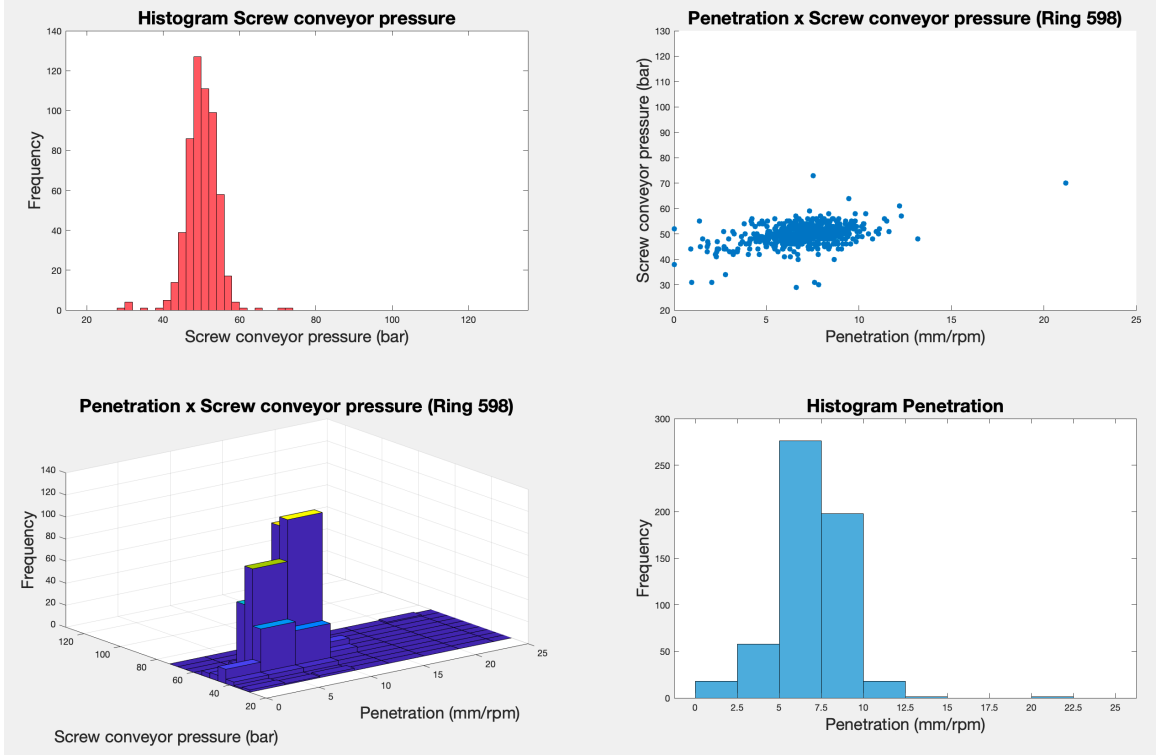
Penetration x Screw Conveyor Pressure

Evaluating the relationship between these two parameters can provide insight on geology. The pressure required to move excavated material varies widely depending on the type and condition of the soil or rock. As a general rule, softer soils require less pressure to move, while harder ground conditions will require more. Next, the sample graphs for each of the chosen ground classes will be presented (figures 4-46, 4-47).

This page intentionally left blank.

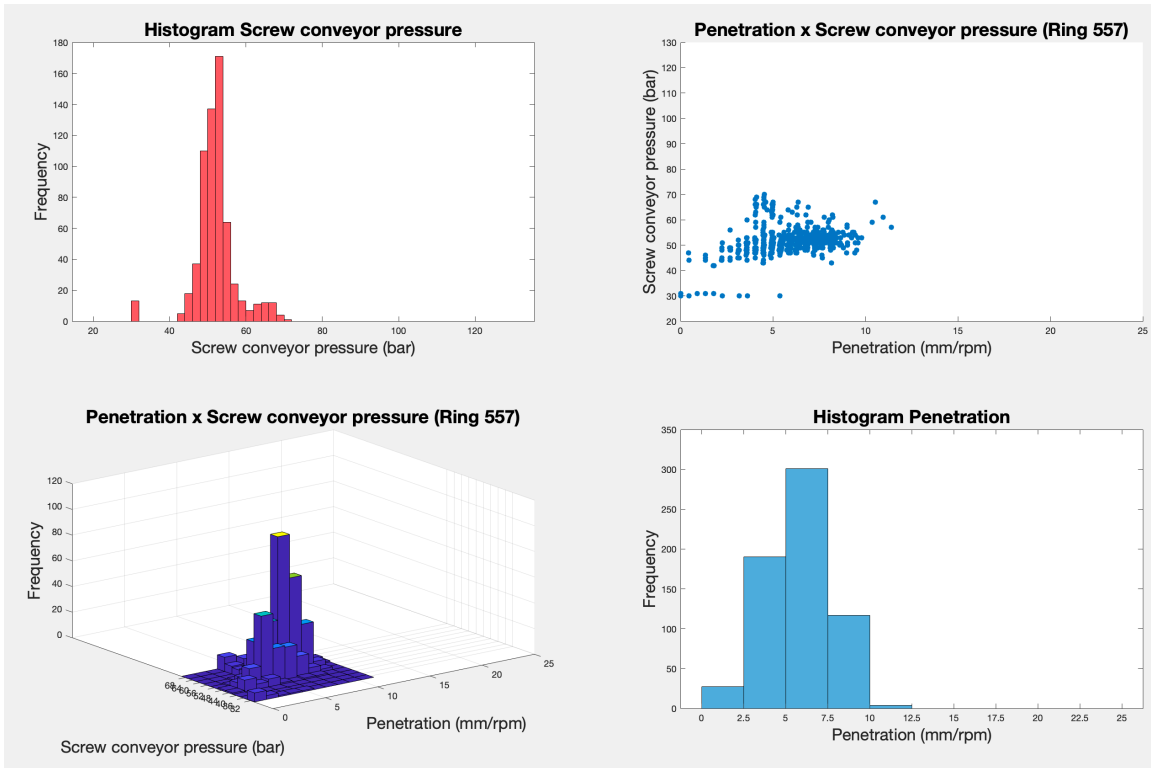


(a) Ring 842: Rock. The data-points are highly concentrated at low values of penetration and screw conveyor pressure.

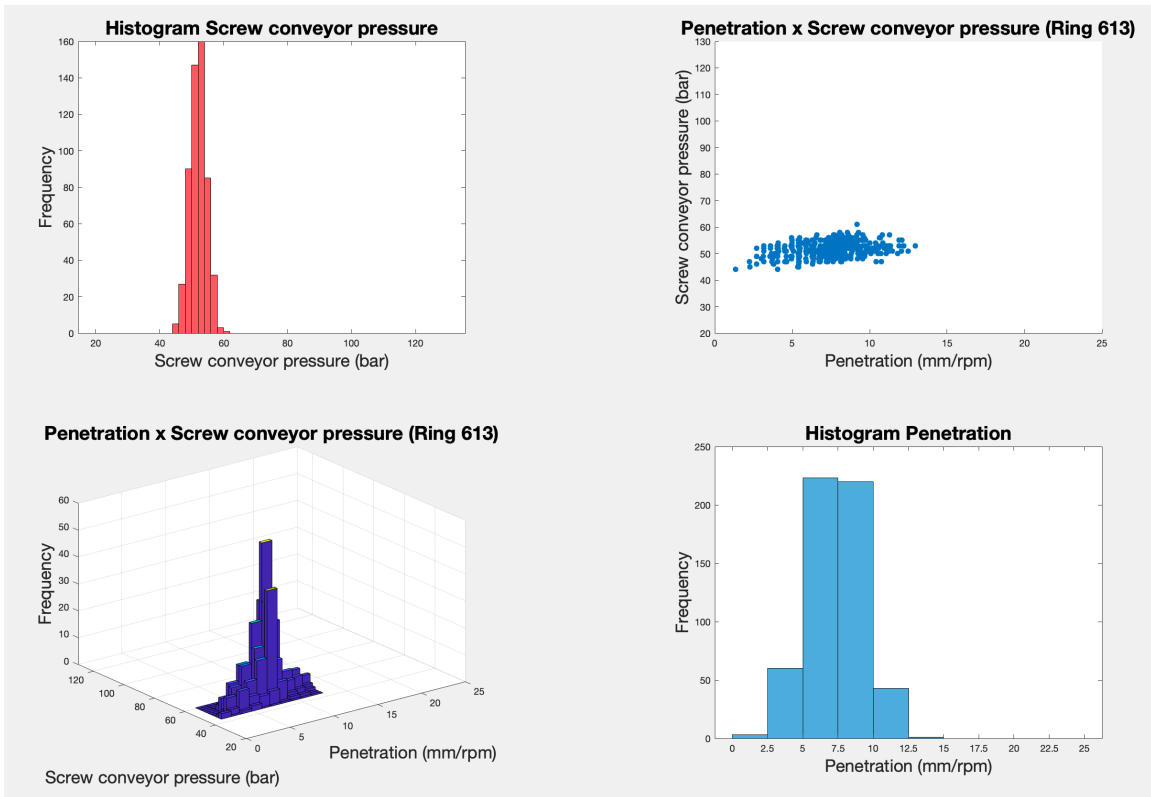


(b) Ring 598: Rock-like mixed. The data-points are highly concentrated around higher values of penetration and screw conveyor pressure.

Figure 4-46: Scatter plots and histograms relating Penetration and Screw Conveyor Pressure for rock and rock-like mixed.



(a) Ring 557: Soil. The scatter plot displays noticeable vertical lines, indicating that penetration rates remain constant at specific values. The screw conveyor pressure rises in tandem with the penetration rates. Few data points that deviate from the trend-line are present.



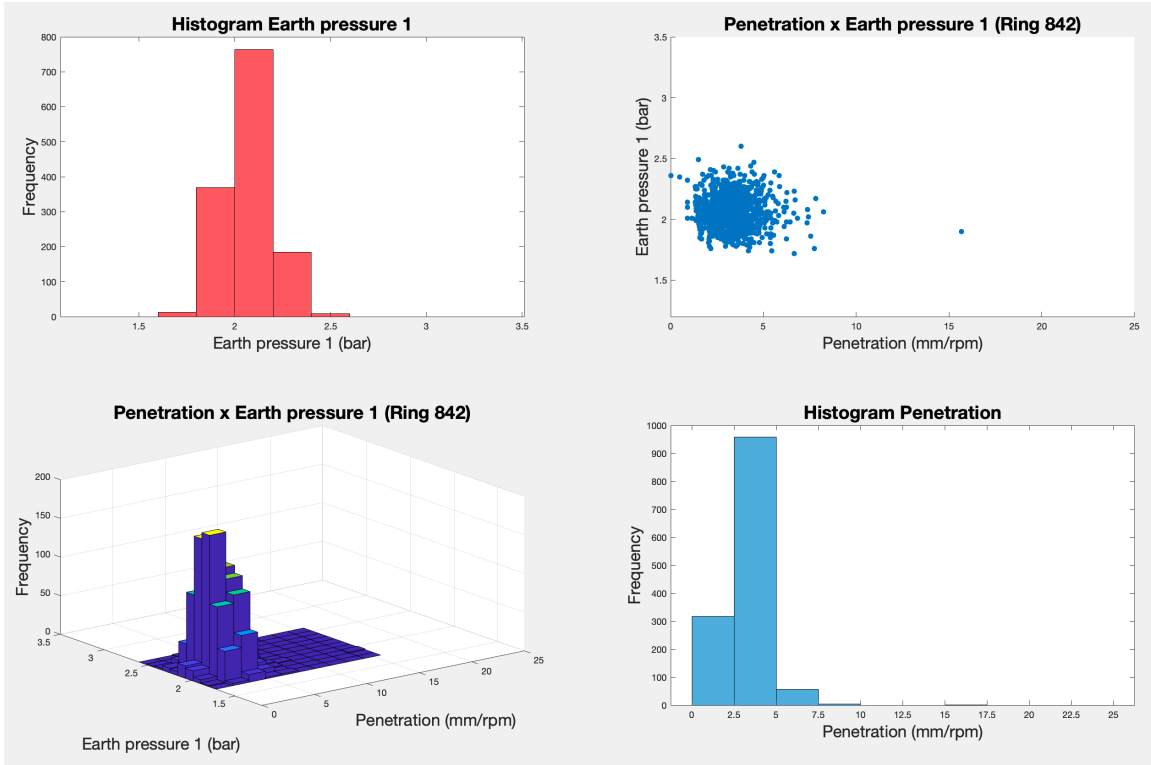
(b) Ring 613: Soil-like mixed. Penetration rates remain constant at specific values, while screw conveyor pressure slightly rises in conjunction with penetration.

Figure 4-47: Scatter plots and histograms relating Penetration and Screw Conveyor Pressure for soil and soil-like mixed.

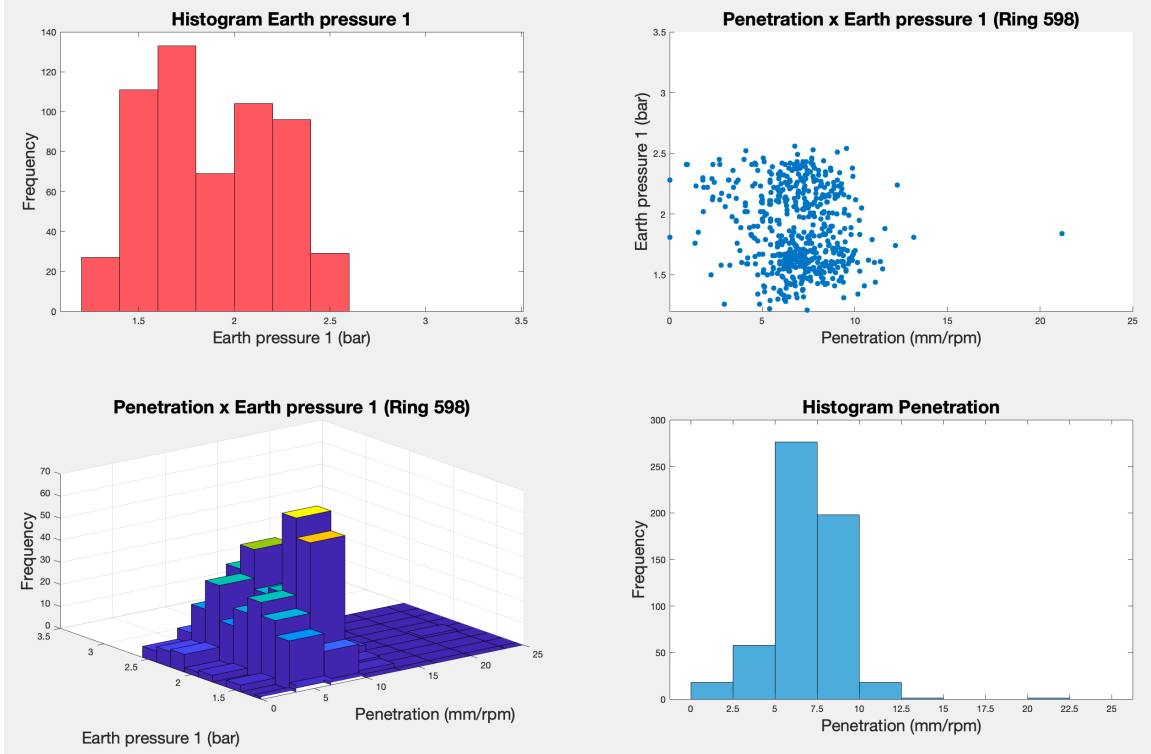
Penetration x Earth Pressure 1

This relationship is especially important for correlating TBM-generated data with ground conditions on-site. Next, the resulting graphical representation of this comparison parameters is presented in figures 4-48 and 4-49.

This page intentionally left blank.

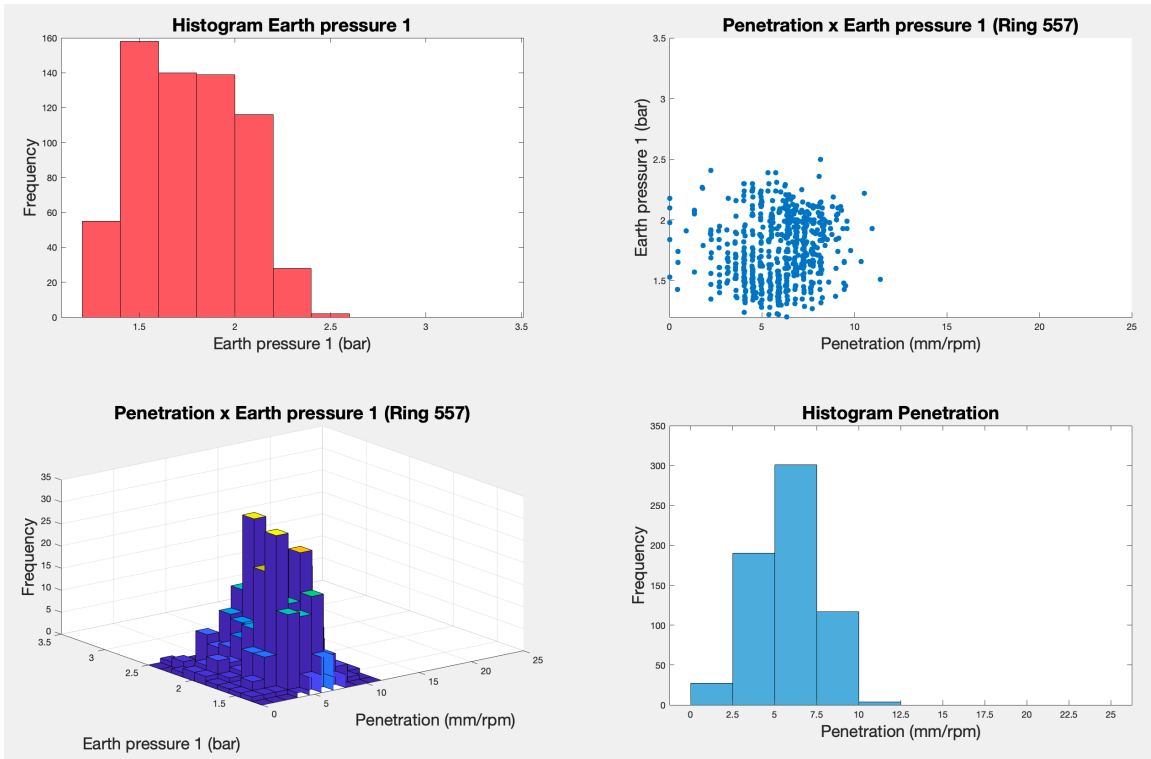


(a) Ring 842: Rock. Data-points are highly concentrated around lower values for both penetration and earth pressure.

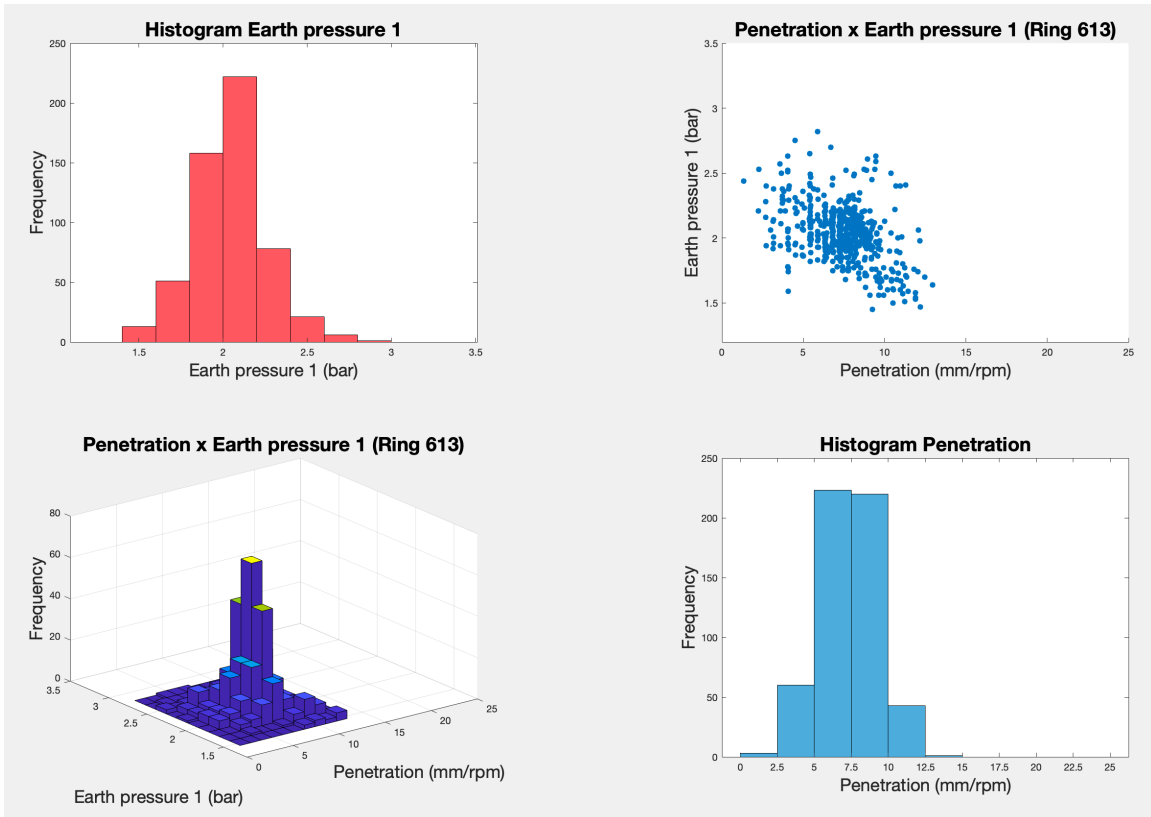


(b) Ring 598: Rock-like mixed. Data-points are spread-out within a threshold of penetration rates and lower earth pressure.

Figure 4-48: Scatter plots and histograms relating Penetration and Earth Pressure 1 for rock and rock-like mixed.



(a) Ring 557: Soil. Somewhat spread-out data-points with vertical lines indicating fixed penetration rates and lower values of earth pressure 1.



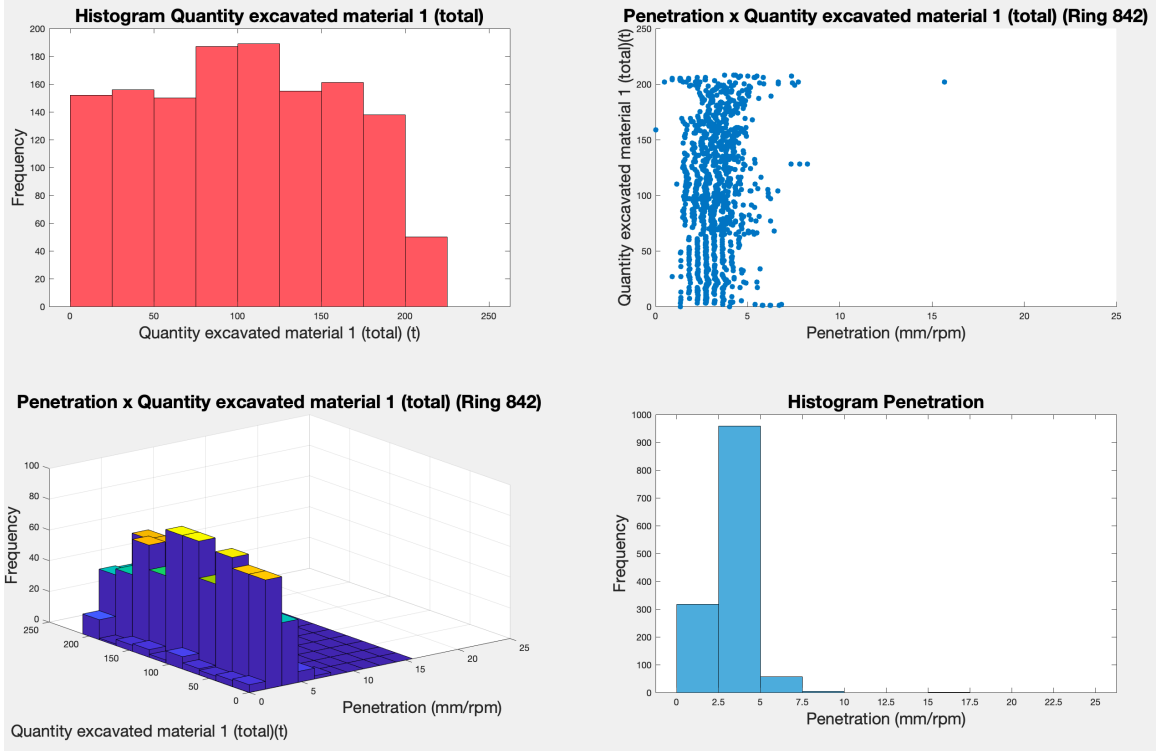
(b) Ring 613: Soil-like mixed. Data-points are somewhat spread-out around higher values of both penetration and earth pressure 1. Vertical lines can again be seen, indicating fixed values for penetration rates.

Figure 4-49: Scatter plots and histograms relating Penetration and Earth Pressure 1 for soil and soil-like mixed.

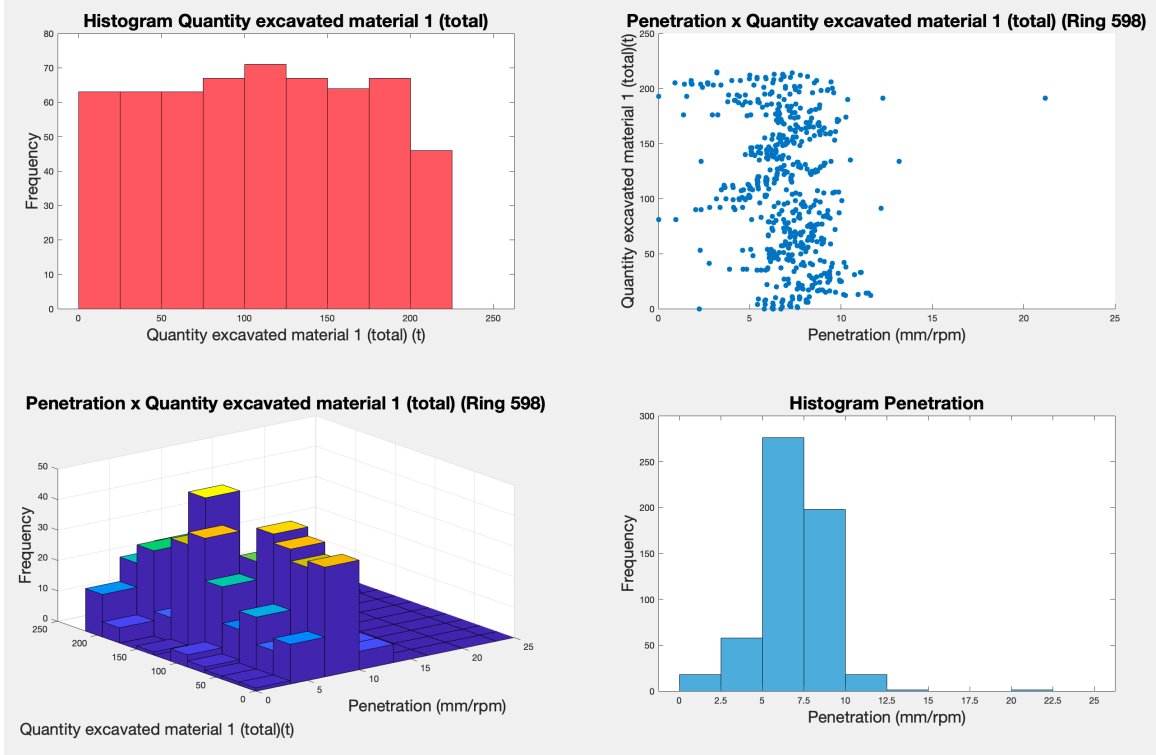
Penetration x Quantity Excavated Material 1 (Total)

Comparing penetration and quantity of excavated material 1 (total) can give insights into the geology encountered during tunneling. In harder rock formations, the TBM will advance at a slower rate excavating less material per unit of time, which results in a lower penetration rate and lower quantity of excavated material 1 (total). For softer soils, the TBM may advance at a faster rate and excavate more material per unit of time, resulting in a higher penetration rate and higher quantity of excavated material 1 (total). The graphs presented next show a sample for each of the evaluated ground classes (figures 4-50, 4-51).

This page intentionally left blank.

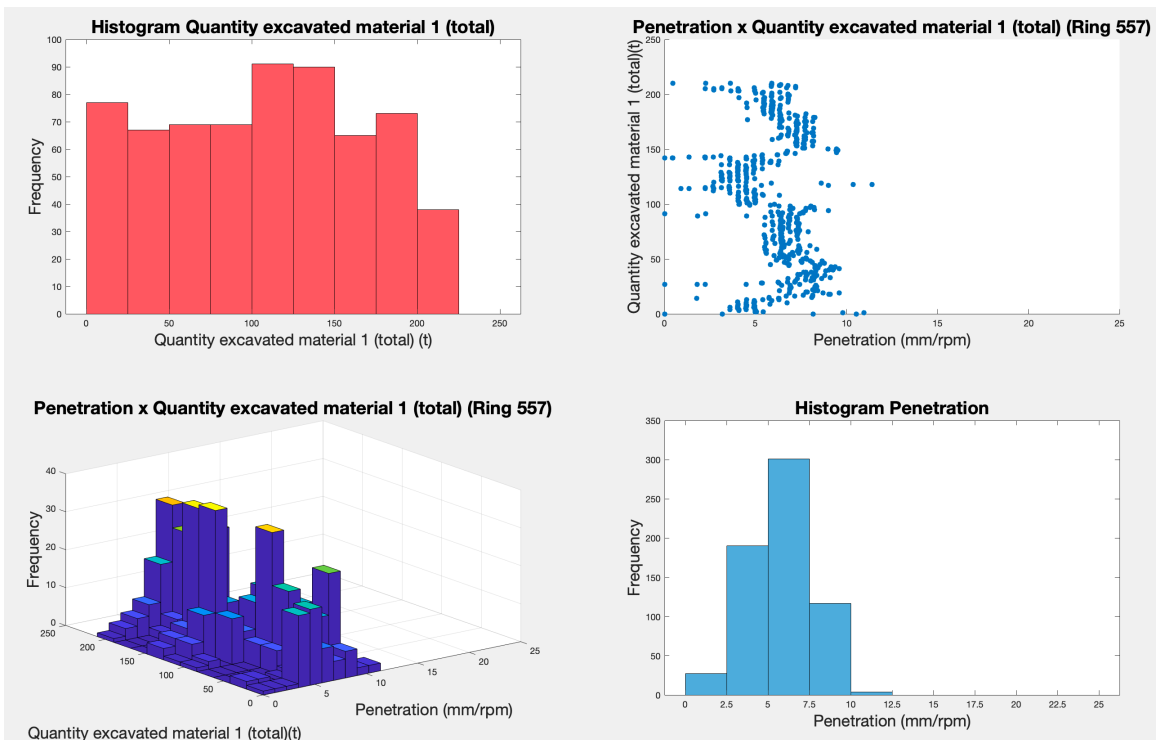


(a) Ring 842: Rock. Distinct columnar shape is displayed, where observations are concentrated around low penetration rates and varying quantity of excavated material (as it is a cumulative parameter).

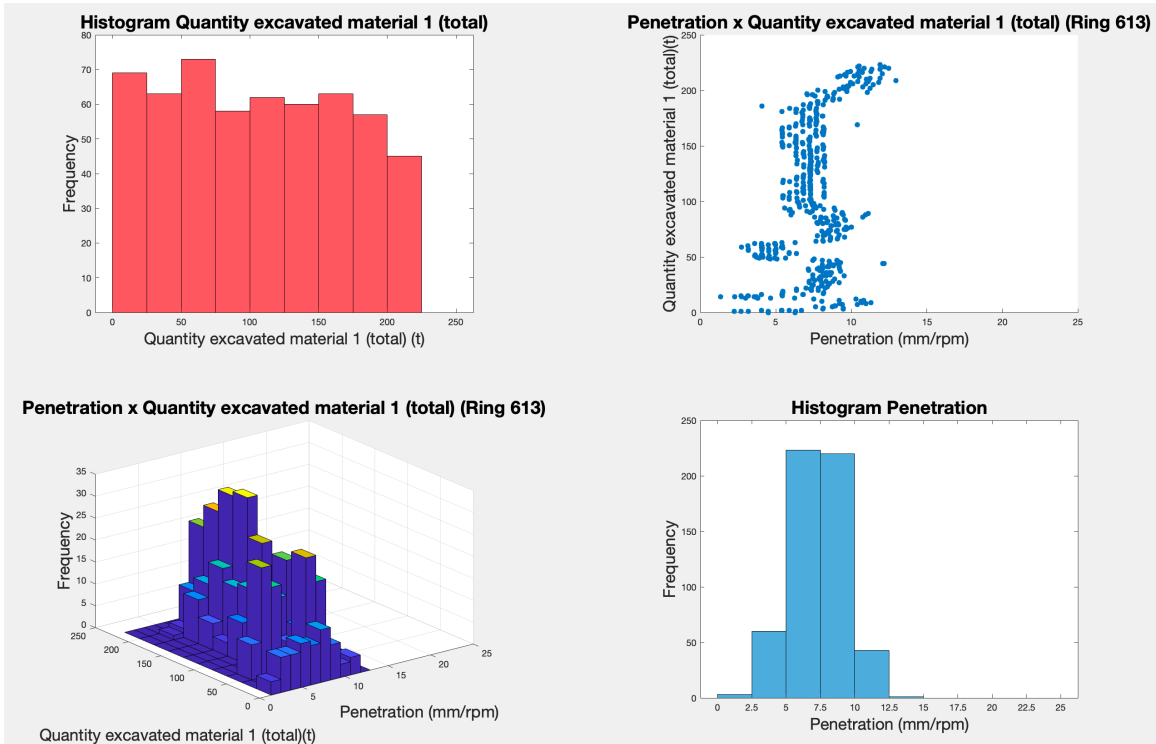


(b) Ring 598: Rock-like mixed. Observations are sparse but record higher penetration rates.

Figure 4-50: Scatter plots and histograms relating Penetration and Quantity Excavated Material 1 (Total) for rock and rock-like mixed.



(a) Ring 557: Soil. Observations vary considerably around specific values of penetration (seen through the presence of vertical line concentrating data-points). Distinct "S" shape is observed.



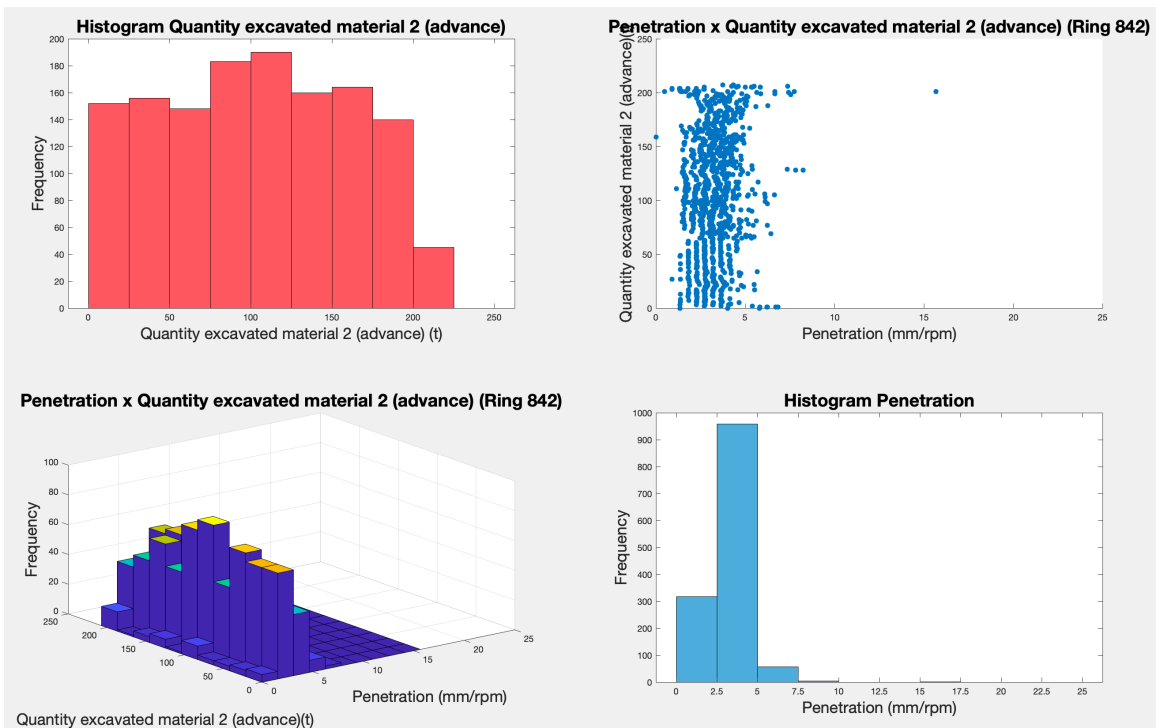
(b) Ring 613: Soil-like mixed. The data-points show considerable variation around specific values of penetration, which can be observed through the presence of a vertical line concentrating the data-points. Distinct "S" shape is observed.

Figure 4-51: Scatter plots and histograms relating Penetration and Quantity Excavated Material 1 (Total) for soil and soil-like mixed.

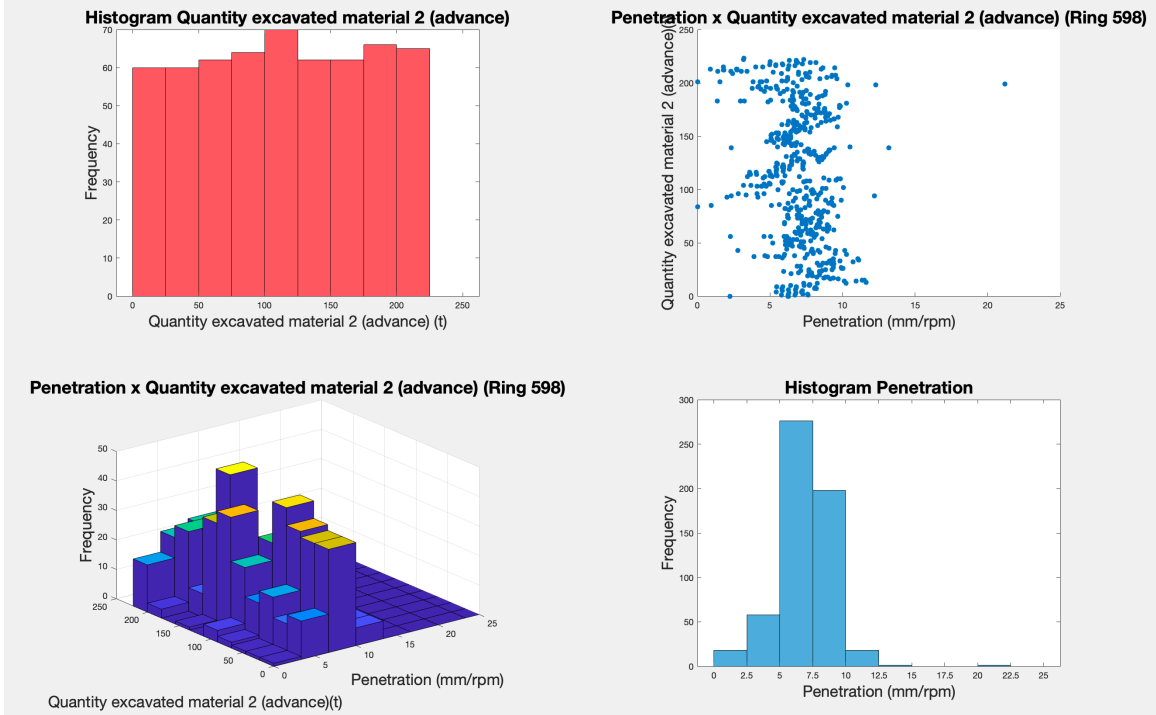
Penetration x Quantity Excavated Material 2 (Advance)

Measured in millimeters per revolution, penetration notes the distance advanced by the TBM during a set time period. On the other hand, quantity of excavated material 2 (Advance) measures the volume of material excavated by the TBM during an equivalent period of time, typically calculated in cubic meters per revolution or per minute. The images below show a sample of this parameter comparison for each of the evaluated ground classes (figures 4-52 and 4-53).

This page intentionally left blank.

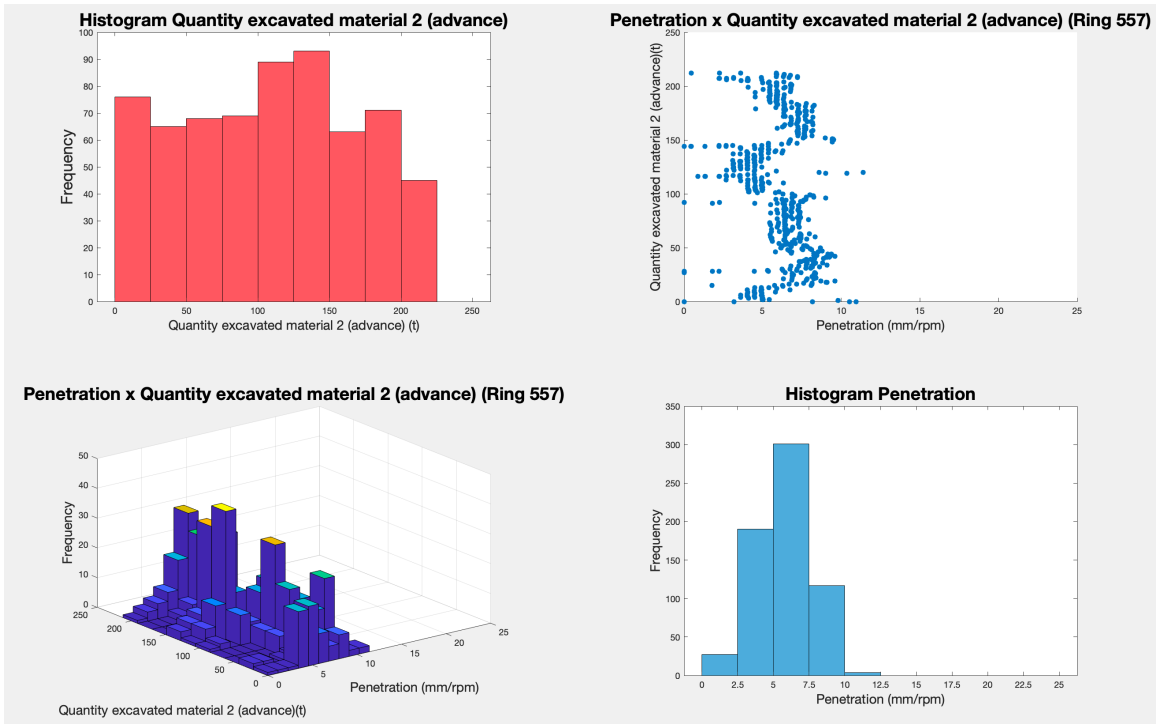


(a) Ring 842: Rock. Distinct columnar shape is displayed, where observations are concentrated around low penetration rates and varying quantity of excavated material (as it is a cumulative parameter).

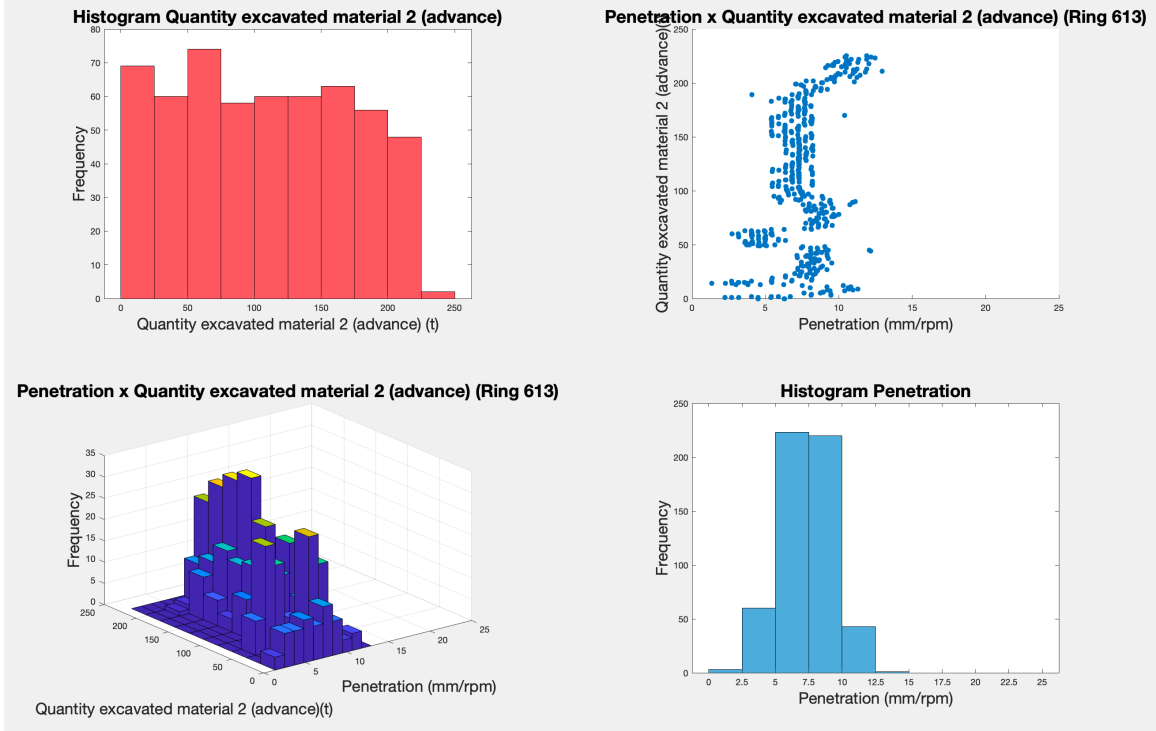


(b) Ring 598: Rock-like mixed. Observations are sparse but record higher penetration rates.

Figure 4-52: Scatter plots and histograms relating Penetration and Quantity Excavated Material 2 (Advance) for rock and rock-like mixed.



(a) Ring 557: Soil. Observations vary considerably around specific values of penetration (seen through the presence of vertical line concentrating data-points). Distinct "S" shape is observed.



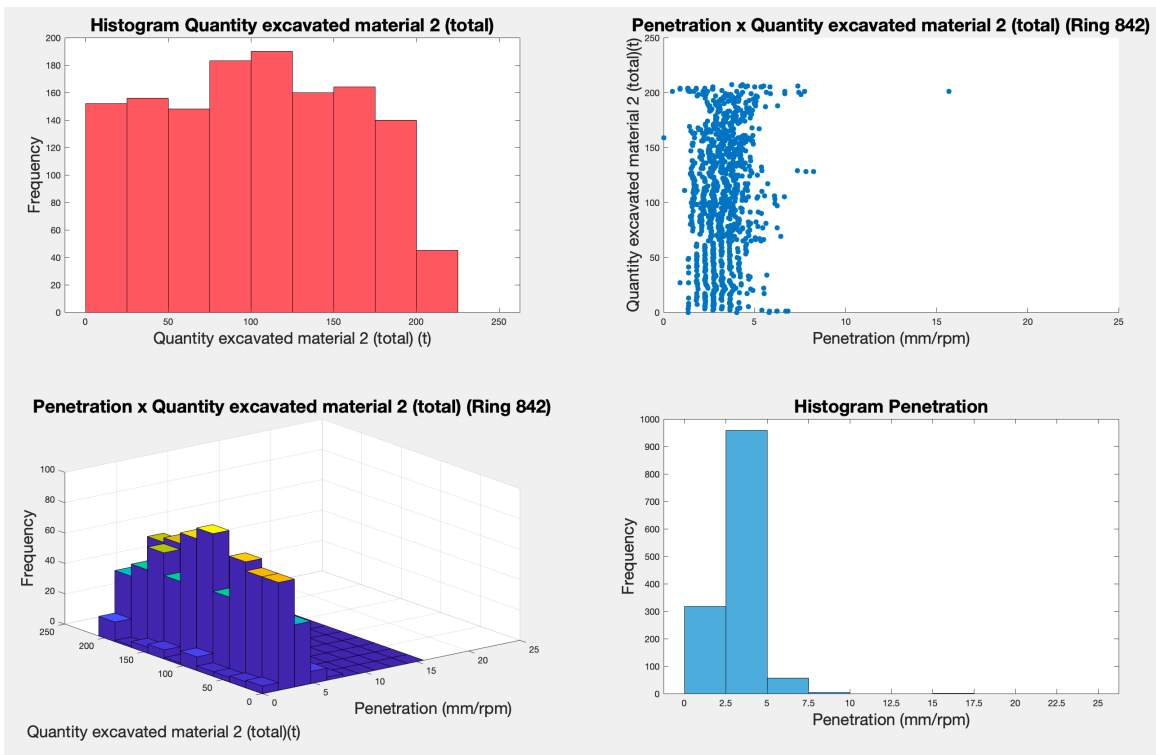
(b) Ring 613: Soil-like mixed. The data-points show considerable variation around specific values of penetration, which can be observed through the presence of a vertical line concentrating the data-points. Distinct "S" shape is observed.

Figure 4-53: Scatter plots and histograms relating Penetration and Quantity Excavated Material 2 (Advance) for soil and soil-like mixed.

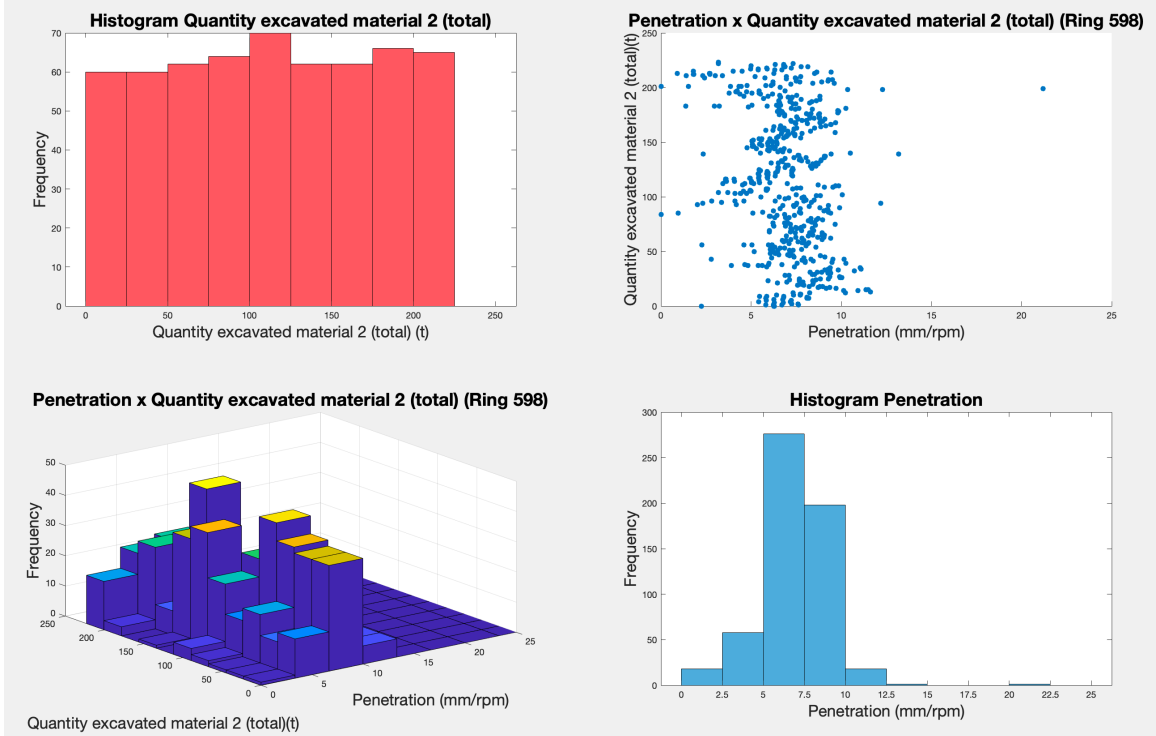
Penetration x Quantity Excavated Material 2 (Total)

As previously discussed, penetration measures, in mm/rpm, the distance advanced by the TBM, while quantity of excavated material 2 (total) is looking at the total amount of material being excavated (measured in cubic meters). This relationship is basically identical to the two parameter comparisons immediately stated above, thus provides similar insights on geology. Figures 4-54 and 4-55 present an example of the comparison between penetration and quantity of excavated material 2 (total) for soil, rock, and mixed rings.

This page intentionally left blank.

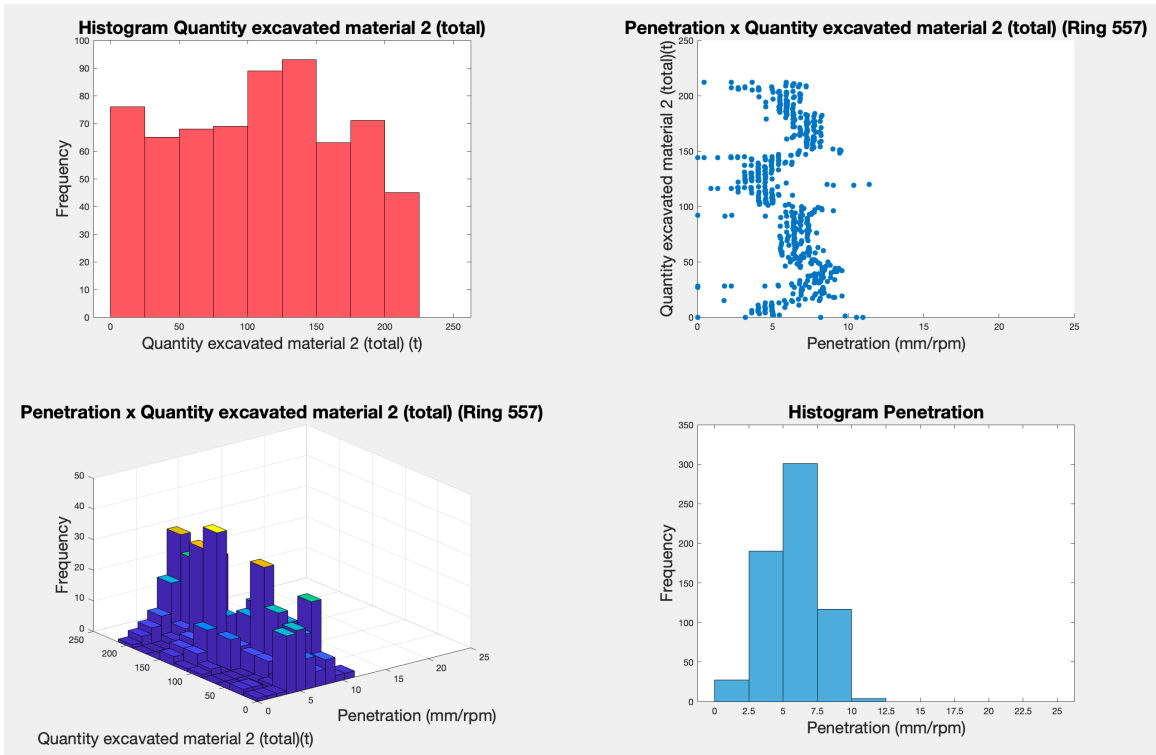


(a) Ring 842: Rock. Distinct columnar shape is displayed, where observations are concentrated around low penetration rates and varying quantity of excavated material (as it is a cumulative parameter).

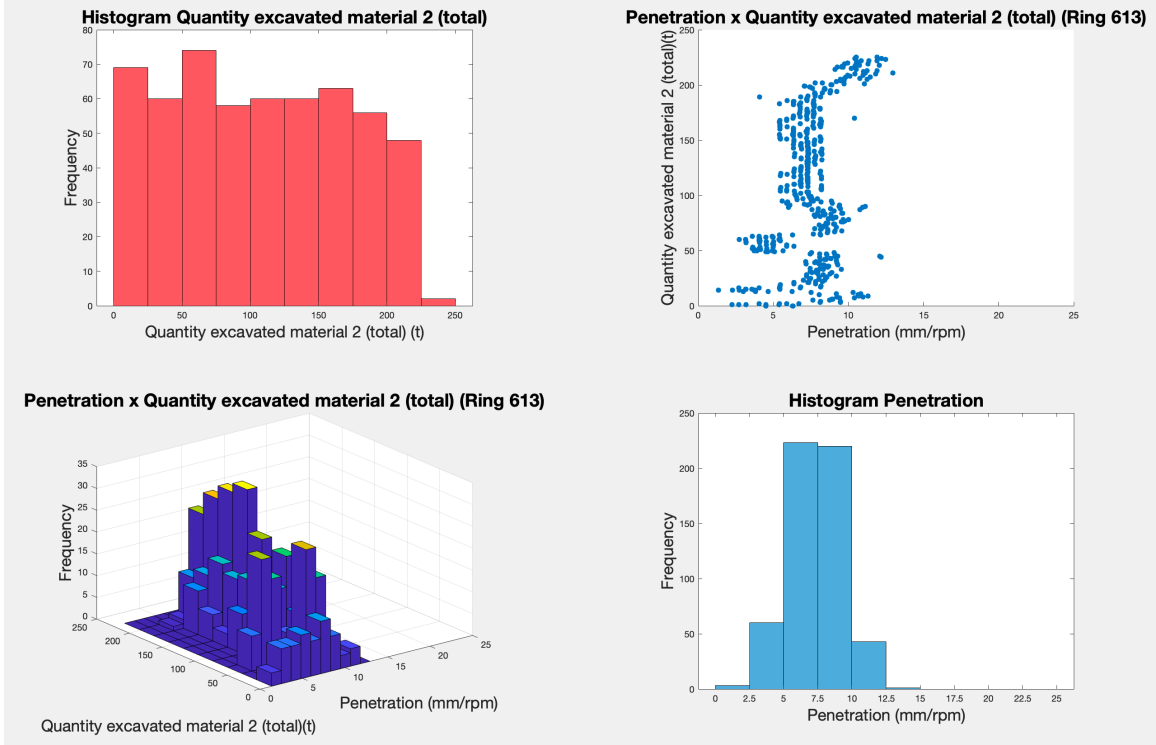


(b) Ring 598: Rock-like mixed. The recorded observations are infrequent, but they exhibit elevated levels of penetration.

Figure 4-54: Scatter plots and histograms relating Penetration and Quantity Excavated Material 2 (Total) for rock and rock-like mixed.



(a) Ring 557: Soil. Observations vary considerably around specific values of penetration (seen through the presence of vertical line concentrating data-points). Distinct "S" shape is observed.



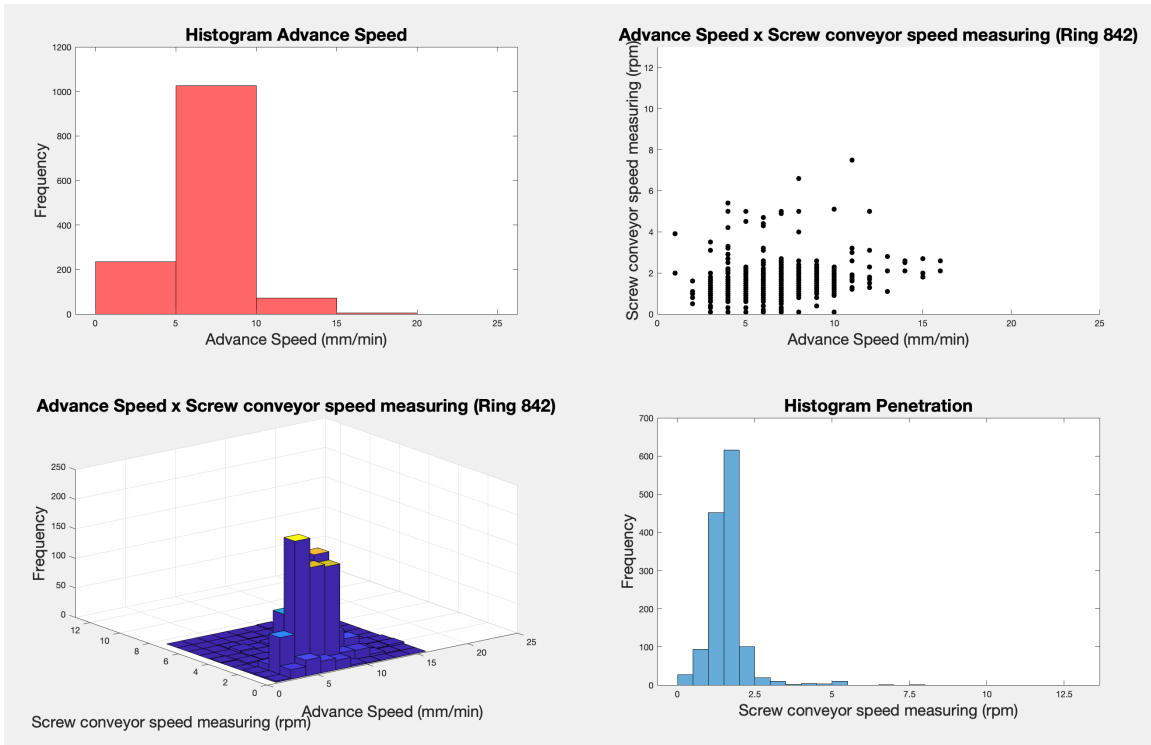
(b) Ring 613: Soil-like mixed. The data-points show considerable variation around specific values of penetration, which can be observed through the presence of a vertical line concentrating the data-points. Distinct "S" shape is observed.

Figure 4-55: Scatter plots and histograms relating Penetration and Quantity Excavated Material 2 (Total) for soil and soil-like mixed.

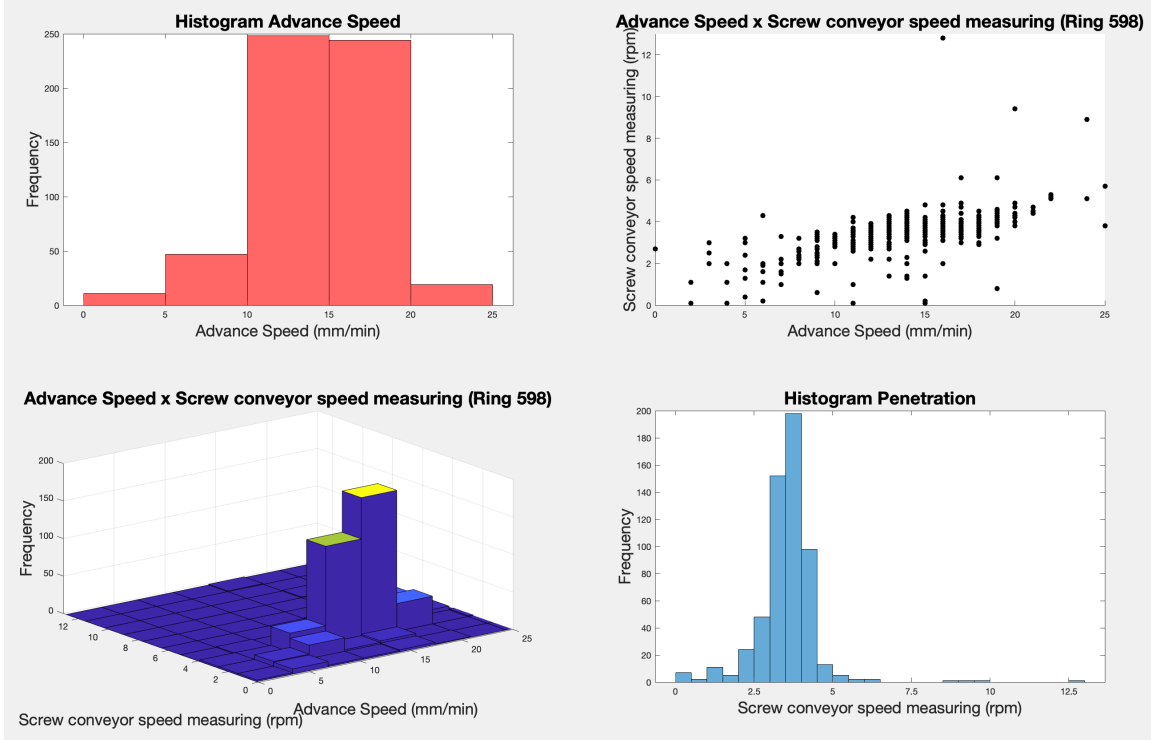
Advance Speed x Screw Conveyor Speed Measuring

Two important parameters measured by the TBM during excavation are advance speed (TBM's forward movement) and screw conveyor speed (movement of excavated material away from TBM). Sensors on the machine record data on speed, torque, and power consumption, and the generated data are used to monitor TBM performance and parameter adjustment to optimize the tunneling process. The figures (figures 4-56 and 4-57) below show the resulting graphs for all the evaluated ground classes (rock, soil, rock-like mixed and soil-like mixed rings).

This page intentionally left blank.

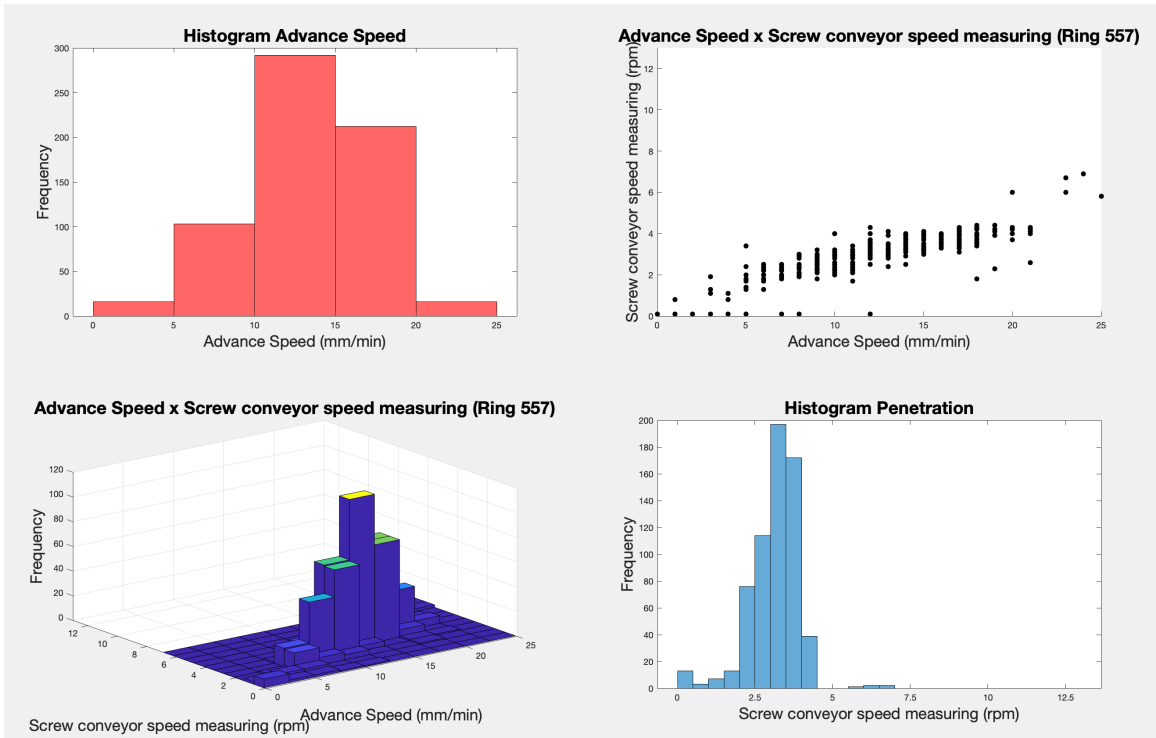


(a) Ring 842: Rock. Distinct lines can be seen at certain advance speed rates, where observations are concentrated. Varies significantly in rock.

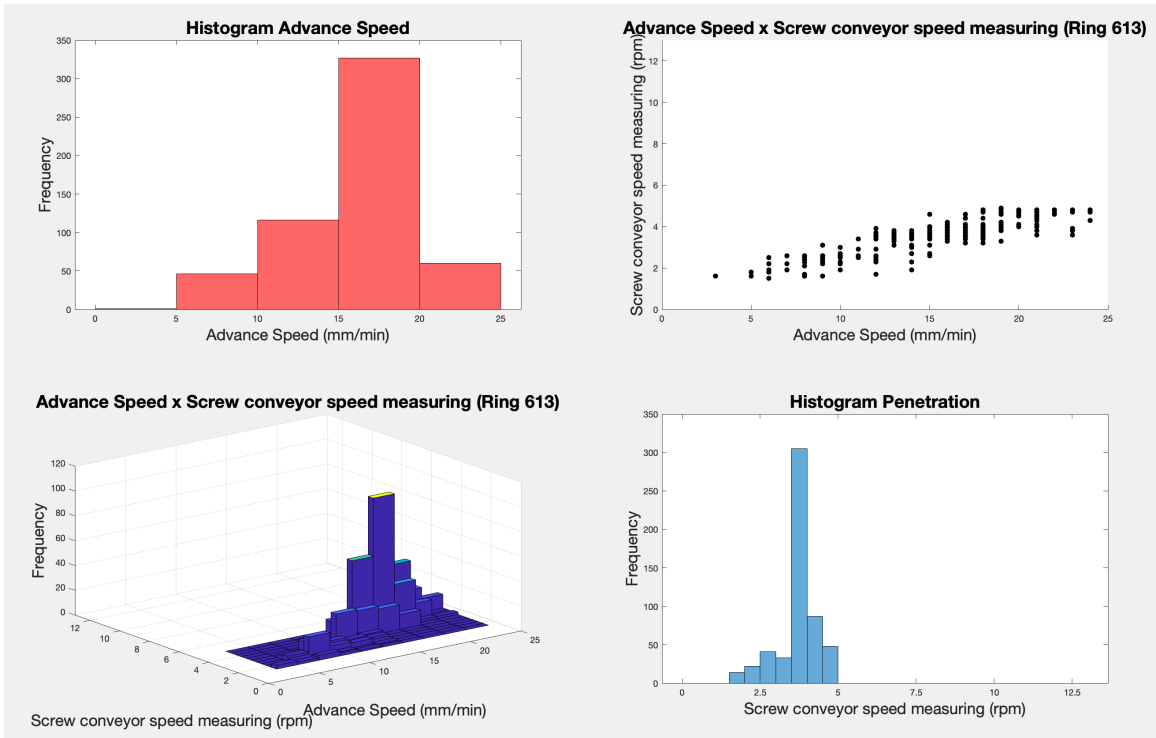


(b) Ring 598: Rock-like mixed. Most observations are concentrated at certain advance speed rates, as seen by the distinct vertical lines.

Figure 4-56: Scatter plots and histograms relating Advance Speed and Screw Conveyor Speed Measuring for rock and rock-like mixed.



(a) Ring 557: Soil. Certain advance speed rates display distinct vertical lines, indicating the concentration of most observations.



(b) Ring 613: Soil-like mixed. Concentration of most observations is evident at distinct vertical lines corresponding to certain advance speed rates.

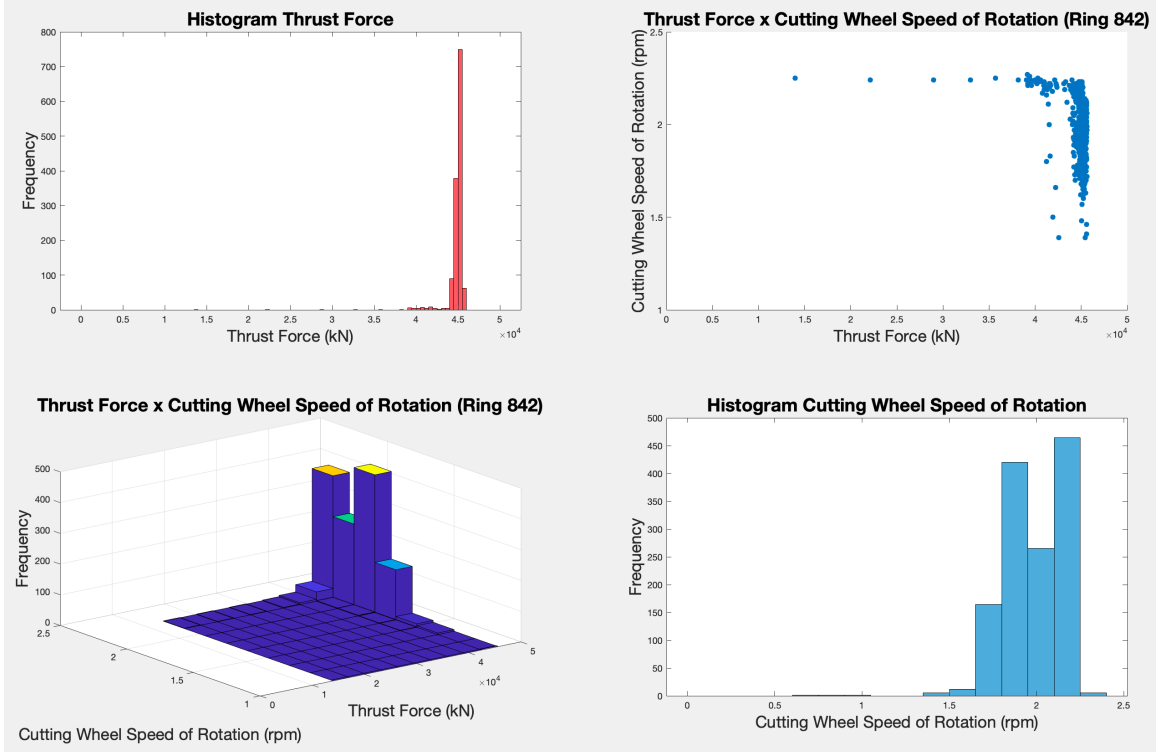
Figure 4-57: Scatter plots and histograms relating Advance Speed and Screw Conveyor Speed Measuring for soil and soil-like mixed.

Thrust Force x Cutting Wheel Speed of Rotation

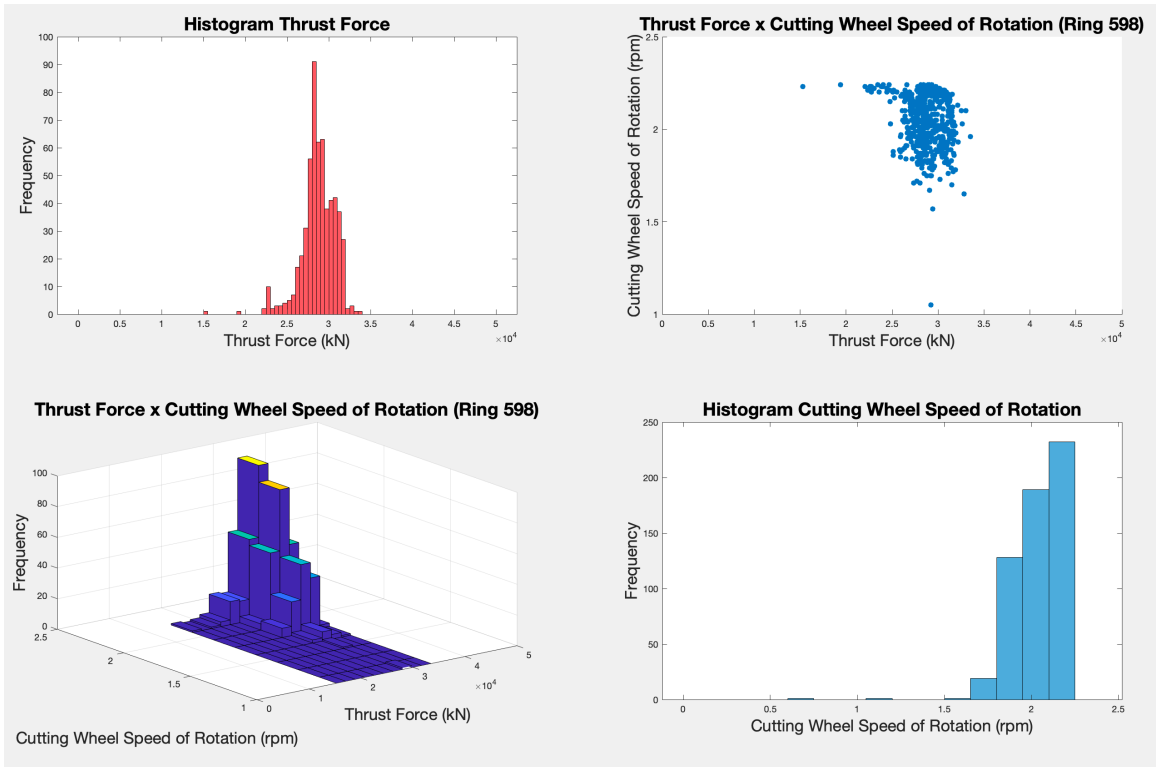
In comparing thrust force and cutting wheel speed of rotation, important indicators of TBM performance, can provide understandings on ground conditions throughout tunnel excavation. Thrust force determines the force exerted by TBM's thrust cylinders against the tunnel face. While cutting wheel speed of rotation measures the rotational speed of the cutting wheel, one of the main components responsible for excavating the tunnel face.

As both parameters have been explored in previous graphs, their comparison is expected to present insights into the geological conditions surpassed by the TBM. Figures 4-58 and 4-59 show sample results for the observed ground classes (rock, rock-like mixed, soil and soil-like mixed rings).

This page intentionally left blank.

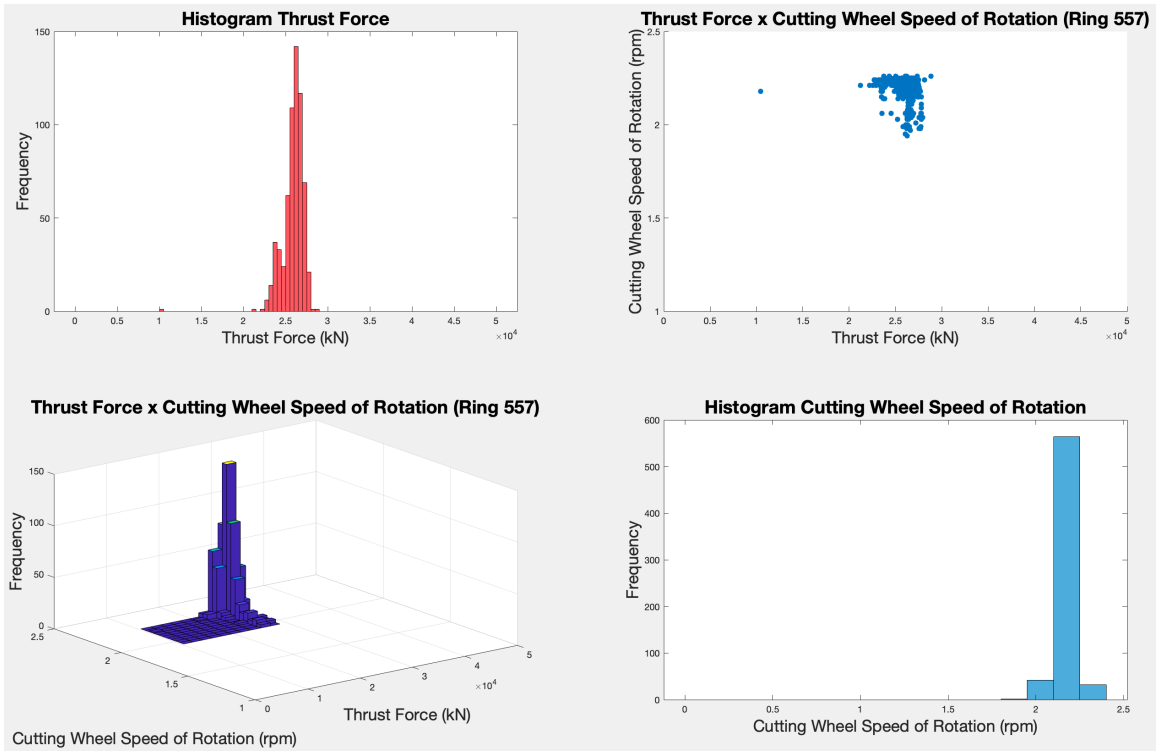


(a) Ring 842: Rock. High concentration of data-points around the highest value of thrust force. Cutting wheel speed of rotation is more variable.

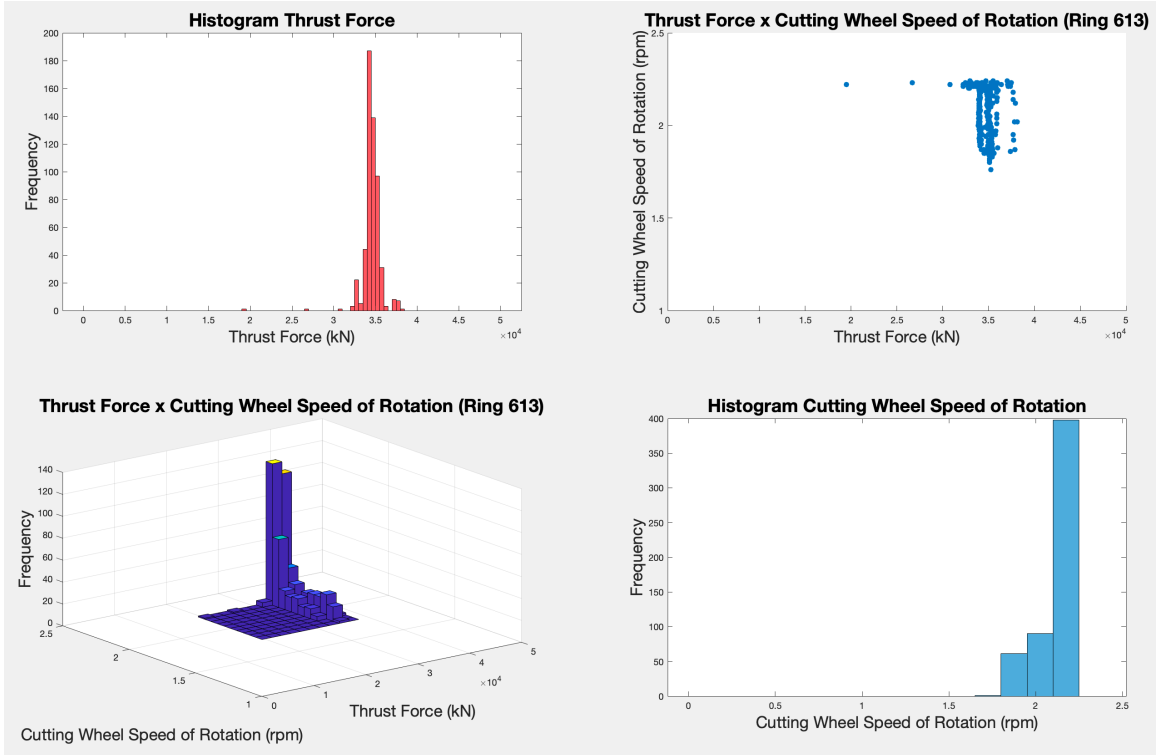


(b) Ring 598: Rock-like mixed. Most observations are concentrated around a thrust pressure threshold, where cutting wheel speed of rotation varies.

Figure 4-58: Scatter plots and histograms relating Thrust Force and Cutting Wheel Speed of Rotation for rock and rock-like mixed.



(a) Ring 557: Soil. Observations concentrated around certain thresholds of both thrust force and cutting wheel speed of rotation.



(b) Ring 613: Soil-like mixed. The data points are concentrated around specific values of both thrust force and cutting wheel speed of rotation.

Figure 4-59: Scatter plots and histograms relating Thrust Force and Cutting Wheel Speed of Rotation for soil and soil-like mixed.

4.5 Interpretation & Conclusions

The aim of this chapter was to find ways to aid the prediction of geological conditions ahead of the TBM tunnel face, using the machine's performance data. Two methods were proposed to achieve this: employing time-series graphs and scatterplots.

Time-series graphs showed distinct patterns between the chosen ground classes (rock, soil, rock-like mixed and soil-like mixed). Rock rings exhibited significantly more variability when parameters were plotted, changing with higher frequency than in other ground classes, making the time-series plots for rock characteristically composed of short and compact "peaks" and "valleys". Also, in rock, the variability seems to be constrained around shorter ranges for the observed parameter comparisons. In soil rings, data presented wider value ranges but often showed a positive correlation between parameters, with some parameter pairs completely overlapping. Rock-like mixed and soil-like mixed rings showed data-point concentration at wider ranges, with positive correlation between parameters, similarly to what was seen in soil rings. A parameter comparison that exemplifies these patterns is Time x Penetration and Advance Speed (see Figures 4-18 and 4-19).

Scatterplots, also revealed significant differences between the compared ground classes (rock, soil, rock-like mixed and soil-like mixed), and since patterns were more easily discernible, they were deemed the best tool to be used for classifying rings. Rock rings had characteristic highly concentrated observations, where data clustered around high-density regions within the plot. In contrast, soil rings had data-points that were somewhat spread-out and variable, with wider ranges of observation values and less concentration or clustering around specific thresholds. Rock-like mixed rings showed similar data-point concentration as in rock rings, however significantly more spread-out than what is seen in rock. Soil-like mixed rings followed patterns similar to soil, with somewhat spread-out data-points and wider ranges of observations. A particular case where this can be seen is in the comparison between Penetration x Screw Conveyor Speed Measuring (Figures 4-44 and 4-45).

Out of all the parameters compared in the scattergrams, five parameter pairs have

been identified as particularly insightful and will be used in the Chapter 5 to develop an AI/ML-based ground class prediction system.

The first comparison that offers valuable insights is Penetration x Torque Screw. When penetration rates are high and torque screw values are low, the material is likely to be softer and easier to excavate. On the other hand, low penetration rates and high torque screw values suggest harder, rock-like materials. For this parameter comparison, rock graphs showed highly concentrated observations around specific thresholds of both parameters, which was characteristic for rock rings throughout the scattergrams. For soils, data-points were located at a wider range of values for both parameters. Also, vertical lines can be seen forming within the data-points, which is consistent with penetration rates being controlled by operators. In rock-like mixed rings, there is still considerable concentration around a certain value-range but data-points fluctuated more widely than what was seen in rock. For soil-like mixed rings, the distribution was somewhat concentrated, with values ranging similarly to soils, also showing the observed vertical lines (fixed penetration rates).

The second comparison is for Penetration x Screw Conveyor Speed Measuring which offered insight into the efficiency of the excavation process and the behavior of the material being extracted from the tunnel face. The graphs reveal that increased screw conveyor speeds that do not result in higher penetration rates indicate harder material (rock), while in softer soils, higher speeds directly result in higher penetration rates. Here, rock rings showed again highly concentrated data-points, clustering around lower thresholds of both parameter values. In soil rings, the data-points were located on a broader spectrum of values for both parameters, concentrating around higher penetration rate values. In addition, vertical lines again appeared within the data-points, which reflects with the operators directly managing penetration rates. In rock-like mixed rings, there was significant concentration around a certain range of values, but the data points showed more variability than in pure rock rings. As for soil-like mixed rings, the distribution was somewhat concentrated around certain thresholds, within somewhat lower ranges than that of soils.

The third comparison, Penetration x Earth Pressure 1, is highly relevant for exca-

vation, where Earth Pressure 1 measures the resistance exerted on the TBM during the excavation process. In rock rings, the characteristically highly-concentrated data-point observations are present, with high-density clustering around lower penetration rate and high values of Earth Pressure 1. For soils, data-points are concentrated around higher value penetration and mid to low-ranging values of Earth Pressure 1. Again, characteristic vertical lines were observed, indicating fixed values of penetration rate. Rock-like mixed rings showed spread-out data-points that varied much more widely, with some clustering around lower values of both parameters. Soil-like mixed rings, similarly to rock-like mixed, had somewhat spread-out observations however having some concentration around higher values of penetration rate and Earth Pressure 1.

For Advance Speed x Screw Conveyor Speed Measuring, rock displayed concentrated observations around lower values of both parameters. Here distinct vertical lines can be seen in all ground classes, suggesting that operators have set values for advance speed. In soils, the data are spread-out across a wide range of advance speed values, while screw conveyor speed measuring is shown to increase slightly with increasing values of advance speed. For rock-like mixed rings, observations are more spread-out, more similar to what was displayed in soil rings. Soil-like mixed, also resembling data-point distributions present in soil rings were more spread-out along the advance speed axis, remaining at lower values of screw conveyor speed.

The fifth and final comparison is for Thrust Force x Cutting Wheel Speed of Rotation. This comparison is vital for understanding the excavation process in different geological conditions and determining specific ground classes. The correlation between the two parameters suggests that as thrust force increases and cutting wheel speed decreases, the machine is likely encountering hard material (rock). Conversely, for soils, higher cutting wheel speed is noted, as well as a concentration of data-points at lower thrust force values. Here in all of the rings, an interesting inverted "L" shape of the data plots is notable (especially clear in rock and soil rings). For rock rings, data-points are highly concentrated at higher values of both parameters, with a clear inverted "L". Here, most observations for thrust force lie near 45,000

kN. In soils, data-points remain in a thrust force range of 20,000-30,000 kN. Here the characteristic inverted "L" can also be observed, although much smaller in size than other ground classes. Rock-like mixed rings showed highly-concentrated data-points in the threshold between 20,000-35,000 kN, and while a shape similar to an inverted "L" can be seen, it is not as clear as in rock and soil rings. For soil-like mixed rings, observations are highly-concentrated at higher thrust force (around 35,000 kN) and cutting wheel speed of rotation.

This page intentionally left blank.

Chapter 5

Novel Approach to Improving Geological Prediction in TBM Operations

5.1 Intent

As presented in previous chapters, the Porto Metro Project has been a significant infrastructure development for the city of Porto, Portugal. With tunnel construction on the rise, the needs for increased productivity and safety in the construction process are paramount. And, at the basis of this is information on geology.

AI/ML models have been used on TBM-generated data to classify and label tunnel sections, furthering efforts to streamline tunneling automation. Although outputting coherent results and seen as an instrumental tool in automating tunnel operations, these models have not been proven using real-time data and have been speculated to generate significant confirmation biases. The accuracy of these models can also be limited by unreliable labels generated.

To overcome this limitation, the present chapter aims to show how the use of scattergrams can aid in the validation of labels generated by a Confidence Learning (CL) model developed in collaboration with a peer researcher, Saadeldin Moustafa.

With the CL model both high and low-quality labels are generated. These were then compared to the ground classification labels generated by the scattergrams.

5.2 Methodologies

5.2.1 Confidence Learning

Confidence learning, or CL, is a powerful machine learning technique that assigns a confidence value to each labeled example in a data-set, indicating the algorithm's certainty in classifying each label [Northcutt et al., 2021b, Zhang et al., 2014]. Traditional machine learning approaches assume that labeled points in the data-set are accurate, which can lead to poor model performance due to mislabeled or incorrectly labeled data-points [Menardi and Torelli, 2014]. To address this, CL applies a probabilistic framework that allows the algorithm to "learn" from both correct and incorrectly labeled data-points [Northcutt et al., 2021b].

Each sample point in the data-set is assigned a confidence value that denotes the degree of uncertainty associated with that particular label [Northcutt et al., 2021a, Xia et al., 2021]. A low confidence value is assigned to a mislabeled example, indicating the algorithm's uncertainty in that label determination [Xia et al., 2021]. Conversely, a high confidence rate is assigned to a correctly labeled example, indicating the algorithm's confidence in that classification [Grunwald et al., 1998] [Xia et al., 2021].

The confidence values are then used to determine the weight of the contribution of each data-point to model training efforts [Northcutt et al., 2021a]. High confidence labels have a greater effect on the model, while low confidence labels are given a smaller influence on the overall performance [Northcutt et al., 2021b]. This enables the algorithm to focus on improving from the most relevant examples [Northcutt et al., 2021a, Zerilli et al., 2022].

CL is a widely used and powerful machine learning technique that can be effectively applied in the classification of tunnel rings based on geological conditions through the analysis of data generated by tunnel boring machines (TBMs). The

Confident Learning (CL) framework was implemented in the Porto Metro data-set using a systematic approach that involves two main steps: counting and rank & prune [Northcutt et al., 2021a, Bardhan et al., 2021]. Initially, the CL model outputs a vector of probabilities for classification labels [Northcutt et al., 2021a], rock, mixed, and soil, for the particular Porto Metro case study. It is interesting to note that confidence learning can include both supervised and unsupervised methods [Loquercio et al., 2020].

In supervised learning, the confidence model is trained using the same input features as the main model, but with the target variable replaced by the residual errors between the predicted and actual values obtained [Loquercio et al., 2020]. This is often done using a regression model, such as linear regression or gradient boosting (e.g. XGBoost, LightGBM, CatBoost, etc.) [Shehadeh et al., 2021].

Gradient Boosting is an iterative machine learning algorithm that produces an ensemble of weak prediction models, usually decision trees, to form a final predictive model [Zhang and Zhan, 2017].

Each tree is trained to predict the residual error of the previous model, with the goal of minimizing a loss function through gradient descent optimization [Bottou, 2010]. The resulting model is a combination of all the individual predictions [Bottou, 2010]. Gradient boosting has many applications, including ranking, recommendation systems, being well-suited for complex data patterns and is known for its high predictive accuracy [Shehadeh et al., 2021]. When it comes to unsupervised learning, different methods are available for training the confidence model, such as clustering or density estimation [Northcutt et al., 2021a].

The Porto Metro case study employed supervised machine learning algorithms, specifically two gradient booster models, Extreme Gradient Boosting (XGBoost) and Adaptive Boosting (Adaboost), used to derive out-of-sample probabilities.

Extreme Gradient Boosting, or simply XGBoost, is a fast and effective ensemble learning algorithm that leverages gradient boosting to create high-performing predictive models [Wade and Glynn, 2020]. It uses decision trees to combine multiple weak models and minimize a loss function through gra-

gradient descent optimization [Wade and Glynn, 2020]. XGBoost is well-known for its capability to handle large datasets with high-dimensional features [Wade and Glynn, 2020].

Adaptive Boosting (Adaboost) is a ML algorithm that combines multiple weak classifiers into a strong classifier [Hatwell et al., 2020]. The algorithm iteratively trains weak classifiers on different subsets of the training data and adjusts the weights of the misclassified samples to emphasize the importance of these samples in subsequent iterations [Hatwell et al., 2020]. By doing so, AdaBoost focuses on the hard-to-classify instances, which results in a more accurate classification model [Hatwell et al., 2020]. Weak classifiers are then combined into strong ones by weighted averaging [Hatwell et al., 2020].

Below, an overview of the model's methodology is explained:

1. **Counting:** The first step involves counting data points that are likely to belong to a different label class than their initially assigned class. This count helps the CL framework calculate the joint probability distribution between "noise labels" and "true labels," as well as a noise transition matrix [Northcutt et al., 2021a].
2. **Rank & Prune:** CL framework cleans the data-set. This is done through two distinct approaches: completely removing mislabeled data points, or eliminating data points based on their probability ranking [Northcutt et al., 2021a]. The probability ranking is determined by a label quality score, which is calculated based on the probability of a data point belonging to the initial noisy class as determined in Step 1 [Northcutt et al., 2021a]. This score serves as an indicator of the reliability of a data point and helps in deciding whether to keep or remove it from the training data-set.
3. **Learning:** The final step of the CL framework involves the algorithm using the now "cleaned" data-set to train and learn the original machine learning

model. This step is crucial as it utilizes the most relevant and accurate examples in the data-set to further improve the model's performance. By removing the mislabeled or low-confidence data points from the training process, the model can better focus on the most informative and reliable examples [Northcutt et al., 2021a].

During the learning process, the algorithm updates the model's parameters by minimizing the chosen loss function [Zhang et al., 2014]. This process involves optimizing the model's weights and biases to minimize the difference between the predicted and actual labels for each example in the data-set [Northcutt et al., 2021b]. By utilizing the high-confidence examples more heavily in the training process, the model can better generalize to new, unseen data and make more accurate predictions [Grunwald et al., 1998].

The learning step of the CL framework is critical in improving the machine learning model's accuracy and generalization capabilities [Grunwald et al., 1998]. By utilizing a cleaned data-set with high-confidence examples, the algorithm can better learn from informative data points and disregard potentially erroneous examples, resulting in a more robust and reliable model [Zerilli et al., 2022].

In the context of confidence learning models, high and low confidence labels are used to describe the level of certainty that a model has in its predictions for a given data point [Grunwald et al., 1998]. High confidence labels are associated with data points that have a probability score close to 1, indicating a high degree of certainty that the label is correct [Grunwald et al., 1998]. Whereas low confidence labels are associated with a probability score close to 0, indicating that the algorithm is uncertain in its classification [Grunwald et al., 1998].

5.2.2 Scattergram Approach

The use of scatterplots to observe ground condition patterns based on TBM data can be a valuable technique for geology prediction. By comparing different machine parameter pairs, such as Penetration x Torque Screw, Penetration x Screw Conveyor

Speed Measuring, Advance Speed x Screw Conveyor Speed Measuring, Thrust Force x Cutting Wheel Speed of Rotation, and Penetration x Earth Pressure 1, we can gain insight into the type of ground the machine is going through. As presented in Chapter 4, these observations show distinct patterns that can be used to verify ground classifications outputted by the confidence learning model presented.

From this analysis, we can observe that rock and rock-like material exhibit a more concentrated and dense data-point distribution than soil and soil-like rings. This means that the data points in a scatterplot for rock tend to cluster more tightly around a central point, while soil data points are more spread out (exemplified in Table 4.7).

The use of scatterplots and parameter comparisons is a powerful tool for observing ground condition patterns and verifying machine-learning based ground classification. In the following sections, both the confidence learning approach and the scatterplot method will be presented for a series of high and low-confidence labels, which will subsequently be compared. By understanding the strengths and weaknesses of each method, we can better understand how they can be used together to improve our understanding of ground conditions and optimize the tunneling process.

5.3 Applications

5.3.1 Confidence Learning Labels

For the Porto Metro case study, the labels generated by the Confidence Learning (CL) framework were evaluated based on their quality score, which is a measure of the probability that a data point belongs to a certain ground class. The quality score is obtained in the first step of the CL framework, where the algorithm calculates the joint probability distribution between the original noisy labels and the true labels generated by the model.

When the quality score is superior to 90%, the label is considered to be high-confidence. Meaning there is a high probability that the ground class assigned to

that data point is correct. Conversely, when the quality score is less than 90%, the label is considered to be low-confidence. Indicating a lower probability that the ground class assigned to the data point is correct.

The choice of the 90% threshold for defining a label as either high or low-confidence is based on the evaluation of the trade-off between precision and recall. A 90% high-confidence threshold allows for significant precision in evaluating machine ground classification, meaning that most high-confidence labels can be deemed correct. However, this may lead to a lower recall, meaning that some of the low-confidence labels that are actually correct may be discarded.

Below, both high and low-confidence labels will be presented, with the scatter-gram method being applied to verify ground classification outputted by the machine learning framework. Lastly, a comparison between the two methods will be discussed.

High Confidence Labels

In the Confidence Learning (CL) model described earlier, the highest confidence labels obtained for each ground class were generated and mapped, as shown in Table 5.1. These high-confidence labels were selected based on the model’s predictions and were used to classify each verified tunnel section (ring).

Table 5.1: High Confidence Labels.

Rings	Label Quality (%)	Ground Class
461	98.60	Rock
842	99.91	
1134	99.99	
1310	99.99	
477	99.99	Mixed
784	99.98	
1233	99.95	
1364	98.74	
557	96.91	Soils
630	99.55	
910	89.66	
877	99.97	

Out of these high confidence rings, a sample of rock, rock-like mixed, soil and

soil-like mixed ring will be evaluated. The highest confidence labels were chosen for each ground class. Thus, rings 1134, 784, 877, and 1233 were chosen to represent each of the four ground classes, respectively.

Low Confidence Labels

In the CL model that was mentioned earlier, the labels with the lowest levels of confidence were created and are listed in Table 5.2.

Table 5.2: Low Confidence Labels.

Rings	Label Quality (%)	Ground Class
453	0.10	Rock
552	2.40	
745	0.70	
772	0.75	
853	0.60	
960	0.10	
421	0.20	Mixed
440	1.40	
720	0.20	
816	2.80	

Out of these low confidence rings, a sample of rock, rock-like mixed, soil and soil-like mixed ring will be evaluated. The highest confidence labels were chosen for each ground class. Thus, rings 816, 853, 552, and 720 were chosen to represent each of the four ground classes, respectively.

5.3.2 Comparison Scattergrams for High Confidence Labeled Rings

This section will present graphical comparisons for rings 1134, 784, 877 and 1233. The following parameter comparisons will be used to validate the labels: Penetration x Torque Screw, Penetration x Screw Conveyor Speed Measuring, Penetration x Earth Pressure 1, Advance Speed x Screw Conveyor Speed Measuring, Thrust Force x Cutting Wheel Speed of Rotation.

Penetration x Torque Screw

Figure 5-1 shows the graphical results for rock ring 1134, rock-like mixed ring 784, soil ring 877 and soil-like mixed ring 1233, respectively, for the parameter pair comparison of Penetration x Torque Screw.

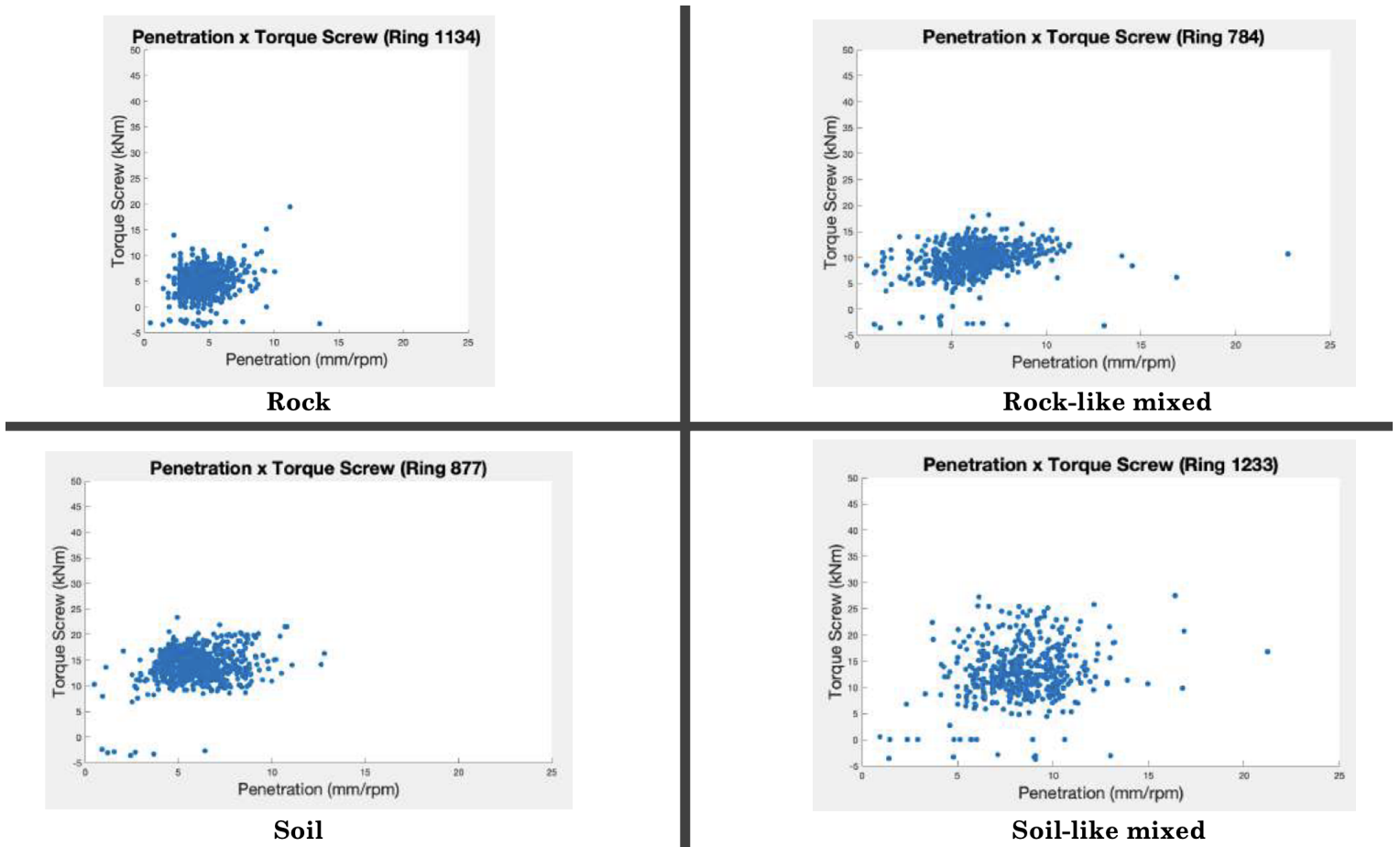


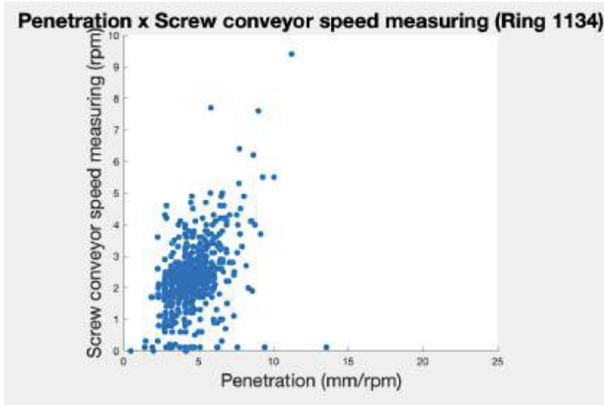
Figure 5-1: Parameter comparison scatterplots for Penetration x Torque Screw for high-confidence labels.

The graphical representation clearly indicates that the data-points for rock rings are highly concentrated at lower values of both penetration rate and torque screw, whereas for soil rings, data are concentrated at higher values for both parameters. Both mixed rings have more spread-out distributions.

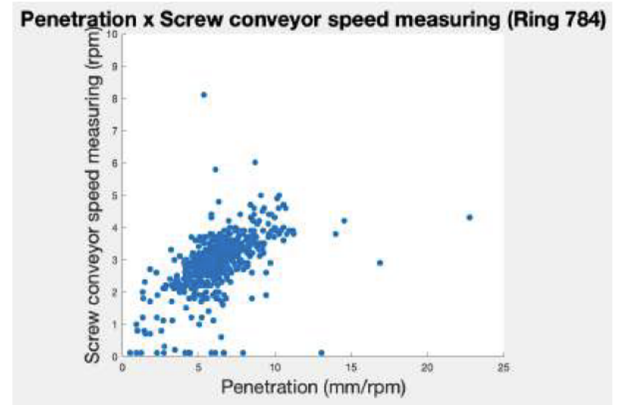
Penetration x Screw Conveyor Speed Measuring

Figure 5-2 shows the graphical results for rock ring 1134, rock-like mixed ring

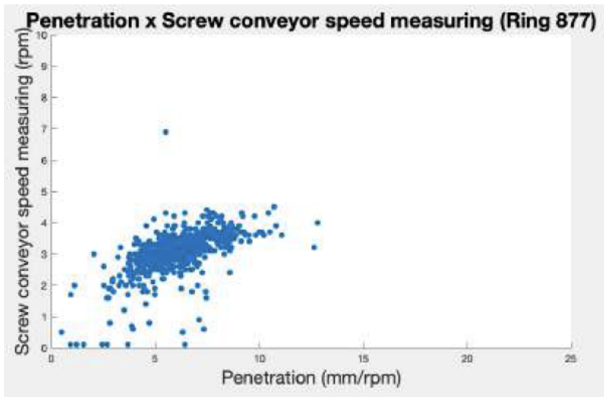
784, soil ring 877 and soil-like mixed ring 1233, respectively, for the parameter pair comparison of Penetration x Screw Conveyor Speed Measuring.



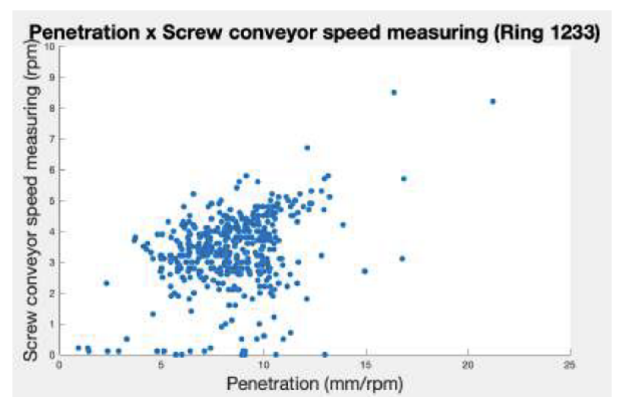
Rock



Rock-like mixed



Soil



Soil-like mixed

Figure 5-2: Parameter comparison scatterplots for Penetration x Screw Conveyor Speed Measuring for high-confidence labels.

The graphs make it evident that the data-points related to rock rings are highly concentrated at lower values of both the penetration rate and screw conveyor speed measuring, whereas for soil rings, data clusters at higher values for both parameters. The mixed rings have a more dispersed distribution, spread-out for soil-like mixed and more concentrated for the rock-like mixed ring.

Penetration x Earth Pressure 1

Figure 5-3 shows the graphical results for rock ring 1134, rock-like mixed ring 784, soil ring 877 and soil-like mixed ring 1233, respectively, for the parameter pair

comparison of Penetration x Earth Pressure 1.

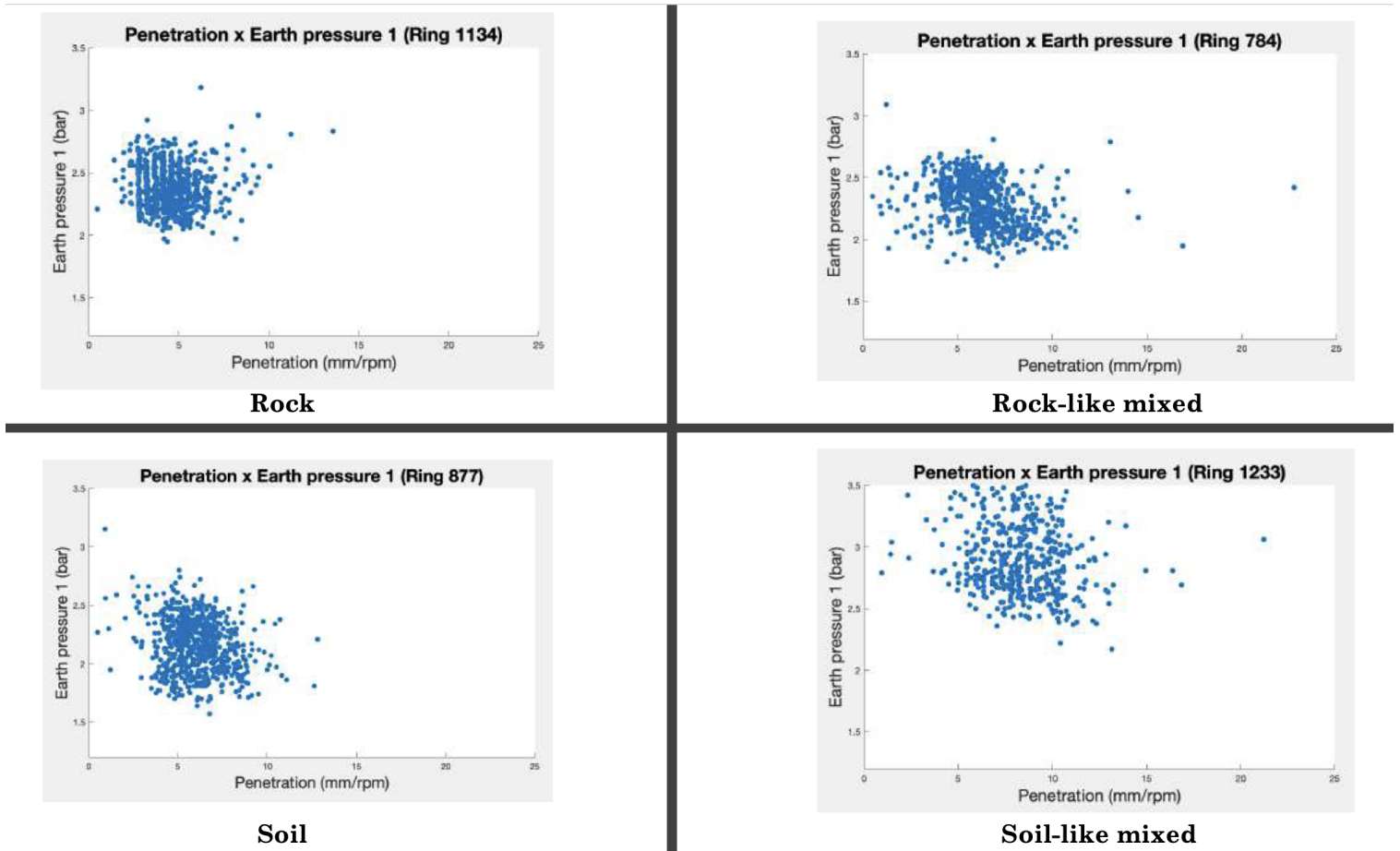
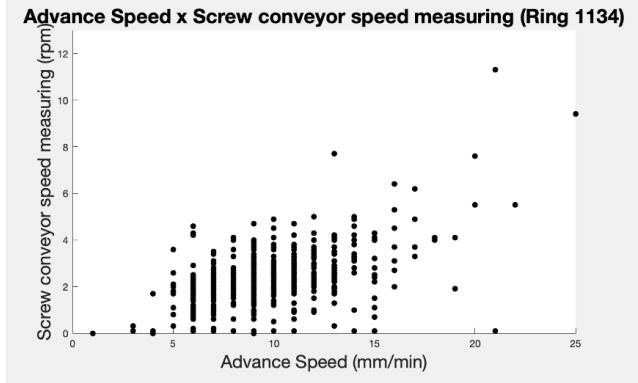


Figure 5-3: Parameter comparison scatterplots for Penetration x Earth Pressure 1 for high-confidence labels.

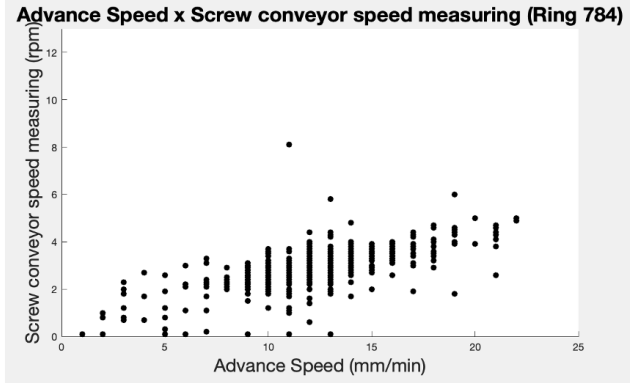
Here, the rock ring has data-points concentrated around higher values of earth pressure while maintaining lower penetration rates. For soils, data are concentrated around higher penetration rates and slightly lower earth pressure. This is in contrast to mixed rings, where both rock and soil-like mixed have a more spread-out distribution.

Advance Speed x Screw Conveyor Speed Measuring

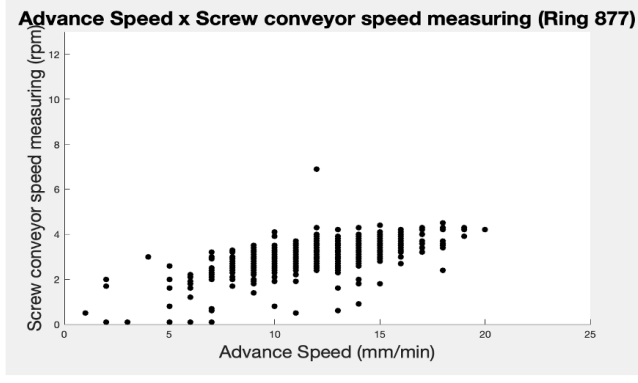
Figure 5-4 shows the graphical results for rock ring 1134, rock-like mixed ring 784, soil ring 877 and soil-like mixed ring 1233, respectively, for the parameter pair comparison of Advance Speed x Screw Conveyor Speed Measuring.



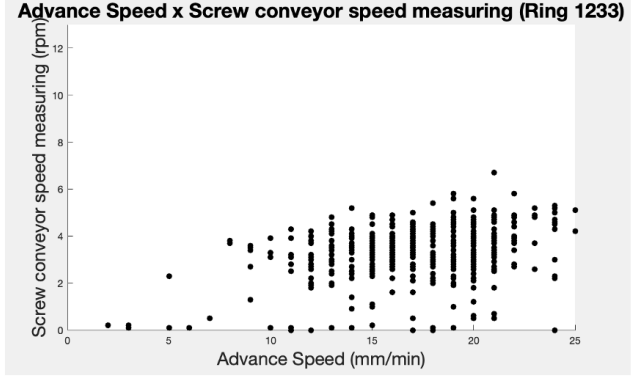
Rock



Rock-like mixed



Soil



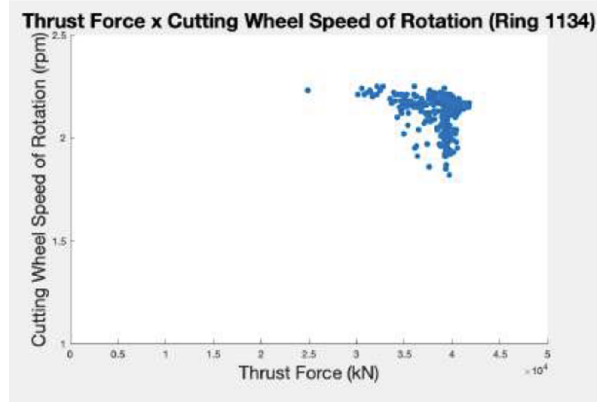
Soil-like mixed

Figure 5-4: Parameter comparison scatterplots for Advance Speed x Screw Conveyor Speed Measuring for high-confidence labels.

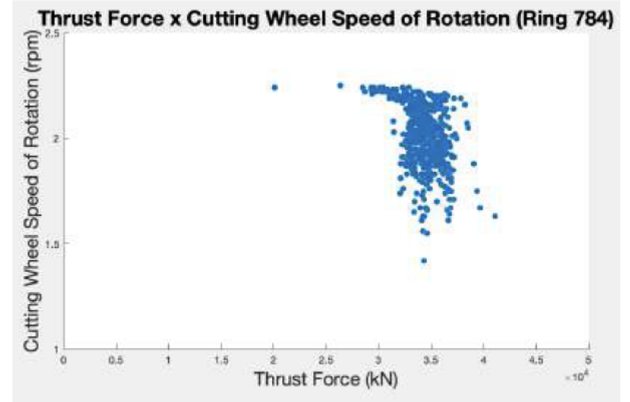
In all of the rings, distinct vertical lines can be seen, which suggest fixed values for advance speed. In rock, the distribution is much more concentrated around lower values of both advance speed and screw conveyor speed measuring. For soils, data-points are considerably more spread-out, with observations concentrated at higher values of both parameters. Both mixed rings show significant data-point concentration, especially in soil-like mixed.

Thrust Force x Cutting Wheel Speed of Rotation

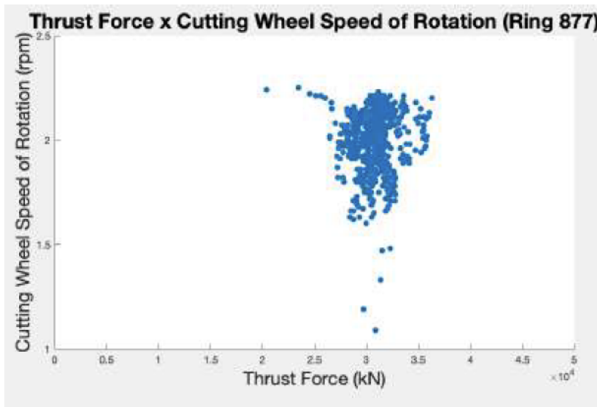
Figure 5-5 shows the graphical results for rock ring 1134, rock-like mixed ring 784, soil ring 877 and soil-like mixed ring 1233, respectively, for the parameter pair comparison of Thrust Force x Cutting Wheel Speed of Rotation.



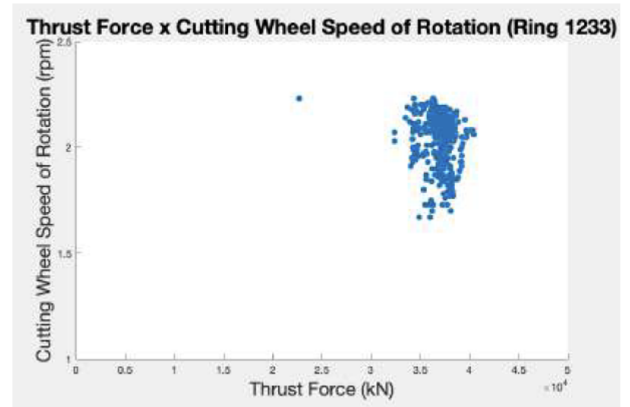
Rock



Rock-like mixed



Soil



Soil-like mixed

Figure 5-5: Parameter comparison scatterplots for Thrust Force x Cutting Wheel Speed of Rotation for high-confidence labels.

For this parameter pair comparison, in rock, the distribution is highly concentrated at higher values of thrust force. While soils present a concentrated distribution at lower thrust force. Both mixed rings present a concentrated distribution at almost identical thrust force and cutting wheel speed of rotation values. Interestingly, there is a distinct inverted "L" shape notable.

Interpretation

Throughout the 5 chosen parameter pairs, rock rings demonstrated a highly concentrated or concentrated distribution, indicating a pattern that can be correlated to the ground class. Soils range from concentrated to spread-out, depending on the parameter pair being analyzed, but are generally in clear contrast to patterns seen

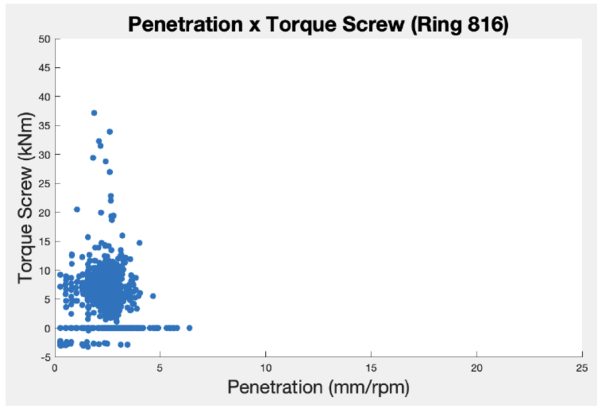
in rock rings. For mixed rings, it is harder to determine their specific ground-class, with behaviors varying significantly throughout the compared parameters. However, still presenting similar characteristics to either rock or soils.

5.3.3 Comparison Scattergrams for Low Confidence Labeled Rings

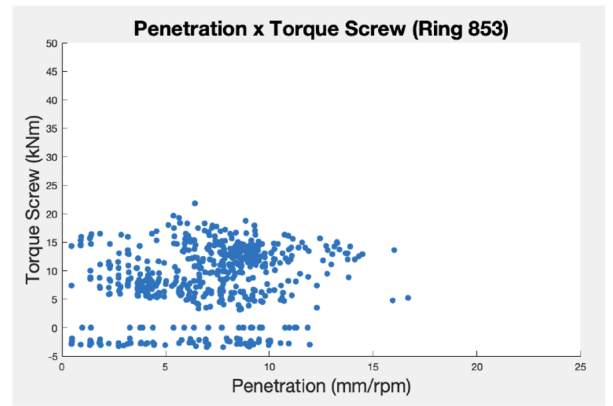
In this section, graphical comparisons for four rings, namely 816, 853, 552, and 720 will be displayed. The comparisons will utilize the following parameter pairs: Penetration x Torque Screw, Penetration x Screw Conveyor Speed Measuring, Penetration x Earth Pressure 1, Advance Speed x Screw Conveyor Speed Measuring, and Thrust Force x Cutting Wheel Speed of Rotation. They will subsequently used to generate labels off of previously presented indicative patterns for each ground class.

Penetration x Torque Screw

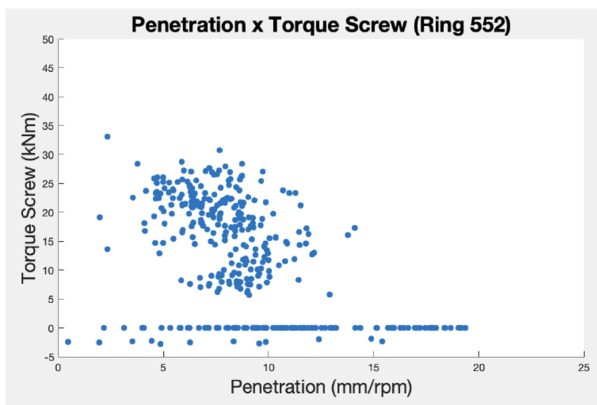
Figure 5-6 shows the graphical results for rock ring 816, rock-like mixed ring 853, soil ring 552 and soil-like mixed ring 720, respectively, for the parameter pair comparison of Penetration x Torque Screw.



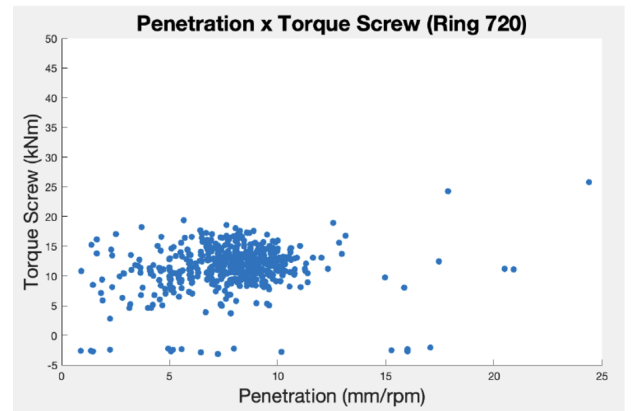
Rock



Rock-like mixed



Soil



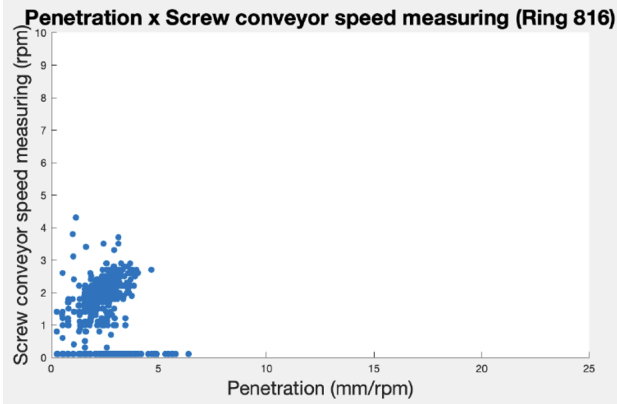
Soil-like mixed

Figure 5-6: Parameter comparison scatterplots for Penetration x Torque Screw for low-confidence labels.

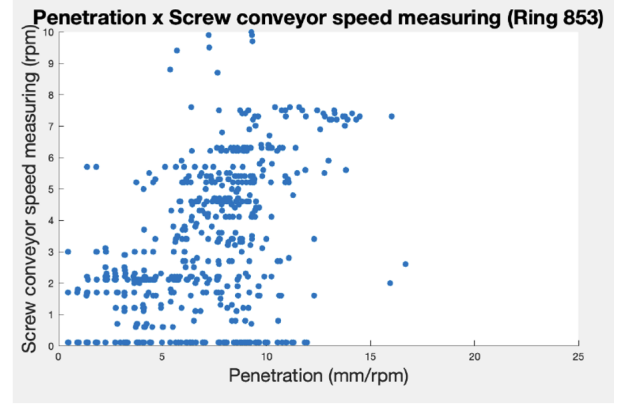
The graphs show that rock rings have a high concentration of data-points with lower values for both penetration rate and torque screw, while soil rings have a high concentration of data-points with higher values for both parameters. In contrast, the distributions for both mixed rings are more dispersed.

Penetration x Screw Conveyor Speed Measuring

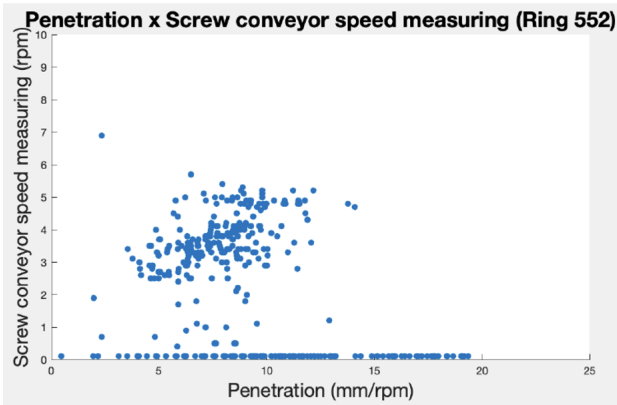
Figure 5-7 shows the graphical results for rock ring 816, rock-like mixed ring 853, soil ring 552 and soil-like mixed ring 720, respectively, for the parameter pair comparison of Penetration x Screw Conveyor Speed Measuring.



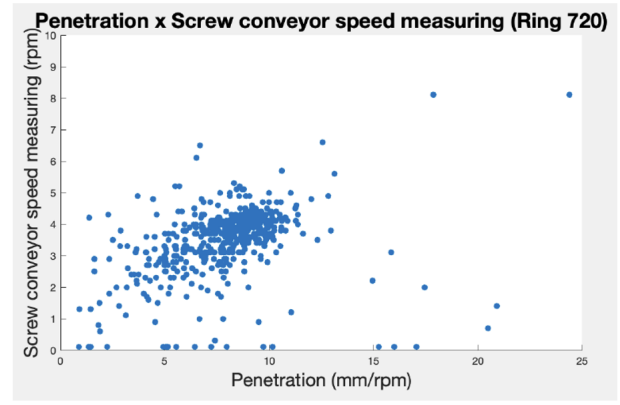
Rock



Rock-like mixed



Soil



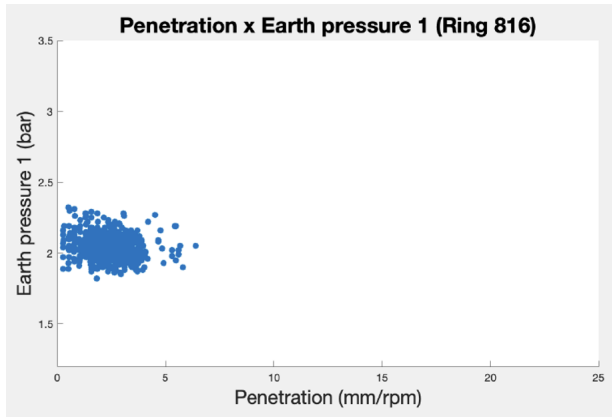
Soil-like mixed

Figure 5-7: Parameter comparison scatterplots for Penetration x Screw Conveyor Speed Measuring for low-confidence labels.

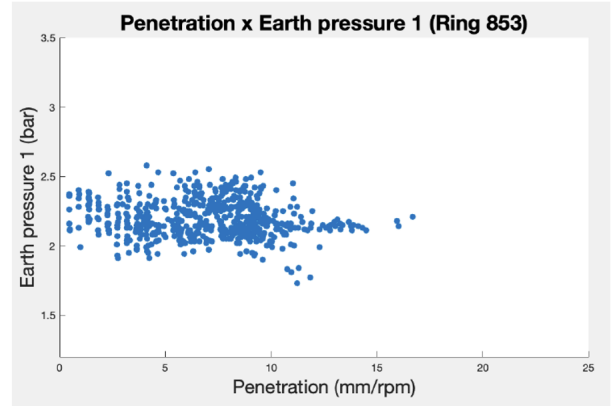
The graphs demonstrate that the data-points pertaining to rock rings are highly concentrated at lower values of both the penetration rate and screw conveyor speed, while for soil rings, data are somewhat spread-out at higher values for both parameters. The rock-like mixed ring exhibits a more spread-out distribution, while the soil-like mixed ring has a more concentrated distribution.

Penetration x Earth Pressure 1

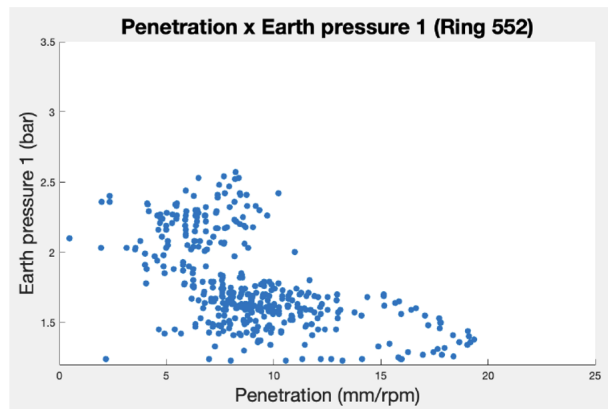
Figure 5-8 shows the graphical results for rock ring 816, rock-like mixed ring 853, soil ring 552 and soil-like mixed ring 720, respectively, for the parameter pair comparison of Penetration x Earth Pressure 1.



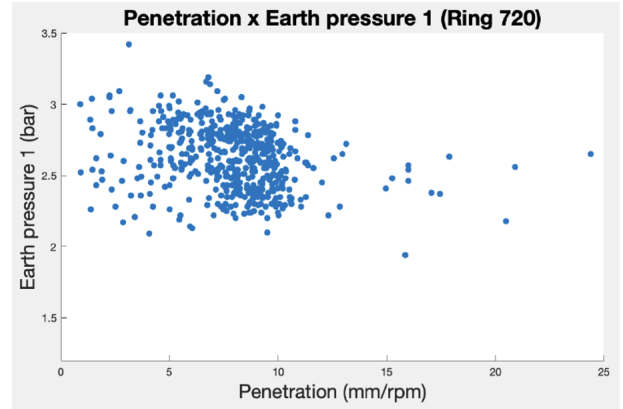
Rock



Rock-like mixed



Soil



Soil-like mixed

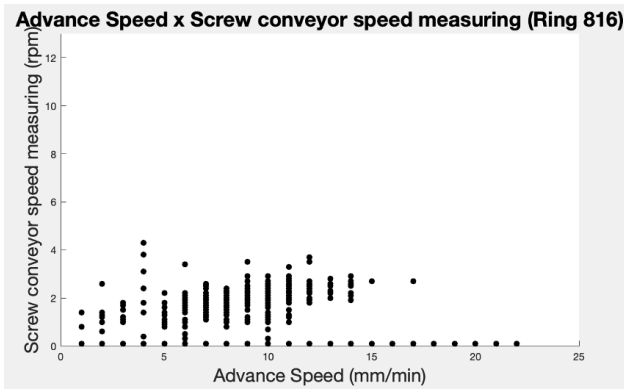
Figure 5-8: Parameter comparison scatterplots for Penetration x Earth Pressure 1 for low-confidence labels.

In this case, the data-points for the rock ring are highly concentrated at higher values of earth pressure and lower penetration rates, whereas for soil rings, data are spread-out around higher penetration rates and slightly lower earth pressure values. The mixed rings, also show data-point concentration. With the rock-like mixed ring concentrating around similar values of earth pressure than the rock ring and varying penetration rates. And the soil-like mixed ring showing data-point concentration at higher earth pressure values and varied penetration rates.

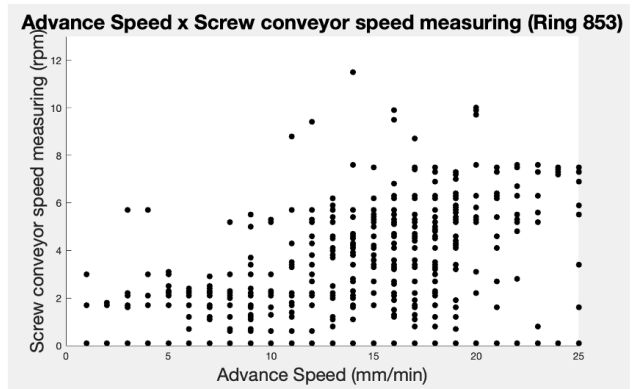
Advance Speed x Screw Conveyor Speed Measuring

Figure 5-9 shows the graphical results for rock ring 816, rock-like mixed ring 853, soil ring 552 and soil-like mixed ring 720, respectively, for the parameter pair

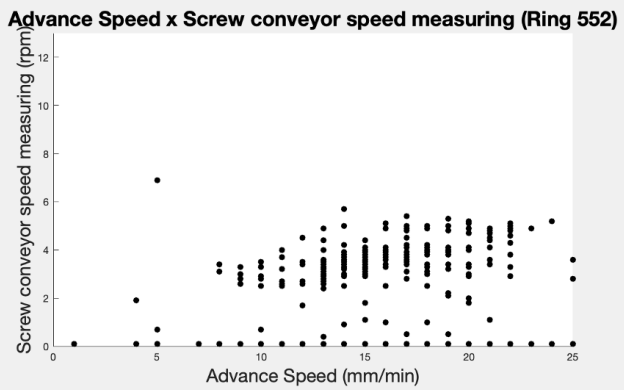
comparison of Advance Speed x Screw Conveyor Speed Measuring.



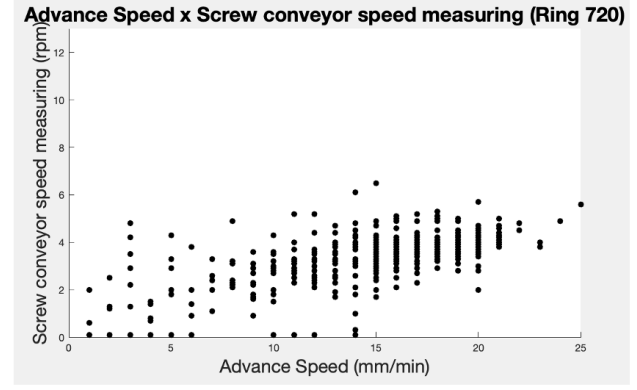
Rock



Rock-like mixed



Soil



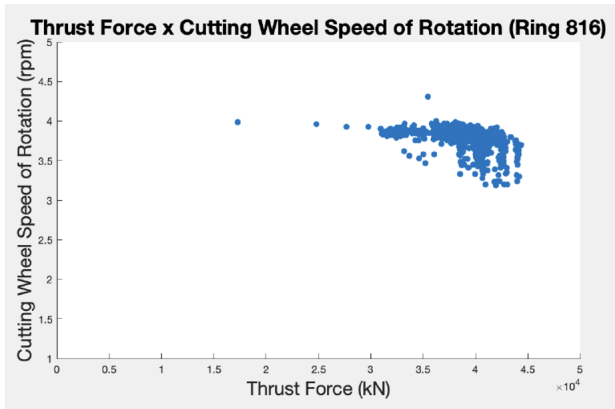
Soil-like mixed

Figure 5-9: Parameter comparison scatterplots for Advance Speed x Screw Conveyor Speed Measuring for low-confidence labels.

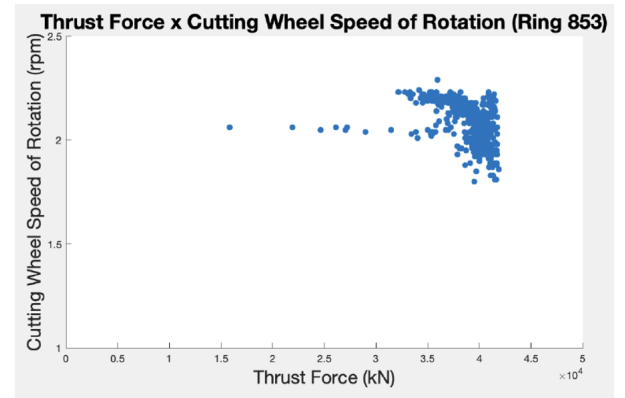
In each of the rings, there are noticeable vertical lines that indicate fixed values for advance speed. The rock rings exhibit a concentrated distribution around lower values of advance speed and screw conveyor speed measurement, while soils exhibit more concentrated data points, especially at higher values of both parameters. The mixed rings, particularly soil-like mixed, have some concentration of data points.

Thrust Force x Cutting Wheel Speed of Rotation

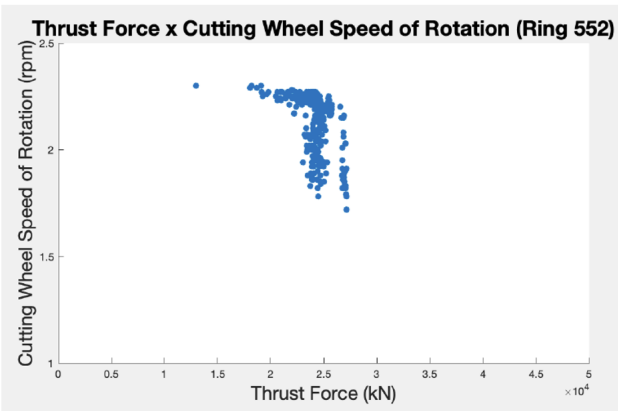
Figure 5-10 shows the graphical results for rock ring 816, rock-like mixed ring 853, soil ring 552 and soil-like mixed ring 720, respectively, for the parameter pair comparison of Thrust Force x Cutting Wheel Speed of Rotation.



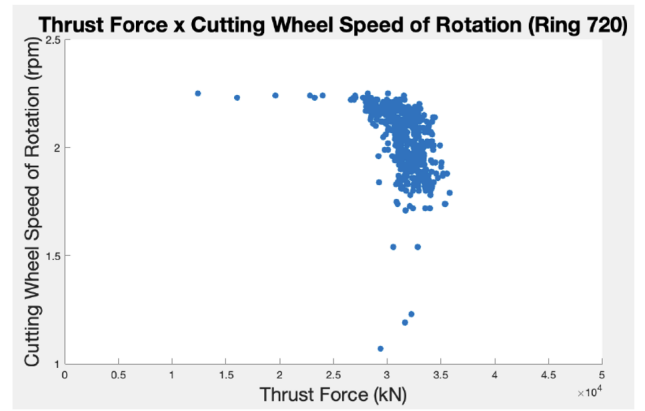
Rock



Rock-like mixed



Soil



Soil-like mixed

Figure 5-10: Parameter comparison scatterplots for Thrust Force x Cutting Wheel Speed of Rotation for low-confidence labels.

When comparing this specific parameter pair, the distribution in rock is heavily focused on higher values of thrust force. Conversely, soils display a concentrated distribution at lower thrust force values. Both mixed rings demonstrate a concentrated distribution with nearly identical values for both thrust force and cutting wheel speed of rotation. Again, the inverted "L" shape can be observed.

Interpretation

The five parameter pairs analyzed revealed that rock rings exhibit a concentrated or highly concentrated distribution, suggesting a correlation with the ground class. Soil rings, on the other hand, vary in distribution from concentrated to spread-out, depending on the parameter pair analyzed, but consistently differ from the patterns

observed in rock rings. Mixed rings are more difficult to classify by ground class, as their behaviors differ significantly across the analyzed parameters, but still present similarities to either rock or soil.

5.4 Comparison & Conclusions

The following table (5.3), shows the comparison of the ground class labels generated by the Confidence Learning (CL) model and their comparison to what was seen in the geologic profiles and face maps presented in Chapter 3.

Table 5.3: Comparison between ground class labels generated by the Confidence Learning Model and Geologic Profiles.

Rings	Label Quality (%)	CL Ground Class	Geologic Profile Ground Class
High Confidence Labels			
461	98.60	Rock	Rock
842	99.91	Rock	Rock
1134	99.99	Rock	Rock
1310	99.99	Rock	Rock
477	99.99	Mixed	Rock-like Mixed
784	99.98	Mixed	Rock-like Mixed
1233	99.95	Mixed	Soil-like Mixed
1364	98.74	Mixed	Soil-like Mixed
557	96.91	Soil	Soil-like Mixed
630	99.55	Soil	Soil-like Mixed
910	89.66	Soil	Soil
877	99.97	Soil	Soil
Low Confidence Labels			
440	1.40	Rock	Soil
816	2.80	Mixed	Rock
421	0.20	Mixed	Soil-like Mixed
453	0.10	Rock	Rock-like Mixed
720	0.20	Mixed	Soil-like Mixed
853	0.60	Mixed	Rock-like Mixed
552	2.40	Rock	Soil
745	0.70	Rock	Soil
772	0.75	Rock	Soil-like Mixed
960	0.10	Rock	Soil

Table 5.4 compares the ground class labels resulting from the scattergrams and what was determined through the information contained in geologic information available in Chapter 3.

Table 5.4: Comparison between ground class labels generated by the Scattergrams and Geologic Profiles.

Rings	Scattergram Ground Class	Geologic Profile Ground Class
1134	Rock	Rock
784	Rock-like Mixed	Rock-like Mixed
877	Soil	Soil
1233	Soil-like Mixed	Soil-like Mixed
816	Rock	Rock
853	Rock-like Mixed	Rock-like Mixed
552	Soil	Soil
720	Soil-like Mixed	Soil-like Mixed

Lastly, Table 5.5 compares the information from Tables 5.3 and 5.4. Here, the ground class labels resulting from high-confidence labeled rings, (1134, 784, 877, and 1233) and low-confidence labeled rings (816, 853, 552 and 720) are compared to the ground classes obtained through the use of scattergrams.

Table 5.5: Comparison between ground class labels generated by the Scattergrams and Geologic Profiles.

Rings	Label Quality (%)	CL Ground Class	Scattergram Ground Class
1134	99.99	Rock	Rock
784	99.98	Mixed	Rock-like Mixed
877	99.97	Soil	Soil
1233	99.95	Mixed	Soil-like Mixed
816	2.80	Mixed	Rock
853	0.60	Mixed	Rock-like Mixed
552	2.40	Rock	Soil
720	0.20	Mixed	Soil-like Mixed

Although useful for outputting machine-generated labels, the Confidence Learning (CL) model presented some discrepancies and low-confidence labels that had misclassified several rings. These were then compared against both the geologic information

(see Chapter 3) and the scatterplots, which verified and changed several ring ground classifications.

Scatterplots, on the other hand, were found to be the most effective tool for classifying rings among different ground classes, including rock, soil, rock-like mixed, and soil-like mixed, being correct in all the evaluated rings (552, 720, 784, 816, 853, 877, 1134, 1233), when verified by the available geologic data (presented in Chapter 3). They revealed notable differences between these ground classes, with rock data-points exhibiting high-density clustering around specific threshold ranges for each compared parameter. In contrast, soil data-points were more widely dispersed with greater variability and less clustering. Mixed rings displayed patterns resembling those of either rock or soil, with data-point concentration being present across parameter comparisons, but less pronounced than in rock rings.

Chapter 6

Techno-Economic Assessment (TEA)

6.1 Contextual Aspects

Techno-economic assessments or TEAs are study tools that seek to understand and assess the technical feasibility of a project or technology while considering its economic implications [Mahmud et al., 2021]. A typical TEA combines a cost-benefit analysis with a technical study of the product/project being evaluated and also studying market factors [Latapí Agudelo et al., 2019]. The techno-economic assessment (TEA) aims to present decision-makers with the data and information needed to establish the validity and worth of a project or product [Rajabi Hamedani et al., 2019]. This informed-decision-making process is extremely important for launching new technologies into markets and attracting investment [Christensen et al., 2005].

Beginning in the early 20th century, techno-economic assessments (TEAs) were developed for large infrastructure projects (usually publicly funded) by joining a team of engineers and economists that would discuss cost-benefit analyses as well as the technical implications of developing projects of this scale [Giacomella, 2021]. The term TEA was coined in the 1950s being popularized only in the 1970s and 1980s as the appraisal of technical and economic aspects of a project became more relevant [Andersen, 1991, Latapí Agudelo et al., 2019].

One of the first detailed TEAs was carried out by the US Atomic Energy Commission for the construction of a nuclear power plant, where it compared the technical

and economic feasibility of nuclear power as a potential substitute for fossil fuels [Hennessey, 1973, Owen, 2011]. By the 1970s the United Nations (UN) began using techno-economic assessments (TEAs) in all large infrastructure projects (like hydroelectric power plants, roads and irrigation systems) that it either financed or was otherwise involved in, especially in the Global South [Andersen, 1991, Sharif, 1988].

By the 1990s TEAs became ubiquitous in the private sector, especially in analyzing new business ideas and products [Gompers and Lerner, 2001]. These assessments were especially helpful in aiding the exponential growth of mobile telecommunications and the internet [Dodgson et al., 2008, Lindmark, 2002]. Currently, techno-economic assessments (TEAs) are employed in a wide array of industries and projects, buttressing the incoming age of artificial intelligence (AI), climate change mitigation technologies, transportation and healthcare [Nagapurkar, 2019, Islam et al., 2022]. The TEA has become an essential tool for decision-makers in gauging new technology.

6.2 The use of Artificial Intelligence (AI) in Tunnel Boring Machines (TBMs)

In this section, a preliminary techno-economic assessment (TEA) of the use of artificial intelligence (AI) in the operation of Tunnel Boring Machines (TBMs) will be discussed. For the evaluation of the uses of AI technology in TBM operations, the following list of steps will be used:

1. **Defining Project Scope:** determine the specific AI application to TBM operations being evaluated.
2. **Conducting Market Analysis:** consult the present market and applications of AI algorithms in TBMs, including market size and growth rate (CAGR ¹), the current main players in the domain, trends and challenges of the technology within the specific industry.

¹Compound Annual Growth Rate (CAGR) is a financial metric that evaluates the rate of return of an investment in a specific period of time [Fernando, 2023]. CAGR is measured by the rate of growth (year-on-year) of an investment over a set time period [Fernando, 2023].

3. **Identifying technical requirements:** delineate the technical aspects of the AI tools that could potentially be applied, including both hardware and software, and note the feasibility and especially the scalability of the proposed technology.
4. **Cost Estimation:** appraise the costs associated with the application of AI/ML to improve TBM operations, including the costs of the operating system, research, maintenance and support costs.
5. **Benefit Analysis:** identify the potential improvements associated with the application of the proposed technology. Including (but not limited to) improved efficiency (or predicted improvement), increased accuracy and worksite safety, and estimating the return on investment (ROI) for applying the technology.
6. **Risks:** determine and weigh potential risks in using the AI/ML technology in the proposed project, also considering any regulatory, compliance and security shortcomings.
7. **Conclusion:** While considering the results and analyses obtained from the aforementioned steps, conclude whether it makes sense for the technology to be applied, understanding if the proposed approach is both technologically and economically feasible and beneficial, further providing recommendations for next steps on how to improve or update the TEA.

The following sections will present the detailed analysis carried out to determine the viability of using Artificial Intelligence (AI) and Machine Learning (ML) to assist real-time decision making for predicting geological conditions ahead of the tunnel face.

6.3 TEA Project Scope

In this section the problem definition for the techno-economic assessment (TEA) will be discussed. The proposed TEA seeks to evaluate the use of artificial intelligence

(AI) through machine learning (ML) algorithms for geology prediction in tunnel boring machine (TBM) operations. The use of AI/ML for predicting ground conditions ahead of the tunnel face has been widely explored in the literature in the past three to four years (see section 4.2.1). As the tunneling industry is expected to grow by approximately 10% per year in the decade from 2022 to 2032, efforts to automate and increase safety and productivity in operations with the aid of AI/ML are being intensely researched [Industry Research, 2022]. The scope of the TEA is listed as follows:

1. Literature review on current work in AI/ML technology for geology prediction in TBMs and potential benefits of this technology (see section 4.2).
2. Identifying relevant stakeholders and the potential effects and consequences incurred if the technology is widely adopted.
3. Development of a simple road-map to envision how the technology will be put into effect.

6.3.1 Literature Review

As presented in section 4.2, much research has been done in recent years exploring the use of AI/ML applications to improving tunneling automation through the analysis of data generated by Tunnel Boring Machines (TBMs). The large data-sets output by the TBM have been used to create real-time analysis and response systems that can potentially inform both machine operators and designers to local ground conditions [Fu et al., 2022, Sun et al., 2018].

Although much progress has been made and increasingly automated TBMs are being deployed, researchers suggest that much progress still needs to be made in order to streamline this technology globally [Akinosho et al., 2020]. Better risk assessments and cost-benefit analyses need to be developed to evaluate this technology [Eskesen et al., 2004, Erharter and Marcher, 2021]. Furthermore, one of the biggest hindrances to the furthering of the field is the lack of unification in data output by

the TBM [Wang et al., 2023]. If data were generated in a single file template, rather than a multitude of files, one for each parameter, using various file formats, it would improve both the quality and productivity of tunneling analysis [Acosta, 2021].

If a master, or all-encompassing, file that could contain the total telemetry² parameters, in a standardized format, would facilitate comparison between different TBM machines (independent of supplier, size, or other specifications) while significantly reducing data pre-processing time [Acosta, 2021]. As the automation revolution is well underway, and data being generated in massive amounts, the ability to share and take insights from this collective data pool would be vastly beneficial for the industry [Mayer-Schönberger and Cukier, 2013]. However, as competing manufacturers might not be willing to freely share information and as governments increasingly regulate data privacy, this might be hindered [Acosta, 2021].

To date, there has not been any techno-economic analysis done for predictive technologies forecasting ground conditions in tunnel construction. Some work has been done in related fields, especially within energy production. The table below (Table 6.1) lists some of these TEAs.

Recent TEAs in the Energy Sector	
Rao, K., et al., 2018.	Improvised Drilling and Blasting Techniques at Underground Metal Mine for Faster Advance to Enhance Linear Excavation and Production—A Techno-Economic Case Study.
Cui, Y., et al., 2019.	Techno-economic assessment of the horizontal geothermal heat pump systems: A comprehensive review.
Continued on next page	

²Telemetry refers to a general term for technologies that compile information through measurements and/or statistical data, forwarding it to information-technology (IT) systems remotely [Rouse, 2015].

Table 6.1 – Continued from previous page

Recent TEAs in the Energy Sector	
Restrepo-Valencia, S., et. al., 2019.	Techno-economic assessment of bio-energy with carbon capture and storage systems in a typical sugarcane mill in Brazil.
Maroušek, J., et al., 2020.	Techno-economic assessment of potato waste management in developing economies
Madlener, R., et. al., 2020.	An Exploratory Economic Analysis of Underground Pumped-Storage Hydro Power Plants in Abandoned Deep Coal Mines.
Zhou, W., et al., 2020.	Selection and techno-economic analysis of hybrid ground source heat pumps used in karst regions.
Sirdesai, N., et al., 2020.	Impact of Rock Abrasivity on TBM Cutter-Discs During Tunnelling in Various Rock Formations.
Pakenham, B., et al., 2021.	A review of life extension strategies for offshore wind farms using techno-economic assessments.
Frey, M., et al., 2022.	Techno-Economic Assessment of Geothermal Resources in the Variscan Basement of the Northern Upper Rhine Graben.
Continued on next page	

Table 6.1 – Continued from previous page

Recent TEAs in the Energy Sector	
Daniilidis, A., et al., 2022.	Techno-economic assessment and operational CO2 emissions of High-Temperature Aquifer Thermal Energy Storage (HT-ATES) using demand-driven and subsurface-constrained dimensioning.

6.3.2 Stakeholders

Tunneling is part of the backbone for transportation, energy, water and other essential services. Thus, from governments to industry professionals, there are many key stakeholders who will be affected by the automation of the tunneling process and real-time prediction of ground conditions on-site. The following list will detail the main stakeholder groups affected.

1. **Tunnel Boring Machine (TBM) Manufacturers:** Automation technology concerns companies that design, produce and provide maintenance for TBMs worldwide as it could enhance the safety, reliability and efficiency of their products.
2. **Construction Industry:** Companies working with large infrastructure projects, especially those specializing in tunnel construction may benefit from increased automation as it has the potential to reduce costs while increasing safety and productivity. The use of AI/ML for real-time geology prediction can boost optimization of the construction process.
3. **Designers, Geologists and Geotechnical Engineers:** The professionals and specialists in the field can potentially be assisted by the proposed tech-

nology, providing them with more accurate and comprehensive information on subsurface conditions that will allow for improved informed decision-making.

4. **Project Proprietors:** Government agencies, private investors and other key stakeholders will be interested in understating how the technology can assist in the development of the project, on-time completion, especially if within predetermined budgets.
5. **Community Advocates:** Organized civil-society groups that are concerned with the socioeconomic and environmental impacts of tunnel construction, including workers unions. This technology would be of interest to them as it has the possibility of reducing accidents, environmental damage but also of changing industry jobs.
6. **Governments and Regulators:** Government agencies and regulators that are responsible for overseeing infrastructure projects would be impacted as increased TBM automation may assist in the compliance of safety and environmental regulation. Also, they would be in charge of regulating and determining the rules of the roll out of this technology.
7. **Data Scientists and Machine Learning Engineers:** Professionals working at the forefront of data science and AI/ML development using Big Data are not only part of the development of the technology but also interested parties as it will provide the opportunity to develop new techniques and research to real-world infrastructure applications.

6.3.3 Implementation

In developing and implementing machine learning (ML) for geologic prediction for tunnel boring machines (TBM), feasibility studies must be conducted to determine if machine learning (ML) is the best alternative for ground condition prediction ahead of the tunnel face. This analysis should include comprehensive information on

the complexity of encountered geology, data availability and existing TBM control systems.

It has still not been proven that machine learning (ML) is appropriate for this use in the tunneling industry. As proposed models have not yet been integrated within TBM operating systems, it is impossible to fully determine the potential value for this technology.

The successful implementation of machine learning techniques for understanding ground conditions ahead of the tunnel face, demands comprehensive application planning, due diligence and direct coordination. Below, a set of steps on what implementation would look like is presented.

1. **Data Collection and Treatment:** Collection of relevant data and preparation. This includes previously presented geotechnical data, geologic maps, boring logs and information on tunnel rings (see Chapters 3 and 4). Treatment of data for application with the proposed methodology, for this case only data-points where advance rate was different from zero were considered.
2. **Integration with TBM Control Systems:** This has not yet been done in practice. As tunneling automation advances, this is the logical next step. In integrating AI/ML algorithms in the machine's control systems, it is expected that models will be able to assist machine operators in identifying geological conditions ahead of the tunnel face. In order to inform real-time decision-making, it would be necessary to establish a connection between TBM control-systems and data collection systems as well as machine learning models, ideally through an adapted interface.
3. **Validation:** Preceding deployment, this integrated system would need to be thoroughly tested and validated, which is where the field currently stands. As more machine learning processes are being explored and tested for the purpose of geologic prediction ahead of the tunnel face, further testing is required, especially in real-world conditions. For this, comprehensive testing would need

to be done over several different ground conditions and geographical locations, validating the methodology based on its accuracy and reliability.

4. **Deployment:** When comprehensive testing and system validation is underway, then AI/ML models can be utilized in actual tunnel construction projects. However, this development is still years away from being applicable to tunneling projects. Also, adequate training would need to be provided to machine operators, as well as continuous system monitoring to determine performance and safety gains.

6.4 Market Analysis

6.4.1 Current Applications

The construction industry has long attempted to predict geological conditions, particularly in tunneling, where knowledge of ground conditions ahead of the tunnel face is critical for safety and productivity. Failure to identify conditions even a few meters ahead of the tunnel can result in accidents. The advent of AI/ML technology presents an opportunity to utilize the vast amounts of raw data generated by Tunnel Boring Machines (TBMs) for data-driven decision making, a unique advantage not commonly available in other areas of construction (where there is significantly less data collection).

The application of machine learning to ground classification is a promising new field of study with the potential of providing valuable insights into geological conditions ahead of the tunnel face. A good example of this is the development of a proprietary A-TBM system by MMC Gamuda, a Malaysian construction company that has been a pioneer in the field [Byrd, 2016]. Although there have been only a few instances of this technology being applied, MMC Gamuda's A-TBM has demonstrated its efficacy in improving tunnel construction processes, which will be explained in further detail in section 6.4.3 [Byrd, 2016]. Figure 6-1 shows a control center for MMC's A-TBMs.



Figure 6-1: Picture of MMC Gamuda's Tunneling Centralized Command and Control Center [Berhad, 2020]).

By using an automated system, adapting to changes in ground conditions during tunneling and predicting maintenance needs can be done more efficiently and quickly. The market for AI/ML applications for tunnel boring machines is projected to expand as construction companies aim to enhance productivity, safety, and cost-effectiveness of projects. Despite its potential benefits, challenges remain, including the requirement for precise and dependable algorithms and the seamless integration of these algorithms into current TBM control systems.

6.4.2 Expected Market Growth

According to an industry report by Kenneth Research [Kenneth Research, 2021], the global market for tunnel boring machines is expected to grow from USD 3.4 billion (2020) to USD 4.7 billion by 2025, at a CAGR of 6.6% [Globe Newswire, 2022]. Figure 6-2 shows this upward trend in TBM sales during the present decade. As increased automation and technological improvements stimulate the market further,

a CAGR of 9% is expected for autonomous tunnel boring machines, at the same period [Kenneth Research, 2021].

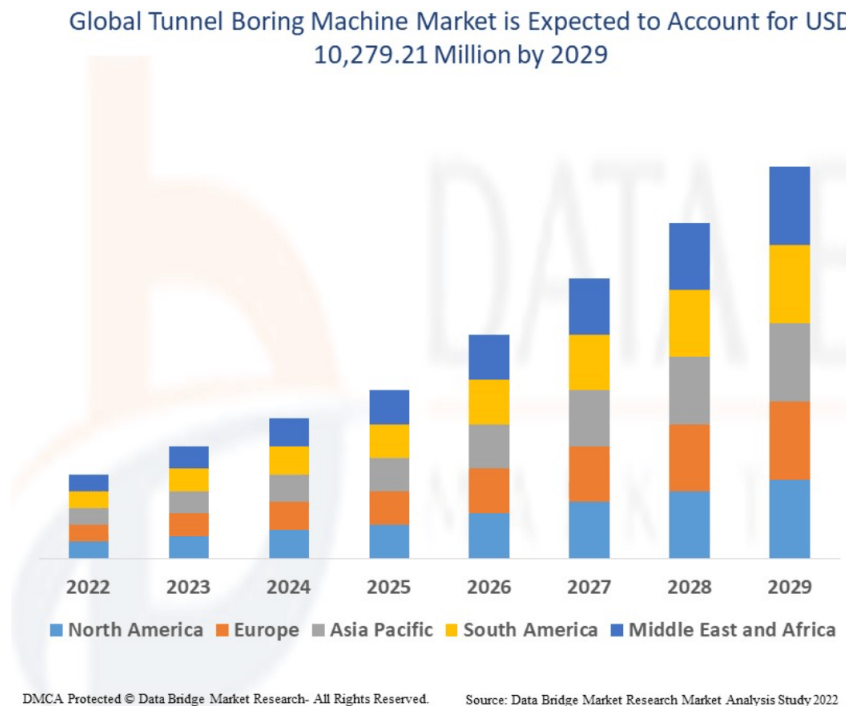


Figure 6-2: Expected Tunnel Boring Machine market growth in the decade from 2020 - 2030 [Data Bridge Market Research, 2021]).

This projected rise in demand for autonomous TBMs³ is based on their advantages over conventional TBMs. Tunneling efforts are also expected to significantly increase in the coming years [Digital Journal, 2019, Mega, 2022]. With a CAGR of 7.6% by 2030 (see Figure 6-3), the tunnel industry is expected to significantly grow, feeding the need for improved TBM-systems [Digital Journal, 2019].

The increasing urbanization in countries such as China, India, and the United States is driving demand for larger and more reliable transportation networks, which in turn drives the demand for tunnel construction and, consequently, the adoption of more advanced and efficient tunneling technologies such as autonomous tunnel boring machines [Avtar et al., 2019]. To meet this demand, it is expected that governments will endorse the use of autonomous tunnel boring machines systems to

³An autonomous tunnel boring machine is a self-propelled excavation device that uses a rotating cutting head to drill tunnels underground with minimal human intervention [Maidl et al., 2014].

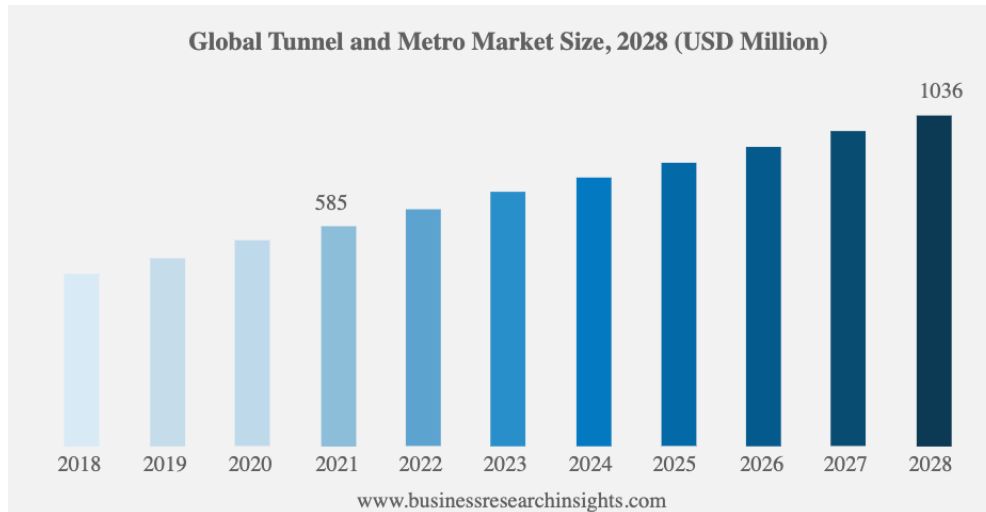


Figure 6-3: Predicted market growth of tunnel construction in the decade from 2018 - 2028 [Business Research Insights, 2021]).

upgrade infrastructure [Melenbrink et al., 2020]. As a result, the demand for autonomous tunnel boring machines systems is likely to increase in the coming years [Melenbrink et al., 2020].

Therefore, the joining of technological enhancements, burgeoning infrastructure projects, and the escalating need for productive and cost-efficient tunneling options, is pushing the market for autonomous tunnel boring machines forward.

6.4.3 Main Players

Still very much in its early stages, the automation of tunnel boring machines (TBMs) has been shaped and driven by a few, highly specialized companies. These companies are developing and deploying prototypes for this incoming TBM technology, and are actively working on MVPs⁴ to bring to market:

MMC Gamuda has implemented an autonomous tunnel boring machine (A-TBM) equipped with proprietary analytics technology for the Klang Valley Mass Rapid Transit (KVMRT) project in Malaysia. MMC Gamuda’s system was trained with data gathered from previous projects as well as a computational simulator. The

⁴MVP stands for Minimum Viable Product. It is a common product development strategy used to fastly generate a basic version of a product with the minimum features necessary to satisfy early customers [Lenarduzzi and Taibi, 2016].

system accurately predicted maintenance requirements such as cutterhead wear and breakage [Hamilton, 2020]. The team also reported increased stability and productivity due to the system's ability to collect data every three seconds and provide corrective feedback to the TBM⁵ [Berhad, 2020]. Adjusting advance speed and screw conveyor to maintain pressure at the face, the system calculates optimal slurry pump speed, selecting the best driving methods based on real-time ground conditions [Hamilton, 2020]. This A-TBM automatically adjusts to upcoming conditions based on real-time data generated during excavation (see Figure 6-4).[Berhad, 2020, Byrd, 2016, Hamilton, 2020].



Figure 6-4: MMC Gamuda's A-TBM on the site of the Klang Valley Mass Rapid Transit (KVMRT), using Herrenknecht hardware [Construction, 2021]).

One of the biggest players in the manufacturing of TBMs, Herrenknecht, is a German company that has been building tunnel boring machines for over 40 years [Schulter and Wagner, 2020]. Currently developing prototypes for an autonomous

⁵Meaning it effectively takes control of machine parameters, changing advance speed, torque cutting wheel speed and others to autonomously steer the machine through changing ground conditions [Hamilton, 2020].

TBM system, Herrenknecht intends to use lasers, hi-def cameras, and sensors to navigate through tunnels [Herrenknecht, 2022]. Having reported completion of successful pilot tests of their autonomous TBM technology [Herrenknecht, 2022].

Another major player is Robbins. A US-based company that has been an important player in the industry since the 1950s, it is currently working on an autonomous TBM system called Robbins i-Bore [Hamilton, 2020]. Their proprietary system, similar to Herrenknecht, uses laser guidance and mechanized drilling to bore tunnels [Knights, 2017]. The company has said to have completed successful tests of their technology in a couple projects around the world [Knights, 2017]. Below is an image of TBM manufactured by Robbins (Figure 6-5).



Figure 6-5: Example of a Robbins TBM [Robbins, 2021]).

China Railway Engineering Equipment Group Co. Ltd (CREG) is also a significant player in the TBM industry [Gao, 2018]. They have been developing their autonomous TBM technology since 2017 and have since completed pilot tests in China [Chan, 2022]. The CREG autonomous TBM system uses 3D scanning and laser-guided navigation to excavate tunnels [Thomas, 2021]. A depiction of the expected autonomous TBM system is presented (see Figure 6-6).

These are the current main players in the automation of TBMs. As the technology

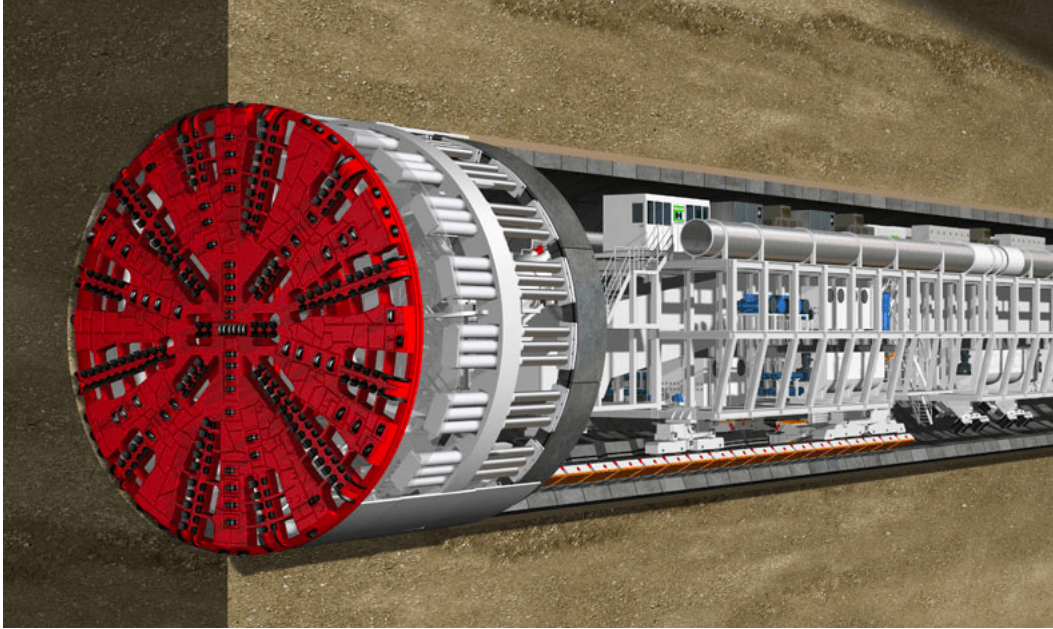


Figure 6-6: Virtual depiction of the CREG's autonomous tunnel boring machine [Chan, 2022]).

continues to develop, it is likely that competitors will enter the market and competition will increase, ultimately leading to more efficient and cost-effective tunneling solutions.

6.4.4 Market Macro-Trends

The TBM market is greatly affected by macro-level changes and trends, which can affect its growth prospects in the present and future. These trends include various factors such as technological advancements, economic shifts, policy changes, and societal preferences. The following list will take a closer look at a couple of these:

1. **Infrastructure Investment:** One of the primary drivers is the increasing demand for infrastructure development around the world. Governments, especially in the Global South and the US, are heavily invested in large-scale transport infrastructure projects ranging from tunnels, to highways, and railways.
2. **Urbanization:** With the world's population expected to be 70% urban by 2050, growing demand for transportation infrastructure, including underground tunnels is apparent. Fast urbanization is greatly influencing demand for TBM

machines in urban areas, where construction space is extremely limited.

3. **Technological Advancements:** Construction is just starting to feel the disruption brought on by increased automation and data-driven decision-making. One of the beachhead markets for these technological advances are TBMs, which are being greatly changed by improvements in machine learning, artificial intelligence, and automation. These technologies are seeking to enable more efficient TBM operation, reduce project timelines, and minimize costs.
4. **Environmental Sustainability, ESG:** The demand for better environmental, social and governance standards in industries worldwide has also been pressuring infrastructure development to be more sustainable. Governments and construction companies are increasingly focusing on minimizing their socio-environmental impact, including in tunneling. Autonomous TBMs can increase safety for operators and existing infrastructure, and productivity, which translates into direct reduction of ESG impacts.
5. **Growing Demand for High-Speed Rail:** The growing demand for high-speed rail networks is also a main driver of growth in the TBM market. High-speed rail networks require extensive underground tunneling, and TBM machines are the preferred method for excavation.
6. **Industry Consolidation:** The TBM market is becoming increasingly consolidated, with a small number of players dominating the industry. Mainly driven by high capital costs, this trend will also be important in shaping the industry's adaptation to automation technology.

Overall, the presented trends are shaping the future of tunneling automation efforts. With increasing investments in infrastructure, and transportation systems for cities, as well as growing demand for high-speed rail networks, tunneling is expected to be an important construction activity driving market growth.

6.4.5 Challenges to Implementation

Having the potential to bring significant progress in the tunneling and construction industries, the implementation of autonomous tunnel boring machines poses significant challenges that need to be considered and addressed. In order to fully realize the potential benefits of autonomous tunnel boring machines, it is essential to understand these difficulties, and develop effective strategies to overcome them. Some of these include:

1. **Cost:** The upfront cost of purchasing and implementing autonomous tunnel boring machine technology is significantly higher than traditional TBMs, as there is a need for specialized operators, control centers and IP/proprietary technology, making it difficult for many companies to justify the investment [Hamilton, 2020, Robbins, 2021]
2. **Infrastructure:** Autonomous TBMs require a robust set of sensors, communication networks, and control systems. The building and maintaining of such infrastructure can be highly costly and time-consuming [Melenbrink et al., 2020].
3. **Technical complexity:** The technology used is complex and requires skilled personnel to operate and maintain it [Anderson et al., 2020]. As AI/ML is an extremely relevant topic in several industries, skilled professionals are scarce [Anderson et al., 2020]. Hindering companies that lack the technical expertise needed to implement and operate such technology [Peres et al., 2020].
4. **Safety:** Safety is a major concern when it comes to autonomous tunnel boring machines. Although showing promising results, the use of autonomous technology in such a high-risk environment requires careful planning and execution [You et al., 2023]. The top priority must be ensuring the safety of both workers and the general public [Berhad, 2019].
5. **Regulation:** There are currently no global standards or regulations governing the use of autonomous TBMs [Huang et al., 2021]. Which can lead to un-

certainty, regulatory push-back, and legal challenges for companies looking to implement the technology.

Despite potential resistance from industry stakeholders, including concerns over safety, reliability, and job displacement, the possible benefits of autonomous tunnel boring machines, including increased productivity, improved accuracy, and reduced operating costs, significantly outweigh the technology's risks and shortcomings. However, the high upfront costs of implementing autonomous TBMs, as well as the need for specialized training for operators and control centers, can make it difficult for many companies to justify the investment. Additionally, some stakeholders in the industry may be hesitant to adopt new technology due to a lack of understanding or familiarity with it.

Despite these challenges, many companies are continuing to heavily invest in research and development in the field of autonomous TBMs, recognizing the potential for significant long-term benefits. As the technology matures and becomes more widely adopted, it is likely that many of these challenges will be overcome through improved safety standards, increased efficiency, and the development of new training and certification programs for operators.

6.5 Technical Requirements

6.5.1 Hardware and Software Requirements

In order to implement AI/ML models for geology prediction in tunneling, several hardware and software specifications are required. They must be thoroughly evaluated and analyzed in order to determine the scalability and feasibility of the technology.

In terms of hardware demands, to deploy autonomous tunnel boring machines, comprehensive central monitoring systems and stations, which include powerful computing systems and servers that can handle large data-sets and process complex algorithms in real-time, are required. There should be sufficient memory and processing capacity to manage high-performance computing, as well as robust communications

systems that created the link between construction sites and command centers. Additionally, for scalability, each particular business must evaluate its specific requirements in terms of computational infrastructure and communications system.

In turn, software requirements include the advanced machine learning algorithms tools for data processing and pre-processing, as well as for visualization, and analysis. Software components should be equipped to treat large and complex data-sets, including vast amounts of live data being fed into automation systems from the TBM, and should thus be capable of processing and analyzing this data in real-time.

The chosen AI/ML models must be able to analyze and interpret geological data, integrating both previously obtained data like rock types, mineralogy, and other geological characteristics, and real-time TBM-data output, comprehensively predicting conditions ahead of the tunnel face and adjusting the machine's parameters to support them. The algorithm should be capable of detecting anomalies and identifying patterns in the data, which can be used to predict ground conditions and identify potential hazards.

As there are very few examples of this, or similar predictive technologies being applied to TBM-based tunneling projects, it is difficult to precisely determine technical requirements. An interesting application of this technology is the case of MMC Gamuda, where the basic setup was the deployment in two command centers, a smaller, local control at the construction site and a more comprehensive central command unit, where the data processed and transmitted to the machine. Figure 6-7 shows the basic setup of MMC's A-TBM system, as applied in the Klang Valley Mass Rapid Transit (KVMRT) project.

Furthermore, the computational model should be able to handle diverse data-sets, including 3D data, seismic data, and other geophysical data, which can be applied to refine existing geological/geotechnical information. It should then be capable to process these robust data-sets in real-time, informing operators and other stakeholders as well as modifying TBM parameters.

Another crucial demand is the AI/ML model being able to learn from new data and adapt itself based on novel information, aiding in the refinement and increased ac-

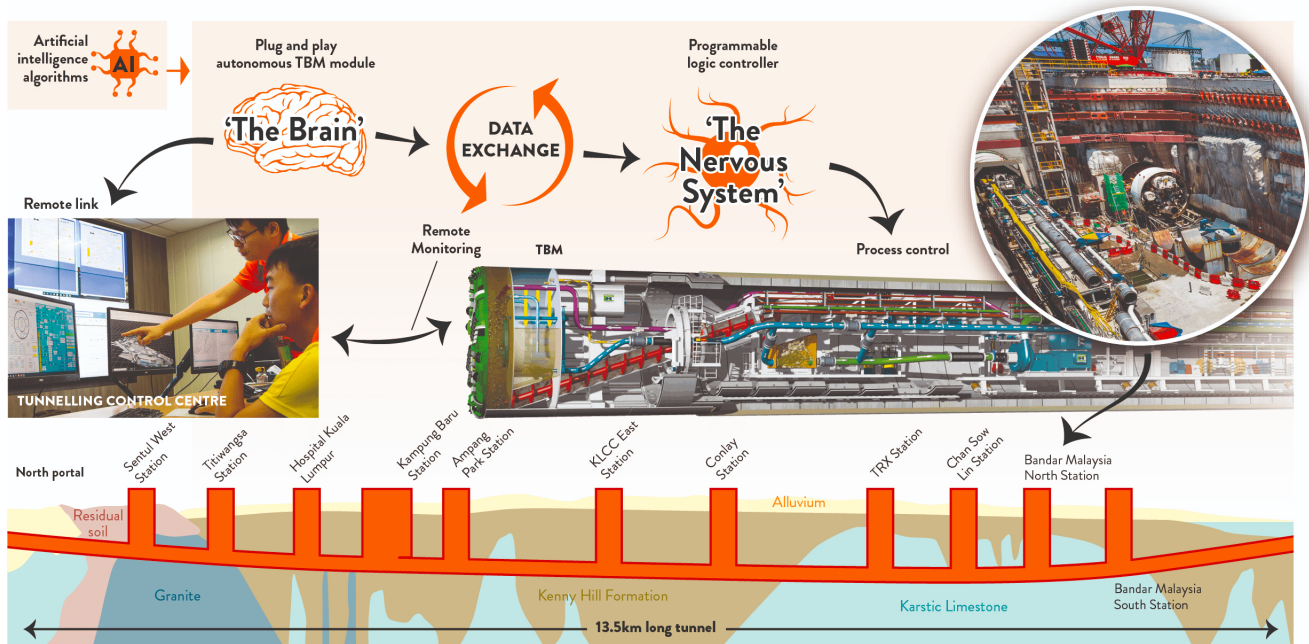


Figure 6-7: MMC Gamuda’s analytics dashboard for its proprietary A-TBM system [Byrd, 2016]).

curacy. The technical requirements for utilizing AI/ML models for geology prediction in tunnels should have the following main characteristics:

1. **Data Collection and Preprocessing:** Collection of relevant data related to geology, such as borehole logs, maps, and geological surveys. Data pre-processing should be done in order to adequately train the chosen AI/ML model, usually data is cleaned, organized and normalized (removing most inconsistencies).
2. **Feature Engineering:** selection of relevant features (or parameters) from the pre-processed data that are most informative in predicting ground conditions ahead of the tunnel face. Can include geophysical data, known geological structures, mineralogical data, and ground resistance parameters.
3. **ML Model Selection:** Some of the commonly used ML models for geology prediction are decision trees, support vector machines, random forests, and neural networks. The ML model should be optimized for accuracy, and scalability.
4. **Hardware Requirements:** Will depend on the size of the data-set and the

complexity of the ML model. Overall, requires high-performance computing systems with specialized hardware such as GPUs ⁶ and TPUs ⁷, commonly used for training large-scale ML models.

5. **Software Requirements:** Can vary widely through each company and use case but would typically include the programming language used for implementing the algorithms, such as Python, R, or Matlab (using libraries such as Scikit-Learn, TensorFlow, and PyTorch).

6.5.2 Feasibility and Scalability

The use of autonomous Tunnel Boring Machine systems has been gaining traction in recent years due to their ability to improve safety, accuracy, and productivity. However, the success of these systems depends on their capability to handle robust and complex data-sets accurately. The models' interpretation and analysis of these data-sets are essential for monitoring and modifying TBM parameters while tunneling.

The feasibility of using AI/ML models for geology prediction in tunnels is strictly dependent on data availability, the geological complexity of the project location, and the availability of computational resources required for training the ML model. The success of AI/ML models in accurately predicting ground conditions ahead of the tunnel face is directly related to the quality and quantity of data available for training. Additionally, the algorithm must be complex enough to identify and interpret intricate geological structures but not too convoluted or highly specialized that it becomes impractical to use.

There is no one-size-fits-all solution when it comes to autonomous TBM systems. It is likely that models will be updated or developed on a case-by-case basis, through

⁶Graphics Processing Unit. Electronic circuitry specifically designed to modify a computer's memory, speeding image generation processes to be outputted to a display device [Foley et al., 1996]. These types of circuits are utilized improve the machine's graphical performance [Foley et al., 1996].

⁷Tensor Processing Unit. Application-specific integrated circuit (ASIC) developed by Google for improving machine learning algorithms based on neural networks using their proprietary TensorFlow software [Google, 2023]. In contrast to GPUs, TPUs are engineered for low-precision computation at higher input/output rates [Armasu, 2016]. TPUs have been designed to optimize neural network operations, providing high efficiency and cost-effectiveness for machine learning tasks [Wang et al., 2019].

a plug-and-play system similar to what MMC Gamuda has presented. This means that the success of AI/ML models in tunneling is essentially dependent on market interest and consequent investment, as well as the proof of concept that these models can significantly improve safety and productivity.

The availability of computational resources is crucial for the scalability of autonomous TBM systems. The infrastructure required to support the system must be able to handle the increasing computational demands as the data-sets and model complexity grow. As technology continues to advance and more data become available, the feasibility and scalability of these systems will continue to improve. Furthermore, as more infrastructure projects adopt these systems, market competition will drive further investment and development of the technology.

Autonomous systems have the potential to significantly improve the efficiency, safety, and precision of infrastructure projects, potentially revolutionizing the way they are carried out. However, successful implementation of these systems requires careful consideration of their feasibility, scalability, and adaptability to ensure that they can be effectively integrated into existing processes and technologies.

6.6 Cost Estimates

To appraise the costs related to applying AI/ML to TBM operations, several factors should be considered out of which the most important will be highlighted below:

1. **Research and Development (R&D):** Developing a comprehensive TBM automation system based on AI/ML models would require significant research and development efforts, from specialized machine learning engineers and data scientists to operators and controllers. Systematic elaboration of data processing, algorithm development and model training must be established, as well as control station planning⁸. The overall cost of these efforts would depend on the scope of the project and the level of complexity involved.

⁸Refers to the process of designing and organizing the control station for an autonomous system.

2. **Hardware and software costs:** Autonomous tunnel boring machine operations require the use specialized hardware and software, such as sensors, processors, and data storage/processing systems (servers, GPUs and TPUs). The cost of these components directly depend on the level of automation and system complexity. Costs include the purchase or leasing of hardware and software components, as well as continuous maintenance and upgrades.
3. **Operating costs:** Ongoing operating costs associated with running and maintaining the system are expected. This includes spending associated with energy consumption, data storage, and system monitoring.
4. **Training and support costs:** To ensure the automation system is being effectively operated, it will be necessary to provide training to TBM operators and other personnel. Incurring in costs associated with hiring trainers or consultants, developing educational material, and conducting training sessions. Ongoing support and learning is also necessary to address arising technical issues.

With regard to these considerations, the cost of implementing an AI/ML system for TBM operations could range widely, depending on the level of automation and complexity involved, project location, contractors⁹, amongst several other factors. However, it is important to mention the potential benefits of such a system (further discussed in section 6.7), which includes improved safety and construction efficiency, that can significantly outweigh costs over time. The table below (Table 6.2) presents approximate cost estimates for the mapped cost categories explored above.

The cost of implementing an AI/ML system for TBM automation can vary widely, from several hundred thousand to several million dollars, depending on the scope, location, complexity and implementation of the project. Potential benefits, which will be discussed in the following section (6.7), may greatly justify the investment for both TBM manufacturers and contractor construction companies in the long run.

⁹Companies or organizations that are responsible for carrying out tunnel boring machine (TBM) operations. Ranging from construction companies, engineering firms, to other specialized project managers who are hired to oversee TBM operations.

Table 6.2: Cost estimation for the implementation components of the use autonomous tunnel boring machine systems, interpreted from the following sources [Janbaz, 2017, Ferrein et al., 2012, Berhad, 2019].

Component	Estimated costs (USD)
Research & Development (R&D)	\$50,000 - \$500,000
Hardware & Software	\$100,000 - \$1,000,000
Operating costs	\$10,000 - \$100,000
Training & Support	\$10,000 - \$100,000

6.7 Benefit Analysis

6.7.1 Potential Improvements

The proposed technology has the potential to bring numerous advancements to the tunneling industry, especially in furthering the automation of tunnel boring machine (TBM) operations. One of these significant improvements is increased efficiency. As the automation of TBM operations has been shown to reduce construction time required to complete a tunneling project (MMC Gamuda reported significant differences between operations of its 10 A-TBMs when compared to conventional counterparts).

By utilizing AI/ML to analyze geology data in real-time and control adjustments to TBM parameters, tunneling can become a more streamlined process. Automation has the potential to address one of the biggest time consuming processes in mechanized tunneling, which are stoppages made for the installation of precast concrete segments, or rings, that are placed every 1.0 - 1.5 meters, greatly improving efficiency and reducing construction time.

Another potential benefit of TBM automation lies in the increased accuracy of geology prediction ahead of the tunnel face, which can significantly reduce the risk of accidents and increase both worksite and overall project safety. Using these computational models to identify potential hazards ahead of the tunnel face will assist project managers in applying necessary countermeasures in a timely manner, thus

reducing the accident risks and worksite injuries. Bettering understanding ground conditions ahead of the construction can also lead to cost savings by reducing the need for manual inspections and investigations.

Improving data analytics can guide important decision-making processes on the excavation process, allowing algorithms to fully control and operate the TBM, adjusting machine parameters live, resulting in a more accurate and efficient excavation process [Byrd, 2016]. For instance, MMC Gamuda's A-TBM system utilizes its custom, proprietary software that fully takes control from the TBM operator and acts as the machine's controller, adapting to various ground conditions with minimal human input [Byrd, 2016].

The system translates data-driven insights into control over steering, machine advance speed, penetration, and muck removal rates, resulting in significantly quicker response times, enhancing accuracy and productivity. With the current A-TBM system, human intervention has been reduced to in less than 1% of the time [Byrd, 2016]. The contractor's experience with its 10 A-TBMs functioning at full capacity in the Klang Valley Transit System project has shown the efficiency and functionality of the technology, being able to reduce construction time by 20-30% [Byrd, 2016].

As the technology went from prototype to being applied in all of this decade-long project's building fronts, stakeholders have noticed the significant improvements in productivity and safety [Byrd, 2016]. According to project engineers responsible for the deployment of the A-TBM, other stakeholders did not have much faith in the success of the technology, which quickly changed as A-TBMs consistently outperformed traditional counterparts [Byrd, 2016].

6.7.2 Return on Investment (ROI)

To estimate the potential return on investment (ROI) of TBM automation, associated costs, maintenance, and support implications must be taken into account, along with the potential benefits of increased efficiency, improved accuracy, and enhanced worksite safety [?].

The benefits of TBM automation include reduced execution timelines, increased

productivity, improved accuracy and safety, and cost and material savings, leading to increased profitability for construction companies [?]. However, estimating the ROI of TBM automation depends on various factors, such as the size of the project, the current level of automation, specific technology used, and the cost of labor and materials. As a result, providing a specific ROI estimate is difficult as it strictly depends on a case-by-case basis. Nonetheless, the potential benefits of this technology suggest it is a worthwhile investment for players in the tunneling industry.

In terms of estimating a range for ROI, studies by the International Tunnelling and Underground Space Association (ITA) found that the tunneling automation can result in cost savings of up to 50% compared to traditional drilling/blasting [International Tunnelling and Underground Space Association, 2008]. Another study, by the University of Cambridge found that the use of AI in TBM operations can reduce the time and cost of tunnel construction by up to 10% [Mair et al., 2007].

Based on these studies, it is reasonable to assume that the application of TBM automation technology could result in significant cost savings for tunneling projects. The exact ROI would depend on the specific project and technology used, but the potential benefits in terms of increased efficiency, accuracy, and safety could outweigh the initial investment costs.

6.8 Associated Risks

Some of the major risks associated with using AI/ML technology for tunneling automation are as follows:

1. **Data quality and availability:** Limited or low-quality data will lead to inaccurate predictions, which could result in accidents or costly mistakes.
2. **Cybersecurity threats:** Automation and allowing the TBM to be fully operated by AI/ML technology has the potential to increase the risk of cybersecurity threats.

3. **Regulatory compliance:** Compliance with current and upcoming regulation, especially on automation efforts and the use of AI/ML, need to be observed.
4. **Technical failures:** Potential hardware and software malfunctioning, which can lead to accidents, delays and increased costs.
5. **Skilled workforce:** Limited availability of skilled engineers and operators.
6. **Resistance to change:** Tunnel companies and other stakeholders are expected to demonstrate initial resistances to the adoption of autonomous tunnel boring machine systems.

6.8.1 Data

The accuracy and reliability of AI/ML models for tunneling automation are highly dependent on the quality and completeness of the data used to train and operate models. The use of inaccurate or low-quality data can lead to incorrect predictions and recommendations, potentially resulting in TBM malfunction or incorrect operation.

If the data used to train an AI/ML model are biased towards a certain type of rock or ground class, the model may become biased and unable to accurately predict the behavior of the TBM in other conditions, or react to them in real-time. In such cases, the TBM may not operate optimally, leading to increased operational costs, and longer construction times.

Additionally, if the data used to train a model are insufficient or outdated, the model may not be able to make accurate predictions using real-time tunneling operational data. In such cases, the AI/ML model may fail to recognize and account for factors that can affect TBM performance, such as changes in ground conditions, shifts in tunnel alignment, and varying excavation parameters. As a result, the TBM may not operate efficiently, leading to increased construction costs, delays, and potential safety risks.

Acosta (2019), has correctly noted that a significant hurdle to furthering the development of autonomous tunnel boring machines is the lack of data unity [Acosta, 2021].

Currently, data is outputted in a diversity of formats and files, which if united under a master file formatting, would be greatly beneficial for analytics. Amassing this structured telemetry data-set into particular files, would greatly advance computer processing time, thus making real-time applications of AI/ML models highly efficient.

The use of Building Information Modeling (BIM), ever more present within civil construction, can greatly further improvements in infrastructure development, and should thus be considered as a simpler next step in improving tunneling construction. BIM executes a digital representation of a project, integrating all relevant data into a single platform, that can be visualized and manipulated by designers, engineers and other project stakeholders. By adopting BIM more widely, tunneling operations can become more efficient and accurate, as it allows for real-time collaboration, leading to a reduction in errors and delays. BIM can also be used to simulate various scenarios, making it easier to identify potential risks and optimize construction.

6.8.2 Cybersecurity Threats

As with any technology that relies on data, there is a risk of cybersecurity threats such as hacking, data breaches, or malicious attacks. In the particular case of autonomous TBMs, as this involves the use of sensitive data related to tunnel construction and the operation of the tunnel boring machine, cybersecurity is probably the biggest concern.

The increased dependence on the internet of things (IoT) in tunneling operations, especially for TBM automation, creates considerable risks. Hackers, malware and other malicious agents can exploit vulnerabilities in software systems used, gaining access to critical information and potentially machine control.

Cybersecurity risks include unauthorized access to sensitive data, such as geotechnical information or confidential project details, as well as tampering with the operation of the TBM or other equipment. A successful cyberattack could disrupt the entire construction site, causing delays, accidents and other safety risks, and financial losses. It is essential to have robust cybersecurity protocols in place to mitigate these risks, including firewalls, comprehensive data encryption, and secure communication

channels. Regular security assessments and updates are also necessary to identify and diminish any potential vulnerabilities in the system.

6.8.3 Regulation

Tunnelling operations is subject to significant regulation. As increased automation and the use of AI/ML technology becomes more widespread, governments around the world are updating and creating new regulation to address potential risks. For infrastructure work, regulation widely varies based on the country where the project will be implemented. Private companies will need to comply with governmental regulation, ensuring that their use of the automation technology complies with these regulations and standards, increasing costs and the complexity of the project.

Risks to the potential for non-compliance with regulations, standards, and laws governing tunneling operations are extremely serious and can even lead to the embargo of the construction. The use of AI/ML technology for TBMs, although currently unregulated, may become subject to regulations related to safety, environmental impact, and worker protection.

For instance, in the United States, the Occupational Safety and Health Administration (OSHA) sets clear standards for the construction industry, including regulations related to tunneling operations. Incoming automation technology used in tunneling must comply with these standards as well as updated ones, promoting the safety of workers and the general public.

As AI/ML continue to advance adoption in a range of industries, concerns about data privacy and protection have been at the forefront of regulation discussions in governments worldwide. The European Union (EU) has been at the forefront of this regulatory crackdown, launching the General Data Protection Regulation (GDPR), having worked mainly against data sharing amongst social media platforms. However, the use of AI/ML technology in tunneling may also be subject to regulation related to data privacy and security. Failure to comply with these regulations can result in significant fines and legal liabilities.

6.8.4 Technical Failure

AI/ML models can sometimes produce unexpected or inaccurate results, which could lead to equipment malfunctions and other considerable safety incidents. Tunnel Boring Machines (TBMs) are highly complex accounting for multiple subsystems that must work simultaneously to allow for adequate advancement. Introducing AI/ML technology, thus, adds considerable layers of complexity to the system, which increases the potential for technical failures.

If the sensors and TBM communication systems used to collect data fail, computational models do not receive accurate or timely information, leading to incorrect predictions and maneuvering. Moreover, the integration of AI/ML technology may require modifications to the TBM system, which can introduce new points of failure or increase existing vulnerabilities. Technical failure has the potential to cause significant delays and cost overruns, as well as considerably compromising worksite safety.

To mitigate technical failure risks, it is crucial to conduct rigorous prototype testing and validation of AI/ML models and the TBM subsystems before deploying them in the field. This includes extensive model testing under a range of operating conditions and scenarios, as well as identifying and addressing any potential failure points. Additionally, a comprehensive maintenance and repair plan should be in place to ensure the proper functioning of autonomous TBM systems over time. Regular monitoring and performance evaluations are also instrumental in identifying and addressing technical issues before they escalate.

6.8.5 Lack of Skilled Labor

In successfully implementing AI/ML technology for tunneling automation, skilled labor force is required. The availability of engineers and machine operators who understand both the technology and the tunneling process, is extremely limited, which may significantly increase costs and slow down comprehensive implementation.

The tunneling process requires a wide range of technical skills, from ground survey-

ing and geotechnical analysis to material science, structural engineering, and equipment maintenance. In order to successfully integrate AI/ML applications into this complex process, it is necessary to have a workforce that has both an understanding of tunneling at a high-level and the ability to work with this novel technology.

Seen in the industry long before the current shortage, several factors have historically contributed to the lack of skilled labor available in the tunneling industry. One of the most significant is the general worldwide decline in vocational education programs that train workers in skilled operational trades. As fewer workers enter the field, and seeing that those who do may not have the necessary skills to work with advanced technologies, a clear shortage is in effect. Another challenge is workforce aging, which is leading to a shortage of experienced workers in various fields, as older workers exit the market.

To address these challenges, it would be necessary for stakeholders, from governments to industry players, to invest in training and qualifying programs, as well as education initiatives that help workers acquire the necessary skills for understanding new technologies, especially when considering AI/ML applications for tunneling. Additionally, efforts to increase diversity and inclusion in the workforce, has the potential to bring in necessary new perspectives and skills to the industry. By addressing the shortage of skilled labor, the implementation of AI/ML technology in tunneling could be more successful and contribute to increased efficiency, safety, and cost savings.

6.8.6 Implementation Pushback

The application of AI/ML technology for TBM-tunneling automation will require significant modifications to the way work is done on-site. Thus, changes can be met with considerable resistance from workers (especially specialized machine operators) and other stakeholders. Major player companies must effectively communicate the benefits and improvements brought on by the technology, as well as address any concerns in order to successfully achieve comprehensive implementation.

Push-back is a common challenge when introducing new technologies, and the adoption of AI/ML for tunneling automation is no exception. Workers and other

stakeholders may resist changes in their workflow status-quo, commonly motivated by fear of obsolescence or concerns about their ability to adapt to new processes. Additionally, as seen in several other industries, workers may view the use of AI/ML technology as an existential threat to their expertise and skills.

To successfully implement the proposed technology, contractors and TBM manufacturers need to effectively inform on the benefits of the technique to machine operators, engineers, designers, and other stakeholders, and address any concerns that may arise. As previously mentioned, this may involve providing training and support to help employees adapt to new processes, ensuring that their expertise is still valued in the new system. Companies should also consider gradual implementation. A phased approach that allows workers to become comfortable with the technology and its benefits over time is preferred to a complete substitution of TBMs.

In addition to addressing worker concerns, private companies will also need to address concerns among other stakeholders, such as regulators and investors. Governments and their regulators may be hesitant to approve the use of AI/ML to automate TBMs without sufficient evidence of its safety and effectiveness. And investors may be hesitant to fund projects involving substantial changes in technology or processes. Companies may need to provide evidence of the benefits of AI/ML technology, such as improved safety and increased productivity, in order to address gain buy-in from stakeholders.

6.8.7 Considerations on Automation Technology

As argued by Erharter (2021), the use of AI in TBM automation holds promise for improving efficiency, accuracy, and safety, but there are still very significant challenges to overcome before these systems can be widely adopted [Erharter and Marcher, 2021].

One of the primary challenges is the need for large amounts of high-quality data to train the models. While it is relatively easy to collect data from sensors on the TBM, it can be challenging to obtain complementary geological data. Erharter suggests that more research is needed to develop better data collection and processing methods [Erharter and Marcher, 2021].

Another challenge is the complexity of the models needed to achieve consistent prediction accuracy. While machine learning algorithms have shown promise in other domains, such as image and speech recognition, they are not yet mature enough to reliably predict geological conditions in a tunnel [Erharter and Marcher, 2021]. More research is needed to develop improved AI models that can take into account the complex interplay between geological conditions and TBM performance [Erharter and Marcher, 2021].

While there is great potential for these systems to improve efficiency, accuracy, and safety in tunneling projects, the use of AI in TBM automation is still in its early stages. Erharter cautions that more research is needed to overcome challenges associated with these systems and to ensure that they are reliable and accurate enough for widespread adoption [Erharter and Marcher, 2021]. It is argued that there are significant changes that can promote improved efficiency and safety in tunneling without necessarily using AI/ML.

6.9 Conclusions and Recommendations

Tunneling is an essential and often complex process that requires meticulous planning, execution, and management. In seeking to achieve better efficiency and productivity, automating technologies for tunneling have been widely discussed within the industry, especially as AI/ML advances to more engineering applications. However, streamlining tunneling automation can be challenging, as it requires a systematic approach that focuses on identifying potential areas for intervention and improvement.

A critical component that can substantially advance tunneling automation is the development of "intelligent" and predictive analytics tools that can optimize the performance of Tunnel Boring Machines (TBMs). This can be achieved by gathering vast amounts of data from various sources, including geotechnical surveys, real-time monitoring, and machine sensors attached along the TBM. Machine learning algorithms can then be utilized to create models that can forecast ground conditions ahead of the TBM tunnel-face and, thus, recommend and even adjust the machine to optimal

operating parameters. Increased automation intends to enhance productivity, reduce machine downtime, and improve safety in construction sites.

After conducting the techno-economic assessment presented in this chapter, it is notable that the proposed technology is not the only approach being considered in the effort to improve tunneling operations. It is important to consider the technological feasibility of widespread adoption of autonomous TBMs, considering their safety, costs, risks and benefits.

The Techno-economic assessment (TEA) presented on the use of autonomous Tunnel Boring Machine technology in tunneling operations has shown that there is still significant work to be done in the field, in order to fully prove and adopt the technology. From what was presented, it can be concluded that autonomous TBMs are yet to be proven at scale, and the use of AI/ML in tunneling operations is still very much in its infancy.

However, the study also showed that the use of AI/ML in tunneling operations can lead to a significant increase in productivity, with an estimated 20-30% increase (based on the case study in Malaysia). This increase in productivity is promising and highlights the potential benefits of continuing to develop predictive technologies for TBM-control systems. It is important to note that this is not the only way to improve tunneling automation, and knowledge-sharing allied to further research are essential for these technologies to be streamlined to other real-world applications.

Overall, while the TEA has shown that there is still work to be done, it has also highlighted the potential benefits of using AI/ML in tunneling operations. With further research and development, there is an opportunity to significantly improve productivity, efficiency, and safety in tunneling operations.

It is important to closely evaluate interventions that explore the potential of robotics and automation for tasks that are traditionally performed by humans. For instance, robots can be used to lay concrete segments, install ventilation systems, and carry out inspections. They can also be used for tasks that require high levels of precision and accuracy, such as drilling and excavation. By automating these tasks, tunneling operations can become faster, more efficient, and less reliant on human

labor (which can lead to important considerations and trade-offs).

The use of Building Information Modeling (BIM) is becoming increasingly common in civil construction and can greatly improve infrastructure development, especially in tunneling construction. BIM creates a digital representation of a project that integrates all relevant data into a single platform, allowing for real-time collaboration and reducing errors and delays. BIM can also simulate various scenarios to identify potential risks and optimize construction. To further the development of autonomous tunnel boring machines, it is important to address the issue of data unity, as currently data is outputted in various formats and files. By consolidating this data into specific file formats, computer processing time can be greatly improved, leading to efficient applications of AI/ML models in real-time.

While these models can potentially improve safety and accuracy, other technologies may be more feasible and beneficial for increasing tunneling productivity. Several companies in the tunneling space are currently exploring ways to eliminate the need for TBM stoppages during the installation of precast concrete segments (rings). This stop-start process is the most time-consuming aspect of tunneling construction, and reducing or eliminating it could significantly improve productivity. While geology prediction is still important for ensuring safety, this alternative technology may be much more relevant when considering productivity in the short-term. Ultimately, a combination of both technologies may be necessary for further optimizing tunneling operations, but careful consideration should be given to the cost-effectiveness and practicality of each option.

Undoubtedly, geology prediction plays a vital role in preventing accidents and ensuring worker safety. While it may not necessarily increase tunneling productivity, in fact, the use of AI/ML for geology prediction in TBM may be deemed useless if the results obtained are simply delayed and slightly altered versions of the input data. While machine learning models trained on recorded TBM data can provide highly accurate forecasts of rock mass conditions ahead of the tunnel face, the lack of predictive value derived from these forecasts is a significant drawback.

As such, further research is needed in this particular field of TBM data analysis

to overcome the current deficits in data-driven forecasts ahead of the tunnel face. Ultimately, the use of AI/ML for geology prediction must be weighed against other potential improvements, such as reducing the stop-start nature of TBM-tunneling, in order to determine the most effective way to increase productivity while maintaining satisfactory levels of safety.

Finally, in hoping to advance the field of TBM automation it is crucial to promote collaboration and knowledge-sharing among companies and stakeholders. This can be achieved through partnerships (such as the example cited of the collaboration between MMC Gamuda and Herrenknecht), knowledge exchange programs, and training initiatives that bring together experts from different fields, including geology, engineering, and data science. By establishing the best practices and state of the art knowledge, the industry can identify new opportunities for innovation, improved work quality, and increase overall efficiency of the tunneling process.

Advancing tunneling automation requires a multifaceted approach that addresses various aspects of tunnel construction. By developing intelligent and predictive analytics tools, exploring the potential of robotics and automation, adopting BIM, and promoting collaboration and knowledge-sharing, stakeholders can achieve better efficiency, productivity, and safety in this key infrastructure sector.

This page intentionally left blank.

Chapter 7

Summary and Conclusions

Throughout history, tunnels have been a vital part of human civilization, from ancient irrigation tunnels to transportation and mining tunnels. The Industrial Revolution brought advancements in tunneling technology, including the rise of shield tunneling, which continued into the 20th century with the growing need for underground infrastructure for transportation. Today, tunnels play a critical role in supporting transit systems, energy production, water supply, sewage, and telecommunications networks in cities worldwide.

As research and technology advances to supply an increasingly urbanized world with infrastructure, Tunnel Boring Machines (TBMs) are being ever improved and automated to build longer, deeper and more complex tunnels. While also ensuring safety, cost-effectiveness and increased productivity. That is where Artificial Intelligence (AI) and Machine Learning (ML) algorithms come into play. With TBMs producing vast amounts of data in real-time throughout tunnel construction, efforts to use this abundant information to inform machine operators, designers, engineers and other stakeholders are under use.

Predicting ground conditions ahead of the tunnel face remains one of the biggest challenges in tunnelling. Designers, operators, and engineers often have only a rough idea of the geological profile and this uncertainty is heightened in urban areas where previous construction may have altered anticipated ground conditions. Consequently, there is a growing effort to utilize TBM-generated data for geological predictions in

TBM operations.

Tunnel boring machines (TBMs) progress incrementally, in line with the main jacks' advancement, which is typically connected to the installation of pre-fabricated concrete liner rings. It is therefore logical to try to assess and predict geologic conditions related to the sections defined by these rings, and the term "ring" was used throughout this thesis to refer to these sections.

The goal of this thesis was to assist in the making of geologic predictions ahead of the TBM tunnel face based on the machine's performance data. This was done in three main ways: through the use of time-series plots, the Confidence Learning (CL) model and the use of scattergrams.

The time-series plots displayed discernible patterns among the different ground classes (rock, soil, rock-like mixed, and soil-like mixed). Rock rings exhibited greater variability with more frequent fluctuations, resulting in plots typically characterized by short and compact "peaks" and "valleys". Moreover, the variability in rock appeared to be confined to smaller value ranges for the observed parameter comparisons. On the other hand, in soil rings, the data exhibited wider ranges and often showed positive correlations between parameters, with some parameter pairs completely coinciding. Rock-like mixed and soil-like mixed rings were more similar to soil rings than rock, with data-point concentration being less dense and occurring at wider ranges.

Scatterplots proved to be particularly effective in distinguishing the different ground classes (rock, soil, rock-like mixed and soil-like mixed). In rock, the graphs showed characteristic high-density areas where the observations were highly concentrated. In contrast, the data-points for soil rings were more spread out and had a wider range of observations, resulting in less concentration. The mixed rings tended to exhibit similar patterns to rock and soil respectively, with data-point concentrations being noticeable throughout the parameter comparisons but not as prominent as in rock rings.

The Confidence Learning (CL) model also proved to be a valuable tool for generating ground class labels for the tunnel rings. However, there were instances where the produced labels exhibited low confidence and some discrepancies, leading to the

misclassification of several rings. To address these issues, a comparison was made between the machine-generated labels and the geologic information presented in Chapter 3, as well as the scatterplots. The scattergrams were then utilized to verify machine-generated labels, allowing for any discrepancies or errors to be rectified. By cross-referencing the machine-generated labels with other sources of data, the accuracy of the classifications was significantly improved. This highlights the importance of utilizing multiple sources of information to verify the outputs of machine learning models and ensure the accuracy of the results.

All three approaches (time-series plots, scatterplots and CL) were deemed successful in identifying ground classes for rings based on TBM performance data. However, scattergrams were considered the most suitable approach for classifying the rings with the highest overall accuracy. If at all possible, combinations of AI/ML approaches are recommended.

It is clear from the work presented that although increased automation shows promise in reducing safety risks associated with tunnel construction, as well as boosting productivity and cost-effectiveness of these large infrastructure projects, much still needs to be done for fully automated Tunnel Boring Machines to be deployed ubiquitously. In the subset of the field of tunneling automation through the use of AI/ML applications for geologic/geotechnical predictions of ground conditions ahead of the tunnel face, better understanding and evaluating the applicability of these applications is necessary.

7.1 Future Research

While significant progress has been made in the use of artificial intelligence and machine learning algorithms in tunneling, further research is still very necessary to comprehensively apply these computational tools ubiquitously and safely. An area that demands further attention is, specifically, the implementation of AI/ML approaches. Both the use of more coherent parameter comparisons and the use of full data-sets is replacing the average values, currently used in models. To achieve this,

researchers should focus on developing more comprehensive algorithms that can work with larger data sets, incorporating more specialized variables or pairwise comparisons, that can potentially provide more accurate predictions.

The methodology proposed in this thesis aims to support researchers in enhancing existing models and developing new software for validating ground classification based on TBM-data. This can be achieved through joining an AI/ML algorithm to a closer examination of key parameter comparisons, informing on areas where the model outputs low-confidence classification labels. The resulting more robust model can help identify differences between chosen ground classes, leading to improved quality and reliability of computational models.

Lastly, any new developed model that proves to be comprehensive and robust for geology prediction in tunneling, should be extensively applied to real-world projects and not just data-sets stemming from completed work. This is instrumental in proving the validity of using AI/ML for geology prediction and the furthering of automation efforts in tunnel construction. The technology shows great promise in improving the quality, safety, and productivity of tunnel boring machine (TBM) operations. To reach its full potential, the field requires intense collaboration between researchers, engineers, construction companies, and other important stakeholders, to ensure the technology is effectively integrated into the construction process.

Bibliography

- [Acosta, 2021] Acosta, C. (2021). Unifying tunnel boring machines data. *Medium*.
- [Akinosho et al., 2020] Akinosho, T. D., Oyedele, L. O., Bilal, M., Ajayi, A. O., Delgado, M. D., Akinade, O. O., and Ahmed, A. A. (2020). Deep learning in the construction industry: A review of present status and future innovations. *Journal of Building Engineering*, 32:101827.
- [Allied Market Research, 2022] Allied Market Research (2022). Mining drills and breakers market to generate \$20.67 bn, globally, by 2030 at 4.1% cagr: Allied market research.
- [Alzubi et al., 2018] Alzubi, J., Nayyar, A., and Kumar, A. (2018). Machine learning from theory to algorithms: an overview. In *Journal of physics: conference series*, volume 1142, page 012012. IOP Publishing.
- [Amato et al., 2000] Amato, L., Evangelista, A., Nicotera, M., and Viggiani, C. (2000). The crypta neapolitana; a roman tunnel of the early imperial age. In *More than two thousand years in the history of Architecture. UNESCO-ICOMOS International Congress*.
- [Andersen, 1991] Andersen, E. S. (1991). Techno-economic paradigms as typical interfaces between producers and users. *Journal of Evolutionary Economics*, 1(2):119–144.
- [Anderson et al., 2020] Anderson, J., Viry, P., and Wolff, G. B. (2020). Europe has an artificial-intelligence skills shortage. *Bruegel-Blogs*.

- [Araújo et al., 2013] Araújo, A., Gomes, A. A., and Soares, L. (2013). Visita de estudo ao litoral de vila nova de gaia. In *VI Congresso Ibérico de Didática da Geografia*.
- [Araújo, 1984] Araújo, M. d. A. (1984). A formação areno-pelítica de cobertura: alguns resultados dum estudo preliminar. *Biblos: revista da Faculdade de Letras*, vol. 40 (1984), p. 71-89.
- [Araújo, 2004] Araújo, M. d. A. (2004). O final do cenozóico na plataforma litoral da região do porto.
- [Araújo, 2014] Araújo, M. d. A. (2014). A plataforma litoral da região do porto: Dados adquiridos e perplexidades. *Estudos do quaternário: revista da Associação Portuguesa para o Estudo do Quaternário*, 1997, n. ^o 1 (1997), p. 3-12.
- [Archives Photographiques, 1906] Archives Photographiques (1906). Paris metro construction. https://en.m.wikipedia.org/wiki/File:Paris_Metro_construction_03300288-3.jpg.
- [Armasu, 2016] Armasu, L. (2016). Google’s big chip unveil for machine learning: Tensor processing unit with 10x better efficiency (updated).
- [Arquivo Municipal do Porto, 2022] Arquivo Municipal do Porto (2022). Oporto.
- [Avtar et al., 2019] Avtar, R., Tripathi, S., Aggarwal, A. K., and Kumar, P. (2019). Population–urbanization–energy nexus: a review. *Resources*, 8(3):136.
- [Balasubramanian, 2014] Balasubramanian, A. (2014). Tunnels-types and importance. Technical report, Technical report.
- [Bardhan et al., 2021] Bardhan, A., Kardani, N., GuhaRay, A., Burman, A., Samui, P., and Zhang, Y. (2021). Hybrid ensemble soft computing approach for predicting penetration rate of tunnel boring machine in a rock environment. *Journal of Rock Mechanics and Geotechnical Engineering*, 13(6):1398–1412.

- [Bastos et al., 2012] Bastos, L., Bio, A., Pinho, J., Granja, H., and da Silva, A. J. (2012). Dynamics of the douro estuary sand spit before and after breakwater construction. *Estuarine, Coastal and Shelf Science*, 109:53–69.
- [Beaver, 1972] Beaver, P. (1972). *A History of Tunnels*.
- [Benato and Oreste, 2015] Benato, A. and Oreste, P. (2015). Prediction of penetration per revolution in tbm tunneling as a function of intact rock and rock mass characteristics. *International Journal of Rock Mechanics and Mining Sciences*, 74.
- [Bennett et al., 1985] Bennett, R. D., Hignett, H. J., Johansson, S., Patrick, D. M., Taylor, P., Smith, H., and McAneny, C. C. (1985). State-of-the-art construction technology for deep tunnels and shafts in rock. Technical report, Army Engineer Waterways Experiment Station VICKSBURG United States.
- [Berhad, 2019] Berhad, G. (2019). Award-winning autonomous tbm operations. <https://gamuda-get.com/award-winning-autonomous-tbm-operations-2/>. Accessed: February 15, 2023.
- [Berhad, 2020] Berhad, G. (2020). Enabling technologies through our people. <https://gamuda.com.my/2020/11/enabling-technologies-through-our-people/blog/>. Accessed: 2023-03-14.
- [Bilgin, 2016] Bilgin, N. (2016). An appraisal of tbm performances in turkey in difficult ground conditions and some recommendations. *Tunnelling and Underground Space Technology*, 57:265–276.
- [Bobet et al., 2019] Bobet, A., Arson, C. F., Elsworth, D., Nelson, P., Tomac, I., and Modiriasari, A. (2019). The role of rock mechanics in the 21st century. *Geotechnical Fundamentals for Addressing New World Challenges*, pages 319–357.
- [Bombardier, 2003] Bombardier (2003). Flexity outlook.
- [Bombardier, 2012] Bombardier (2012). Flexity swift.

- [Bottou, 2010] Bottou, L. (2010). Large-scale machine learning with stochastic gradient descent. In *Proceedings of COMPSTAT'2010: 19th International Conference on Computational Statistics Paris France, August 22-27, 2010 Keynote, Invited and Contributed Papers*, pages 177–186. Springer.
- [Brierley, 1976] Brierley, G. S. (1976). Construction of the hoosac tunnel, 1855 to 1876. *Journal of the Boston Society of Civil Engineers*, 63(3).
- [Burns, 2022] Burns, A. (2022). Hoosac tunnel (massachusetts): Map, length, location, history.
- [Business Research Insights, 2021] Business Research Insights (2021). Tunnel and metro market. <https://www.businessresearchinsights.com/market-reports/tunnel-and-metro-market-100791>. Accessed: 2023-03-14.
- [Byrd, 2016] Byrd, T. (2016). Malaysia’s self driving tbms. <https://www.newcivilengineer.com/tech-excellence/tech-excellence/tunnelling-malaysias-self-driving-tbms-06-04-2016/>. Accessed: February 15, 2023.
- [Caricola et al., 2020] Caricola, I., Breglia, F., Larocca, F., Hamon, C., Lemorini, C., and Giligny, F. (2020). Prehistoric exploitation of minerals resources. experimentation and use-wear analysis of grooved stone tools from grotta della monaca (calabria, italy).
- [Carleo et al., 2019] Carleo, G., Cirac, I., Cranmer, K., Daudet, L., Schuld, M., Tishby, N., Vogt-Maranto, L., and Zdeborová, L. (2019). Machine learning and the physical sciences. *Reviews of Modern Physics*, 91(4):045002.
- [Castellani and Dragoni, 1997] Castellani, V. and Dragoni, W. (1997). Ancient tunnels: from roman outlets back to the early greek civilization. In *Proceedings of 12th International Conference of Speleology, La Chaux-de-Fonds, Switzerland*, pages 12–14.

- [Cedergren, 2013] Cedergren, A. (2013). Designing resilient infrastructure systems: a case study of decision-making challenges in railway tunnel projects. *Journal of Risk Research*, 16(5):563–582.
- [Central Intelligence Agency, 2022] Central Intelligence Agency (2022). Portugal.
- [Chan, 2022] Chan, D. (2022). China railway engineering equipment group co. ltd. *South China Morning Post*. Accessed: March 14, 2023.
- [Chapman et al., 2017] Chapman, D., Metje, N., and Stärk, A. (2017). *Introduction to tunnel construction*. Crc Press.
- [Chapman et al., 1992] Chapman, P., Wrightam, V., Ince, G., and Lewis, R. (1992). Machine-driven tunnels. In *Proceedings of the Institution of Civil Engineers-Civil Engineering*, volume 92, pages 55–86. Thomas Telford-ICE Virtual Library.
- [Chappell and Parkin, 2004] Chappell, M. and Parkin, D. (2004). Tunnel construction. In *Sewers*, pages 150–192. Elsevier.
- [Chen et al., 2018] Chen, Q., de Soto, B. G., and Adey, B. T. (2018). Construction automation: Research areas, industry concerns and suggestions for advancement. *Automation in construction*, 94:22–38.
- [Chester et al., 2019] Chester, M. V., Markolf, S., and Allenby, B. (2019). Infrastructure and the environment in the anthropocene. *Journal of Industrial Ecology*, 23(5):1006–1015.
- [Christensen et al., 2005] Christensen, P., Dysert, L. R., Bates, J., Burton, D., Creese, R., Hollmann, J., et al. (2005). Cost estimate classification system-as applied in engineering, procurement, and construction for the process industries. *AACE International Recommended Practices*, pages 1–30.
- [Cigla et al., 2001] Cigla, M., Yagiz, S., and Ozdemir, L. (2001). Application of tunnel boring machines in underground mine development. In *17th international mining congress and exhibition of Turkey*, pages 155–164.

- [Construction, 2021] Construction, S. A. (2021). Expanding horizons. <https://www.tradelinkmedia.biz/publications/7/news/1872>. Accessed: 2023-03-14.
- [Cottet Dumoulin and Schueler, 2020] Cottet Dumoulin, E. and Schueler, J. (2020). Construction of the first railway routes through the alps (1848-1882).
- [Crighton et al., 1992] Crighton, G., Biggart, A., and Norie, E. (1992). Tunnel design and construction. In *Proceedings of the Institution of Civil Engineers-Civil Engineering*, volume 92, pages 18–42. Thomas Telford-ICE Virtual Library.
- [Cuny University, 2021] Cuny University (2021). Nycdata: Infrastructure.
- [Curley et al., 2011] Curley, R. et al. (2011). *The complete history of railroads: trade, transport, and expansion*. Britannica Educational Publishing.
- [Dal Piaz and Argentieri, 2021] Dal Piaz, G. V. and Argentieri, A. (2021). 150 years of plans, geological survey and drilling for the fréjus to mont blanc tunnels across the alpine chain: an historical review. *Italian Journal of Geosciences*, 140(2):169–204.
- [Dasgupta and Nath, 2016] Dasgupta, A. and Nath, A. (2016). Classification of machine learning algorithms. *International Journal of Innovative Research in Advanced Engineering (IJIRAE)*, 3(3):6–11.
- [Data Bridge Market Research, 2021] Data Bridge Market Research (2021). Global tunnel boring machine market. <https://www.databridgemarketresearch.com/reports/global-tunnel-boring-machine-market>. Accessed: 2023-03-14.
- [De Feo et al., 2014] De Feo, G., Antoniou, G., Fardin, H. F., El-Gohary, F., Zheng, X. Y., Reklaityte, I., Butler, D., Yannopoulos, S., and Angelakis, A. N. (2014). The historical development of sewers worldwide. *Sustainability*, 6(6):3936–3974.
- [Diamond and Kassel, 2018] Diamond, R. and Kassel, B. (2018). A history of the urban underground tunnel (4000 b.c.e. - 1900 c.e.). *Journal of Transportation Technologies*, 08:11–43.

- [Dias, 1993] Dias, J. A. (1993). Causas da erosão costeira. *Estudo de Avaliação da Situação Ambiental e Proposta de Medidas de Salvaguarda para a Faixa Costeira Portuguesa (Geologia Costeira)*, pages 13–38.
- [Dias et al., 2000] Dias, J. M. A., Boski, T., Rodrigues, A., and Magalhães, F. (2000). Coast line evolution in portugal since the last glacial maximum until present—a synthesis. *Marine Geology*, 170(1-2):177–186.
- [Dias, 2013] Dias, R. (2013). *Geologia de Portugal, vol I. Geologia Pré-mesozóica de Portugal*. Escolar Editora.
- [Dias and Ribeiro, 1995] Dias, R. and Ribeiro, A. (1995). The ibero-armoric arc: a collision effect against an irregular continent? *Tectonophysics*, 246(1-3):113–128.
- [Dias R., 2013] Dias R., A. A. (2013). *Geologia de Portugal, vol II, Geologia Mesoceno-zóica de Portugal*. Escolar Editora.
- [Digital Journal, 2019] Digital Journal (2019). Detailed report on tunnel construction market size 2023 - 2029 with industry chain analysis, research by absolute reports. Accessed: 2023-03-14.
- [Disney, 2009] Disney, A. R. (2009). *A history of Portugal and the Portuguese empire: volume 1, Portugal: from beginnings to 1807*, volume 1. Cambridge University Press.
- [Dodgson et al., 2008] Dodgson, M., Gann, D. M., and Salter, A. (2008). *The management of technological innovation: strategy and practice*. Oxford University Press on Demand.
- [Eftekhari et al., 2010] Eftekhari, M., Baghbanan, A., and Bayati, M. (2010). Predicting penetration rate of a tunnel boring machine using artificial neural network. In *ISRM International Symposium-6th Asian Rock Mechanics Symposium*. OnePetro.

- [Entacher et al., 2012] Entacher, M., Winter, G., Bumberger, T., Godor, I., and Galler, R. (2012). Cutter force measurement on tunnel boring machines – system design. *Tunnelling and Underground Space Technology*, 31:97–106.
- [Erharter and Marcher, 2021] Erharter, G. H. and Marcher, T. (2021). On the pointlessness of machine learning based time delayed prediction of tbm operational data. *Automation in Construction*, 121:103443.
- [Eskesen et al., 2004] Eskesen, S. D., Tengborg, P., and Kampmann (2004). Guidelines for tunnelling risk management: international tunnelling association, working group no. 2. *Tunnelling and Underground Space Technology*, 19(3):217–237.
- [Farrokh and Rostami, 2008] Farrokh, E. and Rostami, J. (2008). Correlation of tunnel convergence with tbm operational parameters and chip size in the ghomroud tunnel, iran. *Tunnelling and Underground Space Technology*, 23(6):700–710.
- [Fein, 2012] Fein, M. R. (2012). Highway under the hudson: A history of the holland tunnel.
- [Feio and Daveau, 2004] Feio, M. and Daveau, S. (2004). O Relevo de Portugal. University of Coimbra.
- [Fernando, 2023] Fernando, J. (2023). Compound annual growth rate (cagr) formula and definition. *Investopedia*.
- [Ferrein et al., 2012] Ferrein, A., Kallweit, S., and Lautermann, M. (2012). Towards an autonomous pilot system for a tunnel boring machine. In *2012 5th Robotics and Mechatronics Conference of South Africa*, pages 1–6.
- [Ferreira, 2005] Ferreira, A. B. (2005). *Geografia de Portugal, vol I. O Ambiente Físico*. Círculo de Leitores.
- [Fickling, 2020] Fickling, D. (2020). Naval shipworms (teredo navalis).

- [Flyvbjerg, 2010] Flyvbjerg, B. (2010). Policy and planning for large-infrastructure projects: problems, causes, and curses. In *Dialogues in Urban and Regional Planning*, pages 243–268. Routledge.
- [Foley et al., 1996] Foley, J. D., Van, F. D., Van Dam, A., Feiner, S. K., and Hughes, J. F. (1996). *Computer graphics: principles and practice*, volume 12110. Addison-Wesley Professional.
- [Formiche, 2020] Formiche (2020). Highway a1: Excavation of the santa lucia tunnel with the largest tbm in europe has been completed.
- [Fu et al., 2022] Fu, X., Feng, L., and Zhang, L. (2022). Data-driven estimation of tbm performance in soft soils using density-based spatial clustering and random forest. *Applied Soft Computing*, 120:108686.
- [Fu et al., 2023] Fu, X., Wu, M., Tiong, R. L. K., and Zhang, L. (2023). Data-driven real-time advanced geological prediction in tunnel construction using a hybrid deep learning approach. *Automation in Construction*, 146:104672.
- [Gao et al., 2021] Gao, B., Wang, R., Lin, C., Guo, X., Liu, B., and Zhang, W. (2021). Tbm penetration rate prediction based on the long short-term memory neural network. *Underground Space*, 6(6):718–731.
- [Gao, 2018] Gao, J. (2018). Ceperc accelerator after cdr towards tdr: Status and international collaboration.
- [Garcia et al., 2021] Garcia, G. R., Michau, G., Einstein, H. H., and Fink, O. (2021). Decision support system for an intelligent operator of utility tunnel boring machines. *Automation in Construction*, 131:103880.
- [Garcia, 2022] Garcia, R. (2022). Tatução da linha 6-laranja do metrô volta a funcionar a partir desta quarta, quase 7 meses após acidente na marginal tietê.
- [Gehring, 2009] Gehring, K. (2009). The influence of tbm design and machine features on performance and tool wear in rock. *Geomechanics and Tunneling*, 2(2):140–155.

- [Giacomella, 2021] Giacomella, L. (2021). Techno-economic assessment (tea) and life cycle costing analysis (lcca): Discussing methodological steps and integrability. *Insights into Regional Development*, 3(2):176–197.
- [Gillespie, 2011] Gillespie, A. K. (2011). *Crossing Under the Hudson: The Story of the Holland and Lincoln Tunnels*. Rutgers University Press.
- [Girasa and Girasa, 2020] Girasa, R. and Girasa, R. (2020). Ai as a disruptive technology. *Artificial Intelligence as a Disruptive Technology: Economic Transformation and Government Regulation*, pages 3–21.
- [Girmscheid, 2003] Girmscheid (2003). Tunnel boring machines. *Practice periodical on structural design and construction*, 8(3):150–163.
- [Gleit, 2016] Gleit, J. (2016). The detroit river tunnel few have seen: The michigan central railway tunnel.
- [Globe Newswire, 2022] Globe Newswire (2022). Tunnel boring machine market size is projected to reach usd 10.30 billion by 2030, growing at a cagr of 6.2%: Straits research. Accessed: 2023-03-14.
- [Godfrey, 1910] Godfrey, S. C. (1910). The detroit river tunnel. *Professional Memoirs, Corps of Engineers, United States Army, and Engineer Department at Large*, 2(6):153–167.
- [Goel et al., 2012] Goel, R. K., Singh, B., and Zhao, J. (2012). *Underground Infrastructures*. Butterworth-Heinemann.
- [Gompers and Lerner, 2001] Gompers, P. and Lerner, J. (2001). The venture capital revolution. *Journal of economic perspectives*, 15(2):145–168.
- [Gong et al., 2007] Gong, Q., Zhao, J., and Jiang, Y. (2007). In situ tbm penetration tests and rock mass boreability analysis in hard rock tunnels. *Tunnelling and Underground Space Technology*, 22:303–316.

- [Google, 2023] Google (2023). Cloud tensor processing units (tpus). <https://cloud.google.com/tpu>. Accessed on 20 July 2020.
- [Gradenwitz, 1913] Gradenwitz, A. (1913). The lotschberg or bernese alpine railway. *Scientific American*, 108(20):452–453.
- [Grand Site Canal du Midi, 2020] Grand Site Canal du Midi (2020). Malpas tunnel.
- [Grantz, 1997] Grantz, W. C. (1997). Steel-shell immersed tunnels—forty years of experience. *Tunnelling and underground space technology*, 12(1):23–31.
- [Grunwald et al., 1998] Grunwald, D., Klauser, A., Manne, S., and Pleszkun, A. (1998). Confidence estimation for speculation control. *ACM SIGARCH Computer Architecture News*, 26(3):122–131.
- [Guedes, 2017] Guedes, A. e. a. (2017). Travelling by metro in porto - tips and costs.
- [Guglielmetti et al., 2008] Guglielmetti, V., Grasso, P., Mahtab, A., and Xu, S. (2008). *Mechanized tunnelling in urban areas: design methodology and construction control*. CRC Press.
- [Guo et al., 2022] Guo, D., Li, J., Jiang, S.-H., Li, X., and Chen, Z. (2022). Intelligent assistant driving method for tunnel boring machine based on big data. *Acta Geotechnica*, 17(4):1019–1030.
- [Hamilton, 2020] Hamilton, D. (2020). Big data spurs autonomous tunneling. *ASME.org*.
- [Hammerer, 2015] Hammerer, N. (2015). Influence of steering actions by the machine operator on the interpretation of tbm performance data. *University of Innsbruck: Innsbruck, Austria*.
- [Hansen, 2010] Hansen, B. (2010). The hudson and manhattan railroad tunnels: Digging under pressure. *Civil Engineering Magazine Archive*, 79(1):36–39.
- [Harper, 2011] Harper, J. A. (2011). The history and geology of the allegheny portage railroad, blair and cambria counties, pennsylvania. *Field Guides*, 20:111–141.

- [Hasanpour et al., 2018] Hasanpour, R., Rostami, J., Thewes, M., and Schmitt, J. (2018). Parametric study of the impacts of various geological and machine parameters on thrust force requirements for operating a single shield tbn in squeezing ground. *Tunnelling and Underground Space Technology*, 73:252–260.
- [Hatwell et al., 2020] Hatwell, J., Gaber, M. M., and Atif Azad, R. M. (2020). Ada-whips: explaining adaboost classification with applications in the health sciences. *BMC Medical Informatics and Decision Making*, 20(1):1–25.
- [Hencher, 2004] Hencher, S. (2004). Weathering and erosion processes in rock—implications for geotechnical engineering. In *Proceedings symposium on Hong Kong soils and rocks*, pages 29–79.
- [Hennessey, 1973] Hennessey, J. F. (1973). Licensing of nuclear power plants by the atomic energy commission. *Wm. & Mary L. Rev.*, 15:487.
- [Herrenknecht, 2013] Herrenknecht (2013). Variable density technology – game changer for kuala lumpur. <https://www.herrenknecht.com/en/newsroom/pressreleasedetail/variable-density-technology-game-changer-for-kuala-lumpur/>. Accessed: February 15, 2023.
- [Herrenknecht, 2021] Herrenknecht (2021). Gripper tbn.
- [Herrenknecht, 2022] Herrenknecht (2022). Re-connect: Our joined ingenuity - herrenknecht auf der bauma 2022. <https://www.herrenknecht.com/en/newsroom/pressreleasedetail/re-connect-our-joined-ingenuity-herrenknecht-auf-der-bauma-2022/>. Accessed: 2023-03-14.
- [Hodge, 1992] Hodge, A. T. (1992). *Roman Aqueducts and Water Supply*. Bloomsbury Academic.
- [Huang et al., 2021] Huang, M., Ninic, J., and Zhang, Q. (2021). Bim, machine learning and computer vision techniques in underground construction: Current

status and future perspectives. *Tunnelling and Underground Space Technology*, 108:103677.

[Industry Research, 2022] Industry Research (2022). Global tunnel and bridge market research report 2022. Technical report.

[Instituto Portuário e dos Transportes Marítimos, 2009] Instituto Portuário e dos Transportes Marítimos (2009). Relatório de conformidade ambiental do projecto de execução variante norte de loulé à en270 (2^a fase).

[Intelligent Transport, 2019] Intelligent Transport (2019). Metro do porto: A success story moving 50 million people every year.

[International Tunnelling and Underground Space Association, 2008] International Tunnelling and Underground Space Association (2008). Guidelines for the use of the "natm" tunneling technique with the support of sprayed concrete. Technical report, ITA.

[Ishii, 2017] Ishii, G. (2017). Current issues regarding mechanised and automated tunnelling. In *Tunnels and Underground Structures*, pages 75–86. Routledge.

[Islam et al., 2022] Islam, M. M. M., Kowsar, A., Haque, A. M., Hossain, M. K., Ali, M. H., Rubel, M., and Rahman, M. F. (2022). Techno-economic analysis of hybrid renewable energy system for healthcare centre in northwest bangladesh. *Process Integration and Optimization for Sustainability*, pages 1–14.

[Jain et al., 2015] Jain, P., Naithani, A., and Singh, T. (2015). Performance characteristics of tunnel boring machines and correlation with empirical prediction model - case study from mumbai, india. *ISEG Golden Jubilee Special Publication Journal of Engineering Geology*, pages 642–651.

[Janbaz, 2017] Janbaz, M. (2017). *On the Optimization of Resource Allocation in Cognitive Radio Networks*. PhD thesis, The University of Texas at Arlington, Arlington, TX.

- [Johnston and Gutierrez-Alonso, 2010] Johnston, S. T. and Gutierrez-Alonso, G. (2010). The north american cordillera and west european variscides: Contrasting interpretations of similar mountain systems. *Gondwana Research*, 17(2):516–525.
- [Jung et al., 2019] Jung, J.-H., Chung, H., Kwon, Y.-S., and Lee, I.-M. (2019). An ann to predict ground condition ahead of tunnel face using tbn operational data. *KSCE Journal of Civil Engineering*, 23(7):3200–3206.
- [Kamp and Owen, 2013] Kamp, U. and Owen, L. (2013). *Polygenetic Landscapes*, volume 5, pages 370–393.
- [Kelley, 2017] Kelley, J. (2017). Jerry’s models.
- [Kenneth Research, 2021] Kenneth Research (2021). Global tunnel boring machine market. <https://www.kennethresearch.com/report-details/global-tunnel-boring-machine-market/10352111>. Accessed: 2023-03-14.
- [Kirkland, 1947] Kirkland, E. C. (1947). The hoosac tunnel route: The great bore. *New England Quarterly*, pages 88–113.
- [Knights, 2017] Knights, M. (2017). The changing face of the tunneling industry: The role of the ita, partnership, and innovation. <https://www.robbinstbn.com/category/blog/the-future-of-tunneling/>. Accessed: March 14, 2023.
- [Kolymbas, 2005] Kolymbas, D. (2005). *Tunnelling and tunnel mechanics: A rational approach to tunnelling*. Springer Science & Business Media.
- [Koopialipoor et al., 2019] Koopialipoor, M., Nikouei, S. S., Marto, A., Fahimifar, A., Jahed Armaghani, D., and Mohamad, E. T. (2019). Predicting tunnel boring machine performance through a new model based on the group method of data handling. *Bulletin of Engineering Geology and the Environment*, 78:3799–3813.
- [Lane, 2019] Lane, K. S. (2019). Tunnels and underground excavations.

- [Latapí Agudelo et al., 2019] Latapí Agudelo, M. A., Jóhannsdóttir, L., and Davídsdóttir, B. (2019). A literature review of the history and evolution of corporate social responsibility. *International Journal of Corporate Social Responsibility*, 4(1):1–23.
- [Lenarduzzi and Taibi, 2016] Lenarduzzi, V. and Taibi, D. (2016). Mvp explained: A systematic mapping study on the definitions of minimal viable product. In *2016 42th Euromicro Conference on Software Engineering and Advanced Applications (SEAA)*, pages 112–119. IEEE.
- [Lewis, 2013] Lewis, T. (2013). *Divided highways: Building the interstate highways, transforming American life*. Cornell University Press.
- [Li et al., 2017] Li, S., Liu, B., Xu, X., Nie, L., Liu, Z., Song, J., Sun, H., Chen, L., and Fan, K. (2017). An overview of ahead geological prospecting in tunneling. *Tunnelling and Underground Space Technology*, 63:69–94.
- [Li et al., 2022] Li, W., Yan, P., Lu, A., Huang, S., and Lu, W. (2022). Effect of confining pressure on peak penetration force of the tbm disc cutter. *Arabian Journal of Geosciences*, 15(11):1041.
- [Lindmark, 2002] Lindmark, S. (2002). Evolution of techno-economic systems-an investigation of the history of mobile communications. *Doktorsavhandlingar vid Chalmers Tekniska Hogskola*.
- [Liu et al., 2015] Liu, J., Ren, J., and Guo, W. (2015). Thrust and torque characteristics based on a new cutter-head load model. *Chinese Journal of Mechanical Engineering*, 28(4):801–809.
- [Liu et al., 2020] Liu, Q., Wang, X., Huang, X., and Yin, X. (2020). Prediction model of rock mass class using classification and regression tree integrated adaboost algorithm based on tbm driving data. *Tunnelling and Underground Space Technology*, 106:103595.

- [Liu et al., 2023] Liu, W., Li, A., Fang, W., Love, P. E., Hartmann, T., and Luo, H. (2023). A hybrid data-driven model for geotechnical reliability analysis. *Reliability Engineering & System Safety*, 231:108985.
- [Long, 2014] Long, D. (2014). *A history of London in 100 places*. Simon and Schuster.
- [Loquercio et al., 2020] Loquercio, A., Segu, M., and Scaramuzza, D. (2020). A general framework for uncertainty estimation in deep learning. *IEEE Robotics and Automation Letters*, 5(2):3153–3160.
- [Mahdevari et al., 2014] Mahdevari, S., Shahriar, K., Yagiz, S., and Akbarpour Shirazi, M. (2014). A support vector regression model for predicting tunnel boring machine penetration rates. *International Journal of Rock Mechanics and Mining Sciences*, 72:214–229.
- [Mahmud et al., 2021] Mahmud, R., Moni, S. M., High, K., and Carbajales-Dale, M. (2021). Integration of techno-economic analysis and life cycle assessment for sustainable process design—a review. *Journal of Cleaner Production*, 317:128247.
- [Maidl et al., 2013] Maidl, B., Herrenknecht, M., Maidl, U., and Wehrmeyer, G. (2013). *Mechanised shield tunnelling*. John Wiley & Sons.
- [Maidl et al., 2008] Maidl, B., Schmid, L., Ritz, W., and Herrenknecht, M. (2008). *Hardrock tunnel boring machines*. John Wiley & Sons.
- [Maidl et al., 2014] Maidl, B., Thewes, M., and Maidl, U. (2014). *Handbook of Tunnel Engineering II: Basics and Additional Services for Design and Construction*. John Wiley & Sons.
- [Mair et al., 2007] Mair, R., Soga, K., and Jin, Y. (2007). Automatic prediction of ground movement and support pressure in tunnelling. *Proceedings of the Institution of Civil Engineers-Geotechnical Engineering*, 160(1):3–14.
- [Mair and Taylor, 1997] Mair, R. and Taylor, R. (1997). Theme lecture: Bored tunnelling in the urban environment. In *Proceedings of the fourteenth international*

- conference on soil mechanics and foundation engineering*, pages 2353–2385. Rotterdam.
- [Mapa Metro, 2010] Mapa Metro (2010). Porto metro : Map, lines, schedules and fares.
- [Marchesi, 2019] Marchesi, R. (2019). Metro is not just for big city, as porto city shows in portugal.
- [Mass Rapid Transit Corporation, 2013] Mass Rapid Transit Corporation (2013). Breakthrough of the world’s first variable density tunnel boring machine. Accessed: February 15, 2023.
- [Mathewson and Kentley, 2006] Mathewson, A. and Kentley, E. (2006). *The Brunels’ Tunnel*. Brunel Museum.
- [Mayer-Schönberger and Cukier, 2013] Mayer-Schönberger, V. and Cukier, K. (2013). *Big data: A revolution that will transform how we live, work, and think*. Houghton Mifflin Harcourt.
- [Mediastorehouse, 2019] Mediastorehouse (2019). Prints of a view of the entrance to the wapping-rotherhithe tunnel under the thames.
- [Mega, 2022] Mega, V. (2022). Climate-conscious cities: The critical decade to 2030. In *Human Sustainable Cities: Towards the SDGs and Green, Just, Smart and Inclusive Transitions*, pages 73–103. Springer.
- [Melenbrink et al., 2020] Melenbrink, N., Werfel, J., and Menges, A. (2020). On-site autonomous construction robots: Towards unsupervised building. *Automation in construction*, 119:103312.
- [Menardi and Torelli, 2014] Menardi, G. and Torelli, N. (2014). Training and assessing classification rules with imbalanced data. *Data mining and knowledge discovery*, 28:92–122.
- [Merriam-Webster,] Merriam-Webster. Biomimicry definition & meaning.

- [Metro do Porto, 2010a] Metro do Porto (2010a). História do metro do porto.
- [Metro do Porto, 2010b] Metro do Porto (2010b). Metro em números.
- [Metro do Porto, 2019] Metro do Porto (2019). 70 milhões de obrigados.
- [Metro do Porto S.A., 2006] Metro do Porto S.A. (2006). Relatório e contas. Technical report, Metro do Porto.
- [Mohammadzamani et al., 2019] Mohammadzamani, D., Mahdevari, S., and Bagherpour, R. (2019). Evaluation of required thrust force based on advance rates in shielded tbms under squeezing conditions. *Journal of Geophysics and Engineering*, 16(5):842–861.
- [Mooney et al., 2012] Mooney, M. A., Walter, B., and Frenzel, C. (2012). Real-time tunnel boring machine monitoring: A state of the art review. *North American Tunnelling, 2012 proceedings*, pages 73–81.
- [Mukerji, 2021] Mukerji, C. (2021). Impossible engineering. In *Impossible Engineering*. Princeton University Press.
- [Munfakh, 2003] Munfakh, G. (2003). Ground improvement in transportation projects: from old visions to innovative applications. *Proceedings of the Institution of Civil Engineers-Ground Improvement*, 7(2):47–60.
- [Nagapurkar, 2019] Nagapurkar, P. (2019). *Techno-economic optimization and environmental life cycle assessment of microgrids using genetic algorithm and artificial neural networks*. PhD thesis, Missouri University of Science and Technology.
- [National Parks Service, 2022] National Parks Service (2022). Staple bend tunnel.
- [National Research Council, 2009] National Research Council (2009). *Sustainable critical infrastructure systems: A framework for Meeting 21st Century Imperatives: Report of a workshop*. National Academies Press.
- [Nilsson, 1982] Nilsson, N. J. (1982). *Principles of artificial intelligence*. Springer Science & Business Media.

- [Noronha and Leterrier, 1995] Noronha, F. and Leterrier, J. (1995). Complexo metamórfico da foz do douro. geoquímica e geocronologia. resultados preliminares. In *SODRÉ BORGES, F. & MARQUES, M.(coords). IV Congresso Nacional de Geologia. Mem. Mus. Lab. Min. Geol. Fac. Ciênc. Univ. Porto*, volume 4, pages 769–774.
- [Noronha and Leterrier, 2000] Noronha, F. and Leterrier, J. (2000). Complexo metamórfico da foz do douro (porto). geoquímica e geocronologia. *REVISTA-REAL ACADEMIA GALEGA DE CIENCIAS*, 19:21–42.
- [Northcutt et al., 2021a] Northcutt, C., Jiang, L., and Chuang, I. (2021a). Confident learning: Estimating uncertainty in dataset labels. *Journal of Artificial Intelligence Research*, 70:1373–1411.
- [Northcutt et al., 2021b] Northcutt, C. G., Athalye, A., and Mueller, J. (2021b). Pervasive label errors in test sets destabilize machine learning benchmarks. *arXiv preprint arXiv:2103.14749*.
- [OECD, 2019] OECD (2019). The oecd creates better policies for better lives. read the oecd’s main figures to find out more about their work.
- [Oleson, 2008] Oleson, J. P. (2008). *The Oxford Handbook of Engineering and Technology in the Classical World*. Oxford University Press.
- [O’Reilly, 2002] O’Reilly, M. (2002). Mont cenis: The first trans-alpine tunnel. *Tunnels & Tunnelling International*, 34(3).
- [Owen, 2011] Owen, A. D. (2011). The economic viability of nuclear power in a fossil-fuel-rich country: Australia. *Energy Policy*, 39(3):1305–1311.
- [Pafnutius, 2023] Pafnutius (2023). Gadhara aqueduct, jordan.
- [Pan et al., 2018] Pan, Y., Liu, Q., Peng, X., Kong, X., Liu, J., and Zhang, X. (2018). Full-scale rotary cutting test to study the influence of disc cutter installment radius on rock cutting forces. *Rock Mechanics and Rock Engineering*, 51.

- [Pasalkar, 2023] Pasalkar, A. (2023). The tunnel boring machine market grows stronger day by day as city infrastructure revolutionizes. <https://scoop.market.us/the-tunnel-boring-machine-market-grows-stronger-day-by-day-as-city-infrastructure-revolutionizes/>. Accessed: February 15, 2023.
- [Patatas et al., 2011] Patatas, T. M. d. A. et al. (2011). Processes of transformation in urban development: comparative study of oporto and wroclaw.
- [Pereira, 1997] Pereira, D. (1997). *Sedimentologia e Estratigrafia do Cenozóico de Trás-os-Montes Oriental (NE Portugal)*. PhD thesis, Universidade do Minho.
- [Peres et al., 2020] Peres, R. S., Jia, X., Lee, J., Sun, K., Colombo, A. W., and Barata, J. (2020). Industrial artificial intelligence in industry 4.0-systematic review, challenges and outlook. *IEEE Access*, 8:220121–220139.
- [Place and Cox, 2008] Place, D. and Cox, R. (2008). Bridgeworks on the east london railway line extension, uk. In *Proceedings of the Institution of Civil Engineers- Bridge Engineering*, volume 161, pages 89–98. Thomas Telford Ltd.
- [Pollio, 2011] Pollio, V. (2011). *The Ten Books on Architecture*.
- [Railssystem, 2018] Railssystem (2018). Tunnel boring machine.
- [Railway Technology, 2008] Railway Technology (2008). Porto light rail project.
- [Rajabi Hamedani et al., 2019] Rajabi Hamedani, S., Kuppens, T., Malina, R., Bocci, E., Colantoni, A., and Villarini, M. (2019). Life cycle assessment and environmental valuation of biochar production: Two case studies in belgium. *Energies*, 12(11):2166.
- [Rajoub, 2020] Rajoub, B. (2020). Supervised and unsupervised learning. In *Biomedical Signal Processing and Artificial Intelligence in Healthcare*, pages 51–89. Elsevier.

- [Ramoni and Anagnostou, 2010] Ramoni, M. and Anagnostou, G. (2010). Thrust force requirements for tbms in squeezing ground. *Tunnelling and Underground Space Technology*, 25(4):433–455.
- [Reichstein et al., 2019] Reichstein, M., Camps-Valls, G., Stevens, B., Jung, M., Denzler, J., and Carvalhais, N. (2019). Deep learning and process understanding for data-driven earth system science. *Nature*, 566(7743):195–204.
- [Renard, 2020] Renard, S. (2020). The grotto of posilippo by night in naples.
- [Ribeiro et al., 2010] Ribeiro, H., de Jesus, A. P., Mosquera, D., Abreu, I., Romani, J. V., and Noronha, F. (2010). Sedimentologia e estratigrafia-estudo de um teraço de lavadores. contribuição para a dedução das condições paleoclimáticas no plistocénico médio.
- [Ribeiro da Silva, 2004] Ribeiro da Silva, F. (2004). *Estudos em homenagem a Luís António de Oliveira Ramos*. Universidade do Porto.
- [Ring, 2011] Ring, J. (2011). *How the English made the Alps*. Faber & Faber.
- [Ritchie and Roser, 2018] Ritchie, H. and Roser, M. (2018). Urbanization.
- [Roach and Brunel, 1998] Roach, M. and Brunel, M. (1998). The strengthening of brunel’s thames tunnel. In *Proceedings of the Institution of Civil Engineers-Transport*, volume 129, pages 106–115. Thomas Telford Ltd.
- [Robbins, 2021] Robbins (2021). Single shield.
- [Rodrigue, 2020] Rodrigue, J.-P. (2020). *The geography of transport systems*. Routledge.
- [Romão et al., 2008] Romão, J., Ribeiro, A., Pereira, E., Fonseca, P. E., Rodrigues, J. F., Mateus, A., Noronha, F., and Dias, R. (2008). Desligamentos interplaca e intraplaca em cadeias deformadas: exemplos no bordo do sw dos variscides ibéricos. In *8^a Conferência Anual do CGET*.

- [Rostami, 2016] Rostami, J. (2016). Performance prediction of hard rock tunnel boring machines (tbms) in difficult ground. *Tunnelling and Underground Space Technology*, 57:173–182.
- [Rouse, 2015] Rouse, M. (2015). Telemetry. *Techopedia*.
- [Routledge, 1903] Routledge, R. (1903). *Discoveries and Inventions of the Nineteenth Century*. G. Routledge and Sons.
- [Ruwanpura et al., 2004] Ruwanpura, J., AbouRizk, S., and Allouche, M. (2004). Analytical methods to reduce uncertainty in tunnel construction projects. *Canadian journal of civil engineering*, 31(2):345–360.
- [Schulter and Wagner, 2020] Schulter, A. and Wagner, H. (2020). *Tunnel Boring Machines: Trends in Design and Construction of Mechanical Tunnelling: Proceedings of the International Lecture Series, Hagenberg Castle, Linz, 14-15 December 1995*. CRC Press.
- [Sebbeh-Newton et al., 2021] Sebbeh-Newton, S., Ayawah, P. E., Azure, J. W., Kaba, A. G., Ahmad, F., Zainol, Z., and Zabidi, H. (2021). Towards tbm automation: on-the-fly characterization and classification of ground conditions ahead of a tbm using data-driven approach. *Applied Sciences*, 11(3):1060.
- [Sharif, 1988] Sharif, M. N. (1988). Basis for techno-economic policy analysis. *Science and Public Policy*, 15(4):217–219.
- [Shaw, 2022] Shaw, A. (2022). Tunnels built in their own approaches. *Tunnelling and Underground Space Technology*, 120.
- [Shehadeh et al., 2021] Shehadeh, A., Alshboul, O., Al Mamlook, R. E., and Hamedat, O. (2021). Machine learning models for predicting the residual value of heavy construction equipment: An evaluation of modified decision tree, lightgbm, and xgboost regression. *Automation in Construction*, 129:103827.

- [Sheil et al., 2020a] Sheil, B. B., Suryasentana, S. K., Mooney, M. A., and Zhu, H. (2020a). Machine learning to inform tunnelling operations: recent advances and future trends. *Proceedings of the Institution of Civil Engineers-Smart Infrastructure and Construction*, 173(4):74–95.
- [Sheil et al., 2020b] Sheil, B. B., Suryasentana, S. K., Mooney, M. A., and Zhu, H. (2020b). Machine learning to inform tunnelling operations: recent advances and future trends. *Proceedings of the Institution of Civil Engineers-Smart Infrastructure and Construction*, 173(4):74–95.
- [Singh and Singh, 2006] Singh, T. D. and Singh, B. (2006). *Elsevier Geo-Engineering Book 5: Tunnelling In Weak Rocks*, volume 5. Elsevier.
- [Soldo et al., 2019] Soldo, L., Vendramini, M., and Eusebio, A. (2019). Tunnels design and geological studies. *Tunnelling and Underground Space Technology*, 84:82–98.
- [Sousa, 2010] Sousa, R. (2010). *Risk analysis for tunneling projects*. PhD thesis, Massachusetts Institute of Technology.
- [Sousa and Einstein, 2012] Sousa, R. and Einstein, H. (2012). Risk analysis during tunnel construction using bayesian networks: Porto metro case study. *Tunnelling and Underground Space Technology*, 27(1):86–100.
- [Sousa and Einstein, 2021] Sousa, R. L. and Einstein, H. H. (2021). Lessons from accidents during tunnel construction. *Tunnelling and Underground Space Technology*, 113:103916.
- [Sowers and Royster, 1978] Sowers, G. F. and Royster, D. L. (1978). Field investigation. *Special report*, 176:81–111.
- [Spielmann, 1880] Spielmann, A. e. a. (1880). The hudson river tunnel. *Transactions of the American Society of Civil Engineers*, 9(1):259–272.

- [Stack, 1995] Stack, B. (1995). *Encyclopaedia of tunnelling, mining and drilling equipment*. Mudén Publishing Company.
- [Sun et al., 2018] Sun, W., Shi, M., Zhang, C., Zhao, J., and Song, X. (2018). Dynamic load prediction of tunnel boring machine (tbn) based on heterogeneous in-situ data. *Automation in Construction*, 92:23–34.
- [Sutcliffe, 1996] Sutcliffe, H. (1996). Tunnel boring machines. *Tunnel Engineering Handbook*, pages 203–219.
- [Suthaharan, 2016] Suthaharan, S. (2016). Machine learning models and algorithms for big data classification. *Integr. Ser. Inf. Syst*, 36:1–12.
- [Szabo, 2016] Szabo, S. (2016). Urbanisation and food insecurity risks: Assessing the role of human development. *Oxford Development Studies*, 44(1):28–48.
- [The Port Authority, 2016] The Port Authority (2016). The holland tunnel: Did you know?
- [Thomas, 2021] Thomas, T. (2021). Successful tbn launch for chouer liao river diversion project.
- [Transportes Publicos de Portugal, 2015] Transportes Publicos de Portugal (2015). Transportes publicos portugal e espana: Public transport portugal and spain - andante ticket system.
- [Tunnel Business Magazine, 2017] Tunnel Business Magazine (2017). Hard-rock tunnel boring machines.
- [Ugitech, 2019] Ugitech (2019). Slurry tbn.
- [U.S. Bureau of Economic Analysis (BEA), 2022] U.S. Bureau of Economic Analysis (BEA) (2022). Gross domestic product.
- [Vertovec, 2015] Vertovec, S. (2015). Introduction: Migration, cities, diversities ‘old’and ‘new’. *Diversities old and new: Migration and socio-spatial patterns in New York, Singapore and Johannesburg*, pages 1–20.

- [Vieira et al., 2020] Vieira, G., Zêzere, J., and Mora, C. (2020). *Landscapes and Landforms of Portugal*. World Geomorphological Landscapes. Springer International Publishing.
- [Wade and Glynn, 2020] Wade, C. and Glynn, K. (2020). *Hands-On Gradient Boosting with XGBoost and scikit-learn: Perform accessible machine learning and extreme gradient boosting with Python*. Packt Publishing Ltd.
- [Wang et al., 2020] Wang, F., Zhou, D., Zhou, X., Xiao, N., and Guo, C. (2020). Rock breaking performance of tbm disc cutter assisted by high-pressure water jet. *Applied Sciences*, 10(18):6294.
- [Wang et al., 2023] Wang, K., Zhang, L., and Fu, X. (2023). Time series prediction of tunnel boring machine (tbm) performance during excavation using causal explainable artificial intelligence (cx-ai). *Automation in Construction*, 147:104730.
- [Wang et al., 2019] Wang, Y. E., Wei, G.-Y., and Brooks, D. (2019). Benchmarking tpu, gpu, and cpu platforms for deep learning. *arXiv preprint arXiv:1907.10701*.
- [Washington State Department of Transportation, 2020] Washington State Department of Transportation (2020). Washington state department of transportation-state route 99 tunnel project.
- [West, 2005] West, G. (2005). *Innovation and the rise of the tunnelling industry*. Cambridge University Press.
- [Wilson, 2019] Wilson, R. W. (2019). Fifty years of the wilson cycle concept in plate tectonics: an overview. *Geological Society, London, Special Publications*, 470(1):1–17.
- [Wolmar, 2009] Wolmar, C. (2009). *The Subterranean Railway: how the London Underground was built and how it changed the city forever*. Atlantic Books Ltd.
- [Wonders, 2010] Wonders, R. (2010). The simplon tunnel.

- [World Population Review, 2022] World Population Review (2022). Porto population 2022.
- [Wu et al., 2021] Wu, F., Gong, Q., Li, Z., Qiu, H., Jin, C., Huang, L., and Yin, L. (2021). Development and application of cutterhead vibration monitoring system for tbn tunnelling. *International Journal of Rock Mechanics and Mining Sciences*, 146:104887.
- [Xia et al., 2021] Xia, X., Liu, T., Han, B., Gong, M., Yu, J., Niu, G., and Sugiyama, M. (2021). Sample selection with uncertainty of losses for learning with noisy labels. *arXiv preprint arXiv:2106.00445*.
- [Xu et al., 2019] Xu, H., Zhou, J., G. Asteris, P., Jahed Armaghani, D., and Tahir, M. M. (2019). Supervised machine learning techniques to the prediction of tunnel boring machine penetration rate. *Applied sciences*, 9(18):3715.
- [You et al., 2023] You, K., Zhou, C., and Ding, L. (2023). Deep learning technology for construction machinery and robotics. *Automation in Construction*, 150:104852.
- [Yu et al., 2022] Yu, H., Zhou, X., Zhang, X., and Mooney, M. (2022). Enhancing earth pressure balance tunnel boring machine performance with support vector regression and particle swarm optimization. *Automation in Construction*, 142:104457.
- [Záruba, 2012] Záruba, Q. (2012). *Engineering geology*, volume 10. Elsevier.
- [Zerilli et al., 2022] Zerilli, J., Bhatt, U., and Weller, A. (2022). How transparency modulates trust in artificial intelligence. *Patterns*, page 100455.
- [Zhang and Zhan, 2017] Zhang, L. and Zhan, C. (2017). Machine learning in rock facies classification: An application of xgboost. In *International Geophysical Conference, Qingdao, China, 17-20 April 2017*, pages 1371–1374. Society of Exploration Geophysicists and Chinese Petroleum Society.
- [Zhang et al., 2019a] Zhang, Q., Liu, Z., and Tan, J. (2019a). Prediction of geological conditions for a tunnel boring machine using big operational data. *Automation in Construction*, 100:73–83.

- [Zhang et al., 2019b] Zhang, Q., Liu, Z., and Tan, J. (2019b). Prediction of geological conditions for a tunnel boring machine using big operational data. *Automation in Construction*, 100:73–83.
- [Zhang et al., 2014] Zhang, Z., Coutinho, E., Deng, J., and Schuller, B. (2014). Cooperative learning and its application to emotion recognition from speech. *IEEE/ACM Transactions on Audio, Speech, and Language Processing*, 23(1):115–126.
- [Zhao et al., 2012] Zhao, K., Janutolo, M., and Barla, G. (2012). A completely 3d model for the simulation of mechanized tunnel excavation. *Rock Mechanics and Rock Engineering*, 45(4):475–497.
- [Zheng et al., 2016] Zheng, Y., Zhang, Q., and Zhao, J. (2016). Challenges and opportunities of using tunnel boring machines in mining. *Tunnelling and Underground Space Technology*, 57:287–299.
- [Zheng et al., 2023] Zheng, Z., Wang, F., Gong, G., Yang, H., and Han, D. (2023). Intelligent technologies for construction machinery using data-driven methods. *Automation in Construction*, 147:104711.
- [Zhou et al., 2015] Zhou, S., Kang, Y., Su, C., and Zhang, Q. (2015). Mechanical analysis and prediction for the total thrust on tbms. In *Intelligent Robotics and Applications: 9th International Conference, ICIRA 2015, Portsmouth, UK, August 24–27, 2015, Proceedings, Part III*, pages 436–444. Springer.
- [Zlatanic, 2022] Zlatanic, S. (2022). Tunnels. In *Women in Infrastructure*, pages 263–301. Springer.